

# **Development of Enzymes for Biocatalytic Applications: Protein Engineering, Immobilization and Reactor Concepts**

Inauguraldissertation

zur

Erlangung des akademischen Grades

doctor rerum naturalium (Dr. rer. nat.)

an der Mathematisch-Naturwissenschaftlichen Fakultät

der

Ernst-Moritz-Arndt-Universität Greifswald

vorgelegt von

Hendrik Mallin

geboren am 27.01.1985

in Parchim

Greifswald, August 2014

Dekan:	Prof. Dr. Klaus Fesser
1. Gutachter:	Prof. Dr. Uwe T. Bornscheuer
2. Gutachter:	Prof. Dr. Per Berglund
Tag der Promotion:	17.10.2014

# Content

## Content

Content.....	I
Abbreviations.....	II
Scope and Outline.....	IV
1 Background .....	1
1.1 Protein Engineering of Enzymes in General and of Polyol-Dehydrogenases.....	2
1.2 Application of Baeyer-Villiger Monooxygenases in Organic Synthesis (Article I).....	4
1.3 Immobilization of Transaminases .....	7
1.4 Bioreactors.....	9
2 Biocatalysts Design and Coupling of Enzymatic Steps .....	11
2.1 Protein Engineering of a Polyol-dehydrogenase from <i>Deinococcus geothermalis</i> DSM 11300 (Article II) ....	11
2.2 Biocatalytic Route from Cyclohexanol to $\epsilon$ -Caprolactone (Article III) .....	14
3 Immobilization of Biocatalysts.....	18
3.1 Support Production and Immobilization of (R)-Amine Transaminases on Chitosan Support (Article IV).....	18
3.2 Immobilization of (R)- and (S)-Amine Transaminases on Chitosan Support Using Glutaraldehyde or Divinylsulfone as Linkers (Article V).....	20
4 Application of Biocatalysts in Bioreactors .....	24
4.1 Application of the Rotating Flow Cell Reactor (SpinChem) for Biocatalysis (Article VI) .....	24
5 Concluding Remarks.....	27
6 References .....	28
Author contribution .....	31
Articles.....	32
Article I .....	32
Article II .....	50
Article III .....	59
Article IV .....	65
Article V .....	72
Article VI .....	79
Affirmation .....	84
Curriculum Vitae .....	85
Acknowledgements .....	86

# Abbreviations

## Abbreviations

API	advanced pharmaceutical intermediate	G6PDH	glucose-6-phosphate dehydrogenase
AspFum	( <i>R</i> )-ATA from <i>Aspergillus fumigatus</i>	h	hour
ATA	amine transaminase	HPLC	high-pressure liquid chromatography
BET	Brunnauer-Emmet-Teller	IPA	Isopropylamine
BV	Baeyer-Villiger	IPAc	Isopropylacetate
BVMO	Baeyer-Villiger monooxygenase	ISM	iterative saturation mutagenesis
B-factor	Debye-Waller-factor	kDa	kilodalton
B-fit	B-factor iterative test	L	liter
CALB	<i>Candida Antarctica</i> lipase B	LipA	lipase A from <i>Bacillus subtilis</i>
CHL	cyclohexanol	m <sup>2</sup>	square meter
CHO	cyclohexanone	MD	molecular dynamics
°C	degree Celsius	mg	milligram
CASTing	combinatorial active site saturation test	min	minutes
CAMO	cycloalkanone MO	ml	milliliter
CHMO	cyclohexanone MO	μM	micromolar
CODEHOP	consensus degenerate hybrid oligonucleotide primer	mM	millimolar
CHAPS	3-[(3-cholamidopropyl)dimethylammonio]-1-propanesulfonate	MM	molecular mechanics
CTAB	cetrimonium bromide	MO	monooxygenase
CHES	<i>N</i> -cyclohexyl-2-aminoethane-sulfonic acid	mU	milliunits
DVS	divinylsulfone	NAD(P) <sup>+</sup>	nicotinamide adenine dinucleotide (phosphate) oxidized form
Dgeo	<i>Deinococcus geothermalis</i>	NAD(P)H	nicotinamide adenine dinucleotide (phosphate) reduced form
DSM	“deutsche Sammlung von Mikroorganismen“	n.d.	not determined
2,5-DKCMO	2,5-diketocamphane 1,2-MO	NeoFis	( <i>R</i> )-ATA from <i>Neosartorya fischeri</i>
3,6-DKCMO	3,6-diketocamphane 1,6-MO	nm	nanometer
DMSO	dimethyl sulfoxide	N435	Novozyme 435
<i>E. coli</i>	<i>Escherichia coli</i>	OAT	ornithine amine transaminases
EC	enzyme class	PAMO	phenylacetone MO
e.g.	for example	PCR	polymerase chain reaction
<i>et al.</i>	<i>et alia</i>	pdb	protein data bank
ε-CL	epsilon-Caprolactone	PDH	polyol dehydrogenase
FACS	fluorescence-activated cell sorting	1-PEA	1-phenylethylamine
FAD	flavin adenine dinucleotide	PEI	polyethylenimine
FBR	fixed-bed reactor	pH	<i>pondus hydrogenii</i>
FMN	flavin mononucleotide	PLP	pyridoxal-5'-phosphate
G	gram	PMP	pyridoxamine-5'-phosphate
GA	glutaraldehyde	QM	quantum mechanics
GC	gas chromatography	rpm	rounds per min
GibZea	( <i>R</i> )-ATA from <i>Gibberella zeae</i>	s	seconds
		SCR	SpinChem reactor
		SDR	short chain dehydrogenase
		SDS	sodium dodecyl sulfate
		SEM	scanning electron microscope
		STR	stirred tank reactor
		T	temperature

## Abbreviations

$T_m$	melting point
$T_{50}^{60}$	T where half of initial activity is left after 1 h incubation
U	units
VfTA	(S)-ATA from <i>Vibrio fluvialis</i>
V	volume
3HMu	(S)-ATA from <i>Ruegeria pomeroyi</i>
3I5T	(S)-ATA from <i>Rhodobacter sphaeroides</i> 2.4.1

Moreover, the usual codes for amino acids were used.

### Scope and Outline

Within this thesis the protein engineering, immobilization and application of enzymes in organic synthesis were studied in order to enhance the productivity of diverse biotransformations. **Article I** is a review about Baeyer-Villiger monooxygenases (BVMO) and provides a detailed overview of the most recent advantages in the application of that enzyme class in biocatalysis. Protein engineering of a former uncharacterized polyol-dehydrogenase (PDH) identified in the mesothermophilic bacterium *Deinococcus geothermalis* 11300 is described in **Article II**. **Article III** covers the combination of one PDH mutant with a BVMO in a closed-loop cascade reaction, thus enabling direct oxidation of cyclohexanol to  $\epsilon$ -caprolactone with an internal cofactor recycling of NADP(H). **Article IV** and **Article V** report a process optimization for transamination reactions due to a newly developed immobilization protocol for five (*S*)- and (*R*)-selective aminotransferases (ATA) on chitosan support. Furthermore, the immobilized ATAs were applied in asymmetric amine synthesis. In **Article VI**, an ATA immobilized on chitosan, an encapsulated BVMO whole cell catalyst and a commercially available immobilized lipase were applied in a traditional fixed-bed (FBR) or stirred-tank reactor (STR), and were compared to a novel reactor design (SpinChem, SCR) for heterogeneous biocatalysis.

#### **Article I**      **Discovery, Application and Protein Engineering of Baeyer-Villiger Monooxygenases for Organic Synthesis**

K. Balke\*, M. Kadow\*, H. Mallin\*, S. Saß\*, U.T. Bornscheuer\*, *Org. Biomol. Chem.* **2012**, 10, 6249-6265.

This review provides an overview of the state of the art in applications of BVMOs in biocatalysis. Examples of applications, recently discovered BVMOs and available crystal structures are given and explained in detail. Protein engineering approaches and optimizations, like immobilization, cofactor recycling or reaction condition improvements are summarized and analyzed. To overcome substrate and product inhibition, strategies like substrate feeding or *in situ* product removal are also covered in this perspective.

#### **Article II**      **Protein Engineering of a Thermostable Polyol Dehydrogenase**

H. Wulf\*, H. Mallin\*, U.T. Bornscheuer, *Enzyme Microb. Technol.* **2012**, 51, 217-224.

The mesothermophilic bacterium *Deinococcus geothermalis* 11300 is a possible source for thermostable enzymes. **Article II** describes the identification and cloning of a thermostable PDH in this strain by database search, followed by subsequent extensive protein engineering and characterization of this enzyme. Substitution of a loop region, identified in a homologous enzyme from *Rhodobacter sphaeroides*, lead to a more thermostable variant. A further mutation found by rational design broadened the cofactor specificity towards acceptance of NADP<sup>+</sup>. Studies of the active site by distinct mutations identified residues important for the activity towards 1,2-diols. For a further loop mutant, which accepted NADP<sup>+</sup>, an increase in the specific activity for cyclohexanol was found by analyzing the substrate scope of the variants.

## Scope and Outline

### **Article III      A Self-Sufficient Baeyer–Villiger Biocatalysis System for the Synthesis of $\epsilon$ -Caprolactone from Cyclohexanol**

H. Mallin\*, H. Wulf\*, U.T. Bornscheuer, *Enzyme Microb. Technol.* **2013**, 53, 283-287.

**Article III** shows the combination of a PDH loop mutant capable of using NADP<sup>+</sup> as cofactor with the cyclohexanone monooxygenase (CHMO) from *Acinetobacter calcoaceticus*. Within this closed-loop reaction the cofactor recycling issue of the CHMO was addressed performing the double oxidation of cyclohexanol to  $\epsilon$ -caprolactone. A proof of concept study was carried out, which included expression-optimization of the PDH mutant or co-immobilization of the enzymes. Hereby the CHMO was shown to be the bottleneck in the reaction due to its low stability. Finally,  $\epsilon$ -caprolactone could be isolated in small scale with a yield of 55 % and a purity of 99 % without the necessity of an additional cofactor recycling system.

### **Article IV      Immobilization of two (*R*)-Amine Transaminases on an Optimized Chitosan Support for the Enzymatic Synthesis of Optically Pure Amines**

H. Mallin, U. Menyes, T. Vorhaben, M. Höhne, U. T. Bornscheuer, *ChemCatChem* **2012**, 5, 588-593.

Next to the described protein engineering or cascade approaches to efficiently apply enzymes in industrial processes, immobilization greatly improves the properties of biocatalysts in organic synthesis. Amine transaminases (ATA) were of high impact in the past few years, as they transfer an amino group regio- and stereoselective to a keto-substrate. **Article IV** reports about the efficient immobilization of two (*R*)-amine transaminases on an optimized chitosan support and their application in the production of (*R*)-2-aminohexane from the prochiral ketone. The attachment on chitosan support yielded in highly active ATA preparations (up to 362 U/ g<sub>support</sub>) with greatly improved stability and only a slight reduction in activity by 15 % after four consecutive batch experiments. This study demonstrated that chitosan is an excellent matrix for both enzymes.

### **Article V      Immobilization of (*R*)- and (*S*)-Amine Transaminases on Chitosan Support and their Application for Amine Synthesis using Isopropylamine as Donor**

H. Mallin, M. Höhne, U. T. Bornscheuer, *J. Biotechnol.* 2014, online,  
DOI: 10.1016/j.jbiotec.2014.05.015.

To expand the set of immobilized transaminases, the support developed in **Article IV**, was used to immobilize three recently discovered ATAs. Advantages equal to those reported in **Article IV** were achieved and further properties, e.g. storage stability and activity of the immobilized enzymes were investigated. Furthermore interesting heat activation effects for the free and immobilized transaminase from *Aspergillus fumigatus* were observed. As isopropylamine (IPA) displays advantages as amine donor in the asymmetric amine synthesis from the prostereogenic ketone, interesting scaffolds for protein engineering to improve IPA acceptance were identified.

## Scope and Outline

### **Article VI      Efficient Biocatalysis with Immobilized Enzymes or Encapsulated Whole Cell Microorganism by Using the SpinChem Reactor System**

H. Mallin\*, J. Muschiol\*, E. Byström, U. T. Bornscheuer, *ChemCatChem* **2013**, 5, 3529-3532.

For application of immobilized catalysts the choice of the best reactor system is important for the economical applicability of the process. Traditional set-ups like fixed-bed or stirred-tank reactors display both disadvantages such as reaction compound supply or mechanical forces acting on the catalysts. **Article VI** reports the application of a new reactor design, the rotating flow cell reactor (SpinChem™), used for biocatalysis. Herein, the catalyst is packed within the stirrer and thus protected from mechanical forces. Comparisons to FBR and STR, by performing reactions with an immobilized transaminase as described in **Article IV**, an encapsulated BVMO whole cell catalyst and a commercially available immobilized lipase, were examined. Analysis of these model-reactions revealed that the mass-transfer was not negatively influenced within the SCR and the reusability was greatly improved due the protection of the catalyst and downstream processing was simplified.

\* equal contribution



## 1 Background

Biocatalysis has become an emerging field for the production of compounds on industrial scale by simultaneously reducing process cost and waste produced<sup>[1]</sup>. Therefore traditional chemical catalysts are displaced by enzymes, which catalyze a specific reaction. These work under mild conditions, and in general they display a high activity and selectivity during catalysis<sup>[2]</sup>. In the last decade the application of biocatalysts increased rapidly due to technological advancements in the fields of molecular- and structural biology as well as computational methods. Furthermore, the rapidly increasing number of enzyme encoding sequences available in databases and faster screening systems simplifies the search for a suitable catalyst bearing the required activity. Next to the screening and database approaches, protein engineering has become an established method for the adaption of enzymes to the need of applied biotechnology<sup>[1, 3]</sup>. Especially for the production of advanced pharmaceutical intermediates (API) enzymes displayed important advantages to form the optically pure product since optimized biocatalysts show high enantio-, chemo- and regioselectivity<sup>[4]</sup>. Besides engineering, the applicability of the biocatalyst and the product recovery is important for an economic process<sup>[5]</sup>. Here, immobilization of the enzyme on a solid matrix and the choice of the right reactor/reaction system is an effective way to reduce overall costs. Another important issue in biocatalysis is to find ways of combining certain enzymatic steps to ensure the direct formation of valuable compounds from cheap starting materials in an one-pot reaction.

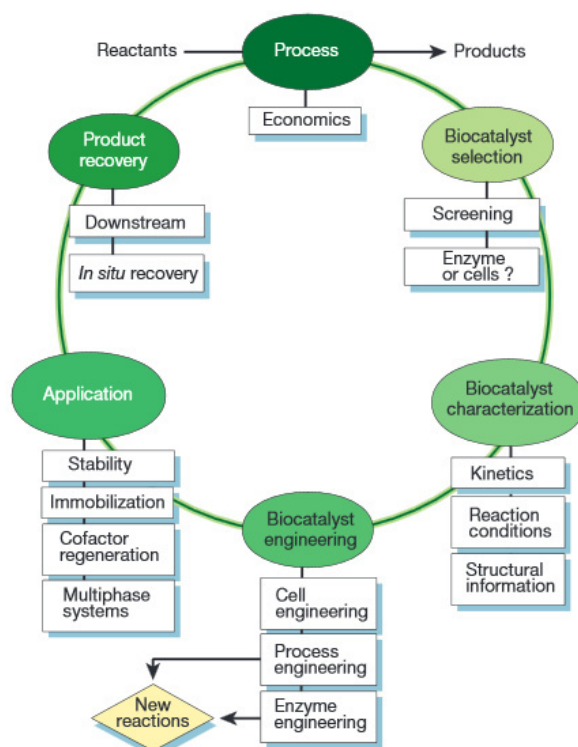


Figure 1: The biocatalytic cycle for application of biocatalysts<sup>[6]</sup>.

Within this study the biocatalytic cycle was intensively investigated using several enzyme classes (Figure 1)<sup>[6]</sup>. An uncharacterized thermostable polyol dehydrogenase (PDH) was selected and cloned. The PDH was then characterized and engineered by rational protein design, facilitating a combination with a Baeyer-Villiger monooxygenase (BVMO). Hence, a new biocatalytic cascade for  $\epsilon$ -caprolactone ( $\epsilon$ -CL) formation from the corresponding alcohol was shown, facilitating an internal cofactor recycling system of NADP(H). Transaminases, important for the production of chiral (*R*)- or (*S*)-amines, were immobilized and stabilized on an optimized chitosan support. Thus, an easy downstream process

# Background

of the catalyst was demonstrated within consecutive batch experiments and the feasibility in chiral amine production was shown. Due to immobilization the biocatalysts could be used in fixed-bed and stirred-tank reactors. Moreover, a novel design of the rotating flow cell (SpinChem™) was successfully applied. This project included several biocatalyst types like calcium alginate encapsulated *E. coli* whole cells harboring a BVMO or a covalently immobilized transaminase. Furthermore a transesterification reaction in organic solvent using a commercially available immobilized lipase was investigated.

## 1.1 Protein Engineering of Enzymes in General and of Polyol-Dehydrogenases

Protein engineering is one of the most powerful tools for the discovery and application of biocatalysts fulfilling the requirements of industrial processes such as stability under reaction conditions and high catalytic activity for the desired substrate without inhibitory effects [1, 3b, 5]. Wildtype enzymes, which were found through screening approaches, e.g. database search, screening microorganisms or metagenome libraries often did not show the properties required in an economic biotechnological process. Besides, an enzyme must be highly enantio-, regio- and chemo-selective to be able to reduce impurities of the final product and thus the purification costs. Protein engineering can address these problems by changing the amino acid sequence of a protein using molecular biology technics or post-translational modifications[7]. Among these techniques, several PCR methods are applied (e.g. QuikChange®, overlap-extension PCR, error-prone PCR, shuffling, mutagenic factors) to quickly introduce mutations using either rational or directed evolution approaches (Figure 2)[8].

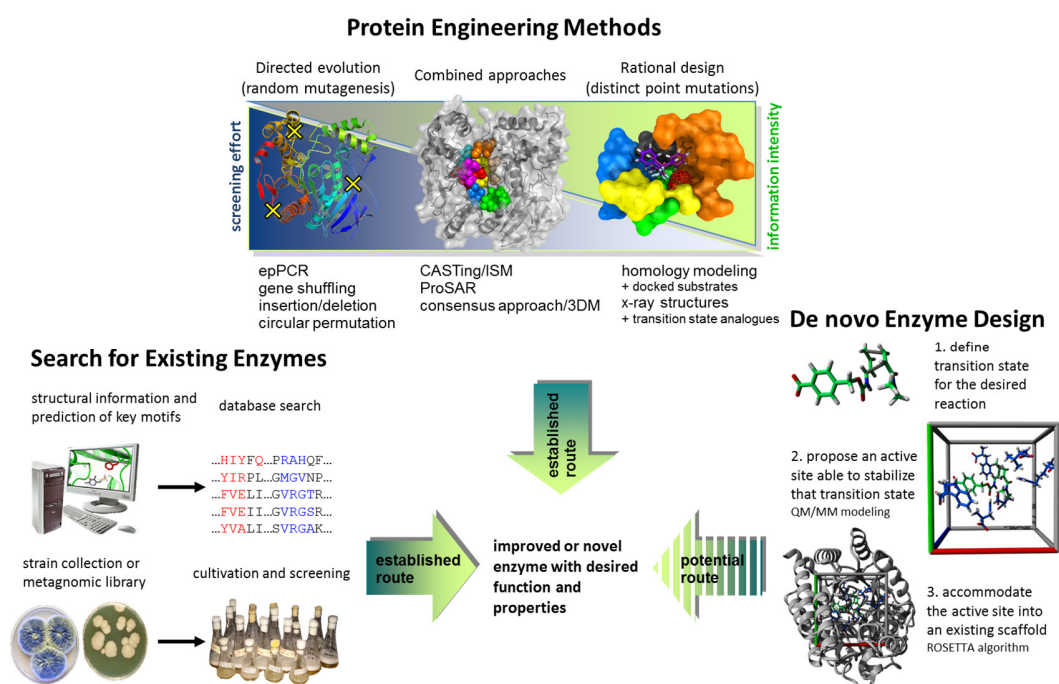


Figure 2: Overview of protein discovery and engineering approaches by rational, evolutionary or combined methods[3b].

In rational design, distinct point mutations are introduced into the protein based on crystal structure information and computational quantum mechanics/molecular mechanics (QM/MM) calculations, but until now a prediction of the best mutations remained challenging and is highly dependent on the available information. In contrast, random mutagenesis is applied in the directed evolution approach. The latter generates random-mutation libraries, which need to be screened for the desired improvement. The size of large libraries, which is generated in this manner, is a limiting factor concerning the rapid identification of improved variants. Nowadays, it becomes apparent that a combination of both methods is the most promising way to identify the desired catalyst within reasonable time. In the combined methods a specific site of

## Background

the protein is targeted for saturation mutagenesis using e.g., degenerate primers. Furthermore, it has been pointed out that synergistic mutations often are necessary, because they can have mutual effects not only on activity, but also on stability. Thus, the crucial amino acid substitutions for the activity are maybe not found during screening if too little exchanges are considered. It was assumed that a screening targeting thermostability prior to activity could increase the chance to identify a catalyst exhibiting increased activity. In this context, Bartsch *et al.* showed that a single mutation had no effect on the enantioselectivity of an esterase from *Bacillus subtilis*, whereas a double mutant displayed inverted enantioselectivity<sup>[9]</sup>. Thus, iterative saturation mutagenesis (ISM) and the combinatorial active site saturation test (CASTing), which were used to combine several interesting mutations by simultaneously reducing the screening effort, essentially contributed to the identification of interesting double mutants<sup>[10]</sup>. During ISM several hot spots are identified within the enzymes structure and then saturated to obtain libraries. The best variants out of these libraries are then subjected to the next mutagenesis round, keeping the first positions conserved while others are saturated. With this strategy the thermostability of lipase A (LipA) from *Bacillus subtilis* could be improved significantly by screening only 8000 clones<sup>[11]</sup>. During CASTing the active site of an enzyme is targeted and several amino acids are saturated simultaneously. Thus, cumulative mutations can be found, but the screening effort increases rapidly. By using the NNK codon, which enables exchanges by all 20 amino acids, for saturation of one position, 94 colonies had to be screened to obtain a statistical coverage of 95 % of all amino acids in the library. If two amino acid position are saturated simultaneously, the number increased to 3066 and for three positions even to 98163 colonies. To manage this library sizes an efficient selection (e.g. growth assay, FACS, phage-display) or high throughput screening system are needed. A strategy to minimize the screening effort is the use of “small, but smart” libraries. When designing small libraries, only frequently occurring amino acids at equivalent positions within structurally related proteins are included<sup>[12]</sup>. With this strategy the screening effort could be reduced significantly, which was shown for stabilization as well as improved enantioselectivity for an esterase from *Pseudomonas fluorescens*<sup>[12-13]</sup>. Nowadays studies show that often a large number of mutations are necessary to obtain an optimal catalyst fulfilling these requirements. Whereas in the beginnings of the 2000s only up to five mutations were introduced, nowadays between 30-40 amino acid substitutions are introduced simultaneously to create the final optimized variant<sup>[1]</sup>.

Especially thermo-stability is often investigated, because there is a high demand for thermostable enzymes in industry as they often show better process performance due to their higher stability and display better scaffolds for extensive protein engineering <sup>[14]</sup>. It is known that salt bridges, H-bonds and  $\pi$ - $\pi$ -stacking effects are increasing the structural rigidity and therefore the thermo-stability of proteins<sup>[15]</sup>. The mutation of flexible amino acids identified by the Debye-Waller-factor (B-factor) of crystal structures represents a major contribution to target this issue (B-factor iterative test, B-fit)<sup>[10c, 13]</sup>. B-factors are measures for the flexibility of a residue displayed by the inability to completely resolve the electron density at this position in a crystal structure.

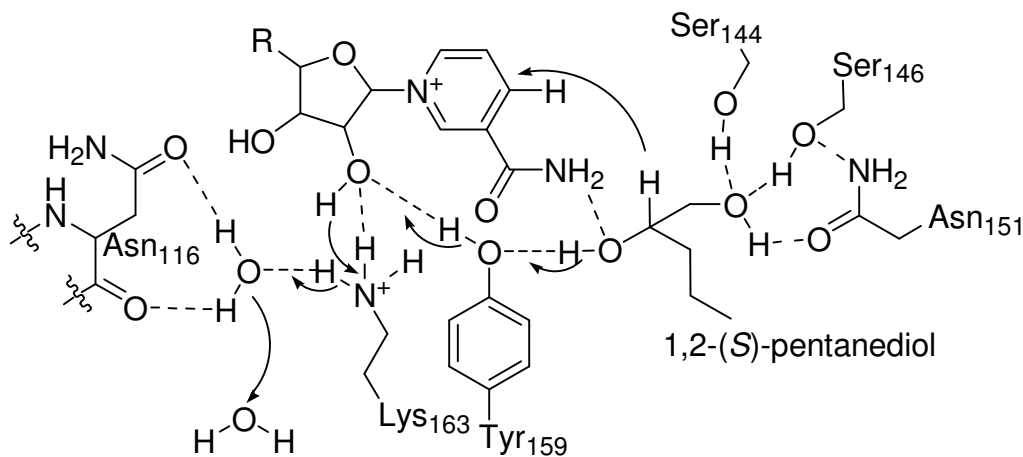
To obtain thermostable enzymes Eijssink *et al.* proposed three ways: (I) isolation from organisms living in extreme environments, (II) rational design based on structural information and (III) directed evolution using an efficient screening system<sup>[14]</sup>. Within this thesis points, (I) and (II) were investigated here in order to identify thermostable polyol dehydrogenases (PDH).

PDHs are enzymes active towards di- or polyhydroxylated compounds and belong to the large family of oxidoreductases (EC 1.x.x.x), which represent around 25 % of all known enzymes<sup>[5]</sup>. A subclass of the oxidoreductases are short chain dehydrogenases (SDR) which require NAD<sup>+</sup> as a cofactor. They are relevant in industry because of their regio- and enantioselectivity towards hydroxylated substrates.

The galactitol-dehydrogenase (EC 1.1.1.16) from *Rhodobacter sphaeroides* D (PDH-D) was obtained from a chemostat culture and shown to catalyze the formation of the sweetener L-tagatose from galactitol. In the enzymes' homotetrameric crystal structure (pdb-entrie: 2WDZ) it was discovered that the typical Rossmann-fold motif for the binding of NADH was present and the residues N116, S144 and Y159XXXK163 were proposed to be the catalytic tetrad (Scheme 1)<sup>[16] [17]</sup>. In this work a slightly varied PDH from the strain *Rhodobacter sphaeroides* DSM 158 (PDH-158) was used, which differed in five amino acids from the PDH-D. The gene Dgeo\_2865 from *Deinococcus geothermalis* DSM

## Background

11300 (PDH-11300) shares 51 % sequence identity with the PDH-158 and was classified as SDR. This strain is a source of thermostable enzymes and thus this protein was assumed to display a good scaffold for rational design using a homology model derived from the structure of the PDH-D<sup>[18]</sup>.



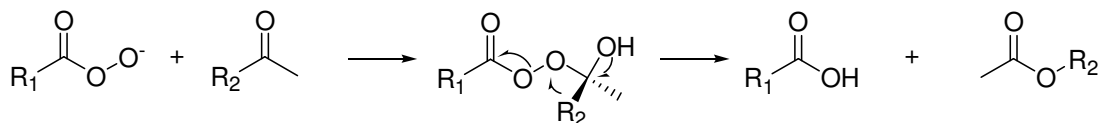
Scheme 1: Catalytic tetrad (Asn-Ser-Tyr-Lys) in the active site of galactitol-dehydrogenase from *Rhodobacter sphaeroides* D. Displayed is the oxidation of 1,2-(S)-pentanediol<sup>[17a]</sup>.

## 1.2 Application of Baeyer-Villiger Monooxygenases in Organic Synthesis (Article I)

The Baeyer-Villiger oxidation enables the production of chiral esters and lactones as valuable building blocks from ketones with preservation of the absolute configuration of the substrate<sup>[19]</sup>. With conventional chemical methods the ketone is oxidized using harmful peracids (Scheme 2), but without high enantio-, regio- or chemoselectivity. These drawbacks can be overcome enzymatically applying Baeyer-Villiger monooxygenases (BVMO), which catalyze the reaction between oxygen and carbon (Scheme 2)<sup>[20]</sup>. This is performed with a flavin redox-cofactor, which is either flavin adenine dinucleotide (FAD) or flavin mononucleotide (FMN). The reduced flavin can react slowly with molecular oxygen due to stabilization in the BVMOs active site by formation of a flavin semiquinone. Thus, a covalent adduct, the reactive C4a-peroxyflavin, is formed, which occurs in an equilibrium with hydroperoxyflavin. During BVMO catalysis a nucleophilic oxygenation is then performed introducing an oxygen atom into the substrate. Then, water is released from the resulting hydroxyflavin thus, regenerating the oxidized flavin. Reduced flavin is formed through the reaction with reduced nicotinamides, which are consumed throughout the reaction.

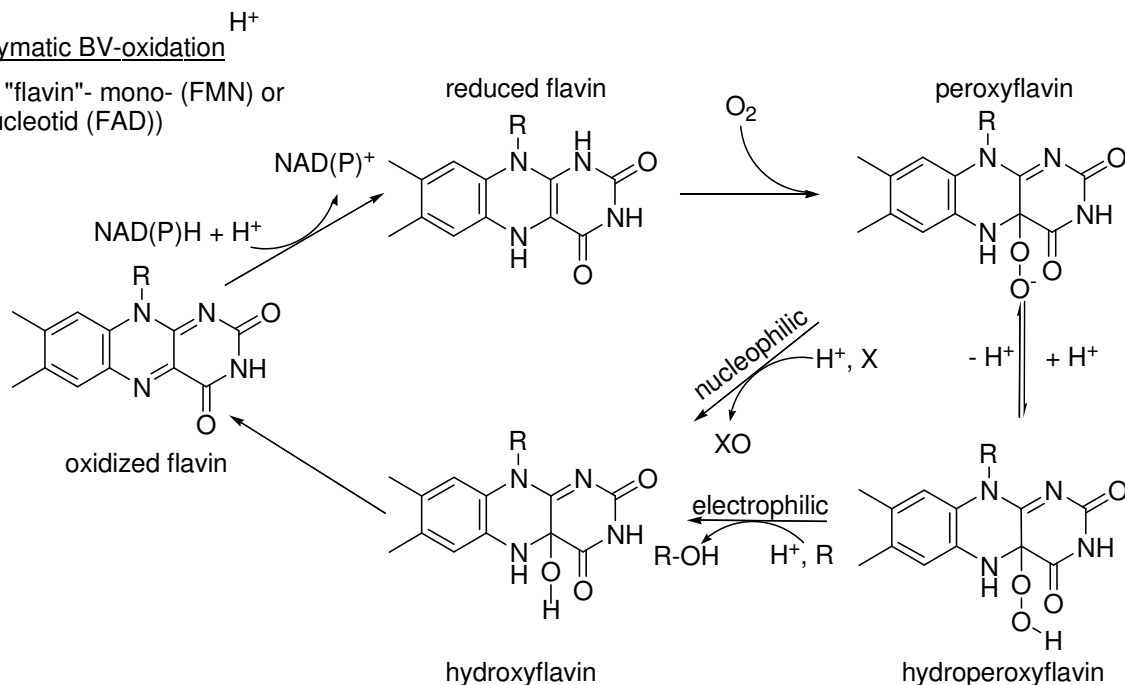
## Background

### chemical BV-oxidation



### enzymatic BV-oxidation

(R= "flavin"- mono- (FMN) or dinucleotid (FAD))



Scheme 2: Chemical and enzymatic BV-oxidation. The type of (hydro-)peroxyflavin performing the oxygenation is dependent on the enzyme environment.

In the fungi *Proactinomyces erythropolis* the first enzymatic BV-oxidation was found in 1948 in the cleavage of the A-ring of steroids to ketoacids. BVMOs are often involved in degradation pathways of various natural compounds, thus enabling the growth of microorganism on these sources. Several BVMOs were identified and cloned, whereby the best-characterized example is the cyclohexanone monooxygenase from *Acinetobacter calcoaceticus* (CHMO) which converts cyclohexanone (CHO) to  $\epsilon$ -caprolactone ( $\epsilon$ -CL) with high catalytic activity<sup>[21]</sup>. A few examples also report about BVMOs involved in the catabolic metabolism (synthesis of sesquiterpenoid, antibiotic pentalenolactone D and neopentalenolactone D in *Streptomyces* sp. or cytochalasin E in the eukaryote *Aspergillus clavatus*)<sup>[22]</sup>.

Since 2009 structures of phenylacetone monooxygenase from *Thermobifida fusca* (PAMO) and CHMO enabled a better understanding of the structural mechanism during BVMO catalysis by showing the enzyme in its reduced and oxidized form with bound FAD/NADP(H)<sup>[23]</sup>. The NADPH is coordinated near the flavins N5-atom and after hydride donation it slides over the flavin to stabilize the peroxide. Then the crucial residue R337 (for PAMO) interacts with the negatively charged reduced flavin, making it accessible for oxygen. After the flavin (hydro)peroxide is formed, it shifts back because of the missing negative charge. Thus, the active site becomes accessible for the substrate, which can be subsequently oxidized by the flavin (hydro)peroxide.

According to Van Berkel *et al.* BVMOs belong to the subclasses B and C of flavin-dependent monooxygenases<sup>[24]</sup>. The subclass B contains the bifunctional Type I BVMOs, because they combine the reductive and oxidative half-reaction in one polypeptide chain by using NADPH and FAD. In contrast, monofunctional Type II BVMOs belongs to the subclass C, because they are multicomponent monooxygenases dependent on NADH and FMN. Here, the oxidation is performed by the oxygenase subunit, whereas a second protein (usually a reductase) reduces the oxidized flavin.

Recombinantly available Type I BVMO were mainly isolated from prokaryotic sources, until Leipold *et al.* reported the expression of the cycloalkanone monooxygenase (CAMO) cloned by CODEHOP-PCR from the ascomycete

## Background

*Cylindrocapsa radicola* in 2011<sup>[25]</sup>. This enzyme represented the first eukaryotic Type I BVMO, which was recombinantly produced in *E. coli*. Interestingly, the CAMO showed high activity for cyclobutanones, but did not accept steroids as substrates. Since *C. radicola* was reported to convert progesterone, further BVMOs active for steroids must be encoded in the genome of this fungus.

Typically, new Type I BVMOs are found by searching for unique motifs in sequence databases, like the fingerprint motif FXGXXXHXXXW[P/D] or the N-terminal Rossmann-fold motif GXGXXG.<sup>[26]</sup> The phenylacetone monooxygenase (PAMO) from *Thermobifida fusca* was found using the fingerprint motif and until now it represents the only thermostable BVMO with an available crystal structure<sup>[27]</sup>.

In contrast, Type II BVMOs lack these motifs and only a few are known, as e.g. the luciferases from *Photobacterium phosphoreum* NCIMB 844 and from *Vibrio fischeri* ATCC 7744 or the 2,5-diketocamphane-1,5-monooxygenase (2,5-DKCMO) and the 3,6-diketocamphane-1,6-monooxygenase (3,6-DKCMO) *Pseudomonas putida* ATCC 17453<sup>[28]</sup>. These enzymes are of special interest for industrial application as they use the much cheaper cofactor NADH to reduce the flavin.

The application of BVMOs is addressed in several reviews, which showed the synthetic utility of these enzymes leading to valuable compounds for drug production and organic synthesis<sup>[1, 29]</sup>. Even not expected products from a typical BV-oxidation can be achieved as for example the access to  $\beta$ -amino acids as well as  $\beta$ -amino alcohols after hydrolysis of the produced normal and abnormal esters<sup>[30]</sup>. Furthermore the applicability for the oxygenation of heteroatoms like sulfur, nitrogen, phosphorus, boron and selenium was shown. For instance valuable selenium containing compounds, which are highly interesting for organic synthesis were produced using a PAMO mutant<sup>[31]</sup>. Another important example is the industrial application of a BVMO engineered by the company Codexis Inc. for the production of the drug Esomeprazole by sulfoxidation (Codexis, WO/2011/071982).

The performance of BVMOs for organic synthesis is approved by many examples, but still there are several major drawbacks considering their application on industrial scale. Many of the available BVMOs show low stability in organic solvents and only low substrate/product concentrations are tolerated. Furthermore oxygen must be available in stoichiometric amounts, which therefore needs to be supplied continuously when using higher substrate concentrations. Immobilization can often overcome the stability issues and was therefore applied for the CHMO and PAMO. Until now, these studies did not reveal that any effective attachment to a support yield in a suitable catalyst for industrial application was achieved. The most promising results were obtained by encapsulation of the CHMO in a polyacryl-amide gel or a PAMO fusion enzyme in peroxisomes<sup>[32]</sup>. The use of encapsulated *E. coli* whole cells containing a BVMO in polyelectrolyte complex capsules was also shown to be promising, but the encapsulated cells showed a five times decrease of the initial BV-activity<sup>[33]</sup>. This effect might be explained by the additional diffusion barrier caused by the encapsulation and cell walls. The application of whole cells profits from the main advantage that the supply of the required cofactor NAD(P)H is produced by the cell metabolism. Using isolated enzymes the expensive cofactor must be supplied and thus an effective recycling system had to be used. Regarding the cofactor recycling for BVMOs several dehydrogenase-depending systems were applied, were glucose-dehydrogenase, glucose-6-phosphate-dehydrogenase (G6PDH) or sodium phosphite dehydrogenase (PTDH) turned out to be the best enzymes so far<sup>[34]</sup>. The cofactor regenerating reaction serves the BVMO, but requires an additional substrate. A major contribution was the design of fusion BVMOs genetically linked to PTDH, which seemed to be a promising catalysts for application in organic synthesis<sup>[35]</sup>. Application of additional cofactor recycling enzymes is a good example, why scientist try to establish biocatalytic routes using a combination of several enzymatic steps. A cheap starting material is thus converted to the final product without accumulation of intermediates.

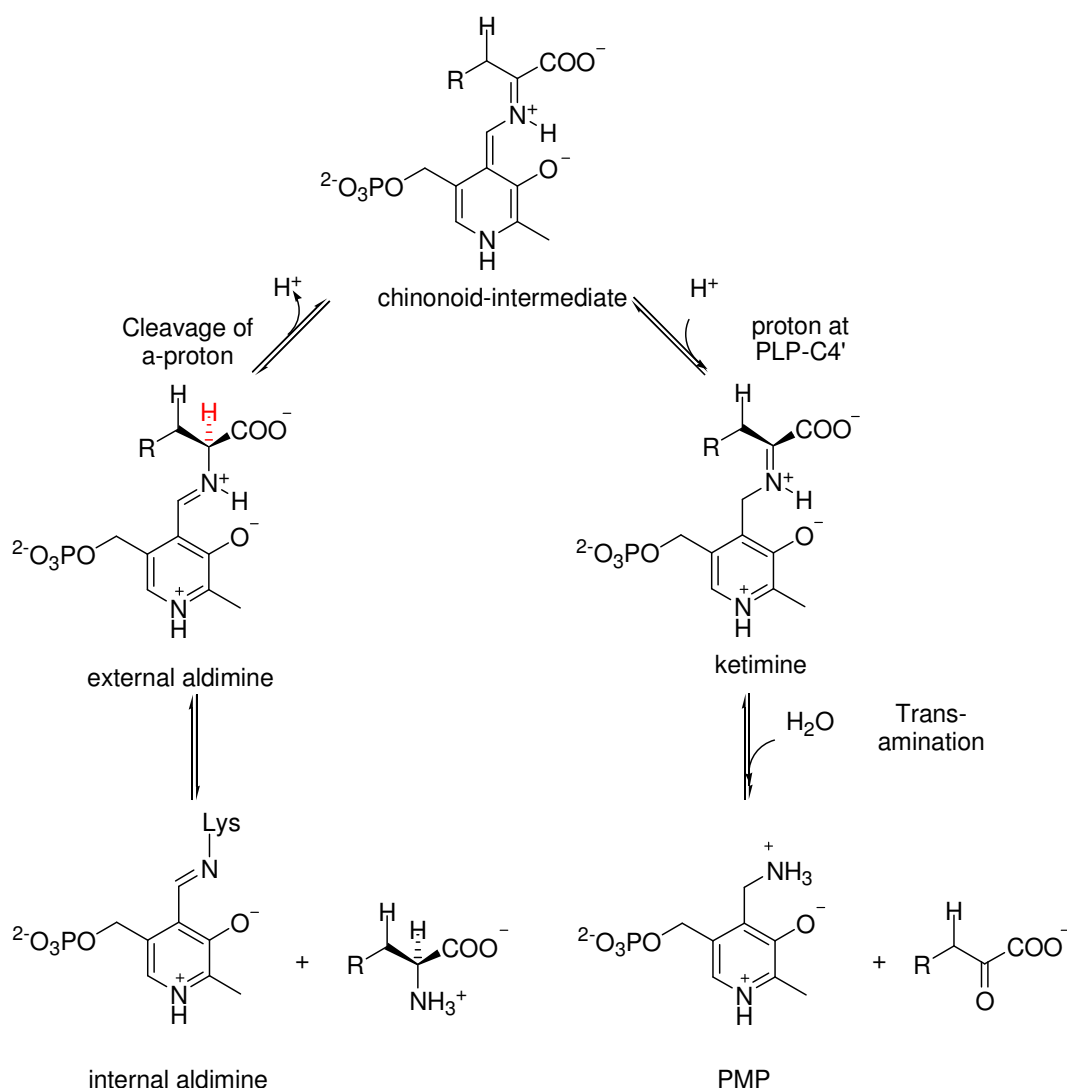
Nowadays  $\epsilon$ -CL is an important precursor for the biodegradable thermoplastic poly- $\epsilon$ -CL and is produced chemically by BV-oxidation of CHO with peracetic acid with annual amounts between 40000 to 60000 tons<sup>[36]</sup>. In the chemical reaction the peroxy-group of peracetic acids performs a nucleophilic attack on the carbonyl group of CHO and acetic acid is released by the formation of the lactone or ester<sup>[37]</sup>. To apply a new biocatalytic route to  $\epsilon$ -CL and simultaneously address the problem of cofactor regeneration, the direct enzymatic double oxidation of cyclohexanol (CHL) to  $\epsilon$ -CL using an internal cofactor recycling seemed attractive. The "closed-loop" reaction involving BVMOs was first described

## Background

by Willets *et al.*, using an isolated dehydrogenase from *Thermoanaerobium Brockii* in combination with CHMO for the conversion of bicyclic alcohols to their corresponding lactones<sup>[38]</sup>.

### 1.3 Immobilization of Transaminases

In recent years amine transaminases (ATA) became interesting especially for the pharmaceutical industry, as they were often found in building block for drugs. The application of ATA in asymmetric syntheses of chiral amines has been investigated thoroughly<sup>[39]</sup>. These reactions interconvert a preferably cheap amino donor and prostereogenic ketones the 'amino acceptors' into a keto product and the desired chiral amine. It is performed by reactions within the enzymes at the cofactor pyridoxal-5'-phosphate (PLP, Scheme 3)<sup>[40]</sup>. First, the nitrogen of the amino donor is transferred to the enzyme bound cofactor, the 'internal aldimine' forming pyridoxamine-5'-phosphate (PMP) and the keto product. The nitrogen group is then further transferred to the amino acceptor and the product amine is released by the regeneration of the internal aldimine.

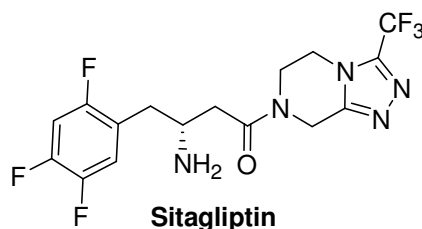


Scheme 3: Mechanism of the transaminase reaction.

The transamination is of special interest for the production of API's (in this case chiral amines) which are found in several pharmacological applied drugs<sup>[41]</sup>. The biocatalytic route to optically pure amines represents an alternative to

## Background

classical transition metal catalysis and shows several advantages, which made their application attractive for pharmaceutical companies<sup>[39, 42]</sup>. Biocatalytic reactions can be run in aqueous media at mild conditions, whereas most classical chemical alternatives are run at harsh conditions like high temperature, involving toxic transition metal catalysts and organic solvents. Applying transaminases for amine synthesis could therefore reduce the waste, reach higher product purity and due to their high regio-selectivity, avoid protection steps. This was shown by the companies Merck & Co. and Codexis Inc. for the manufacturing of sitagliptin, a drug for the treatment of *Diabetes mellitus* Type II (Scheme 4). The chemical reaction based on rhodium-catalyzed sitagliptin production was replaced by a biocatalytic route using an engineered ATA, which reduced the total waste by 19 %, increased the total yield by 13 % and the productivity by 53 %<sup>[43]</sup>. In further investigations this engineered ATA was immobilized on Sepabeads®, a highly hydrophobic octadecyl functionalized poly methacrylate carrier, which additionally increased process productivity. This simplified the product purification and enabled a reuse of the biocatalyst<sup>[44]</sup>. Moreover, the immobilized ATA could be applied in isopropylacetate (IPAc) wherein the free ATA was completely inactive. Immobilization often stabilizes biocatalysts, allows for long-term operations and simplifies the overall downstream processing if applied in heterogeneous reactions<sup>[5, 45]</sup>. Especially for process development the immobilization of biocatalysts widens the spectrum of their applications, as e.g. continuous or fixed-bed operations are not possible with free enzymes. Therefore immobilization of enzymes is an important part of the biocatalytic cycle because it is usually required for economical industrial application. The mode of an enzyme's attachment (adsorptive or covalent) is depending on the functional groups of the carrier and the protein's surface thus requiring a screening for the best enzyme/support combination. Unfortunately general and reliable predictions of favorable combinations are not yet possible<sup>[46]</sup>.



Scheme 4: Chemical structure of Sitagliptin, a drug for the treatment of *Diabetes mellitus* Type II. Merck & Co. and Codexis Inc. replaced the final chemical step for the manufacturing of this compound by a biocatalytic process utilizing an engineered transaminase.

In this thesis the immobilization of (*R*)- and (*S*)-selective transaminases on chitosan support was investigated to improve their applicability in biotechnology processes. For transaminases several immobilization approaches have been reported, where chitosan has shown to be a promising support for this enzyme class<sup>[44, 47]</sup>. Chitosan is well known for offering a variety of possibilities for enzyme immobilization, because of its free hydroxyl- and one amino group (Scheme 5c)<sup>[48]</sup>. Because of its high hydrophilicity it is suitable for adsorptive attachment and due to its solubility in acids and bases it can be applied for cell flocculation<sup>[47f, 47g]</sup>. Furthermore the free amino group can be linked by e.g. glutaraldehyde (GA) to the  $\epsilon$ -amino group of lysine residues of an enzyme under neutral conditions (Scheme 5c)<sup>[49]</sup>. When covalently linked to the carrier, no leaching of the immobilized catalyst will occur during the reaction.

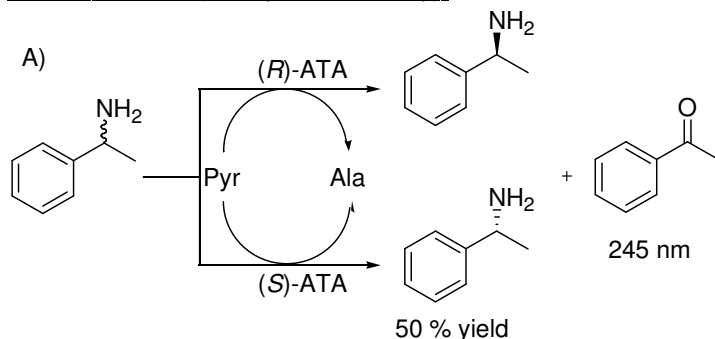
In 2010 a pool of 17 (*R*)-ATAs was discovered by a sequence-function relation based search algorithm in a database of 5000 related sequences<sup>[50]</sup>. Seven of these proved to be particularly interesting for the asymmetric synthesis of twelve (*R*)-amines<sup>[51]</sup>. Among these, especially GibZea from *Gibberella zeae*, NeoFis from *Neosartorya fischeri* and AspFum from *Aspergillus fumigatus* showed high activity towards the model substrate (*R*)-1-phenylethylamine (Scheme 5A). These enzymes could be expressed with good yields and no immobilization study for these biocatalysts had been reported. Good conversions in asymmetric amine synthesis mode (Scheme 5B) were obtained with NeoFis and AspFum while the highly active GibZea only displayed a modest stability thereby resulting in relatively low conversions. Recently, the crystal structure of AspFum was solved thus allowing for a better understanding of the immobilization on a molecular level<sup>[52]</sup>. These (*R*)-selective ATAs belong to the PLP-fold type IV according to Jansonius<sup>[53]</sup>. In contrast (*S*)-ATAs belong to the fold type I, where the (*S*)-ATAs 3HMU from *Ruegeria pomeroyi* and 3I5T from *Rhodobacter sphaeroides* 2.4.1 were immobilized<sup>[53]</sup>. For both no immobilization was described elsewhere and they displayed reasonable activity



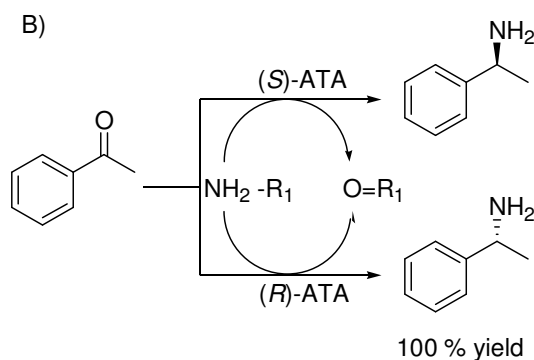
## Background

against (S)-1-phenylethylamine. Both (S)-ATAs were found by revealing of crystal structures in the cluster of ornithine-aminotransferase (OAT)-like proteins annotated with unknown activity<sup>[54]</sup>.

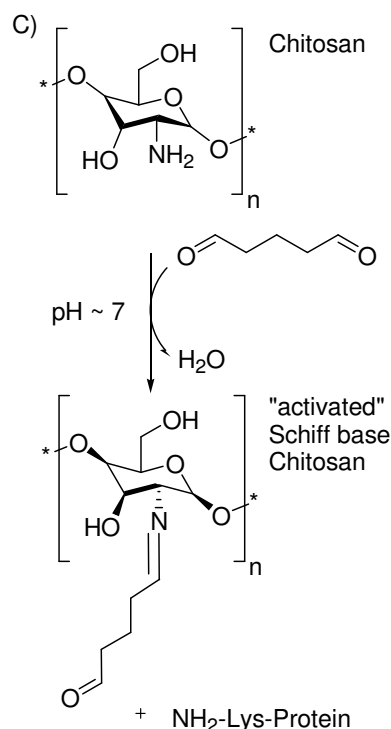
kinetic resolution (acetophenone assay):



asymmetric synthesis:



Glutaraldehyde activation:



Scheme 5: Reaction catalyzed by (R)- or (S)-selective aminotransferases (A and B). (C) Chitosan activation by glutaraldehyde for covalent enzyme attachment via Schiff base.

## 1.4 Bioreactors

To apply a biotechnological process, a suitable reactor concept is necessary for immobilized enzymes to achieve high and cost effective production<sup>[5, 45a, 46b, 55]</sup>. Established systems use immobilized catalysts in a packed column in a continuous flow process. These fixed-bed reactors (FBR) are for example used in the lipase-catalyzed large scale production of chiral amines or esters for the cosmetic industry<sup>[56]</sup>. The simple stirred tank reactor is a batch reactor with a mostly attached overhead stirrer to ensure mixing of the solution. Therefore it is more flexible usually, but mechanical forces can lead to destruction of the catalyst. With respect to downstream processing and reusability of the biocatalyst, the filtration process is rather laborious and challenging for enzymes immobilized on small particle supports. FBRs can circumvent these problems, but here other disadvantages depending on the length, diameter, and particle size in the reactor occur. High/low flow rates, the pressure drop within the column, reactant- and pH-gradients as well as deactivation of the biocatalyst after long-term use (e.g. by accumulation of reaction compounds) are problematic and need to be overcome to enable a process. Another major disadvantage appears in gas-dependent reactions, which are difficult to adjust since the columns need to be air-free. The rotating flow cell reactor (SpinChem S6530 reactor, Nordic ChemQuest AB, SCR) was shown in **Article VI** to provide an alternative concept for the application of immobilized biocatalysts. Herein, mixing and efficient liquid flow through the packed catalyst are achieved simultaneously by a rotating device bearing specially designed hollows (Figure 3). The immobilized enzymes are fixed within a chamber, which then provides mixing of the liquid by rotation. The reaction solution is sucked from top and bottom into the middle of the compartment and thereby passes through the catalysts within the SCR walls by centrifugal forces. This enables an optimized mass-transfer and the catalyst is not exposed to mechanical forces compared to conventional stirring.

## Background

Besides these advantages, the downstream processing is simplified and thus the reuse of the catalyst. The first systems describing a related design are the basket reactors developed by Carberry and Mahoney in the 1960s and 1970s<sup>[57]</sup>. Here four baskets are rotating within the gas/ solid reaction. The SCR can thus be regarded as an evolution of the basket reactor as the special design enables a greater mixing of the reaction solution and flexibility.

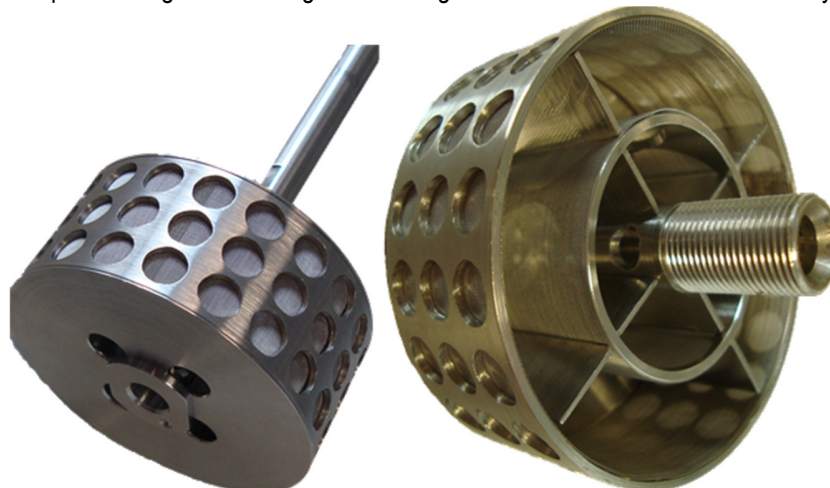


Figure 3: The rotating flow cell SpinChem S6530 (Nordic Chemquest AB).

## 2 Biocatalysts Design and Coupling of Enzymatic Steps

### 2.1 Protein Engineering of a Polyol-dehydrogenase from *Deinococcus geothermalis* DSM 11300 (Article II)

Within this work a polyol dehydrogenase from *Rhodobacter sphaeroides* DSM 158 (PDH-158) and one from *Deinococcus geothermalis* 11300 (PDH-11300) were cloned and investigated. The study included characterization of the enzymes and an extensive protein engineering, which was performed with respect to substrate scope, thermostability and cofactor dependency.

A highly homologous enzyme to the PDH-158 was the galactitol dehydrogenase from *Rhodobacter sphaeroides* D (PDH-D). For this enzyme a crystal structure (pdb-code: 2WDZ) was resolved, which could be used for homology modeling and structural analysis of the PDH-158. During analysis of the B-factors of PDH-D a flexible loop (E195-R203, EMTLKM<sup>R</sup>ER) next to the active site was identified (Figure 4). Since Carius *et al.* described it as a “flexible substrate binding loop”, we decided to build a chimeric enzyme by transferring this loop into the scaffold of the more thermostable PDH-11300<sup>[17a]</sup>. Using sequence alignments the corresponding loop in the PDH-11300 (P196-T204, PLTRRGLET) was identified and exchanged by overlap-extension PCR<sup>[58]</sup>, which resulted in a construct of PDH-11300 possessing the loop of PDH-158 (PDH-loop).

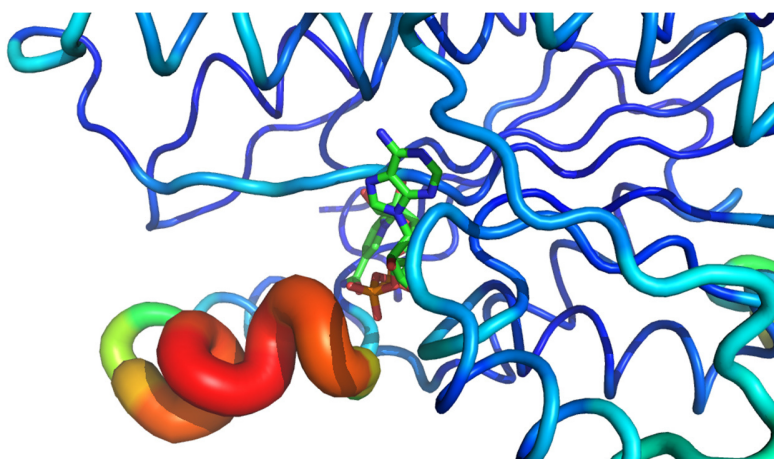


Figure 4: Shown is the loop (EMTLKM<sup>R</sup>ER) displaying high B-values (red color displays the highest and light blue color the lowest B-factor) next to the active site of galactitol dehydrogenase with the bound cofactor NAD<sup>+</sup> *Rhodobacter sphaeroides* D (pdb: monomer 2WZD).

Recombinant expression in *E. coli* BL21 (DE 3) revealed a good yield of PDH-158, PDH-11300 and PDH-loop. Purification was performed by using a N-terminal His<sub>6</sub>-tag, thus facilitating a thorough characterization of the pure enzymes. The pH-profile was examined and PDH-11300 and PDH-loop showed their highest activity at 45°C, which resembles the optimal growth temperature of *D. geothermalis* 11300. The stability was investigated by incubation of the enzymes for 6 h at certain temperatures. This revealed that PDH-158 was unstable at only 30°C, whereas PDH-11300 was stable up to 40°C (Figure 5a-b). A rather unexpected finding was the high stability of the PDH-loop variant at 50°C (Figure 5c), because it contained the flexible loop of the non-thermostable PDH-158 (merely stable for 6 h at 25°C).

## Biocatalyst Design and Coupling of Enzymatic Steps

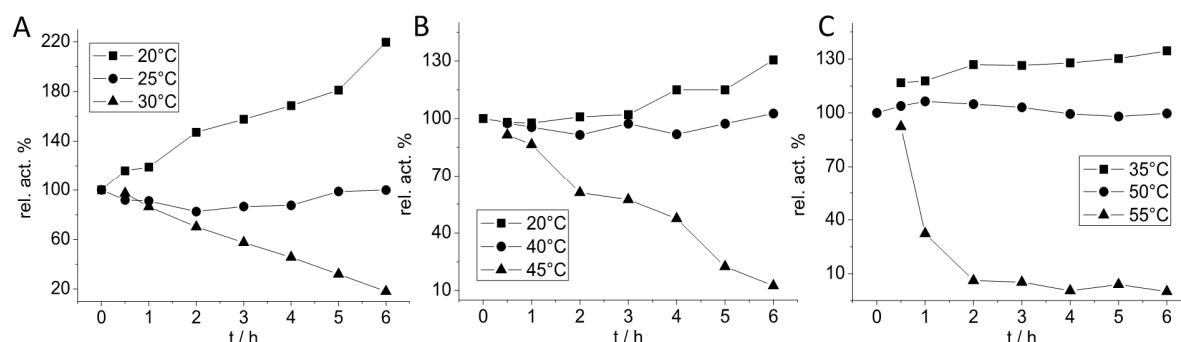


Figure 5: Stability of PDH-158 (A), PDH-11300 (B) and PDH-loop (C) after incubation up to 6 h at the given temperatures. Each measurement point corresponds to the initial activity determined spectrophotometrically at 340 nm and 30°C after the incubation period.

We confirmed this finding by determination of  $T_{50}^{60}$ , which is the temperature where 50% of the initial activity remains after one hour of incubation and the melting point ( $T_m$ ) by circular dichroism spectroscopy. As the PDH-11300 showed a  $T_{50}^{60}$  of 48.3°C and a  $T_m$  of 48.4 our initial finding was approved as the loop chimera showed an increased  $T_{50}^{60}$  of +7°C and an increased  $T_m$  of + 5.2°C. Stabilization of enzymes is reported as a gain of rigidity or as stabilization by substitution of flexible residues. A possible explanation for the increased thermostability of PDH-loop of +10°C compared to the wildtype might be that the original loop from PDH-11300 was much more flexible than the one from PDH-158, but that seems unlikely because theoretically the loop in the less stable PDH-158 should be more flexible. An enhancement of subunit interaction could also be a reason for multimeric enzyme-stabilization but the loop regions were not located at the multimerization interfaces<sup>[59]</sup>. Therefore no additional H-bonds or hydrophobic interactions were introduced, but longer ranging conformational changes due interactions or repulsions between residues inside the subunits might be possible. To the best of our knowledge, the PDH-loop is the first example for the stabilization of an enzyme by introduction of a loop from a less into a more stable enzyme.

Furthermore, an approach for the redesigning of the active site of the *D. geothermalis* enzyme was conducted by alignment of PDH-158 and PDH-11300 to identify possible hot spots involved in determining activity. Four differing amino acids were found and the amino acids from PDH-158 were introduced into the scaffold of PDH-loop (V97A, N99L, Q157A and N161M). The loop mutant was chosen as template as it showed a higher stability and therefore increased tolerance against destabilizing mutations. Five mutants were constructed, expressed and the  $T_m$  examined (Table 1). For all mutants the  $T_m$  was higher or equal compared to the  $T_m$  of the wildtype, showing that none of the mutations destabilized the enzyme.

Table 1:  $T_m$  and  $T_{50}^{60}$  values of wildtype and mutated polyol dehydrogenases.

PDH (variant)	$T_m$ [°C]	$T_{50}^{60}$ [°C]
158	43.2 ± 1.0	35.6 ± 0.4
11300	48.4 ± 0.5	48.3 ± 0.3
loop	53.6 ± 0.2	55.3 ± 0.2
loopD55N	65.5 ± 1.0	56.1 ± 0.2
loopQ157A	52.9 ± 0.2	n.d.
loopN99L	56.9 ± 0.3	n.d.
loopV97A/N99L	53.8 ± 0.3	n.d.
loopV97A/N99L/Q157A	48.5 ± 0.3	n.d.
loopV97A/N99L/Q157A/N161M	48.8 ± 0.4	n.d.

The investigated polyol dehydrogenases are restricted to the use of the cofactor  $NAD^+$ , so in our next protein engineering approach we targeted the cofactor dependency of the PDH-loop variant. An acceptance of the cofactor

## Biocatalyst Design and Coupling of Enzymatic Steps

NADP<sup>+</sup> would enable the application in reactions where a cofactor regeneration of NADP(H) is necessary (e.g. when a BVMO is used). Computational analysis revealed that, after substitution of the NAD<sup>+</sup> C2 hydroxyl-group with the phosphate group and two consecutive energy minimizations, the NADP<sup>+</sup> moved out of the binding pocket. Fan *et al.* showed for horse liver dehydrogenase that the crucial residue was an aspartate, probably due to the repulsion of the negatively charged phosphate groups<sup>[60]</sup>. As an aspartate at position 55 pointing towards the ribose C2 hydroxyl group of the NAD<sup>+</sup> moiety could be identified in the homology model of PDH-loop this residue was further investigated (Figure 6). *In silico* MD analysis revealed by creating mutant D55N, the NADP<sup>+</sup> was found well orientated in the binding cleft by coordination between the amide groups of N57 and D55N and the backbone of the amino acids Q34, L56 and N57 (Figure 6).

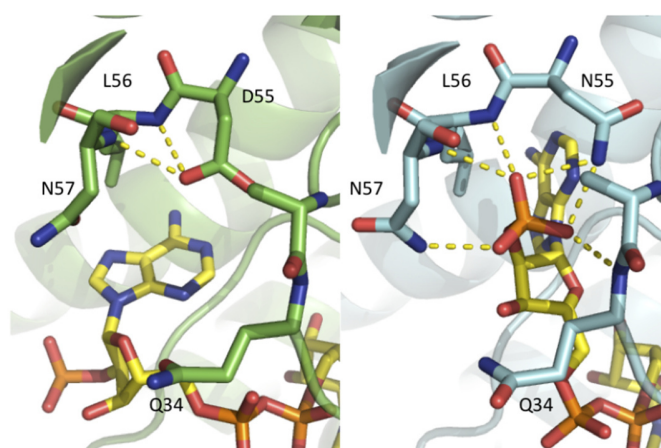


Figure 6: Simulation of positioning of NADP<sup>+</sup> in the PDH-loop variant cofactor binding cleft (left) and the cofactor bound to the mutant PDH-loopD55N (right).

As PDH-11300 and PDH-loop showed no activity with NADP<sup>+</sup> and a  $K_m$  for NAD<sup>+</sup> of 150  $\mu$ M, it could be assumed that the introduction of the loop did not influence the cofactor binding. Nevertheless, for PDH-loop an increased turnover of 68% could be observed. However, the mutant PDH-loopD55N, which was predicted by rational design, was proved to be active with NAD<sup>+</sup> and NADP<sup>+</sup> with  $K_m$  of 440  $\mu$ M and 410  $\mu$ M respectively. Anyway, the  $k_{cat}$  were comparable to PDH-11300 and the mutation did not affect the  $T_{50}$ <sup>[60]</sup> (Table 1). A minor drawback of the PDH-loopD55N was the poor expression of this mutant. This was addressed in **Article III**, which reports about the application of this PDH variant in combination with a BVMO.

Having nine PDH-variants at hand, an extensive substrate profiling was performed to gain more information about the substrate specificity and the residues involved therein (Table 2). Regarding the activity of the wildtype enzymes PDH-158 and PDH-11300 a clear preference for 1,2-diols with increasing activity for longer carbon chains and the oxidation at the secondary hydroxyl group was observed. For PDH-158 the best substrate was 1,2-hexandiol (11298 mU/ mg) whereas it was only the second best for PDH-11300. Here, xylitol was found to be the best substrate (4659 mU/ mg). Interestingly for PDH-158, galactitol was found to be a worse substrate (263 mU/ mg) although the highly homologous PDH-D was annotated as a galactitol dehydrogenase. In contrast, PDH-11300 showed much higher activity towards galactitol of 1427 mU/ mg, which was its third best substrate. PDH-loop revealed a changed substrate scope compared to its wildtype and concerning the order of substrates that were preferred, it resembled more the PDH-158 than the PDH-11300. When analyzing the substrate scope of the active site mutants N99L, Q157A, V97A/N99L, V97A/N99L/Q157A and V97A/N99L/Q157A/N161M, it could be shown that the residues Q157 and N161 seem to be involved in catalysis of 1,2-diol-dehydrogenation because variants bearing mutations at this positions exhibited decreased activities. Mutations at V97 and N99 did not drastically affect the activity and could thus be targets for engineering the substrate-binding pocket by CASTing or ISM.

# Biocatalyst Design and Coupling of Enzymatic Steps

Table 2: Substrate oxidation scope of PDH wild-types and mutants determined with 0.5 mM NAD<sup>+</sup> in bicine-buffer (pH 9.0; 100 mM). For mutant PDH-loopD55N NADP<sup>+</sup> was used. The numbers denote activities in mU/ mg.

Substrate	158	11300	loop	loopD55N	N-L <sup>a</sup>	Q-A <sup>a</sup>	2x <sup>a</sup>	3x <sup>a</sup>	4x <sup>a</sup>
1-Butanol	20	49	35	17	89	95	58	15	85
1-Methoxy-2-propanol	72	63	75	72	108	101	130	25	102
1-Phenylethanol	217	485	360	421	379	231	366	154	140
1-Propanol	23	47	43	20	81	89	82	14	79
1,2-Butanediol	3250	1013	1491	1447	901	194	736	90	95
1,2-Hexanediol	11298	2742	1960	2265	1583	389	2665	423	246
1,2-Propanediol	1028	311	403	325	405	118	323	44	110
1,3-Butanediol	146	182	74	87	166	141	141	54	127
1,3-Dihydroxyacetone	180	324	130	323	176	185	272	85	199
1,3-Propanediol	15	38	20	52	97	114	93	10	94
2-Butanol	460	303	605	349	473	456	540	367	186
2-Ethyl-1,3-Hexanediol	47	120	60	21	119	127	99	25	80
2-Methyl-1-propanol	39	120	221	50	218	153	212	65	49
2-Propanol	341	142	195	88	206	159	213	112	66
2,3-Butanediol	998	664	1218	1326	1052	338	1014	210	89
3-Methyl-1-butanol	44	136	35	75	118	130	100	26	81
Cyclohexanol	305	654	1021	2076	1005	626	714	337	232
Cyclopentanol	500	383	466	207	464	427	576	343	234
Ethanol	37	55	23	53	89	131	66	17	56
Ethanolamine	30	23	23	23	86	91	61	7	54
Galactitol	263	1427	508	213	206	95	172	2	61
Glycerinaldehyde	75	72	86	44	116	104	137	28	128
Glycerol	698	145	193	98	156	109	111	23	54
Hydroxyacetone	56	100	43	50	120	145	89	26	57
Sorbitol	72	936	763	400	230	102	166	19	73
Thioglycerin	221	782	1036	1459	276	147	239	40	71
Xylitol	6651	4659	1521	1435	1096	128	1722	40	60

<sup>a</sup>Mutants from PDH-loop including following mutations N-L= N99L, Q-A= Q157A, 2x= V97A/N99L, 3x= V97A/N99L/Q157A, 4x= V97A/N99L/Q157A/N161M.

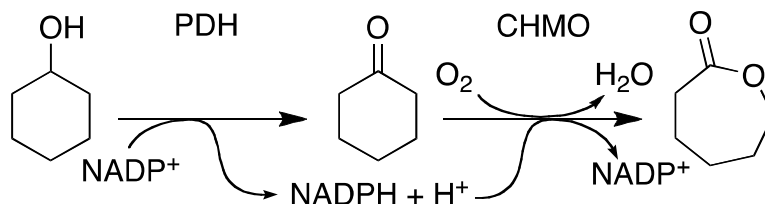
The mutant PDH-loopD55N, which revealed an altered cofactor-specificity/preference showed a remarkably increased activity towards cyclohexanol (CHL) of 2076 mU/ mg using NADP<sup>+</sup> as a cofactor, but at the same time no decreased thermo-tolerance (Table 1). This result led to the follow up study described in **Article III**, wherein an application of the mutant in combination with an enzymatic BV-oxidation was investigated.

## 2.2 Biocatalytic Route from Cyclohexanol to $\epsilon$ -Caprolactone (Article III)

The extensive protein engineering of the PDH-11300 at multiple positions led to the mutant PDH-loopD55N (**Article II**), which enabled an application of this catalyst in a cascade reaction with a BVMO. The mutant exhibited a good activity for the oxidation of cyclohexanol (CHL) to cyclohexanone (CHO) by simultaneously reducing NADP<sup>+</sup> to NADP(H).

## Biocatalyst Design and Coupling of Enzymatic Steps

Therefore a self-sufficient biocatalytic route from CHL to  $\epsilon$ -caprolactone ( $\epsilon$ -CL) via CHO was established by combination of PDH-loopD55N with the NADPH-consuming CHMO (Scheme 6).



Scheme 6: Double oxidation of cyclohexanol with the cofactor  $\text{NADP}^+$  catalyzed by the polyol-dehydrogenase (PDH) in combination with a Baeyer-Villiger monooxygenase (CHMO) in a "closed-loop" recycling of  $\text{NADP(H)}$ .

Since in **Article II** the poor expression of PDH-loopD55N was found as a major disadvantage, the first goal in this study was to optimize the overexpression of the mutant in *E. coli*, but even at lower expression temperatures a large insoluble fraction was found. Therefore, to support correct folding, coexpression of several plasmids encoding chaperones GroEI-GroES, dnaK-dnaJ-grpE, and tig in certain combinations (pGro7, pGKJE8, pKJE7, pGTF2 and pTF16 from TaKaRa chaperone plasmid set #3340), different *E. coli* strains (BL21 (DE3), C41 (DE3) and Shuffle (DE3)) were investigated. By comparison of the plasmids encoding the different chaperones using the strain *E. coli* BL21 (DE3), it was found that the pGro7 plasmid (bearing only the chaperones groES-groEL) showed the highest formation of soluble protein. Consequently, the mentioned expression strains were used with the pGro7 plasmid, which gave a final yield of 1592 U/ L culture broth (activity towards xylitol) of the mutant PDH-loopD55N in the strain *E. coli* C41 (DE3). Thus, the overall yield of soluble enzyme could be increased 4.9 times compared to the initial expression in *E. coli* BL21 (DE3) without additional chaperones.

After a good expression system for PDH-loopD55N was established, biocatalysis was performed using purified PDH-loopD55N and CHMO and a mixture (0.3 mM each) of the reduced and oxidized cofactor  $\text{NADP(H)}$ . Enzyme amounts of 0.5 U/ ml led to a conversion of 84 and 80 % (5 mM and 10 mM CHL, respectively) after 2 h based on the detection of  $\epsilon$ -CL. After 4 h the conversion only slightly increased, because 95 % of the CHL was already consumed after 2 h. This demonstrated that both enzymes worked in combination, because otherwise only  $\epsilon$ -CL concentrations corresponding to the initial  $\text{NADPH}$ -concentration of 0.3 mM (refers to 3 % conversion at 10 mM CHL) would be detected. To determine if one of the enzymes was a bottleneck in the two-step approach, several enzyme ratios (PDH-loopD55N:CHMO= 1:1, 1:3, 3:1) were used in an one pot reaction. Enzyme concentrations five times lower compared to the initial biocatalysis-experiment were applied, to ensure that maximum conversion was not reached within 2 h. The CHMO could be identified to be the bottleneck in the reaction, because the highest conversion (84 %) was achieved when this enzyme was added in excess. In contrast, by applying a shortage of CHMO the lowest conversion (23 %) was obtained.

To identify the reason for this observation, initial activities of CHMO and PDH-loopD55N were studied by applying increasing CHL-concentrations during spectrophotometrical measurements, which was monitoring  $\text{NADP(H)}$  at 340 nm (Figure 7). For the PDH-loopD55N an increasing activity up to a CHL-concentration of 90 mM was observed, whereas the CHMO seemed to be inhibited by CHL. Already at 10 mM CHL-concentration only 30 % residual activity was observed.



## Biocatalyst Design and Coupling of Enzymatic Steps

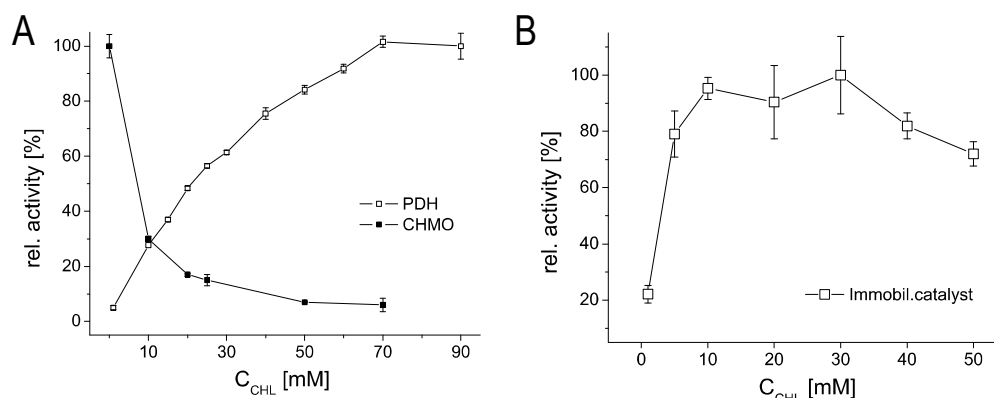


Figure 7: A) Activity of separately applied soluble CHMO or PDH-loop55N at increasing concentrations of cyclohexanol (CHL). B) Activities of the covalently co-immobilized enzymes are shown.

Due to the observed inhibition of the pure CHMO by CHL only 10 mM CHL was applied during small preparative scale biotransformations using both enzymes. After extraction with dichloromethane, followed by evaporation of the solvent, the yield was determined to be 55 %  $\epsilon$ -CL with a purity of >99 %. CHL is highly volatile and the downstream process was not optimized, which explains the low yield. These issues can easily be addressed in large scale biocatalysis.

This “proof-of-principle”-study illustrates the application of our engineered PDH-variant in a “closed-loop” reaction together with a BV-oxidation. The PDH oxidized CHL to CHO in the reversible redox interconversion, and provides the cofactor NADPH. Then the CHMO withdraws irreversible the product CHO. Therefore the reaction is driven towards the final product  $\epsilon$ -CL, which can easily be obtained in high purity by dichloromethane extraction after quantitative substrate conversion. The purified CHMO was identified to be the bottleneck in the system. Therefore, one strategy for further process optimization could be stabilization of the BVMO by protein engineering. This could involve facilitating the covalent binding of the so far only weakly attached cofactor FAD, screening for a CHMO-variant with bound FAD, like it has been shown for e.g. alditol oxidase or the berberine enzyme<sup>[61]</sup>.

Immobilization of enzymes on solid supports represents an opportunity to improve their properties and to facilitate their easy separation from the reaction media. As a strong decrease in activity was observed for the CHMO at higher CHL concentrations, a covalent co-immobilization of the purified enzymes on Relizyme™ HA403 (hexylamine functionalized poly methacrylate support) was carried out to improve stability. The identified enzyme ratio of 10:1 (CHMO:PDH) for immobilization using glutaraldehyde gave the highest  $\epsilon$ -CL formation and was thus applied in further studies. The specific activity of 500 mU/ g dry carrier for the combined approach and an immobilization yield of 28 % showed that the immobilization was successful, but could be further optimized. As assumed, the co-immobilized catalysts were significantly stabilized against higher CHL concentrations, showing nearly no loss in activity up to 40 mM (Figure 7). In contrast, a residual activity of 17 % at 20 mM CHL was detected using the free CHMO. The co-immobilized enzymes furthermore showed a faster initial conversion when performing the double oxidation of CHL compared to the free enzymes, but unfortunately the reaction stopped at 34 % conversion. This low conversion could be assigned to the CHMO, encouraged by the finding observed by using the immobilized catalysts in consecutive 1 h batch experiments by addition of dissolved CHMO or PDH. When PDH was added, no effect compared to the control (without soluble enzymes) was observed with 10 % activity in the fifth batch compared to the initial activity (Figure 8). In contrast, by addition of dissolved CHMO the decrease in activity was highly reduced with a residual activity of 53 % after the fifth batch. In terms of re-obtaining the free enzymes by filtration through a 10 kDa membrane, a residual activity of only 10 % was obtained in the second batch, which showed that no effective catalyst-recycling could be performed without immobilization.



## Biocatalyst Design and Coupling of Enzymatic Steps

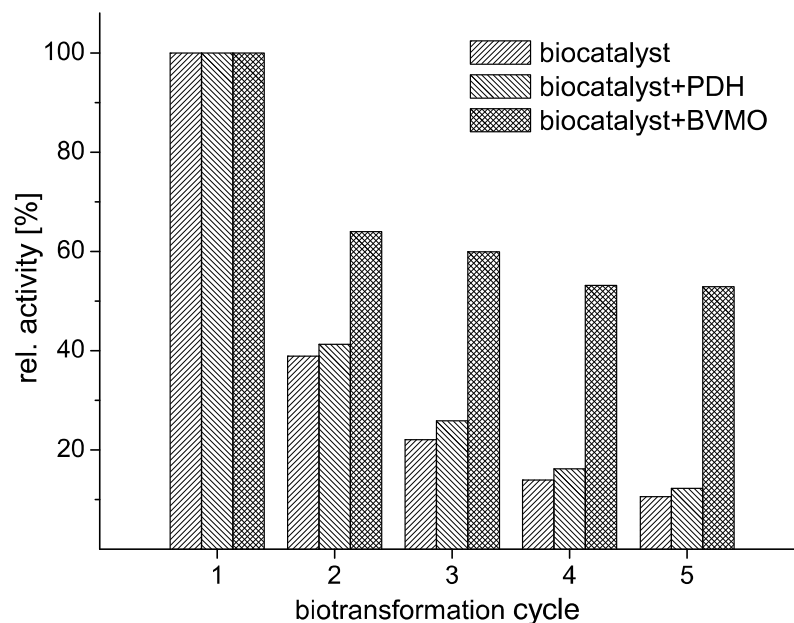


Figure 8: Recycling studies of co-immobilized enzymes (biocatalysts) compared to biocatalysis reactions with additional soluble PDH in excess (biocatalysts+PDH) and reactions with additional soluble CHMO in excess (biocatalysts+BVMO).

Through the immobilization a single catalyst containing PDH- and CHMO-activity was obtained, which can consequently be reused and applied in fixed-bed reactors or designs like the rotating flow cell investigated in **Article VI**. This example shows the impact of immobilization of enzymes to improve their properties for further process application and establishment of cost efficient biotechnological processes. In **Article IV and V** this part of the biocatalytic cycle was investigated in more detail for (*R*)- and (*S*)- amine transaminases, which were covalently immobilized on a solid chitosan support.

## 3 Immobilization of Biocatalysts

### 3.1 Support Production and Immobilization of (*R*)-Amine Transaminases on Chitosan Support (Article IV)

Within this study the opportunities for process optimization through immobilization of (*R*)- and (*S*)-amine transaminases on chitosan support have been investigated. **Article IV** describes the establishment of the protocol for chitosan support production and for the immobilization of the transaminases from *Gibberella zeae* (GibZea, (*R*)-selective) and *Neosartorya fischeri* (NeoFis, (*R*)-selective). In **Article V** the immobilization procedure described in **Article IV** is extended to the ATAs from *Aspergillus fumigatus* (AspFum, (*R*)-selective), *Ruegeria pomeroyi* (3HMU, (*S*)-selective) and *Rhodobacter sphaeroides* 2.4.1 (3I5T, (*S*)-selective). As model reaction for characterization studies, the transamination of (*R*)- or (*S*)-1-phenylethylamine ((*R*)- or (*S*)-1-PEA) to acetophenone using pyruvate as amino acceptor was applied for characterization studies. This reaction provided the advantage of spectrophotometrical determination of the formed acetophenone concentration by following the absorbance at 245 nm (Scheme 5A)<sup>[62]</sup>.

Yi et al. showed that chitosan beads were a suitable support for the (*S*)-amine transaminase from *Vibrio fluvialis* (VfTA)<sup>[47h]</sup>. Therefore, this support was chosen for our (*R*)-amine transaminases<sup>[50]</sup>. In **Article IV** GibZea and NeoFis were chosen as they displayed a high specific activity against the model substrate (*R*)-1-phenylethylamine (19.6 and 7.4 U/ mg respectively).

Two production protocols for beads were investigated, which were both based on the property of chitosan being soluble in acidic (e.g. 1 % acetic acid) and insoluble in basic solutions. In the first approach, the solubilized acidified chitosan was dropped into sodium hydroxide solution (NaOH) as Nasratun et al. reported for the immobilization of a *Candida rugosa* lipase. In the second method, described by Yi et al., a chitosan/ toluene emulsion is prepared to form the beads, which have been poured into a NaOH solution.

We adapted the described protocols by introducing a vacuum-drying step of the gel-like beads to change their physical properties. The obtained dried, solid beads showed a very low swelling behavior and were therefore more useful for application as they will not block columns or filter devices so easily like a gel-like bead. The activity of GibZea and NeoFis was 3.8- and 2.4-fold higher on beads obtained by the emulsion method compared to the dropping method. Thus this protocol was subjected to further optimization: chitosan concentrations were varied when utilizing GibZea as model enzyme, which resulted in a clear trend of increasing activity with decreasing concentration (Figure 9A). As 0.5 % is the critical chitosan concentration for bead formation, we chose to not investigate concentrations lower than 1 %. With 1 % chitosan beads a 4.1-fold increased activity compared to a concentration of 2 %. Three independently produced carrier batches of 1 % chitosan beads using the emulsion method revealed a good reproducibility with a mean activity of  $246 \pm 46$  U/ g for GibZea. Furthermore, approximately 80 % of the enzyme activity missing from the supernatant after immobilization could be retrieved on the carrier. After the production of the support was established, important properties for enzyme carriers, like pore-size distributions and specific surface areas were determined by Brunauer-Emmet-Teller (BET) measurements. For the sponge-like structure (Figure 9B) a specific surface area of  $31 \pm 0.8$  m<sup>2</sup>/ g could be calculated and around 39 % of all pores were between 20 and 80 nm in size.

## Immobilization of Biocatalysts

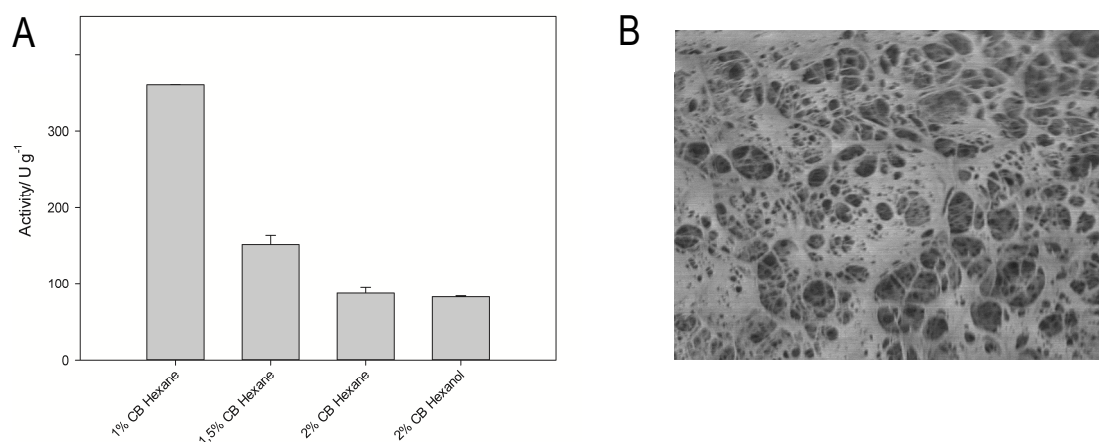


Figure 9: A) Activity of the GibZea immobilized on chitosan supports (CB) at different concentrations as determined by the acetophenone assay. B) Scanning electron microscope (SEM) picture of a chitosan bead (magnification x 4000), which shows its sponge like structure.

After the support production had been established to yield high reproducibility, the immobilization conditions were optimized. By the addition of 0.5 M sodium chloride to the *E. coli* crude extracts of GibZea and NeoFis, thereby preventing polar interactions during covalent immobilization, the activity of GibZea on the carrier increased 1.6-fold. As it had no effect on NeoFis, we assume that GibZea has a more polar surface and thus its native structure might be distorted by ionic interactions in the highly hydrophilic support. Due to the lack of structural information at this time this could not be verified. To prevent the dissociation of the cofactor pyridoxal-5'-phosphate (PLP) from the enzyme and thereby to improve the stability and activity of the bound enzymes, PLP was added in excess. To prevent heat inactivation and high shear forces, the immobilization itself was carried out at 4°C with orbital shaking. Next, immobilizations were carried out and stopped after certain time intervals. Here after a maximum in immobilized activity was reached, which only slightly increased further at 3 h. Thus we decided to stop all immobilizations after 3 h, which yielded high bound activities for GibZea (362 U/ g) and NeoFis (216 U/ g). As the immobilization of the VftA was described before, we used this enzyme too and achieved a significantly lower immobilized activity (71 U/ g) compared to GibZea and NeoFis<sup>[47h]</sup>. Nevertheless, we found a hyper activation of VftA leading to a recovered activity of 120 %, which might result from the use of pure enzyme. In contrast, GibZea and NeoFis were directly immobilized from *E. coli* crude cell extracts.

The immobilized GibZea and NeoFis showed good immobilization yields and specific activities per gram carrier and important parameter, like pH- and temperature optima and reusability were investigated. A shift in the pH optima from 7.5 to 8 was determined for immobilized GibZea. This effect could not be observed for NeoFis as free and immobilized preparations had a pH optima of 9. The temperature optimum for the immobilized GibZea was increased from 30°C to 40°C (Figure 10A). As the free GibZea was inactive at 40°C, this data indicated a strong increase in the enzyme stability by the attachment to the chitosan support. This effect could be also observed for the immobilized NeoFis, but was less pronounced: smaller changes in the relative activities shifted the optimum from 40°C to 50°C (Figure 10B). Additionally to the increased temperature optima, a good recycling performance for the immobilized GibZea and NeoFis was found. Four consecutive 1 h transaminations of (*R*)-1-PEA and pyruvate to acetophenone and D-alanine were followed by gas chromatography (GC). After the fourth batch only slight reductions in relative activity by 15 % (GibZea) and 14 % (NeoFis) were observed. This low decrease could be associated to bound enzymes by non-specifically hydrophobic interactions, a slow deactivation of exposed enzyme layers, the slow accumulation of inhibiting reaction compounds during the consecutive batches or deactivation of the catalyst due to the recovery process from the reaction solution. A reason for the good reusability during this consecutive batches could be the reduced leaching of enzyme molecules due to the covalent attachment with glutaraldehyde.

# Immobilization of Biocatalysts

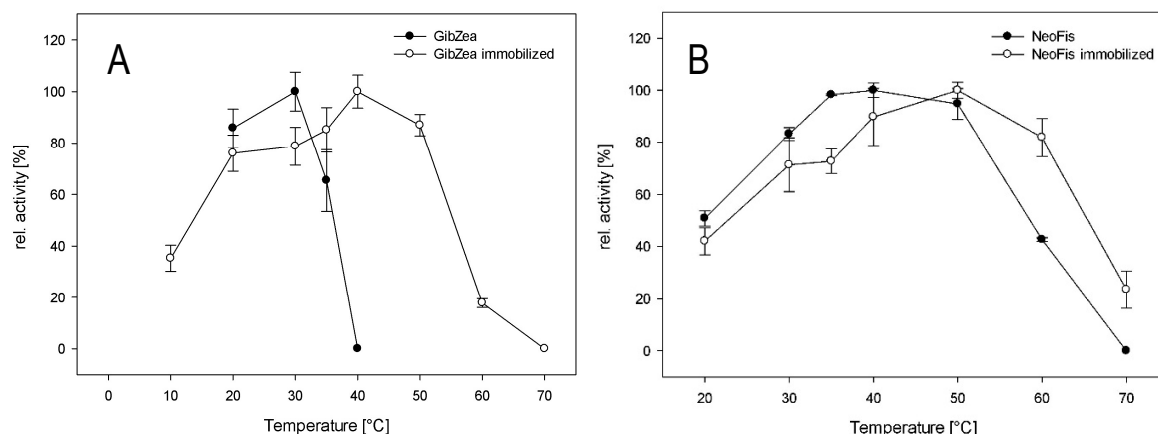


Figure 10: Temperature profiles (relative initial activity) of soluble and immobilized transaminases from *Gibberella zeae* (A) and from *Neosartorya fischeri* (B).

After these important properties of the immobilized enzymes were determined, the application in small-scale asymmetric syntheses was investigated. This reaction mode has the advantage of theoretically allowing 100 % yield of optically active amine from a prochiral ketone. We performed the asymmetric synthesis of (*R*)-2-aminohexane from 2-hexanone by applying D-alanine as amino donor. As the equilibrium of the reaction strongly favors the substrates' side, the formed pyruvate was removed with the previously described lactate dehydrogenase/glucose dehydrogenase system to shift the equilibrium to the products side<sup>[51]</sup>. The reactions with free and immobilized NeoFis showed no significant differences in product formation after 24 h ( $79 \pm 13$  % and  $71 \pm 3$  % conversion) which suggests an already stable free enzyme. However, the immobilization of GibZea resulted in a 13.4-fold higher conversion ( $>99 \pm 3$  %) compared to the free enzyme. This finding correlates with an earlier study, where the free GibZea only reached 14 % conversion after 72 h even though relatively high initial activities were used<sup>[51]</sup>. It can therefore be concluded that the immobilization of GibZea on Chitosan beads significantly stabilized the enzyme. Furthermore the immobilized GibZea showed a 1.3-fold higher conversion after 24 h under same reaction conditions compared to NeoFis, which showed a 7.1-fold higher conversion than GibZea in the earlier study.

In order to extend our pool of immobilized transaminase preparations, we tested three further promising transaminases with the established protocol described in **Article V**.

## 3.2 Immobilization of (*R*)- and (*S*)-Amine Transaminases on Chitosan Support Using Glutaraldehyde or Divinylsulfone as Linkers (Article V)

In **Article IV** an immobilization protocol on chitosan beads is described to achieve highly stable and active immobilized ATA preparations. We decided to test this concept also for the (*R*)-ATA from *Aspergillus fumigatus* (AspFum) and the (*S*)-ATAs from *Ruegeria pomeroyi* (3HMU) and *Rhodobacter sphaeroides* 2.4.1 (3I5T). The enzymes were chosen because no immobilization was described so far and the successful application in asymmetric amine synthesis were shown<sup>[51, 54]</sup>. These enzymes belong to two different PLP fold types, e.g. fold type I ((*S*)-ATAs) and IV ((*R*)-ATAs), and subsequent the chitosan was investigated as carrier for this enzymes. As we also wanted to study the effect of the linker for the covalent attachment on the immobilized enzymes, divinylsulfone (DVS) was used as an alternative to GA. The immobilized ATAs were investigated for temperature profile and long-term storage stability. As AspFum displayed interesting heat activation effects, the thermo-stability was examined in more detail.

As GA mainly reacts with the  $\epsilon$ -amino group of lysine, we investigated DVS as alternative linker, which additionally links thiol and hydroxyl groups (e.g. cysteine and serine/threonine) to the chitosan support's amino and hydroxyl groups<sup>[63]</sup>. GibZea and NeoFis that have been described in **Article IV** were also included in this study to compare the effect of DVS as linker to GA.

# Immobilization of Biocatalysts

First, the optimal assay conditions for the ATAs had to be investigated. For (*R*)-ATAs the use of several buffers was investigated by Schätzle *et al.* and therefore sodium phosphate at pH 7.5 was used<sup>[64]</sup>. For 3HMU and 3I5T the use of CHES at pH 9.5 was reported as reaction buffer<sup>[54]</sup>. Interestingly it turned out in this study that the highest activity for 3I5T could be obtained in bicine buffer at pH 9.5, whereas it was only half in CHES buffer at the same pH.

As the linker concentration was not investigated in **Article IV**, the first goal in this study was the determination of the optimal GA and DVS amounts for activating the support. GibZea was used to test several GA (1.5 to 3 % v/v 25 % stock solution) and DVS (1-5 % v/v) concentrations. 1.5 % GA and 2.5 % DVS gave the highest activities (319 and 407 U/ g<sub>carrier</sub> respectively) and were used for further experiments. Investigations of the immobilization duration revealed, as previously found, that 3 h was optimal for all enzymes. Both linkers resulted in actively immobilized ATAs, but the DVS immobilization of AspFum, 3HMU and 3I5T reduced the specific activities by 2-3 fold compared to GA (Table 3). Only for GibZea and NeoFis equal bound activities on the carrier were obtained with both linkers. Regarding the use of DVS as linker molecule all further experiments revealed that it was in some cases equal to GA, but mostly it was less efficient. Therefore only results obtained from the experiments using GA as linker are further discussed.

Table 3: Specific<sup>a</sup> and recovered activities<sup>b</sup> of different covalently immobilized (*R*)- and (*S*)-ATAs. The attachment to the chitosan beads was achieved either with GA or DVS as linker molecule.

Enzyme	Activity (GA)	Recovered activity (GA)	Activity (DVS)	Recovered activity (DVS)
GibZea	322 ± 22	63 ± 4	291 ± 29	38 ± 4
NeoFis	165 ± 6	39 ± 2	168 ± 15	54 ± 5
AspFum <sup>c</sup>	99 ± 7	54 ± 2	51 ± 3	85 ± 6
3HMU	157 ± 2	21 ± 0	52 ± 22	26 ± 11
3I5T	163 ± 8	23 ± 3	50 ± 6	9 ± 1

<sup>a</sup> Activities are given in U g<sub>dry</sub><sup>-1</sup> against the model substrate (*R*)- or (*S*)-1-PEA.

<sup>b</sup> Refers to the percentage of activity bound to the carrier after immobilization.

The storage stability was generally increased by using GA (Figure 11A-C). Except the instable 3I5T, all GA preparations showed a hyperactivation after one month of storage at 4°C.

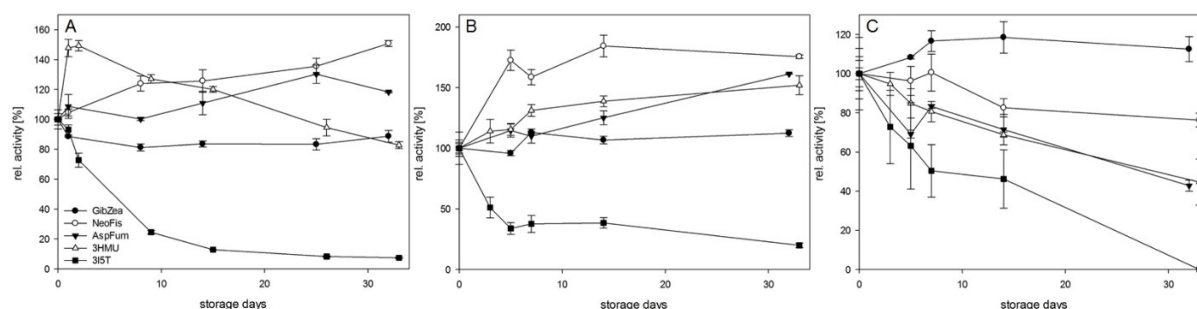


Figure 11: Storage stability at 4°C for the free (A), the glutaraldehyde (B) or divinylsulfone (C) immobilized transaminases on chitosan support. Activity was determined spectrophotometrical at 30°C using (*R*)- or (*S*)-1-PEA.

In contrast to GibZea that showed a strong shift in the temperature optimum in **Article IV** immobilization of the additional enzymes only displayed small effects on this property. Only AspFum showed substantially increased activity at 70°C: the free enzyme showed 23 % relative activity compared to 70 % of the immobilized one. Therefore the free and immobilized AspFum were incubated at elevated temperatures (40, 50 and 60°C, Figure 12A) for 4 h. Interestingly the immobilized AspFum showed a strong activation at all temperatures (up to 3.6-fold at 50°C), which was also observed for the free enzyme at 40 and 50°C. Nevertheless, a strong stabilization of the AspFum due to the covalent attachment was demonstrated at 60°C where the free enzyme was inactive after 4 h.

# Immobilization of Biocatalysts

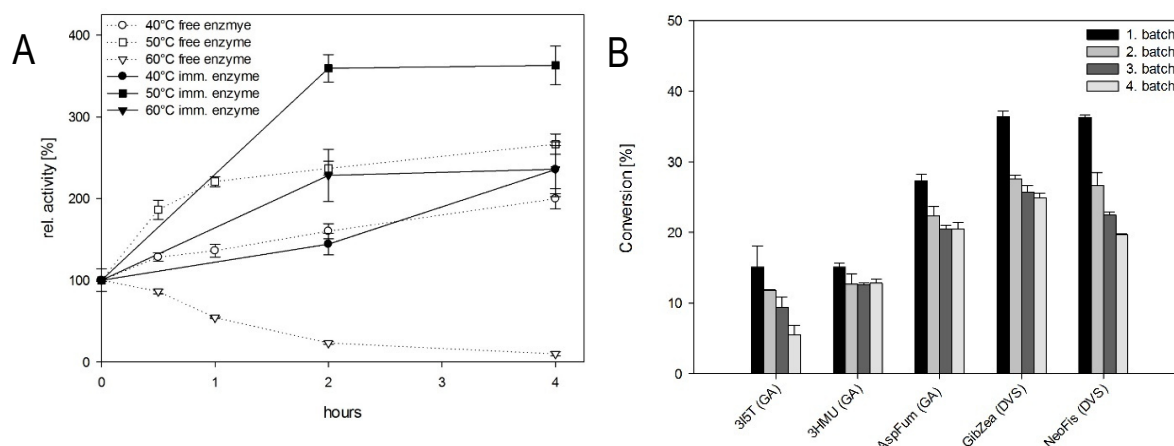


Figure 12: A) Relative initial activities of free (dots) and GA-immobilized (line) AspFum at 30°C after incubation at 40°C, 50°C and 60°C for 4 h are shown. B) Recycling studies with GA immobilized 3I5T, 3HMU and AspFum for four consecutive cycles of 1 h batches in the kinetic resolution of *rac*-1-PEA are given.

Additionally to the stabilization effects, the reusability of the GA immobilized AspFum, 3HMU and 3I5T were investigated. Like described in **Article IV** four consecutive 1 h batches for the transamination of 1-phenylethylamine to acetophenone were carried out, but in this case the racemic substrate was used (Figure 12B). As previously observed for GA immobilized GibZea and NeoFis a small reduction in activity was also seen for AspFum and 3HMU after the fourth batch (75 % and 85 % compared to initial conversion). A fast deactivation was found for 3I5T, confirming the modest stability from previous experiments.

After the immobilized ATAs had been characterized, the free enzymes and the GA preparations were applied in the asymmetric synthesis of (*R*)- or (*S*)-1-methyl-3-phenylpropylamine using isopropylamine (IPA) as amino donor. IPA was chosen, because it is cheap and the unfavorable reaction equilibrium can be shifted by using a high excess or by removal of the formed acetone<sup>[65]</sup>. As IPA normally is less accepted by the ATAs as amino-donor, protein engineering is often necessary to create a suitable biocatalyst. Thus the identification of wildtype enzymes that are already stable enough and accept IPA are highly desired. By using IPA as donor in 30-fold excess to shift the equilibrium for our asymmetric synthesis experiments, we could identify 3HMU, AspFum, NeoFis and GibZea as interesting scaffold for an protein engineering attempt (Table 4). Immobilized 3HMU, 3I5T and AspFum only showed slightly higher conversions than the free enzymes after 40 h, whereas the immobilized GibZea showed a 120-fold ( $36 \pm 1.9$  %) higher conversion than the free enzyme. With this finding we confirmed the results in **Article IV**, that the immobilized GibZea becomes a suitable catalyst for amine synthesis through the attachment on chitosan using GA. Despite the low stability of the free GibZea, which was overcome due to the immobilization, GibZea displayed several advantages: it could be recombinantly expressed in the highest yield compared to all other investigated (*R*)-ATAs and furthermore it showed the highest immobilized specific activity on chitosan support. In contrast, the free GibZea was not feasible at all for application. Interestingly, the opposite was obtained for NeoFis, where the free enzyme displayed a 2.7-fold higher conversion ( $46 \pm 1.5$  %) than the GA immobilized one. As crystal structure determination of immobilized enzymes is impossible, it can only be speculated that the binding of IPA in NeoFis is changed due to the immobilization and therefore the activity is decreased.

## Immobilization of Biocatalysts

Table 4: Conversions<sup>a</sup> observed in biocatalysis<sup>b</sup> using the free and GA immobilized enzymes. IPA was used as amino donor in 30-fold excess to shift the equilibrium.

Enzyme	Free enzyme	Immobilized enzyme
GibZea	<1	36 ± 2
NeoFis	46 ± 2	17 ± 0
AspFum <sup>b</sup>	44 ± 2	50 ± 1
3HMU	67 ± 1	75 ± 1
3I5T	10 ± 0	18 ± 1

<sup>a</sup> Conversion in % after 40 h at a substrate concentration of 10 mM as determined by HPLC for (*R*)- or (*S*)-1-methyl-3-phenylpropylamine produced.

<sup>b</sup> Heat activated.

We demonstrated that the established immobilization protocol from **Article IV** could be successfully transferred to the (*R*)-ATA AspFum and to the (*S*)-ATAs 3HMU and 3I5T which broadened the applicability of the established protocol from **Article III** to other transaminase from different fold types.

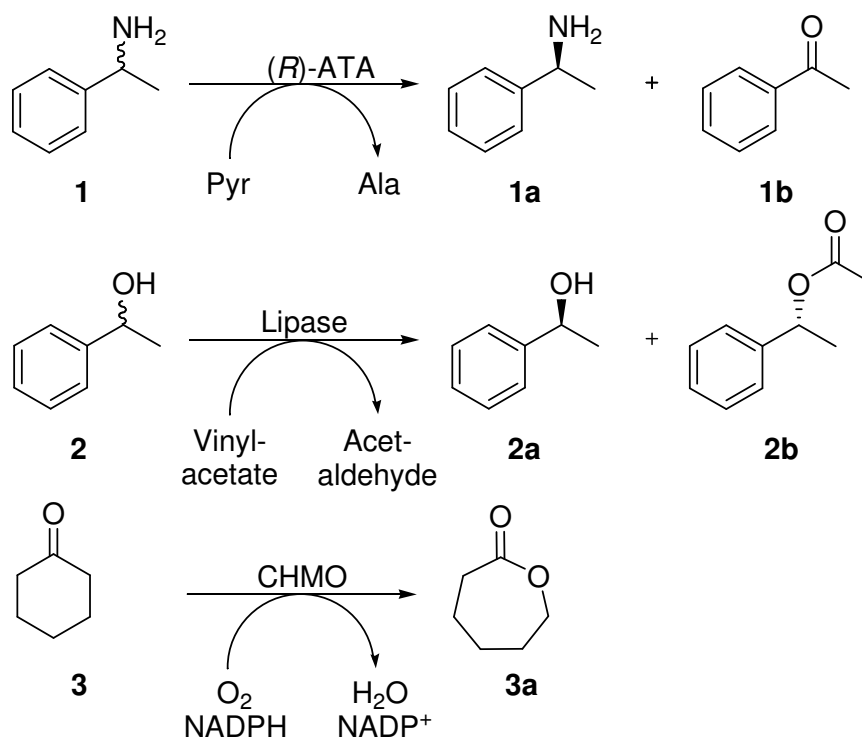
**Article IV and V** showed that the immobilization protocol on chitosan support yielded in active immobilized ATA preparations for the investigated transaminases, resulting in highly active and stable immobilized GibZea, NeoFis, AspFum and 3HMU preparations. Especially GibZea showed a better performance in both asymmetric syntheses e.g. a 13.4- and 120-fold increase in conversion. For immobilized NeoFis we only found in the asymmetric synthesis of (*R*)-2-aminohexane a good conversion, whereas for the synthesis of (*R*)-1-methyl-3-phenylpropylamine the free enzymes showed a 2.7-fold higher conversion. Two main advantages of immobilized enzymes are the easy recovery of the catalyst from the reaction and the possible application in different fixed bed reactor types. We decided to investigate the second one in more detail and applied the highly active GibZea in reactions with different reactor set-ups, which is reported in **Article VI**.

Because of this results further application of the immobilized ATAs was promising. Therefore we used the immobilized GibZea in our study on a novel reactor design for biocatalysis in **Article VI**. It was compared in three reactors: the continuous flow fixed-bed reactor (FBR), a common stirred tank reactor (STR) or the rotating-flow-cell (SpinChem, SCR) at 0.5 L volume scale to investigate its potential in larger scale transamination reactions.

## 4 Application of Biocatalysts in Bioreactors

### 4.1 Application of the Rotating Flow Cell Reactor (SpinChem) for Biocatalysis (Article VI)

Next to designing a biocatalyst, another important part in developing a productive process is the choice of the appropriate reactor concept. Within this study a basket reactor of novel design, the rotating flow cell (SpinChem, SCR), was applied in biocatalysis and compared to a standard fixed-bed (FBR) and a stirred tank reactor (STR). Special focus was put on the reusability, since we assumed that the protection of the catalysts from mechanical forces would be greatly improved by using the SCR.



Scheme 7: Reactions studied for comparison of SpinChem, fixed bed and stirred tank reactor. (R)-ATA: (R)-amine transaminase, CHMO: cyclohexanone monooxygenase.

For this comparison, three different enzymatic conversions were tested in a reaction volume of 0.5 L (Scheme 7). First, the kinetic resolution of (R,S)-1-phenylethylamine by using the immobilized GibZea (**1**) described in **Article IV and V** was investigated. In a second approach the transesterification of (R,S)-1-phenylethanol using immobilized *Candida antarctica* lipase B (CAL-B, Novozyme 435, N435) in *n*-hexane was explored (**2**)<sup>[66]</sup>. Finally, the production of  $\epsilon$ -CL from CHO using calcium-alginate-encapsulated *E. coli* whole cells (**3**) that harbor CHMO from *Acinetobacter calcoaceticus* NCIMB 9871 was performed using SCR<sup>[21a, 67]</sup>. Especially for  $O_2$  dependent enzymes stability is a challenging issue and the application in FBRs is difficult because gas supply is required. The use of the SCR would address both problems, because the catalyst is protected within the flow cell and oxygen can easily be supplied.

The first upcoming task was the encapsulation of the *E. coli* whole cells bearing the CHMO. After expression at 30°C for 5 to 6 h good CHMO activity within the cells was obtained. As cells walls display a strong diffusion barrier, we performed a permeabilization of the cells to support substrate, product and oxygen diffusion. Among different reagents that were tested (CHAPS, CTAB, SDS, Triton™ X-100, DMSO, Tween® 20, PEI), 1 % DMSO turned out to increase the activity for oxidation of CHO by 40 % . As the cells displayed reasonable activity ( $5.4 \pm 0.4$  U/ g<sub>cells</sub>), encapsulation was



## Application of Biocatalysts in Bioreactors

performed using 1.8 % calcium-alginate and a cell mass of 50 g/ L<sup>[68]</sup>. This reduced the activity to 28 %, which can be explained by the formation of additional diffusion barriers due to the encapsulation. Here, for example oxygen supply is a critical factor because the BVMO activity is dependent on available O<sub>2</sub>.

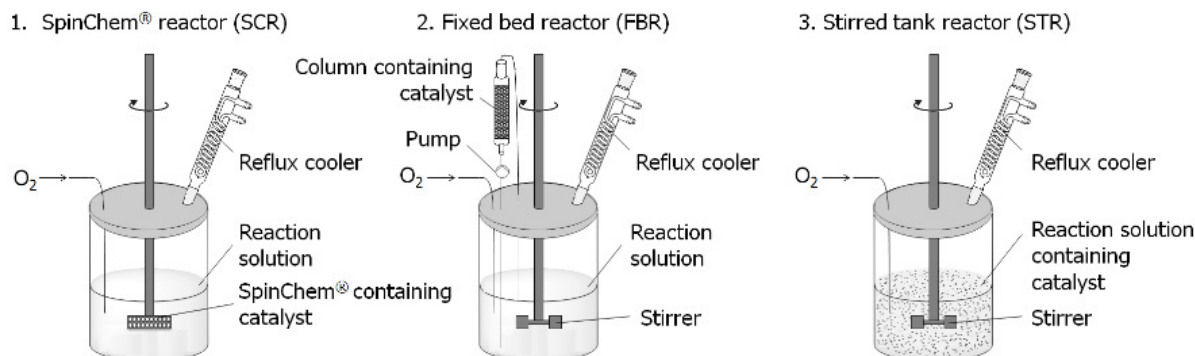


Figure 13: Reaction-setups for the investigated reactor types. Only for BVMO reactions oxygen supply and reflux cooler were necessary.

When immobilized biocatalysts were available for every reaction to be investigated, they were consequently tested using the SCR, STR and FBR (Figure 13). For the FBR a reservoir was applied and the reaction solution was circularly pumped through a column containing the catalysts. Biocatalysis was carried out at high substrate concentrations of 122.17 g/ L and 16.12 g/ L in case of lipase and ATA, respectively. For the CHMO a lower concentration of 1.96 g/ L was applied, to ensure full activity of this BVMO. Since the stirring speed is an important parameter for optimal mass transfer in SCR, 100 to 1000 rpm were tested and a speed of 500 rpm was found to give maximum activity in all reactions. During kinetic resolution using a transaminase (Table 5) after 6 h equal conversions were found for the SCR and STR, whereas the FBR gave a 1.2 times lower conversion. The same trend was observed for the lipase-catalyzed reaction after 4 h. Since the reaction was performed in organic solvent, which leads to several problems in the column like e.g. back pressure due to high volatility a FBR was not applied in this case. For the BVMO-catalyzed reaction the STR and SCR showed similar conversions after 24 h as well, but they were found to be nine times lower using the FBR. An explanation for this could be the problematic oxygen supply in the column. In all reactions using three completely different immobilized catalysts (covalently attached ATA, adsorptive immobilized lipase, encapsulated whole cells bearing a BVMO), the same trend regarding conversion was observed when SCR and STR were compared. Therefore it could be assumed that the mass transfer was not negatively influenced in the SCR through the packing of the catalysts within the chamber.

Table 5: Conversion determined after certain time periods for various investigated reactions

Enzyme/ Conv. [%]	SCR	STR	FBR
<b>Transaminase<sup>a</sup></b>	37 ± 8.0	37 ± 11	30 ± 4.3
<b>Lipase<sup>b</sup></b>	45 ± 1.0	46 ± 1.0	n.d.
<b>CHMO<sup>c</sup></b>	36 ± 6.1	35 ± 6.0	4 ± 0.2

<sup>a</sup>after 6 h, <sup>b</sup>after 4 h, <sup>c</sup>after 24 h; n.d.: not determined

As mentioned in **Article IV and V**, apart from possible application in reactor concepts, easy downstream processing and the reusability is a major advantage of immobilized enzymes. We therefore investigated these aspects by comparing SCR and STR in this terms. By using the SCR the downstream process and reusability of the catalysts was greatly simplified by the opportunity to take out the stirrer of the solution. It was washed three times with acetone (lipase)

## Application of Biocatalysts in Bioreactors

or washing buffer (ATA or BVMO) for 30 s in small beakers and was then ready for the next batch. In contrast, the entire reaction solution from the STR had to be filtered to recover the catalyst, which was then washed several times before it could be subjected to the next batch. Furthermore, the SCR was highly superior compared to the STR in the ATA and BVMO reaction, as in both cases a significantly higher relative activity was seen in the last batch (Figure 14A and B). Here, to improve the stability of the calcium-alginate capsules the addition of 10 mM  $\text{CaCl}_2$  to the reaction and washing solution was necessary. The increased performance of the SCR, that was observed confirmed our assumption that the catalysts were protected more efficiently from mechanical forces or that deactivation during the recovery process was reduced compared to the STR. Using the lipase a slightly different trend was noticed since the SCR was superior until the fourth batch, whereas in the sixth batch the conversion was equal in both reactors (Figure 14C). This can be addressed to the high stability of CALB and the accumulation of reaction compounds in the immobilized catalyst after several uses.

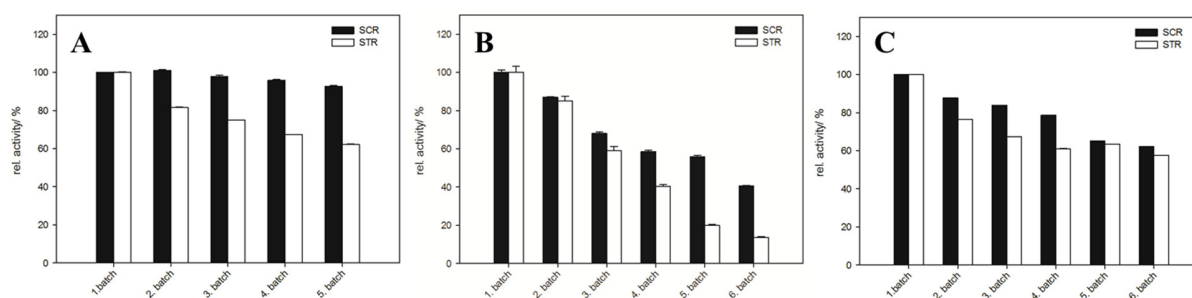


Figure 14: Recycling studies performed with a covalently immobilized GibZea (A), encapsulated whole cells harboring a CHMO (B) and an immobilized lipase (CALB) (C). Each batch was performed for 2 h in 0.5 L volume scale.

Within this study the SCR was successfully established for biocatalysis using encapsulated whole cells or immobilized enzymes. The system displayed a valuable alternative to the conventional STR and FBR, which was demonstrated for several reaction types to be equal or superior regarding conversion. Recycling studies showed that the loss of activity circumvented in the SCR compared to the STR for the ATA- and BVMO-catalyzed reactions with approximately 30 % higher residual activities in the fifth batch for the SCR. For the lipase this effect could only be shown in the initial batches. This revealed that the catalysts are protected more efficiently from mechanical stirring-forces with the same reaction rate as in the STR. A major advantage of the SCR was the easy recovery and reuse of the catalysts, which could be performed in less than 5 min compared to 1-2 h required for filtration and washing when using the STR. Furthermore with the SCR, reactions could be performed efficiently without the need for special laboratory equipment. This is important for fast and easy reactor set-ups in small to medium scale biocatalysis-reactions required for scientific research.

### 5 Concluding Remarks

The application of enzymes has been proven to extend the available toolbox of catalysts for organic chemistry. Nevertheless, the biocatalysts and reaction conditions need to be improved to match an economical process (Figure 1). Within this thesis the engineering to apply biocatalysts in synthesis reactions was studied extensively.

First, a new biocatalytic route to  $\epsilon$ -caprolactone was developed using a polyol dehydrogenase (PDH) from the mesothermophilic strain *Deinococcus geothermalis* 11300. For this, the biocatalyst selection by database search, the biochemical characterization and improvement by protein engineering was successfully applied. The temperature optimum of 45°C achieved for the PDH-variant (PDH-loop) corresponded well to the expected finding for a moderate thermophile enzyme, like reported for other proteins of this strain. It was shown throughout mutational studies that the new PDH had a great potential for further optimization. The thermostability was increased by 7°C by a rather unexpected way, introducing a loop region from a homologue enzyme. Furthermore, two crucial amino acid residues for the conversion of 1,2-diols were identified by analyzing active site mutants. Moreover, the substrate scope of PDH-loop showed an increased activity towards cyclohexanol and was therefore subjected for the alteration of the cofactor dependency. The relaxed variant, bearing the mutation D55N, was able to accept both NAD<sup>+</sup> and NADP<sup>+</sup>. Therefore PDH-loopD55N could be combined with a Baeyer-Villiger monooxygenase (CHMO) in a one-pot-two-step biocatalysis for the double oxidation of cyclohexanol to  $\epsilon$ -caprolactone facilitating an internal cofactor regeneration system. With this proof-of-concept, enabled by protein design, a new biocatalytic route to  $\epsilon$ -caprolactone was established successfully.

Furthermore, industrially useful biocatalysts normally require immobilization, as this often increases stability, downstream processing is simplified and application in long-term operations is possible. Studies by subjecting the CHMO to increasing cyclohexanol concentrations showed that only 30 % residual activity were left at already 10 mM. Co-immobilization of PDH-loopD55N and CHMO was found to improve the stability of CHMO against cyclohexanol, as the preparation showed at 30 mM concentration still full activity. Transaminases, important for the synthesis of chiral amines, were also immobilized to improve their process properties. Optimized chitosan beads were found to be a suitable support for the covalent immobilization of five (*R*)- or (*S*)- selective transaminases. From these, four could be successfully immobilized, whereas enzyme 3I5T showed even immobilized a poor stability. Especially for the transaminases GibZea and NeoFis high specific activities (362 and 216 U/ g<sub>carrier</sub>, respectively) were achieved and a shift in the temperature optimum by +10°C was determined. AspFum showed a significant stabilization at 60°C compared to the free enzyme and unusual heat activation effects of the immobilized catalyst were found. The immobilized ATAs could be stored for up to 30 days at 4°C and showed a good reusability in consecutive batch experiments. After the properties of the ATAs were improved due to the immobilization, their application in asymmetric synthesis of chiral amines was shown. Herein immobilized GibZea was greatly improved for the synthesis of (*R*)-2-aminoheptane with full conversion after 24 h, whereas the free GibZea reached only 7 % within the same time period. Using isopropylamine as unnatural amine donor, scaffolds for protein engineering were identified for optimization of the stability of the enzyme against this cheap donor.

Finally, to obtain a productive process an optimal reactor system had to be chosen. Established systems revealed disadvantages like mechanical forces occurring in a simple stirred-tank reactor or a rather challenging set-up for fixed-bed reactors. Therefore a new reactor design (the SpinChem™ reactor, SCR) was successfully applied for biocatalysis using immobilized enzymes in the SCR, STR and FBR. Examining three types of enzymatic reactions (chitosan immobilized GibZea, immobilized lipase CALB, and encapsulated *E. coli* whole cells bearing CHMO) in 0.5 L reaction volume, it was shown that the mass transfer is not disturbed by packing the biocatalyst into the rotation chamber. It was assumed that the catalyst is more protected within the SCR, which was demonstrated by performing consecutive batch experiment. Next to the highly simplified recovery process of the catalyst after each batch in the SCR compared to the STR, it was demonstrated that after the last batch the biocatalyst showed a highly improved stability in the new reactor design.

## Reference List

### 6 References

- [1] U. T. Bornscheuer, G. W. Huisman, R. J. Kazlauskas, S. Lutz, J. C. Moore, K. Robins, *Nature* **2012**, 485, 185-194.
- [2] J. M. Woodley, *Trends Biotechnol.* **2008**, 26, 321-327.
- [3] a) U. T. Bornscheuer, *Synlett* **2013**, 150-156; b) G. A. Behrens, A. Hummel, S. K. Padhi, S. Schätzle, U. T. Bornscheuer, *Adv Synth Catal* **2011**, 353, 2191-2215; c) J. M. Woodley, *Curr. Opin. Chem. Biol.* **2013**, 17, 310-316.
- [4] D. J. Pollard, J. M. Woodley, *Trends Biotechnol.* **2007**, 25, 66-73.
- [5] K. Buchholz, V. Kasche, U. T. Bornscheuer, *Biocatalysts and Enzyme Technology*, 2nd ed., Wiley-VCH, Weinheim, **2012**.
- [6] A. Schmid, J. S. Dordick, B. Hauer, A. Kiener, M. Wubbolts, B. Witholt, *Nature* **2001**, 409, 258-268.
- [7] S. Lutz, U. T. Bornscheuer, *Protein Engineering Handbook*, Vol. 1 and 2, Wiley-VCH, **2009**, **2012**.
- [8] a) U. T. Bornscheuer, *Biocatal. Biotransf.* **2001**, 19, 84-96; b) U. T. Bornscheuer, M. Pohl, *Curr. Opin. Chem. Biol.* **2001**, 5, 137-143.
- [9] S. Bartsch, R. Kourist, U. T. Bornscheuer, *Angew. Chem. Int. Ed.* **2008**, 47, 1508-1511.
- [10] a) C. G. Acevedo-Rocha, S. Kille, M. T. Reetz, *Methods Mol Biol.* **2014**, 1179, 103-128; b) M. T. Reetz, L.-W. Wang, M. Bocola, *Angew. Chem. Int. Ed.* **2006**, 45, 1236-1241; c) M. T. Reetz, J. D. Carballera, A. Vogel, *Angew. Chem. Int. Ed.* **2006**, 45, 7745-7751.
- [11] M. T. Reetz, J. D. Carballera, J. Peyralans, H. Hobenreich, A. Maichele, A. Vogel, *Chem. Eur. J.* **2006**, 12, 6031-6038.
- [12] H. Jochens, U. T. Bornscheuer, *ChemBioChem* **2010**, 11, 1861-1866.
- [13] H. Jochens, D. Aerts, U. T. Bornscheuer, *Prot. Eng. Des. Sel.* **2010**, 23, 903-909.
- [14] V. G. H. Eijssink, S. Gaseidnes, T. V. Borchert, B. van den Burg, *Biomol. Eng.* **2005**, 22, 21-30.
- [15] F. H. Arnold, P. L. Wintrode, K. Miyazaki, A. Gershenson, *Trends Biochem. Sci.* **2001**, 26, 100-106.
- [16] U. Oppermann, C. Filling, M. Hult, N. Shafqat, X. Wu, M. Lindh, J. Shafqat, E. Nordling, Y. Kallberg, B. Persson, H. Jörnvall, *Chem.-Biol. Interact.* **2003**, 143-144, 247-253.
- [17] a) Y. Carius, H. Christian, A. Faust, U. Zander, B. U. Klink, P. Kornberger, G.-W. Kohring, F. Giffhorn, A. J. Scheidig, *J. Biol. Chem.* **2010**, 285, 20006-20014; b) M. G. Rossmann, D. Moras, K. W. Olsen, *Nature* **1974**, 250, 194-199; c) B. Gerratana, W. W. Cleland, P. A. Frey, *Biochemistry* **2001**, 40, 9187-9195.
- [18] A. C. Ferreira, M. F. Nobre, F. A. Rainey, M. T. Silva, R. Wait, J. Burghardt, A. P. Chung, M. S. Da Costa, *Int. J. Syst. Bacteriol.* **1997**, 47, 939-947.
- [19] A. Baeyer, V. Villiger, *Ber. Dtsch. Chem. Ges.* **1899**, 3625-3633.
- [20] M. D. Mihovilovic, B. Müller, P. Stanetty, *Eur. J. Org. Chem.* **2002**, 3711-3730.
- [21] a) N. A. Donoghue, P. W. Trudgill, *Eur. J. Biochem.* **1975**, 60, 1-7; b) N. A. Donoghue, D. B. Norris, P. W. Trudgill, *Eur J Biochem* **1976**, 63, 175-192; c) Y.-C. Chen, O. P. Peoples, C. T. Walsh, *J. Bacteriol.* **1988**, 170, 781-789; d) C. T. Walsh, Y.-C. J. Chen, *Angew. Chem. Int. Ed.* **1988**, 27, 333-343.
- [22] K. Qiao, Y.-H. Chooi, Y. Tang, *Metab. Eng.* **2011**, 13, 723-732.
- [23] a) I. A. Mirza, B. J. Yachnin, S. Wang, S. Grosse, H. Bergeron, A. Imura, H. Iwaki, Y. Hasegawa, P. C. K. Lau, A. M. Berghuis, *J. Am. Chem. Soc.* **2009**, 131, 8848-8854; b) R. Orru, H. M. Dudek, C. Martinoli, D. E. Torres Pazmiño, A. Royant, M. Weik, M. W. Fraaije, A. Mattevi, *J. Biol. Chem.* **2011**, 286, 29284-29291.
- [24] W. J. H. van Berkel, N. M. Kamerbeek, M. W. Fraaije, *J Biotechnol* **2006**, 124, 670-689.
- [25] F. Leipold, R. Wardenga, U. T. Bornscheuer, *Appl. Microbiol. Biotechnol.* **2012**, 94, 705-717.
- [26] M. W. Fraaije, N. M. Kamerbeek, W. J. H. v. Berkel, D. B. Janssen, *FEBS Lett.* **2002**, 518, 43-47.
- [27] a) E. Malito, A. Alfieri, M. W. Fraaije, A. Mattevi, *Proc. Natl. Acad. Sci. U.S.A.* **2004**, 101, 13157-13162; b) M. W. Fraaije, J. Wu, D. P. H. M. Heuts, E. W. van Hellemond, J. H. L. Spelberg, D. B. Janssen, *Appl. Microbiol. Biotechnol.* **2005**, 66, 393-400.
- [28] a) K. H. Jones, R. T. Smith, P. W. Trudgill, *J. Gen. Microbiol.* **1993**, 139, 797-805; b) H. Leisch, R. Shi, S. Grosse, K. Morley, H. Bergeron, M. Cygler, H. Iwaki, Y. Hasegawa, P. C. Lau, *Appl. Environ. Microbiol.* **2012**, 78, 2200-2212; c) M. Kadow, K. Loschinski, S. Sass, M. Schmidt, U. T. Bornscheuer, *Appl. Microbiol.*

## Reference List

- Biotechnol.* **2012**, 96, 419-429; d) D. G. Taylor, P. W. Trudgill, *J. Bacteriol.* **1986**, 165, 489-497; e) R. Villa, A. Willetts, *J. Mol. Catal. B: Enzym.* **1997**, 2, 193-197.
- [29] a) H. Leisch, K. Morley, P. C. K. Lau, *Chem. Rev.* **2011**, 111, 4165-4222; b) D. E. Torres Pazmino, H. M. Dudek, M. W. Fraaije, *Curr. Opin. Chem. Biol.* **2010**, 14, 138-144; c) G. de Gonzalo, M. D. Mihovilovic, M. W. Fraaije, *ChemBioChem* **2010**, 11, 2208-2231; d) J. Rehdorf, U. T. Bornscheuer, M. C. Flickinger, in *Encyclopedia of Industrial Biotechnology*, John Wiley & Sons, Inc., **2009**, pp. 1-35.
- [30] a) J. Rehdorf, M. D. Mihovilovic, M. W. Fraaije, U. T. Bornscheuer, *Chemistry* **2010**, 16, 9525-9535; b) J. Rehdorf, A. Lengar, U. T. Bornscheuer, M. D. Mihovilovic, *Bioorg. Med. Chem. Lett.* **2009**, 19, 3739-3743.
- [31] L. H. Andrade, E. C. Pedrozo, H. G. Leite, P. B. Brondani, *J. Mol. Catal. B: Enzym.* **2011**, 73, 63-66.
- [32] a) O. Abril, C. C. Ryerson, C. Walsh, G. M. Whitesides, *Bioorg. Chem.* **1989**, 17, 41-52; b) S. A. Meeuwissen, A. Rioz-Martinez, G. de Gonzalo, M. W. Fraaije, V. Gotor, H. J. C. M. van, *J. Mater. Chem.* **2011**, 21, 18923-18926.
- [33] a) M. Hucík, M. Bučko, P. Gemeiner, V. Štefuca, A. Vikartovská, M. Mihovilović, F. Rudroff, N. Iqbal, D. Chorvát, I. Lacík, *Biotechnol. Lett.* **2010**, 32, 675-680; b) M. Bučko, A. Schenk Mayerová, P. Gemeiner, A. Vikartovská, M. D. Mihovilovic, I. Lacík, *Enzyme Microb. Technol.* **2011**, 49, 284-288.
- [34] a) C.-H. Wong, J. Gordon, C. L. Cooney, G. M. Whitesides, *J. Org. Chem.* **1981**, 46, 4676-4679; b) C.-H. Wong, G. M. Whitesides, *J. Am. Chem. Soc.* **1981**, 103, 4890-4899; c) C. Rodríguez, G. de Gonzalo, V. Gotor, *J. Mol. Catal. B: Enzym.* **2012**, 74, 138-143; d) M. J. McLachlan, T. W. Johannes, H. M. Zhao, *Biotechnol. Bioeng.* **2008**, 99, 268-274; e) T. W. Johannes, R. D. Woodyer, H. Zhao, *Appl. Environ. Microbiol.* **2005**, 71, 5728-5734; f) J. M. Vrtis, A. K. White, W. W. Metcalf, W. A. van der Donk, *Angew. Chem. Int. Ed.* **2002**, 41, 3257-3259.
- [35] D. E. T. Pazmino, R. Snajdrova, B. J. Baas, M. Ghobrial, M. D. Mihovilovic, M. W. Fraaije, *Angew. Chem. Int. Ed.* **2008**, 47, 2275-2278.
- [36] a) L. T., in *OECD Screening Information Data Set. (Brussel: UNEP Publications)* **2005**; b) L. Yu, K. Dean, L. Li, *Prog. Polym. Sci.* **2006**, 576-602; c) M. Breulmann, A. Kunkel, S. Philipp, V. Reimer, K. O. Siegenthaler, G. Skupin, M. Yamamoto, in *Ullmann's Encyclopedia of Industrial Chemistry, Vol. 29*, Wiley-VCH, Weinheim, **2009**.
- [37] M. Renz, B. Meunier, *Eur. J. Org. Chem.* **1999**, 1999, 737-750.
- [38] A. J. Willetts, C. J. Knowles, M. S. Levitt, S. M. Roberts, H. Sandey, N. F. Shipston, *J Chem Soc Perk T 1* **1991**, 1608-1610.
- [39] H. Kohls, F. Steffen-Munsberg, M. Höhne, *Curr. Opin. Chem. Biol.* **2014**, 19, 180-192.
- [40] A. C. Eliot, J. F. Kirsch, *Annual Review of Biochemistry* **2004**, 73, 383-415.
- [41] E. Teuscher, M. F. Melzig, U. Lindequist, *Biogene Arzneimittel*, Wissenschaftliche Verlagsgesellschaft Stuttgart, Stuttgart, **2004**.
- [42] a) M. Höhne, U. T. Bornscheuer, in *Enzyme Catalysis in Organic Synthesis*, Wiley-VCH, Weinheim, **2012**, pp. 779-820; b) M. Höhne, U. T. Bornscheuer, *ChemCatChem* **2009**, 1, 42-51; c) S. Mathew, H. Yun, *ACS Catal.* **2012**, 2, 993-1001; d) R. C. Simon, N. Richter, E. Busto, W. Kroutil, *ACS Catal.* **2013**, 4, 129-143.
- [43] a) C. K. Savile, J. M. Janey, E. C. Mundorff, J. C. Moore, S. Tam, W. R. Jarvis, J. C. Colbeck, A. Krebber, F. J. Fleitz, J. Brands, P. N. Devine, G. W. Huisman, G. J. Hughes, *Science* **2010**, 329, 305-309; b) A. A. Desai, *Angew. Chem. Int. Ed.* **2011**, 50, 1974-1976.
- [44] M. D. Truppo, H. Strotman, G. Hughes, *ChemCatChem* **2012**, 4, 1071-1074.
- [45] a) U. T. Bornscheuer, *Angew. Chem. Int. Ed.* **2003**, 42, 3336-3337; b) B. Brena, P. González-Pombo, F. Batista-Viera, in *Immobilization of Enzymes and Cells, Vol. 1051* (Ed.: J. M. Guisan), Humana Press, **2013**, pp. 15-31; c) C. Mateo, J. M. Palomo, G. Fernandez-Lorente, J. M. Guisan, R. Fernandez-Lafuente, *Enzyme Microb. Technol.* **2007**, 40, 1451-1463; d) R. A. Sheldon, *Adv. Synth. Catal.* **2007**, 349, 1289-1307.
- [46] a) U. Hanefeld, L. Gardossi, E. Magner, *Chem. Soc. Rev.* **2009**, 38, 453-468; b) A. Liese, L. Hilterhaus, *Chem. Soc. Rev.* **2013**.
- [47] a) D. Koszelewski, N. Müller, J. H. Schrittwieser, K. Faber, W. Kroutil, *J. Mol. Catal. B: Enzym.* **2010**, 63, 39-44; b) H. Mallin, M. Höhne, U. T. Bornscheuer, *J. Biotechnol.* **2014**, online, DOI: 10.1016/j.jbiotec.2014.05.015; c) H. Mallin, U. Menyes, T. Vorhaben, M. Hohne, U. T. Bornscheuer, *ChemCatChem* **2013**, 5, 588-593; d) M. Cardenas-Fernandez, W. Neto, C. Lopez, G. Alvaro, P. Tufvesson, J. M. Woodley, *Biotechnol. Prog.* **2012**, 28, 693-698; e) M. Päiviö, L. T. Kanerva, *Process Biochem.* **2013**, 48, 1488-1494; f) G. Rehn, C. Grey, C.

## Reference List

- Branneby, P. Adlercreutz, *J. Biotechnol.* **2013**; g) G. Rehn, C. Grey, C. Branneby, L. Lindberg, P. Adlercreutz, *Process Biochem.* **2012**, 47, 1129-1134; h) S.-S. Yi, C.-w. Lee, J. Kim, D. Kyung, B.-G. Kim, Y.-S. Lee, *Process Biochem.* **2007**, 42, 895-898.
- [48] B. Krajewska, *Enzyme Microb. Technol.* **2004**, 35, 126-139.
- [49] I. Migneault, C. Dartiguenave, M. J. Bertrand, K. C. Waldron, *BioTechniques* **2004**, 37, 790-802.
- [50] M. Höhne, S. Schätzle, H. Jochens, K. Robins, U. T. Bornscheuer, *Nat. Chem. Biol.* **2010**, 6, 807-813.
- [51] S. Schätzle, F. Steffen-Munsberg, M. Höhne, K. Robins, U. T. Bornscheuer, *Adv. Synth. Catal.* **2011**, 353, 2439-2445.
- [52] M. Thomsen, L. Skalden, G. J. Palm, M. Hohn, U. T. Bornscheuer, W. Hinrichs, *Acta Cryst. Sect. D* **2014**, 70, 1086-1093.
- [53] J. N. Jansonius, *Curr. Opin. Struc. Biol.* **1998**, 8, 759-769.
- [54] F. Steffen-Munsberg, C. Vickers, A. Thontowi, S. Schätzle, T. Tumlrish, H. M. Svedendahl, H. Land, P. Berglund, U. T. Bornscheuer, M. Höhne, *ChemCatChem* **2013**, 5, 150-153.
- [55] a) L. Cao, *Carrier-Bound Immobilized Enzymes*, Wiley-VCH, Weinheim, **2005**; b) P. Adlercreutz, *Chem. Soc. Rev.* **2013**; c) R. Dicosimo, J. McAuliffe, A. J. Poulou, G. Bohlmann, *Chem. Soc. Rev.* **2013**; d) U. Hanefeld, L. Cao, E. Magner, *Chem. Soc. Rev.* **2013**, 42, 6211-6212; e) R. A. Sheldon, S. van Pelt, *Chem. Soc. Rev.* **2013**, 42, 6223-6235.
- [56] a) F. Balkenhohl, K. Ditrach, B. Hauer, W. Ladner, *J. Prakt. Chem.* **1997**, 339, 381-384; b) G. Hills, *Eur. J. Lipid Sci. Technol.* **2003**, 105, 601-607.
- [57] a) J. J. Carberry, *Ind. Eng. Chem.* **1964**, 56, 39-46; b) J. A. Mahoney, K. K. Robinson, E. C. Myers, *Chemtech* **1978**, 8, 758-763.
- [58] S. N. Ho, H. D. Hunt, R. M. Horton, J. K. Pullen, L. R. Pease, *Gene* **1989**, 77, 51-59.
- [59] R. Fernandez-Lafuente, *Enzyme Microb. Tech.* **2009**, 45, 405-418.
- [60] F. Fan, J. A. Lorenzen, B. V. Plapp, *Biochemistry* **1991**, 30, 6397-6401.
- [61] a) F. Forneris, D. P. Heuts, M. Delvecchio, S. Roviola, M. W. Fraaije, A. Mattevi, *Biochemistry* **2008**, 47, 978-985; b) A. Winkler, F. Hartner, T. M. Kuchan, A. Glieder, P. Macheroux, *J. Biol. Chem.* **2006**, 281, 21276-21285.
- [62] S. Schätzle, M. Höhne, E. Redestad, K. Robins, U. T. Bornscheuer, *Anal. Chem.* **2009**, 81, 8244-8248.
- [63] a) M. S. Masri, M. Friedman, *J. Protein Chem.* **1988**, 7, 49-54; b) M. Friedman, J. W. Finley, *Int. J. Pept. Protein Res.* **1975**, 7, 481-486; c) J. Morales-Sanfrutos, J. Lopez-Jaramillo, M. Ortega-Munoz, A. Megia-Fernandez, F. Perez-Balderas, F. Hernandez-Mateo, F. Santoyo-Gonzalez, *Org. Biomol. Chem.* **2010**, 8, 667-675.
- [64] S. Schätzle, M. Höhne, K. Robins, U. T. Bornscheuer, *Anal. Chem.* **2010**, 82, 2082-2086.
- [65] a) K. E. Cassimjee, C. Branneby, V. Abedi, A. Wells, P. Berglund, *Chem. Commun.* **2010**, 46, 5569-5571; b) G. W. J. Matcham, M. Bhatia, W. Lang, C. Lewis, R. Nelson, A. Wang, W. Wu, *Chimia* **1999**, 53, 584-589.
- [66] E. M. Anderson, K. M. Larsson, O. Kirk, *Biocatal. Biotransform.* **1998**, 16, 181-204.
- [67] J. D. Stewart, *Curr. Org. Chem.* **1998**, 2, 195-216.
- [68] Y.-W. Zhang, P. Prabhu, J.-K. Lee, *Bioproc. Biosyst. Eng.* **2010**, 33, 741-748.

## Author contribution

### **Article I      Discovery, Application and Protein Engineering of Baeyer-Villiger Monooxygenases for Organic Synthesis**

K. Balke\*, M. Kadow\*, H. Mallin\*, S. Saß\*, U.T. Bornscheuer\*, *Org. Biomol. Chem.* **2012**, 10, 6249-6265.

\* All authors contributed equally.

### **Article II      Protein Engineering of a Thermostable Polyol Dehydrogenase**

H. Wulf, H. Mallin, U.T. Bornscheuer, *Enzyme Microb. Technol.* **2012**, 51, 217-224.

H.M. and H.W. contributed equally to this work. H.M., H.W. and U.T.B. designed the experiments. H.M. and H.W. conducted the experiments and wrote the manuscript, U.T.B. revised the manuscript.

### **Article III      A Self-Sufficient Baeyer–Villiger Biocatalysis System for the Synthesis of $\epsilon$ -Caprolactone from Cyclohexanol**

H. Mallin, H. Wulf, U.T. Bornscheuer, *Enzyme Microb. Technol.* **2013**, 53, 283-287.

H.M. and H.W. contributed equally to this work. H.W. conceived the concept, H.M. and U.T.B. designed the experiments. H.M. conducted the experiments, H.M., H.W. and U.T.B. wrote the manuscript and revised the manuscript.

### **Article IV      Immobilization of two (R)-Amine Transaminases on an Optimized Chitosan Support for the Enzymatic Synthesis of Optically Pure Amines**

H. Mallin, U. Menyes, T. Vorhaben, M. Höhne, U. T. Bornscheuer, *ChemCatChem* **2012**, 5, 588-593.

H.M. conceived the concept. H.M., U.M., T.V. and U.T.B. designed the experiments. H.M. conducted the experiments, U.M. the BET measurements. H.M. and U.T.B. wrote the manuscript, H.M., M.H. and U.T.B. designed the journals inside back cover. H.M., U.M., T.V., M.H. and U.T.B. revised the manuscript.

### **Article V      Immobilization of (R)- and (S)-Amine Transaminases on Chitosan Support and their Application for Amine Synthesis using Isopropylamine as Donor**

H. Mallin, M. Höhne, U. T. Bornscheuer, *J. Biotechnol.* 2014, online, DOI: 10.1016/j.jbiotec.2014.05.015.

H.M., M.H. and U.T.B. designed the experiments. H.M. conducted the experiments. H.M. and U.T.B. wrote the manuscript. H.M., M.H. and U.T.B. revised the manuscript.

### **Article VI      Efficient Biocatalysis with Immobilized Enzymes or Encapsulated Whole Cell Microorganism by Using the SpinChem Reactor System**

H. Mallin, J. Muschiol, E. Byström, U. T. Bornscheuer, *ChemCatChem* **2013**, 5, 3529-3532.

H.M. and J.M. contributed equally to this work. H.M., J.M. and U.T.B. designed the experiments, H.M. and J.M. conducted the experiments. H.M., J.M., E.B. and U.T.B. wrote and revised the manuscript.

---

Prof. Dr. Uwe T. Bornscheuer

## Articles

### Articles

#### Article I



## Discovery, application and protein engineering of Baeyer–Villiger monooxygenases for organic synthesis

Kathleen Balke, Maria Kadow, Hendrik Mallin, Stefan Saß and Uwe T. Bornscheuer†\*

Received 10th April 2012, Accepted 8th June 2012

DOI: 10.1039/c2ob25704a

Baeyer–Villiger monooxygenases (BVMOs) are useful enzymes for organic synthesis as they enable the direct and highly regio- and stereoselective oxidation of ketones to esters or lactones simply with molecular oxygen. This contribution covers novel concepts such as searching in protein sequence databases using distinct motifs to discover new Baeyer–Villiger monooxygenases as well as high-throughput assays to facilitate protein engineering in order to improve BVMOs with respect to substrate range, enantioselectivity, thermostability and other properties. Recent examples for the application of BVMOs in synthetic organic synthesis illustrate the broad potential of these biocatalysts. Furthermore, methods to facilitate the more efficient use of BVMOs in organic synthesis by applying *e.g.* improved cofactor regeneration, substrate feed and *in situ* product removal or immobilization are covered in this perspective.

### Introduction

Baeyer–Villiger monooxygenases (BVMOs) catalyze the enzymatic counterpart of the chemical Baeyer–Villiger oxidation and both are important for synthetic organic chemistry. In contrast to standard chemical oxidants such as peracids or hydrogen peroxide, BVMOs offer the unique advantage that they show usually excellent regio- and stereoselectivity and hence provide

an easy and mild method to obtain optically and regioisomerically pure products. Furthermore, the use of protecting groups and formation of by-products can be avoided in enzymatic processes.

The occurrence and properties of natural and recombinant enzymes, and the broad synthetic utility of BVMOs have been reviewed in the past few years.<sup>1–5</sup> This article will concentrate therefore on two aspects: (i) the recent advances in discovery and protein engineering of BVMOs to broaden their synthetic utility and (ii) new applications in organic synthesis, optimized reaction systems and immobilization methods to enable the efficient use of BVMOs in biotransformation.

*Institute of Biochemistry, Dept of Biotechnology & Enzyme Catalysis, Greifswald University, Felix-Hausdorff-Str. 4, 17487 Greifswald, Germany. E-mail: uwe.bornscheuer@uni-greifswald.de; Fax: +49 3834 8679 4367; Tel: +49 3834 864367*

† All authors contributed equally.



Kathleen Balke

*Kathleen Balke (born 1986) studied biochemistry at the University of Greifswald. During her studies she performed research internships at Dr Reddy's Chirotech Technology in Cambridge, UK and in the group of A. Achour at the Karolinska Institute in Stockholm, Sweden. She finished her diploma thesis in 2012 in the group of Prof. Bornscheuer on Baeyer–Villiger monooxygenases.*



Maria Kadow

*Maria Kadow (born 1984) studied biochemistry at the University of Greifswald and obtained her diploma degree in 2009. Since then she performs her PhD studies in the group of Uwe Bornscheuer. Her research topics deal with the identification of novel Baeyer–Villiger monooxygenases and the synthetic application of these enzymes.*

## Discovery and recombinant expression

Until the mid-1990s, research with Baeyer–Villiger mono-oxygenases was mostly restricted to two microorganisms, *Acinetobacter calcoaceticus*<sup>6</sup> and *Pseudomonas putida*.<sup>7</sup> *A. calcoaceticus* produces a BVMO with high activity in the conversion of cyclohexanone to  $\epsilon$ -caprolactone and hence the enzyme is usually named cyclohexanone monooxygenase (CHMO<sub>Acineto</sub>). The limitation that this strain is pathogenic and can only be grown in laboratories with proper permission (L2) was overcome by Stewart *et al.* as they succeeded first in the cloning and functional expression of this CHMO<sup>8,9</sup> paving the way for easier studies of this enzyme. The *Pseudomonas putida* strain NCIMB 10007 was shown to contain three BVMOs<sup>7,10–14</sup> but until recently (see below), the enzymes could only be used as purified proteins isolated after cultivation of the strain.

## Novel BVMOs from prokaryotic origin

In the past few years a tremendous increase in the number of new BVMOs took place due to the fast-growing information deposited in public sequence databases, which in combination with BVMO-specific amino acid motifs led to the identification, cloning, expression and characterization of numerous enzymes. Almost all recombinantly available BVMOs belong to the class of type I BVMOs. Type I BVMOs are NADPH and FAD dependent. Type II BVMOs that are FMN and NADH dependent have not been investigated in detail until recently. Type I BVMOs contain some typical motifs – such as FXGXXXHXXXW[P/D] described in 2002 by Fraaije *et al.*<sup>15</sup> – that facilitate identification of putative BVMOs from sequence data and are therefore called fingerprint motifs. Another conserved motif in type I BVMOs is the N-terminal GXGXXG Rossmann-fold motif of which two enclose the fingerprint. One example of an enzyme that has been identified by genome mining using the fingerprint motif is the phenylacetone monooxygenase (PAMO) from *Thermobifida fusca*.<sup>16</sup> Until now PAMO is the only available thermophilic BVMO and it was the first type I BVMO of which the structure was determined.<sup>17</sup> The most impressive example of newly identified BVMOs is the discovery of over 20 putative BVMOs

found in the genome of *Rhodococcus jostii* RHA1.<sup>18,19</sup> Even though BVMOs are present in a variety of bacteria and fungi, usually only a few BVMOs are encoded in the genome of one specific strain and hence *Rhodococcus jostii* RHA1 is exceptional. Recently Riebel *et al.* succeeded in cloning and expressing 22 BVMOs from this strain.<sup>18</sup> Additionally, 39 substrates were tested with each of these BVMOs in order to explore their substrate scopes. In earlier studies the investigation of those BVMOs was incomplete due to problems expressing some of the BVMOs.<sup>19</sup> In comparison to Szolkowy *et al.*, the Fraaije group was also able to identify one additional BVMO (BVMO24) in the proteome by comparing the protein sequences of PAMO and CHMO with potential BVMOs and completed the gene of another BVMO that had been suggested to lack a large part of the C-terminus (BVMO8). One of the earlier identified BVMOs was discarded from the recent study since it was found to be an FMO (BVMO22; FMOs are human flavin-containing monooxygenases) and BVMO23 was excluded because it only differed in one amino acid from BVMO21. By comparing the sequences of the thus obtained 22 BVMOs, the typical BVMO motifs mentioned above and slightly mutated forms of the fingerprint motif were found in all these BVMOs. Additionally, another motif, which is located between the N-terminal and the BVMO motif, was identified ([A/G]GXWXXXX[F/Y]P[G/M]-XXXD). This motif was supposed to be more suitable for identifying new BVMOs because it contains more conserved residues and allows differentiation between BVMOs and FMOs. Of the 22 investigated BVMOs eight did not show any activity to the substrates tested and five BVMOs converted ten or more substances. Two of these BVMOs (BVMO4 and BVMO24) seemed to be very potent biocatalysts since they accepted a large number of substrates. Their substrate scope was similar to that of cyclopentanone monooxygenase from *Comamonas testosteroni* NCIMB 9872 (CPMO<sub>Coma</sub>). For BVMO9 and 15, the substrate scope was shown to be similar to 4-hydroxyacetophenone monooxygenase from *Pseudomonas fluorescens* ACB (HAPMO<sub>ACB</sub>) as they converted mostly aromatic ketones. In addition to a spectrophotometric assay used for these studies, some of the BVMOs were also analyzed with typical BVMO substrates including prochiral sulfides by GC analyses. Phenylacetone and



**Hendrik Mallin**

immobilization of proteins, protein engineering and plasma techniques for process improvement.

Hendrik Mallin (born 1985) studied biochemistry in Greifswald, Germany. During his diploma thesis in the Bornscheuer group he worked on protein engineering of oxidative enzymes. In 2010 he started his PhD under supervision of Uwe Bornscheuer in which he investigates process development for organic synthesis with oxidative enzymes and transaminases. His research interests include



**Stefan Saß**

Stefan Saß (born 1982) studied biochemistry at the University of Greifswald and obtained his diploma degree in 2009. His PhD thesis under supervision of Uwe Bornscheuer is focused on the establishment of screening systems for Baeyer–Villiger monooxygenases and the application of protein engineering.

bicyclo[3.2.0]hept-2-en-6-one were converted by all BVMOs even though conversions differed somewhat. BVMO8 showed the lowest conversions and BVMO24 differed from the other enzymes with respect to preferred substrate and extent of conversion, and it showed opposite enantioselectivity towards the prochiral sulfides. Hence this study alone substantially extended the number of characterized BVMOs.

A very promising representative of newly available BVMOs is the cyclopentadodecanone monooxygenase (CPDMO) from *Pseudomonas* HI-70. This enzyme was already isolated in 2006<sup>20</sup> when its low protein sequence similarity to the enzymes known at that time was ascertained. While highest catalytic efficiency of this BVMO was detected for cyclopentadecanone, good activity towards large ring ketones (C11–C13) and substituted cyclohexanones was also shown. Later, the enzymes' activity and high selectivity on ketosteroids was confirmed.<sup>21</sup> Recently, extensive profiling of the substrate scope of CPDMO and its revisited integration in the phylogenetic relationship of currently known BVMOs yielded interesting new features of this enzyme.<sup>22</sup> From a present day perspective, CPDMO belongs to a newly identified branch of BVMOs, which was then named after this specific enzyme. Cycloketone- and arylketone-converting enzymes can be found in the vicinity of the CPDMO-branch, whereas these enzymes appear to be separated from the CHMO- and CPMO-clusters. Interestingly, another class of newly identified enzymes, the 1-deoxy-11-oxopentalenic acid monooxygenases, which will later be discussed in detail, also belongs to the CPDMO-branch. For an actual example of a comprehensive phylogenetic tree, we refer to the article by Leipold *et al.* where a newly discovered cycloalkanone monooxygenase from eukaryotic origin is described.<sup>23</sup> CPDMO was shown to oxidize a variety of substituted cyclobutanones and -hexanones as well as fused and bridged bi- and tricyclic ketones. These results were compared to the best-known candidates for the respective compound.<sup>22</sup> Within desymmetrization reactions a similar

substrate scope and identical stereopreference compared to known members of the CHMO-cluster were detected. While conversion and enantioselectivity in general did not exceed other BVMOs like CHMO from *Xanthobacter* sp. ZL5 (CHMO<sub>Xantho</sub>),<sup>24</sup> improved performance concerning sterically demanding substituted cyclohexanones was observed. This however did not pertain to 4-methyl-4-phenyl substituted cyclohexanone, wherefore it was assumed that the ability of CPDMO to oxidize large compounds is not a general feature of this enzyme, but rather restricted to particular substrates.

There are only a few type II BVMOs known and two of them are involved in the camphor degradation pathway of *Pseudomonas putida* ATCC 17453 (identical to NCIMB 10007). These BVMOs were named 2,5-diketocamphane-1,5-monooxygenase (2,5-DKCMO) and 3,6-diketocamphane-1,6-monooxygenase (3,6-DKCMO) and are responsible for the conversion of the two isomers of diketocamphane that are formed through the degradation of (+)- and (–)-camphor.<sup>10,25</sup> The other known type II BVMOs are two FMN and NADH dependent luciferases from *Photobacterium phosphoreum* NCIMB 844 and from *Vibrio fischeri* ATCC 7744 for which a Baeyer–Villiger oxidation of 2-tridecanone and some mono- and bicyclo[3.2.0]-ketones was observed.<sup>26</sup> Moreover, a type II BVMO being involved in the degradation of limonene in *Rhodococcus erythropolis* has been described.<sup>27</sup> Type II BVMOs are of special interest for industrial application since they depend on the cofactor NADH, which is much cheaper than NADPH and therefore the recent identification of the genes encoding the type II BVMOs in the camphor degradation pathway, their recombinant expression and characterization has been a gain for biocatalysis.<sup>12,13</sup> It was shown that the DKCMOs mainly convert bicyclic ketones such as camphor and (±)-*cis*-bicyclo[3.2.0]hept-2-en-6-one, but they are also able to convert monocyclic ketones and α,β-unsaturated monocyclic ketones (Table 1).

However, the great limitation in the efficient application of the DKCMOs is their additional need for a suitable reductase. In contrast to type I BVMOs, where oxygenating and flavin



**Uwe T. Bornscheuer**

In 2008, he received the Biocat2008 Award for his innovative work in biocatalysis and in 2012 the Chevreul Medal for his pioneering work in enzymatic lipid research. His current research interest is focused on protein engineering of enzymes from various classes with special emphasis on applications in organic synthesis.

*Uwe T. Bornscheuer (born 1964) studied chemistry and completed his doctorate in 1993 at the University of Hannover. He then was a postdoc at the University of Nagoya (Japan). In 1998, he completed his Habilitation at the University of Stuttgart and was appointed Professor at Greifswald University in 1999. Bornscheuer edited and wrote several books and is Co-Chairman of the journal Chem-*

**Table 1** Ketones converted by 2,5-DKCMO and 3,6-DKCMO (both crude extract) as determined by GC-analyses<sup>12,13</sup>

Substrate	Conv. <sup>a</sup> (%)	Conv. <sup>b</sup> (%)
(+)-Camphor	66	88
(–)-Camphor	25	91
Cyclobutanone	n.d.	13
Cyclopentanone	n.d.	24
Cyclohexanone	n.d.	3
Acetophenone	n.d.	80
4-Phenyl-2-butanone	n.d.	48
2-Decanone	n.d.	11
Norcamphor	98	77
(±)- <i>cis</i> -Bicyclo[3.2.0]hept-2-en-6-one	100	99
( <i>R,R</i> )-Bicyclo[2.2.1]heptanes-2,5-dione	94	26
2-Cyclopenten-1-one	38	48
3-Methyl-2-cyclopenten-1-one	11	10
2,3,4,5-Tetramethyl-2-cyclopenten-1-one	44	43
2-Cyclohexen-1-one	58	50
3-Methyl-2-cyclohexen-1-one	19	20
3,5,5-Trimethyl-2-cyclohexen-1-one	27	21

<sup>a</sup> With 2,5-DKCMO. <sup>b</sup> With 3,6-DKCMO; n.d. = not determined.



reducing subunits are combined in one polypeptide chain, type II BVMOs need a separate FMN reductase for regeneration of the cofactor. Until now, it is not known how the reduced flavin reaches the monooxygenase active site and if the reductase is bound to the monooxygenase throughout the reaction. Type II BVMOs lack the typical structural features of type I BVMOs such as the fingerprint domain and the GXGXXG-motifs.

The only available structure of a type II BVMO has been determined for 3,6-DKCMO,<sup>28</sup> while there are a few known structures of type I BVMOs. Recently the structure of 2-oxo- $\Delta^3$ -4,5,5-trimethylcyclopentenylacetyl-CoA-monooxygenase (OTEMO) has been published.<sup>11</sup> This enzyme is the third BVMO involved in the degradation of camphor to isobutyrate. Its natural function seems to be the conversion of a cyclopentenylacetyl-CoA derivative, leading to the assumption that it is a suitable biocatalyst for monocyclic ketones. Two separate studies have investigated the biochemical properties and substrate specificity of recombinant OTEMO.<sup>11,12</sup> Kadow *et al.* found that OTEMO prefers bicyclic ketones over monocyclic ketones and that it is a good catalyst for unsaturated cycloketones (Table 2). It was proposed that this is due to the fact that the natural substrate of OTEMO is a CoA-derivative and that possibly the corresponding monocyclic-CoA derivatives would be better accepted. In the work by Leisch *et al.* it was then shown that OTEMO indeed exhibits the highest affinity to the CoA-activated 2-oxo- $\Delta^3$ -4,5,5-trimethylcyclopentenylacetic acid ( $K_M$  18  $\mu$ M) and also converts the CoA-derivative with a higher rate ( $k_{cat}$  4 s<sup>-1</sup>) than the free acid ( $k_{cat}$  0.13 s<sup>-1</sup>).<sup>11</sup> Kinetic parameters were determined for several other substrates as well (Table 2). Additionally, kinetic resolutions of racemic ketones have been performed, revealing a high enantioselectivity (*E*-value) of

OTEMO towards 2-methylcyclopentanone (*E* > 200) in comparison to CHMO from *Rhodococcus* sp. HI-31 (CHMO<sub>Rhodo</sub>), where an *E*-value of only 1.4 was determined. On the other hand *E*-values for cyclohexanone-derivatives were much lower than the ones determined for CHMO<sub>Rhodo</sub>. Desymmetrization reactions with prochiral 4-substituted cyclohexanones showed that OTEMO provides enantiocomplementarity behavior to the CHMO<sub>Rhodo</sub>. Thus, both antipodes of the lactones derived from these prochiral ketones are available when using OTEMO or CHMO<sub>Rhodo</sub>. In contrast to CHMO<sub>Rhodo</sub> and PAMO, OTEMO functions as a dimer. The monomer structure of OTEMO, however, is closely related to the structures of CHMO<sub>Rhodo</sub> and PAMO. The published structure of OTEMO (pdb-code: 3UP5) is the first dimeric structure of a BVMO with bound cofactors.

The first report on fungal Baeyer–Villiger oxidation of steroids over 50 years ago discussed the conversion of progesterone to testolactone in *Penicillium* species and *Aspergillus flavus*.<sup>29</sup> In an actual study, focus was given on the capability of producing steroidal lactones by strains outside the genera *Penicillium* and *Aspergillus*.<sup>30</sup> The soil fungus *Beauveria bassiana* KCH 1065 was chosen because differences in its metabolic pathway of dehydroepiandrosterone (DHEA), androstenedione and progesterone were reported in the literature.<sup>31,32</sup> BVMOs acting on steroids (steroid monooxygenases) in general exhibit a rather narrow substrate spectrum, as they are able to catalyze oxidation of steroidal substrates only. Thereby the most common reaction is the oxidation of the C-17 and/or C-20 carbonyl group in 4-en-3-oxo steroids. The BVMO-activity of *B. bassiana* is distinguished from those enzymes by the fact that it oxidizes solely substrates with an 11 $\alpha$ -hydroxyl group. The presence of the D-lactone without the 11 $\alpha$ -hydroxyl group was not detected. Although this approach provides interesting new insights on BVMO activity in fungal steroid metabolism, the identification of the responsible enzymes and their cloning is strongly awaited as it would render experimental proof on the distinct role of the enzyme in the pathway and this might open a large field of new applications keeping in mind that steroid lactones provide anticancer, antiandrogenic, and antihypercholesterolemic properties.

### Novel BVMOs from eukaryotic origin

Until 2011 all recombinantly produced type I BVMOs have been of prokaryotic origin. The first BVMO from a eukaryotic organism to be cloned and expressed was the cycloalkane monooxygenase (CAMO) from the ascomycete *Cylindrocarpum radiculicola* ATCC 11011.<sup>23</sup> This strain, also known as *Ilyonetria radiculicola* DSM 837, was reported to convert progesterone via androstenedione towards  $\Delta$ 1-dehydrotestolactone.<sup>29</sup> Those Baeyer–Villiger-reactions were supposed to be catalyzed by only one enzyme.<sup>33</sup> Additionally, *C. radiculicola* was known to convert bicyclic ketones representing typical CHMO substrates as well.<sup>34</sup> Leipold *et al.* recently succeeded in identifying a BVMO gene in this strain by CODEHOP PCR. This BVMO showed 46.4% sequence identity to the CHMO from *Rhodococcus* sp. Phil<sup>35</sup> and 44.1% to CHMO<sub>Acineto</sub><sup>36</sup> and was thus claimed to be a CHMO-like BVMO. However, this newly identified BVMO differs from typical known CHMOs. Firstly, the consensus motif in this BVMO is FXGXXHXXWD and not

**Table 2** Conversion of ketones and kinetic data determined for purified OTEMO<sup>11,12</sup>

Substrate	Conv. (%)	$k_{cat}/K_M$ (s <sup>-1</sup> mM <sup>-1</sup> )
(+)-Camphor	44	n.d.
(-)-Camphor	22	n.d.
Cyclobutanone	36	14.7
Cyclopentanone	19	n.d.
Cyclohexanone	19	n.d.
Acetophenone	67	n.d.
4-Phenyl-2-butanone	54	n.d.
2-Decanone	7	n.d.
Norcamphor	96	n.d.
( $\pm$ )-cis-Bicyclo[3.2.0]hept-2-en-6-one	100	49.3
( <i>R,R</i> )-Bicyclo[2.2.1]heptanes-2,5-dione	87	n.d.
2-Cyclopenten-1-one	62	n.d.
3-Methyl-2-cyclopenten-1-one	13	n.d.
2,3,4,5-Tetramethyl-2-cyclopenten-1-one	34	n.d.
2-Cyclohexen-1-one	74	n.d.
3-Methyl-2-cyclohexen-1-one	13	n.d.
3,5,5-Trimethyl-2-cyclohexen-1-one	22	n.d.
OTE-CoA	n.d.	270
2-Oxocyclopentylethylacetate	n.d.	22
2-Oxocyclohexylethylacetate	n.d.	5.6
2-Methylcyclohexanone	n.d.	4
4-Methylcyclohexanone	n.d.	3
2- <i>n</i> -Hexylcyclopentanone	n.d.	430

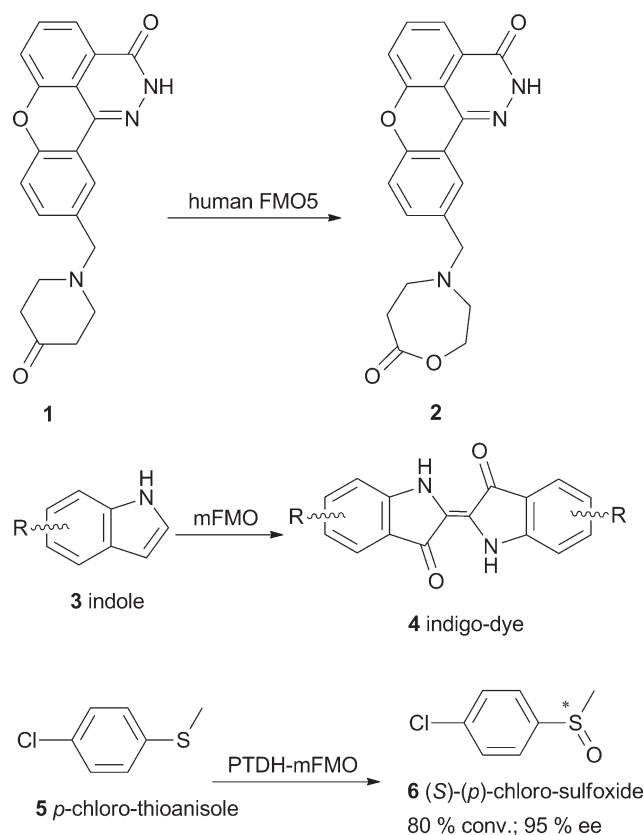
n.d. = not determined, OTE-CoA: 2-oxo- $\Delta^3$ -4,5,5-trimethylcyclopentenylacetyl-CoA.

FXGXXXHXXXWP as was found for certain type I BVMOs like CHMOs and PAMO. Also the temperature at which the enzyme retains half of its initial activity determined for CAMO is with 26 °C significantly lower than for CHMO<sub>Acineto</sub> with 36 °C. Leipold *et al.* suggested that this might be due to a methionine residue (Met57) in close proximity to the reactive C4 atom from FAD, which is not present in CHMOs or PAMO. Additionally, two of the ten residues forming the binding pocket of CAMO differ from the ones found in CHMOs, where all of these residues are conserved. In CAMO, residues 435 and 437 are alanine and phenylalanine, whereas in CHMOs those residues are threonine and leucine, respectively. Since the residues present in CAMO are smaller, leading to a larger binding pocket, the acceptance of a broad range of substrates might be explained. CAMO was shown to convert cycloaliphatic ketones, open-chain ketones and bicyclic ketones. Indeed, the highest  $k_{\text{cat}}/K_{\text{M}}$  value was observed for cyclobutanone. However, CAMO did not convert any of the tested steroids, which means that this enzyme is not responsible for the conversion of progesterone, indicating that there are several BVMOs encoded in the genome of *C. radicola*.

### BVMO-activity of flavin-containing monooxygenases

During the previous years it was thought that BVMOs were fully absent in the genomes of archaea, plants and higher organisms, but recently the performance of Baeyer–Villiger reactions by human enzymes was observed.<sup>37</sup> In that study, the oxidation of a 4-hydroxypiperidine moiety by human flavin-containing monooxygenase 5 (FMO5) in a Baeyer–Villiger reaction was observed. The BVMO-substrate 10-((4-hydroxypiperidin-1-yl)-methyl)chromeno[4,3,2-*de*]phthalazin-3(2*H*)-one (**1**, Scheme 1) is a potential anticancer agent because it acts as an inhibitor of poly(ADP-ribose) polymerase. The apparent oxidation and ring opening of this compound has been observed during preclinical studies on animals. In humans, five FMO isoforms are present that show a tissue-specific distribution while FMO5 occurs in adult human liver and small intestine. Their biological role is the detoxification of drugs and other xenobiotics into more hydrophilic metabolites. Typical FMO-catalyzed reactions are the monooxygenation of heteroatoms such as nitrogen, sulfur, and phosphorus, but the Baeyer–Villiger oxidation of salicylaldehyde to pyrocatechol by human FMO1 and the existence of an almost identical sequence motif in the active sites of FMOs and BVMOs have been shown as well.<sup>15</sup> Due to the identification of the ring-opened hydroxyl carboxylic acid in incubations of hepatocytes from different species, it was assumed that these cells provide the necessary enzymes to first transform the 4-hydroxypiperidine into a ketone by an oxidoreductase and then oxidize this intermediate *via* a Baeyer–Villiger reaction to lactone **2** in liver microsomes. The lactone could afterwards be hydrolyzed to produce the ring-opened acid. This hypothesis was confirmed by investigations using recombinant enzymes.

Inspired by the close homology between FMOs and BVMOs, different typical BVMO-substrates like 2-octanone, cyclohexanone and acetophenone have recently been subjected to mFMO from *Methylophaga* sp. strain SK1.<sup>38</sup> This enzyme aroused researchers' interest because it originates from bacteria and is therefore soluble in contrast to human FMOs, which are often membrane-bound. Although no activity towards the substrates



**Scheme 1** Substrate scope of human flavin monooxygenases and mFMO from *Methylophaga* sp.

mentioned could be detected, the oxidation of indole **3** and analogues into the corresponding indigoid pigment **4**, which represent interesting dyes, was observed (Scheme 1). Moreover, enzymatic sulfoxidation of prochiral sulfides like *p*-chlorothioanisole **5** with excellent enantioselectivity was observed. Although FMOs have only rarely been shown to catalyze typical Baeyer–Villiger oxygenations, their potential use in biotransformation appears interesting due to their dependency on NADH as a cofactor.

Very recently, the BV-oxidation of bicyclo[3.2.0]hept-2-en-6-one by the flavin-containing monooxygenase from *Stenotrophomonas maltophilia* (SMFMO) was described.<sup>39</sup> The 38.6 kDa FAD-containing protein was shown to favor NADH over NADPH as a cofactor and to catalyze the conversion of prochiral aromatic thioethers like *p*-chlorophenyl methyl sulfide with 80% ee of the (*R*)-product. Furthermore, the 3D-structure of SMFMO (Uniprot B2FLR2) was reported in this work. Within FMOs and BVMOs with available structures, the enzyme showing highest sequence similarity to SMFMO was a thio-redoxin reductase from *Thermus thermophilus*, but similarity to PAMO and CHMO<sub>Rhodo</sub> was also observed.

### BVMOs in natural catabolic processes

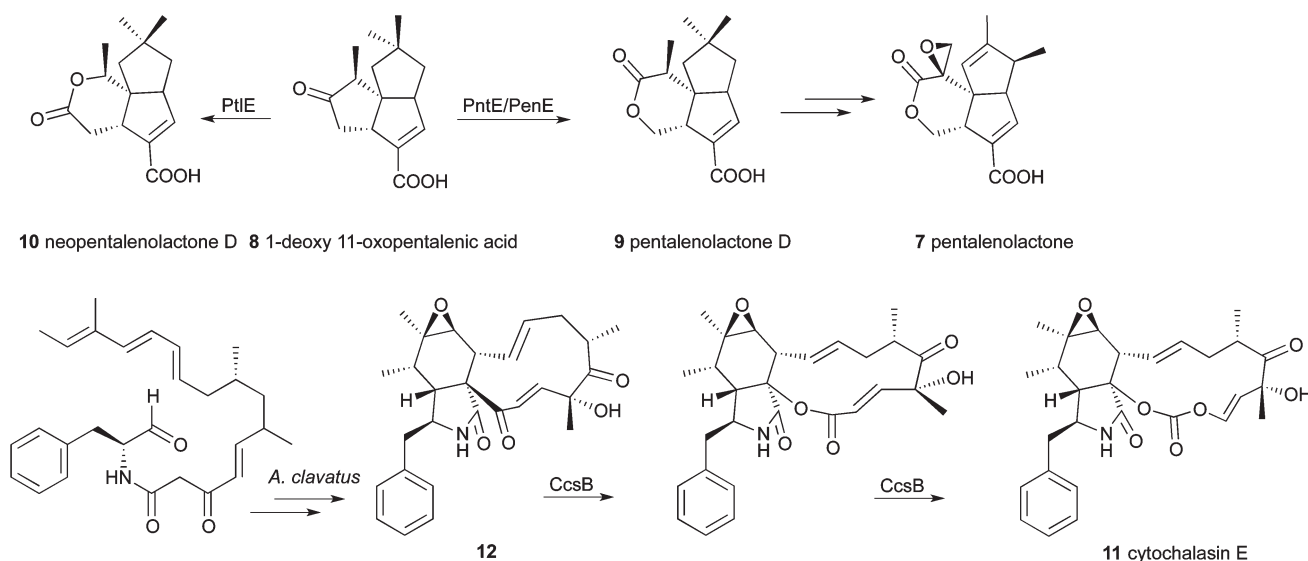
While in the past, the important role of BVMOs in the metabolism of compounds like acetone, bulky cyclic, bicyclic and aliphatic ketones, linear ketones and steroids was shown, recently

the involvement of these enzymes in catabolic pathways was reported.<sup>40</sup> One of the few examples of BVMOs that has been assigned a specific biosynthetic role and a defined substrate are the 1-deoxy-11-oxopentalenic acid-monooxygenases.<sup>41,42</sup> These enzymes are involved in pentalenolactone D and neopentalenolactone D biosynthesis by three different *Streptomyces* species (Scheme 2). The gene clusters responsible for the whole metabolic pathway were cloned and sequenced. Pentalenolactone 7 is a sesquiterpenoid antibiotic, which is active against gram-positive and gram-negative bacteria as well as fungi because of its electrophilic epoxide moiety, which inactivates the glutaraldehyde-3-phosphate-dehydrogenase of those organisms. Pentalenolactone was isolated from numerous *Streptomyces* species. In 2009, a 13.4 kb gene cluster from *Streptomyces avermitilis* was cloned implicating 13 unidirectional ORFs. Among these genes was the putative flavin containing monooxygenase PtlE, which was recombinantly expressed in *E. coli*.<sup>41</sup> Indeed, this enzyme turned out to be a FAD-dependent type I BVMO, catalyzing the Baeyer–Villiger oxidation of 1-deoxy-11-oxopentalenic acid 8 (Scheme 2). Surprisingly, the formation of the expected product pentalenolactone D 9 could not be observed. Instead, the formation of the regioisomer (and the more likely BVMO product) neopentalenolactone D 10 was found. That compound had never been isolated from *Streptomyces* or any other source before and it was concluded that the biosynthetic pathway of pentalenolactone debranches at the BVMO-reaction step and a new path was thereby identified (Scheme 2).

Since wild-type *S. avermitilis* showed the formation of new metabolites of sesquiterpenoids, but not pentalenolactone D itself, the gene clusters of two other representatives of *Streptomyces* species were investigated.<sup>42</sup> The strains *S. arenae* and *S. exfoliatus* were known producers of the desired compound. The relevant ORFs of the pentalenolactone biosynthetic gene clusters of these strains were determined to be not only identical in organization, but also to exhibit a high degree of sequence identity. The PtlE-orthologous enzymes PntE and PenE showed about 80% similarity to the *S. avermitilis* protein

PtlE. They were purchased as codon-optimized synthetic genes and overexpressed in *E. coli* to enable detailed investigations. For both enzymes, the exclusive FAD- and NADPH-dependent formation of the Baeyer–Villiger oxidation product pentalenolactone D (9) from 1-deoxy-11-oxopentalenic acid (8) was proven. PenE and PntE can therefore be considered as paralogues of PtlE, which catalyze the analogous oxidation of the same substrate, but yield the regioisomeric product. All three enzymes were found to be highly regio-specific. From mutational analyses, it was concluded that the N-terminal region, especially the region around the FAD-binding motif, influences the regio-specificity of the Baeyer–Villiger oxidation. Regarding the advantage of the availability of a catalyst for the formation of each regioisomer of a sesquiterpenoid, application of these enzymes in organic synthesis approaches seems promising.

Lately, researchers detected further strong hints for the contribution of another BVMO in a catabolic process. The intended study of the 30 kb *ccs*-gene cluster responsible for the biosynthesis of cytochalasin E (11) by *Aspergillus clavatus* NRRL 1 furthermore reports on BVMO activity in a eukaryote.<sup>43</sup> Cytochalasins belong to secondary metabolites of the fungus and are of significant value because of their complex molecular structure and bioactivity (Scheme 2). The sequenced genome of *A. clavatus* NRRL 1 was searched for genes encoding a hybrid iterative type I polyketide synthase–nonribosomal peptide synthetase (PKS–NRPS). Next to a putative hit, which was identified, additional genes possibly involved in cytochalasin biosynthesis were observed. Based on the deduced gene functions of the *ccs* gene cluster, the biosynthetic pathway for cytochalasin E and K was proposed. It comprises, amongst others, six oxidative steps including two hydroxylations, one alcohol oxidation, one epoxidation and two Baeyer–Villiger oxidations. The enzyme responsible for the latter steps (CcsB) was assumed to be located directly downstream of the PKS–NRPS gene, because the ORF revealed about 25% identity to CHMO<sub>Acineto</sub> and CPMO<sub>Coma</sub>. Moreover, it exhibits high sequence identity towards the recently characterized CPDMO from *Pseudomonas* sp. HI-70 (41%).



**Scheme 2** Involvement of BVMOs in the biosynthetic pathways of pentalenolactone and cytochalasin E.



It was found that CcsB contains the two intact conserved Rossmann fold motifs GxGxxG and GxGxxA, as well as the BVMO fingerprint. The 11-membered carbocyclic intermediate **12** resembles a very large BVMO substrate and the presumed ability of CcsB to convert it coincides with its close relation to CPDMO, which is capable of lactonizing C15 cycloketones. The fact that no additional genes encoding BVMO-like enzymes are located in the *ccs* cluster led the authors to the assumption that CcsB might be responsible for two consecutive Baeyer–Villiger oxidations resulting in compound **11**. Since there are only slight hints available in the literature, experimental confirmation of this hypothesis is still required.

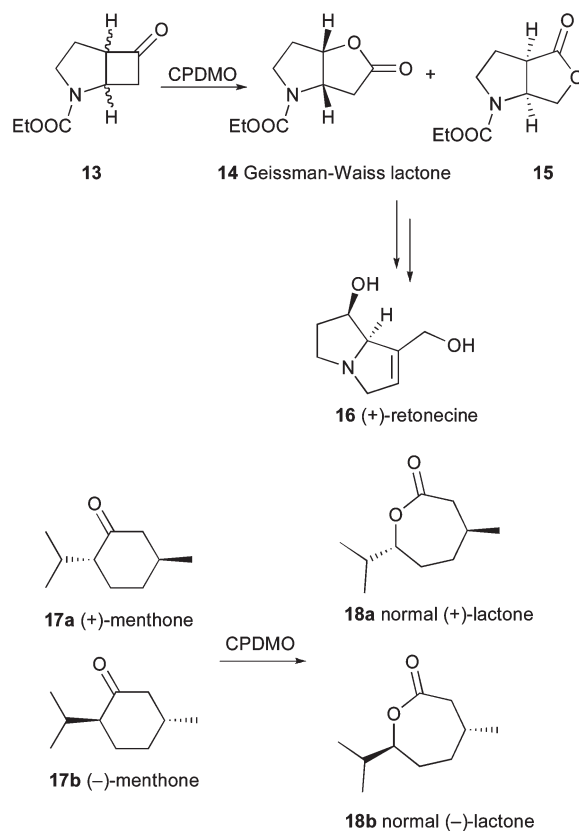
## Novel synthetic applications

The overwhelming diversity of catalytic properties of BVMOs permits access to many different classes of valuable chemicals. An overview about the huge number of examples can be found in recent reviews.<sup>1–5</sup> Recent studies reveal further powerful examples of the broad synthetic utility of these enzymes often leading to compounds one would not consider as products of a typical BVMO-mediated oxidation.

The identification of CPDMO from *Pseudomonas* sp. HI-70 was discussed earlier in this perspective. As a valuable application, Fink *et al.* showed that CPDMO-catalyzed kinetic resolutions of racemic substituted cyclopentanones yielded full conversion to racemic lactones whereas it was possible to selectively oxidize only the (–)-enantiomer of 2-methylcyclohexanone to the normal lactone with  $E = 41$ .<sup>22</sup> This behavior has only been observed for CDMO from *Rhodococcus ruber* CD4 (CDMO<sub>Rhodo</sub>) before. 2-Substituted cycloheptanones were not accepted by CPDMO. Regiodivergent transformation of the N-heterocyclic bicyclic ketone **13** led to formation of products distinct from a tested collection of ten BVMOs from various microbial origin and provided access to the antipodal Geissman–Waiss lactone (*S,S*)-**14** as well as the abnormal product (*R,S*)-**15** in a 50 : 50 mixture (Scheme 3). This means that the non-natural enantiomer of the naturally occurring alkaloids retronecine **16** and other necine bases are accessible *via* this chiral intermediate. Another non-conformity between CPDMO and CHMO-type BVMOs was observed for the conversion of menthone **17**, where no regio-divergence was observed. Instead, both enantiomers (**17a** and **17b**) were oxidized to the optical antipodes (**18a** and **18b**). In conclusion, this approach discovered a number of novel biooxygenations extending the substrate scope within the BVMO family.

### Aliphatic ketones

Until a few years ago, BVMOs were investigated mostly for the conversion of mono- and bicyclic ketones, camphor, a few aryl-aliphatic ketones and some steroids. More recently, it was discovered that BVMOs also catalyze the oxidation of aliphatic ketones to the corresponding esters. This also identified a possible physiological role of BVMOs. As was described for the BVMO from *Pseudomonas fluorescens* DSM 50106, a cascade of enzymes was found to be encoded in an operon including an alkane hydroxylase, an alcohol dehydrogenase, the BVMO and

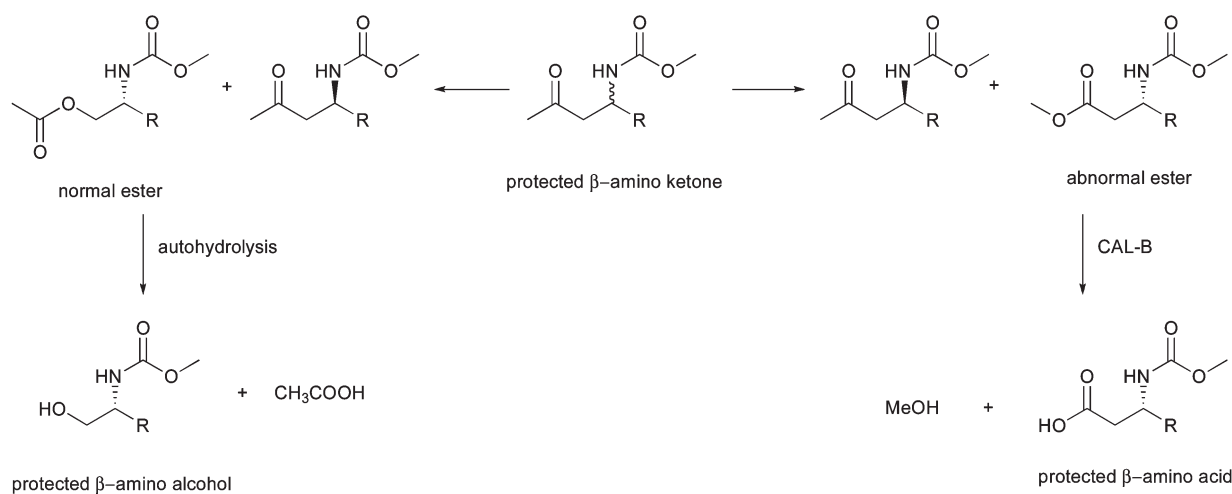


**Scheme 3** CPDMO from *Pseudomonas* sp. HI-70 provides access to the Geissman–Waiss lactone and is able to oxidize menthone.

an esterase presumably being involved in the degradation of alkanes and thus enabling *Ps. fluorescens* growth on this carbon source.<sup>44</sup> A similar pathway was later also found in *Ps. putida* KT2440.<sup>45</sup>

It has been shown that not only simple aliphatic ketones are accepted as substrates, but that also  $\beta$ -hydroxy-substituted linear aliphatic ketones are oxidized in an enantioselective manner by eleven BVMOs of different bacterial origin and especially those of the CHMO-type.<sup>46</sup> This observation is synthetically very useful as the kinetic resolution of these racemic compounds provides access to chiral  $\beta$ -hydroxyesters, which undergo acyl migration and ester hydrolysis by the whole-cell biocatalyst. This leads to the formation of optically pure 1,2-diols, which are valuable compounds in the synthesis of polyesters and antimicrobial agents. Moreover, the enantioconvergent conversion of racemic substrates by different enzyme candidates was observed.

Recently, the potential of BVMOs to form the abnormal ester of N-protected  $\beta$ -amino ketones was described. Coupling of a lipase for hydrolysis of the resulting ester provided access to enantiopure  $\beta$ -amino acids under mild reaction conditions<sup>46</sup> (Scheme 4). This new enzymatic route also grants access to N-protected  $\beta$ -amino alcohols. In this recent approach, whole-cell experiments with 16 BVMOs from various bacterial strains were investigated for their acceptance of protected 5-amino-3-one as substrates in the kinetic resolution mode. This revealed that four enzymes (a CHMO from *Arthrobacter* BP2 (CHMO<sub>Arthro</sub>), a CHMO from *Brachymonas petroleovorans*



**Scheme 4** Enzymatic Baeyer–Villiger oxidation of protected  $\beta$ -amino ketones provides access to  $\beta$ -amino alcohols and  $\beta$ -amino acids.

(CHMO<sub>Brachy</sub>) and CHMO<sub>Xantho</sub> as well as CDMO<sub>Rhodo</sub>) showed activity. Interestingly, the non-protected amino alcohols were not converted by any enzyme. When biocatalysis was performed in 24-well microtiter plates, all four enzymes formed roughly 1 : 1 ratios of normal and abnormal products and all were obtained with excellent enantioselectivity with *E*-values > 200 except for the formation of the normal ester by CDMO, where 81% ee was measured. Interestingly, the ratio of regioisomers formed turned out to be dependent on reaction conditions, which amongst other factors was explained by the availability of oxygen as higher conversion of the substrate was observed, when the reaction was performed under conditions with improved oxygen supply. Due to their pharmaceutical relevance in the synthesis of  $\beta$ -peptides, alkaloids, terpenoids and  $\beta$ -lactam antibiotics,  $\beta$ -amino acids represent desirable compounds for organic synthesis. Because of their enhanced stability towards human proteolytic enzymes, these compounds are particularly interesting for the design of drugs.

This collection of enzymes was also used in a subsequent study to investigate the formation of  $\beta$ -amino alcohols, which are of great pharmaceutical interest because this motif occurs in many different drugs.  $\beta$ -Amino alcohols are difficult to access in enantiopure form by chemical means and only a few enzymatic methods for the synthesis of these compounds have been described before. Rehdorf *et al.* investigated the conversion of linear aliphatic, branched linear and arylaliphatic  $\beta$ -amino ketones.<sup>47</sup> Whole cell preparations of ten BVMOs converted these racemic N-protected compounds. Throughout the linear aliphatic substrates, the CHMO-type enzymes preferred the medium chain length (C8) and conversion decreased dramatically when the chain length was increased to 12 carbon atoms. A complementary trend was observed for HAPMO<sub>ACB</sub> and CDMO, which have been known to prefer structurally demanding ketones. Detailed analyses of the relationship between time and enantiomeric excess at approximately 50% conversion revealed that the C8 aliphatic  $\beta$ -amino ketone was converted the fastest by CHMO<sub>Brachy</sub> with  $E > 200$ . Similar results were obtained for CHMO<sub>Xantho</sub> and CDMO<sub>Rhodo</sub> for chain lengths of 10 carbons. The branched chain aliphatic  $\beta$ -aminoketones were converted with moderate activity, but enantioselectivity was poor

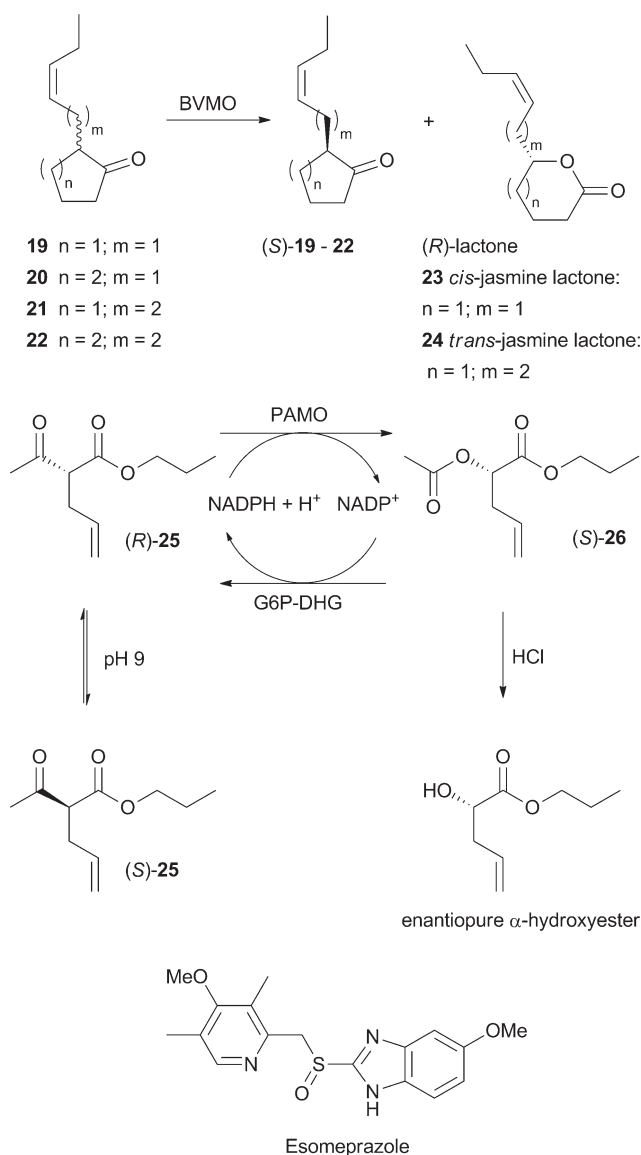
except for CHMO<sub>Arthro</sub> ( $E > 200$ ). For these substrates it was observed that the opposite enantiomer is converted by almost all tested enzymes when the side chain and the keto-function were separated by one more carbon. For the aryl-aliphatic substrate, high activity was observed for almost all enzymes, but only PAMO and cyclohexanone monooxygenase from *Brevibacterium* sp. HCU (CHMO<sub>Brevi</sub>) showed good enantioselectivity. An alignment of the amino acid sequences of seven enzymes active towards arylaliphatic ketones led to the identification of a loop segment, which occurs in PAMO, CDMO and CHMO<sub>Brevi</sub> and is missing in the other CHMOs. The two amino acids reduce the size of the binding pocket in PAMO and this could therefore explain the high enantioselectivity observed.

The  $\beta$ -amino alkylesters formed by the BV-oxidation underwent spontaneous hydrolysis due to the increasing pH in the whole-cell system and hence the N-protected optically active  $\beta$ -amino alcohol became accessible. Regarding the possibility to regulate which product enantiomer will be formed by choice of the appropriate enzyme as catalyst, BVMOs were shown in the recent work by Rehdorf *et al.* to be an essential tool in the synthesis of chiral compounds and even offer access to unexpected compounds like 1,2-diols,  $\beta$ -amino alcohols or  $\beta$ -amino acids.

The strategy of subjecting the entire BVMO collection to a set of compounds was used by the group of Mihovilovic who thus succeeded in the identification of two enzymes for the kinetic resolution of 2-substituted cycloketones.<sup>48</sup> The recovered substituted chiral  $\delta$ -valerolactones and  $\epsilon$ -caprolactones are known as flavor and fragrance compounds. They have been identified in plants like jasmine ((*R*)-**23**), agaves ((*S*)-**23**) as well as natural mango aroma (Scheme 5). In the screening step seven enzymes from known cycloketone-converting BVMO families were identified, which readily transformed substrates **19–22** into the expected lactones with the same regio- and enantioselectivity at 50% conversion. CHMO<sub>Arthro</sub> showed excellent enantioselectivity in the resolution of **19–21** and CDMO<sub>Rhodo</sub> for **22**. This work resembles the first example of BVMOs employed in the preparation of aroma lactones.

The pallet of compounds contrivable by BVMOs was recently widened by a dynamic kinetic resolution (DKR) approach. In this study, aliphatic acyclic  $\alpha$ -substituted  $\beta$ -keto esters were





**Scheme 5** Application of BVMOs in the synthesis of aroma compounds, DKR of  $\alpha$ -substituted  $\beta$ -keto esters and production of the drug Esomeprazole.

subjected to PAMO, its mutant M446G and CHMO<sub>Acinetobacter</sub><sup>49</sup> with spontaneous racemization of the starting material at pH 9. Although the BVMOs chosen normally exhibit substrate preferences for aromatic ketones, the aliphatic acyclic racemic  $\alpha$ -alkyl  $\beta$ -ketoesters were also accepted albeit with low conversion by the PAMO mutant. In a DKR with **25** complete conversion to **26** was found after 24 h (Scheme 5). Selective hydrolysis of the diesters was performed chemically using catalytic amounts of hydrochloric acid and resulted in enantiopure  $\alpha$ -hydroxyesters, which are widely applicable in the pharmaceutical production of anticancer drugs and antibiotics as well as in the food industry.

### Heteroatom-substituted compounds

In addition to the broad number of compounds accessible with BVMOs through the oxygenation at a keto moiety, the

oxygenation of heteroatoms like sulfur, nitrogen, phosphorus, boron and selenium widens the applicability of this enzyme class. In one approach, achiral aromatic and vinylic boron compounds as well as racemic ones have been evaluated as target substrates where oxidation aiming at the carbon–boron bond would afford the corresponding alcohols by elimination of boronic acid.<sup>50</sup> Five different acetophenone derivatives bearing boron substituents at the *m*- or *p*-position were employed. PAMO, its mutant M446G, HAPMO<sub>ACB</sub> and CHMO<sub>Acinetobacter</sub> were chosen as biocatalysts. PAMO and its mutant were equally chemoselective for the boron oxidation of all substrates affording the corresponding phenols, but mutant M446G showed lower activity. In HAPMO-catalyzed reactions boron oxidation as well as BV-oxidation was observed. CHMO showed high chemoselectivity in favor of boron oxidation, but low activity. Using this enzyme, only the 3- or 4-hydroxyacetophenones were afforded, but at poor conversions. Moreover, the oxidation of vinyl boron compounds was explored in that work to evaluate the chemoselectivity between boron oxidation and a possible epoxidation reaction, which has previously been described.<sup>51,52</sup> Thereby, aliphatic vinylic boron compounds turned out to be no substrates for the chosen catalysts, but aromatic substrates of this class were oxidized exclusively at the boron and no epoxidation was observed at all. M446G was furthermore applied to evaluate the enzymatic kinetic resolution of a chiral boron-compound. It was observed that exclusively the (*S*)-borane was transformed into the corresponding (*S*)-alcohol with high enantiomeric excess. These results are valuable since boron-containing compounds are versatile intermediates in synthetic organic chemistry. The same is true for organo selenoxides, which find application as mild oxidation reagents and catalysts in hydrogen peroxide activation, therefore a further study was aimed at evaluating the chemoselectivity of PAMO in the biooxidation of organoselenium acetophenones.<sup>53</sup> Conversion of acetophenone derivatives bearing selenide substituents at all three possible positions on the aromatic ring yielded the corresponding selenoxides in high conversion after 24 h while PAMO was chemoselective by only catalyzing selenium oxidation.

In addition, a Baeyer–Villiger monooxygenase was engineered by the company Codexis Inc. for a sulfoxidation to yield the drug Esomeprazole (Scheme 5). Protein engineering was used to invert the enantiopreference and to improve the enzyme with respect to activity, stability, and chemoselectivity.<sup>54</sup>

### Limitations of BVMO-catalyzed reactions

Although a variety of new biocatalysts have been identified during recent years and novel synthetic applications have been shown, still a number of drawbacks have to be overcome to enable the use of most BVMOs on an industrial scale. One of the major obstacles is the limited stability, low substrate and hence product concentrations, adequate oxygen transfer as well as tolerance of organic cosolvents.<sup>55</sup> To circumvent these limitations several strategies have been developed during the last years.

### Optimization of biotransformation conditions

The addition of a water miscible organic solvent to improve substrate solubility is often encountered with reduced enzyme

stability. In a recent study the stability and activity of PAMO and CHMO<sub>Acineto</sub> in the presence of organic solvents such as methanol, ethanol, 1,4-dioxane, acetonitrile and 1,1,1-trifluoro-ethanol were analyzed.<sup>56</sup> PAMO turned out to be significantly more stable than CHMO<sub>Acineto</sub> concerning the percentage of solvent added as well as the long-term stability at given concentrations. Interestingly, the addition of 20% methanol resulted in an about five-fold increase of PAMO activity while CHMO<sub>Acineto</sub> activity was only 1.2-fold higher at a maximum of 2% methanol. Fluorescence data and circular dichroism analyses indicated that the decrease in catalytic activity for both enzymes at increasing concentrations of organic solvent was caused by a loss in tertiary and secondary structures. Computational comparison of PAMO and CHMO structures identified the number of salt bridges in both enzymes, which are known to increase the protein thermal stability. So the higher amount of salt bridges in PAMO (41) compared to CHMO<sub>Acineto</sub> (31 or 20 depending on whether the closed or the open form model was used) also seems to enhance the stability of the BVMOs in water–organic solvent mixtures.<sup>56</sup> Another approach aimed at analyzing substrate acceptance and enantioselectivity of the PAMO mutant M446G in the presence of varying concentrations of hydrophilic organic solvents.<sup>57</sup> In the oxidation of benzyl methyl sulfide, the addition of 10% PEG or MeOH led to an almost complete formation of the sulfoxide whereas in EtOH, iPrOH or CH<sub>3</sub>CN the sulfone was the major product. Cyclohexyl propyl sulfide and *rac*-2-phenyl-3-heptanone could only be oxidized to the corresponding sulfone and ester in the presence of an organic solvent. In a DKR, the addition of 5% MeOH enabled up to 90% conversion of *rac*-3-phenylbutan-2-one with Lewatit MP62 (89% ee of the product) and for various benzylketones also high yield and optical purity could be achieved.<sup>57</sup>

The addition of water-immiscible organic solvents creates a biphasic system, which on the one hand acts as a substrate reservoir and on the other hand as an extraction medium for *in situ* product removal from the aqueous phase. Thus, both the substrate and the product concentration can be kept below inhibitory levels and therefore the biocatalyst can be stabilized significantly by the addition of the cosolvent for a longer period of time.<sup>58</sup>

Alternatively, ionic liquids (ILs) can be used instead of organic solvents. The advantage of ILs is that the polarity, hydrophobicity, viscosity and solvent miscibility can be tuned by altering the type of cation and anion. This allows the design of media for different purposes.<sup>59</sup> It was found that besides their expected solvent properties, ILs can have a particular impact on enzyme activity and selectivity. In a recent study the PAMO-catalyzed kinetic resolution of *rac*- $\alpha$ -acetylphenylacetone nitrile was investigated. Employment of the IL [bmp]PF<sub>6</sub> reduced the formation of the by-product phenylacetone nitrile from 56 to 3% while the yield of the BVMO product could be increased from 4 to 48% with excellent optical purity of >99% ee. Additionally, the space-time-yield could be improved by increasing the substrate concentration from 10 to 120 mM. Unfortunately, PAMO was inactivated in the presence of IL after 72 h.<sup>59</sup>

In addition, it was shown for PAMO that also the buffer system and the ionic strength had a strong influence as exemplified in the kinetic resolution of *rac*-3-phenylbutan-2-one. Tris- and phosphate buffers gave best results leading to fast conversion of the substrate and an excellent *E* = 120. Other buffer

systems either led to faster product formation, but reduced enantioselectivity or extremely slow conversion.<sup>60</sup> This phenomenon might be explained by neutralization of electrostatic interactions on the protein surface due to high salt concentrations that finally affect the protein structure.<sup>61</sup>

As most BVMOs require reduction equivalents and the stoichiometric addition of the cofactor NAD(P)H is expensive, an efficient cofactor regeneration system is needed. Besides the use of a whole cell system with ‘integrated’ cofactor recycling by the addition of glucose, the PAMO-catalyzed oxidation of phenylacetone was explored with isolated enzymes coupled to several enzymatic cofactor recycling systems such as glucose/GDH,<sup>62</sup> glucose-6-phosphate/G6PDH,<sup>63</sup> iPrOH/TBADH,<sup>64</sup> sodium phosphite/PTDH or using a fusion protein (CRE2-PAMO).<sup>65–68</sup> The use of glucose dehydrogenase (GDH) at pH 8.0 and 30 °C and glucose-6-phosphate dehydrogenase (G6PDH) at pH 9.0 and 30 °C exhibited highest productivities (~40 mmol mL<sup>-1</sup> h<sup>-1</sup>) similar to the phosphite dehydrogenase (PTDH) system. The alcohol dehydrogenase (TBADH) gave poor results. Highest total turnover number and turnover frequency were observed in the presence of only 2  $\mu$ M NADPH. Interestingly, the PTDH and the G6PDH systems also gave higher selectivity (*E* > 100 for *rac*-3-methyl-4-phenylbutan-2-one) but rather slow conversion, whereas with GDH faster conversion but lower selectivity was observed.<sup>60</sup> Similar results were observed for the oxidation of thioanisole to the corresponding (*S*)-methyl phenyl sulfoxide.

### Substrate feeding and product removal approaches

The use of whole cells of the microorganism expressing the BVMO of interest has the advantage that cofactor regeneration is substantially facilitated. However, whole cell biocatalysts are more sensitive to the addition of cosolvents and especially high substrate or product concentrations, which also affect the performance of isolated enzymes. For example, CHMO<sub>Acineto</sub> has been shown to be inhibited by concentrations of 3 mM of *rac*-bicyclo[3.2.0]hept-2-en-6-one as the substrate and 36 mM of the resulting two lactones, respectively.<sup>69</sup> A couple of further examples were published by the group of Woodley<sup>70</sup> and are covered in a recent review.<sup>1</sup>

One strategy to circumvent biocatalyst inactivation by critical substrate concentration is the continuous feeding aiming to maintain the substrate concentration below an inhibitory level.<sup>71,72</sup> A further strategy focuses on an appropriate *in situ* removal of the product formed.<sup>73</sup> Combining both approaches leads to the *in situ* SFPR (substrate feed and product removal) concept that has been utilized in several studies.<sup>74,75</sup> While most published examples employ the CHMO<sub>Acineto</sub><sup>74,76</sup> only one example used HAPMO from *Ps. putida* JD1.<sup>77</sup> In this study the scale-up as well as the *in situ* SFPR strategy were investigated for the kinetic resolution of 3-phenyl-2-butanone, which served as a chiral model substrate for this enzyme.<sup>78</sup> First attempts with 1.4 mM substrate gave 45.6% conversion with excellent optical purity of the product (99.2% ee) and *E* > 100.<sup>77</sup> Already at 5.4 mM the conversion dropped drastically due to the lack of proper oxygen supply, which could be simply overcome by changing the reaction vessel. In order to further increase the substrate

concentration, various adsorption resins were investigated and Dowex® Optipore® L-493 and Lewatit® VP OC 1064 MD PH gave the best results if an optimal ratio between the resin and the substrate is ensured. This resulted in 39% (Dowex®) and 45% (Lewatit®) conversion at substrate concentrations >26 mM. Hence, variation of type and concentration of the resin enabled optimal conditions avoiding inhibition at higher substrate and product levels.

## Immobilization of BVMOs

As outlined above, the application of BVMOs in industrial processes is still hampered by several factors. Immobilization of the biocatalysts (Table 3) can circumvent stability issues and facilitate enzyme recovery, but can also enable easier cofactor regeneration if the recycling enzyme is co-immobilized. Although free enzymes can be recycled by ultrafiltration, in the case of BVMOs the low mechanical stability usually prevents this method as shown by Zambianchi *et al.* for the oxidation of bicyclo[3.2.0]hept-2-en-6-one (5 g L<sup>-1</sup>).<sup>64</sup> 125 U of CHMO and 125 U of the alcohol dehydrogenase from *Thermoanaerobium brockii* (TBADH) were used in repeated batches (each 24 h) with recycling by membrane filtration. After three cycles only 40% conversion was reached and it was shown that this activity loss was due to the inactivation of CHMO<sub>Acineto</sub> during the

process. As is typical in enzyme immobilization, the identification of the best carrier and immobilization method is a rather tedious trial and error task. The first reported immobilization of a BVMO was the entrapment of the CHMO<sub>Acineto</sub> in a polyacrylamide gel.<sup>79</sup> The cofactor regeneration was realized with the G6PDH system, which was separately entrapped in the polyacrylamide gel. The immobilized preparations were used for the biooxidation of different cyclic ketones with concentrations ranging between 40 and 100 mM in a 1 L reaction volume. Within five to ten days it was possible to isolate between 75 and 89% of pure lactones. For the conversion of 2-norbornanone the retained activity of CHMO was 77% and for G6PDH 80%. Co-immobilization of CHMO and G6PDH was tried by attachment on glyoxyl-agarose coated with polyethyleneimine (PEI).<sup>80</sup> The immobilized CHMO<sub>Acineto</sub> showed a broader pH profile in the conversion of 2-oxocyclohexyl acetic acid to the corresponding lactone and the temperature optimum was increased by 5 °C, however the method was not very efficient as only 0.26 U g<sub>Support</sub><sup>-1</sup> could be attached to the surface and large amounts of NADPH were required. The activity of the immobilized cofactor regenerating enzyme was not experimentally confirmed. Another co-immobilization of CHMO<sub>Acineto</sub> was done with the TBADH on Eupergit® C. The immobilized enzymes showed good stability during oxidation of thioanisole (80% conversion after 17 batches, each 24 h) or bicyclo[3.2.0]hept-2-en-6-one (80% conversion after 4 batches, each 24 h). Recently,

**Table 3** Selected examples for immobilization of Baeyer–Villiger monooxygenases

Enzyme	Amount of biocatalyst	Substrate	Conc. (mM)	Support (binding mode)	Reaction time	Conv. (%)	Comment	Ref.
CHMO <sub>Acineto</sub> <sup>a</sup>	50 U CHMO	2-Norbornanone	100	Polyacrylamide	5 d	100	30% immobilization yield (by protein concentration); CHMO recovered with 77% activity (after complete conversion of 2-norbornanone); G6PDH entrapped separately	79
	100 U G6PDH	L-Fenchone	100	Gel (entrapping) <sup>c</sup>	8 d	100		
		D-Fenchone	100		10 d	100		
		(+)-Camphor	50		10 d	n.r.		
CHMO <sub>Acineto</sub>	10 U	(+)-Dihydrocarvone	40	Eupergit® C (Covalent) <sup>f</sup>	10 d	n.r.	80% conversion in 17th cycle (thioanisole); 80% in 4th cycle (bicyclo[3.2.0]hept-2-en-6-one); half-life at 25 °C increased 2.5-fold	64
		Thioanisole	38 <sup>d</sup>		24 h	100		
		Bicyclo[3.2.0]hept-2-en-6-one	46 <sup>d</sup>		24 h	100		
CHMO <sub>Acineto</sub>	n.r.	(2-Oxocyclohexyl) acetic acid	n.r.	PEI coated glyoxyl-agarose (adsorption) <sup>e</sup>	24 h	67	G6PDH activity experimentally not confirmed; T <sub>opt</sub> +5 °C; pH <sub>opt</sub> broader; γ-irradiation improves stability; 0.26 U g <sup>-1</sup> for cyclohexanone	80
PAMO	20 mg	Phenylacetone	~9.5 <sup>d</sup>	Polyphosphazene (covalent) <sup>e</sup>	24 h	n.r.	Low recovered activity on support; 80% activity loss after 5 cycles; co-immobilization: 3.2 U g <sup>-1</sup>	81
CRE2-PAMO	n.r.	Phenylacetone	2.5	Peroxisome (encapsulation) <sup>e</sup>	15 h	100	CRE2-PAMO higher activity then co-encapsulation of both enzymes; activity reduced	82
CPMO <sub>Coma</sub> <sup>a</sup>	n.r.	8-Oxabicyclo[3.2.1]oct-6-en-3-one <sup>b</sup>	5.7	Polyelectrolyte complex capsule (encapsulation)	48 h	91	5-fold lower activity compared to free cells; 94% cells viable after encapsulation; 0.12 U g <sup>-1</sup> cells; storage stability improved	83
CHMO <sub>Acineto</sub> <sup>a</sup>		rac-Bicyclo[3.2.0]hept-2-en-6-one <sup>c</sup>	1.85	Polyelectrolyte complex capsule (encapsulation)	12 h	77	0.12 U g <sup>-1</sup> cells; 14th cycle; storage stability improved	108

<sup>a</sup> Whole cells. <sup>b</sup> Oxygen aeration. <sup>c</sup> Bubble free oxygen aeration and continuous flow reactor. <sup>d</sup> Reaction volume ≤2 ml; cofactor recycling with <sup>e</sup> G6PDH (glucose-6-phosphate dehydrogenase) or <sup>f</sup> alcohol dehydrogenase from *Thermoanaerobium brockii*; n.r. not reported.



PAMO was immobilized with G6PDH on a polyphosphazene support and used for the oxidation of phenylacetone,<sup>81</sup> but the recovered activity on the support and the stability were rather low. Another example for PAMO used encapsulation in peroxisomes.<sup>82</sup> The authors could show that the fusion enzymes CRE2-PAMO showed higher activity than the single co-encapsulated enzymes. Nevertheless, the encapsulated CRE2-PAMO showed decreased activity compared to the soluble enzymes, which was explained by diffusion problems. Until now no immobilization system could be identified, which leads to a highly active and stable biocatalyst with satisfying performance. Whole cell immobilization was shown for *E. coli* cells expressing CPMO<sub>Coma</sub> in polyelectrolyte complex capsules (PEC) used for the oxidation of 8-oxabicyclo[3.2.1]oct-6-en-3-one.<sup>83</sup> The encapsulation process was visualized using confocal laser scanning microscopy (CLSM) and around 94% of cells were viable. The encapsulated cells showed significant improvement of storage stability, but a 5 times lower activity (0.12 U g<sup>-1</sup> cells) compared to free cells. During biooxidation, the immobilized cells showed the same conversion (over 90%) of the ketone after 48 h with comparable enantioselectivity to the free cells, but reusability was not reported. For the encapsulation of *E. coli* cells with CHMO<sub>Acineto</sub> in PEC a recycling and storage stability study showed that the cells showed high stabilization benefits due to the encapsulation. The cells could be reused for 14 repeated biotransformations of *rac*-bicyclo[3.2.0]hept-2-en-6-one (each 12 h) with a starting conversion of 77% in the first and 75% conversion in the 14th cycle. The storage ability of the cells was increased drastically with conversions of 80% after 60 days and 50% after 91 days. These approaches show the potential for encapsulation of BVMO expressing whole cells ensuring a high stabilizing effect. However, until now encapsulation in PEC matrixes is limited by the low activity of the entrapped cells, which appears to be unsuitable for industrial application. Diffusion problems and limited oxygen supply could be one explanation for these low activities.

Recently, a new expression system in *Corynebacterium glutamicum* for CHMO<sub>Acineto</sub> was established, overcoming substrate inhibition of cells and enabling high productivity during fed batch biotransformation.<sup>84</sup> The high conversion was explained by a more efficient cofactor regeneration system.<sup>85</sup> To circumvent diffusion problems through the cell wall, permeabilization was achieved with ethambutol.<sup>86</sup> For molecules >170 g mol<sup>-1</sup>, the affinity could be increased by 30%, which indicates a permeabilized cell wall. These new host cells hence appear to be a more suitable system to overcome the low activity of entrapped cells.

## Crystal structures of BVMOs

Since 2011, different 3D-structures of PAMO<sup>88</sup> and the newly characterized OTEMO were solved.<sup>11,12</sup> Orru and coworkers crystallized PAMO during different steps of BVMO catalysis with a focus on the structural mechanism of the oxidation process (Table 4, Fig. 1). The snapshots provided deep insights into the PAMO structure with bound FAD/NADPH and the enzyme in its oxidized and reduced form. For the oxidized wild-type with bound FAD and NADP<sup>+</sup>, the authors predicted that

NADPH binds near the flavin N5 atom for hydride donation as it was described for CHMO<sub>Acineto</sub>.<sup>89</sup> Then the NADP<sup>+</sup> slides over to the flavin and stabilizes the flavin (hydro)peroxide. With a reduced form of the wild-type enzyme they gained insight into the flavin-peroxide formation. The carboxamide group from NADP<sup>+</sup> forms a H-bond to the N5 atom of the reduced flavin to prevent intermediate collapse of the flavin (hydro)peroxide. In contrast, in the oxidized form the crucial R337 residue forms H-bonds to the nicotinamide and interacts with D66. In the reduced enzyme state R337 moves to the pyrimidine moiety of the flavin ring and can interact with the negatively charged reduced flavin. Due to this movement Orru and coworkers predicted that flavin is accessible to O<sub>2</sub> to form the flavin (hydro)peroxide. The flavin (hydro)peroxide shifts back and interacts with the nicotinamide – because of the loss of the negative charge – and the active site becomes accessible. With the mutant D66A the authors could show that R337 directs the substrate into the active site. In the snapshot (pdb-code: 2YLT) they demonstrated that R337 had two functions, which is first the increased nucleophilic attack against the flavin peroxide and second that it compensates the negatively charged Criegee intermediate. Mutant R337K confirmed that the enzyme in its oxidized form can still form a stable Criegee intermediate. In its reduced form, the mutant could still bind 2-(*N*-morpholino)-ethanesulfonic acid (MES) despite the lack of the guanidine group. Mutant M446 showed a widened pocket, which explains the broader substrate specificity and conversion of aromatic compounds.

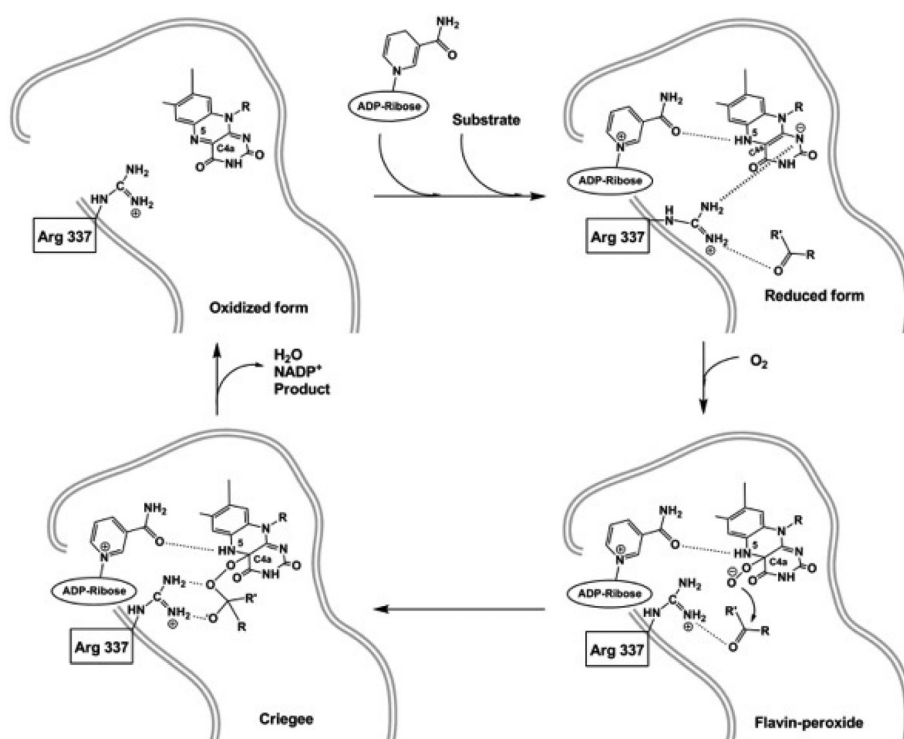
## Assay systems to identify BVMOs

In order to allow fast and reliable identification of novel BVMOs or variants within protein engineering derived mutant libraries, it is crucial to have high-throughput assays available. Assay systems to measure product formation from BVMO-catalyzed reactions are based either on a pH shift after hydrolysis of the resulting ester or lactone, respectively, or on the formation of chromo- or fluorogenic compounds liberated after cleavage of the resulting ester BVO-product. In 2002 Littlechild *et al.* introduced an assay employing pig-liver esterase (PLE) to induce a pH shift that occurs in a non- or weakly-buffered system through a pH-indicator.<sup>92</sup> However, this method was only applicable to washed cell suspensions, as various factors in a whole cell system can lead to a change in pH, which again can entail erroneous results. A fluorogenic assay was based on the detection of umbelliferone (7-hydroxycoumarin) formed from 4-oxopentyl umbelliferyl ether by a BVMO reaction and subsequent oxidation of the formed alcohol, which was first reported in 2003.<sup>93</sup> Umbelliferone also served as a reporter in another assay in which the oxidation product of 2-coumaryloxy ketones was subsequently cleaved by PLE to release the fluorescent dye.<sup>94</sup> Both assays require the multi-step synthesis of the non-commercially available starting material and acceptance of the bulky substrates by the BVMO. The successful adaptation of an assay based on adrenalin conversion, initially described by Wahler and Reymond,<sup>95</sup> was used by our group to identify mutants of a BVMO from *Pseudomonas fluorescens* DSM 50106 that showed enhanced conversion and enantioselectivity in the kinetic resolution of 4-hydroxy-2-decanone.<sup>96</sup> After BVO and subsequent

**Table 4** Protein structures of BVMOs

Enzyme	Pdb-code	Resolution (Å)	Comment	Ref.
PAMO	1W4X <sup>a</sup>	1.7	2 domains (one for FAD and one for NADP <sup>+</sup> binding; active site in cleft of domain interface); R337 <i>re</i> side to flavin, R337 in “IN” and “OUT” conformation	17
	2YLR <sup>a,b</sup>	2.26	Oxidized form; structure shows NADP <sup>+</sup> binding and its stabilization of flavin-(hydro)peroxide; R337 interacts with NADP <sup>+</sup> and side chain D66	88
	2YLS <sup>a,b</sup>	2.26	Reduced form; structure shows flavin-peroxide formation; carboxamide group of NADP <sup>+</sup> makes H-bond with N5 from reduced FAD to prevent reaction with flavin-peroxide; R337 interacts with negatively charged reduced flavin favoring accessibility for O <sub>2</sub>	88
	2YLT <sup>a,b,c</sup>	2.65	MES in the active site is shown to be in direct contact with R337 and the ribose group of NADP <sup>+</sup>	88
PAMO N337K	2YLV <sup>a,b,c</sup>	2.9	Mutant can still bind MES <sup>c</sup> , but cannot interact with NADP <sup>+</sup> , D66 and ligand simultaneously	88
	2YM1 <sup>a,b,d</sup>	2.28	Oxidized form; K337 interacts with carboxamide group of NADP <sup>+</sup> and side chain of D66	88
	2YM2 <sup>a,b</sup>	2.70	Reduced form; K337 moves to the flavin to a similar conformation as R337 in WT	88
PAMO D66A	2YLY <sup>a,b,c</sup>	2.20	Mutant showed lower <i>k</i> <sub>cat</sub> for NADPH; negative charge facilitates positioning of NADPH	88
PAMO M446G	2YLZ <sup>a</sup>	2.00	Mutant accepts aromatic compounds; showed no conformational changes, but widened pocket	88
MtmOIV	3FMW <sup>a,e</sup>	2.89	Dimer; R52 (similar to R337 in PAMO), but in <i>si</i> side orientation to flavin; class A flavoprotein monooxygenase; needs peroxyflavin intermediate	90
CHMO closed	3GWD <sup>a,b</sup>	2.30	2 domains (one for FAD and one for NADP <sup>+</sup> binding); R329 (similar to R337 in PAMO) pushes nicotinamide head deeper to stabilize peroxyflavin and “Criegee” intermediate (causing “sliding” of NADP <sup>+</sup> ); represents enzyme in post-flavin reduction state; structure confirms novel role of BVMO sequence motif as it coordinates domain movements during catalysis	89
CHMO open	3GWF <sup>a,b</sup>	2.20	R329 in “OUT” conformation (similar to R337 in PAMO); structure shows final step of NADP <sup>+</sup> release in the catalytic cycle	89
3,6-DKCMO	2WGK	2.00	Structure determined only by non-crystallographic symmetry (NCS) exhaustive search	91
OTEMO	3UOV <sup>a</sup>	2.05	Dimer	11
	3UOX <sup>a</sup>	1.96		11
	3UOY <sup>a,b</sup>	2.00		11
	3UOZ <sup>a,b</sup>	2.41		11
	3UP4 <sup>a,b</sup>	2.80	Closed form	11
	3UP5 <sup>a,b</sup>	2.45		11

<sup>a</sup> FAD<sup>+</sup>. <sup>b</sup> NADP<sup>+</sup>. <sup>c</sup> 2-(*N*-Morpholino)-ethanesulfonic acid. <sup>d</sup> Oxygen. <sup>e</sup> 1,2-Ethenediol.

**Fig. 1** Mechanism of PAMO-catalyzed Baeyer–Villiger oxidation as derived from 3D structure analysis.

**Table 5** Summary of most recent protein engineering approaches for BVMOs

Target enzyme	Method	Mutations	Desired objective	Results/comments	Ref.
PAMO	Saturation mutagenesis using degenerate primers	S441A/A442W/L443Y/S444T	Increasing the activity toward a substrate that is hardly converted by WT PAMO	Alignment of WT PAMO with seven other BVMOs, limited number of amino acids at positions 411–444, mutant screening on <i>rac</i> -2-phenyl-cyclohexanone identified quadruple mutant with $E = 70$ favoring the ( <i>R</i> )-enantiomer in contrast to ( <i>S</i> )-selective wild-type. This mutant also oxidized 2-(4-chlorophenyl)-cyclohexanone with excellent selectivity ( $E > 200$ ).	102
PAMO	CASTing, saturation mutagenesis	“Second sphere” residue P440N	Expanding the substrate scope; higher $E$ -values, maintenance of thermostability	Screening with <i>rac</i> -2-ethylcyclohexanone (not converted by wild-type enzyme) resulted in five highly active hits, which were analyzed in kinetic resolutions using various 2-substituted cyclohexanones; best mutants converted all cyclic ketones with $E > 200$ ; some mutants gave formation of ‘abnormal lactone’ with <i>rac</i> -bicyclo [3.2.0]hept-2-en-6-one.	103
PAMO	Site directed mutagenesis, saturation mutagenesis using NDT codon degeneracy	Q93N/P94D	Expanding the substrate scope	Introduction of distal mutations at positions Q93/P94 induced allosteric interactions between the N-terminal region of an $\alpha$ -helix (Ala91–Glu95) and the loop segment Tyr56–Tyr60 (FAD-binding domain) causing movement of the loop segment Trp177–Glu180 (NADP-binding domain). A double mutant Q93N/P94D gave good to excellent selectivity in the conversion of 2-substituted cyclohexanones and desymmetrization of 4-substituted cyclohexanones. MD simulations suggested new H-bonds (Asp94/Arg59 and Trp57/Trp177) and a strong salt bridge between Asp94 and Arg59.	104
PAMO	Site directed mutagenesis	H220N, H220Q, K336N	Changing the cofactor specificity to NADH	3-fold increase of the catalytic efficiency of mutants using NADH as reduction equivalent compared to wild-type enzyme, mutant K336N showed a significantly increased $E$ -value in the kinetic resolution of <i>rac</i> -3-methyl-4-phenylbutane-2-one for both NADH and NADPH.	105
PAMO	CASTing, site directed mutagenesis	V54, I67, Q152, A435	Expanding the substrate scope	Comprehensive inspection of the active site of PAMO (crystal structure) and CPMO (homology model based on PAMO). Exchange of various active site amino acid residues in PAMO to its counterparts in CPMO. Single and multiple mutants (15 each) were analyzed in oxidation reactions of 14 different ketones and sulfides. Amino acids V54, I67, Q152, and A435 in PAMO contributed to the substrate specificity and enantioselectivity; a partially inverted enantioselectivity similar to CPMO/CHMO was observed too.	106
PAMO	Structure-inspired subdomain exchanges by the SLIC method	Chimeric BVMOs	Expanding the substrate scope	Blending of the substrate specificities of sequence-related BVMOs (STMO, CHMO and a putative BVMO from a metagenome screening effort <sup>107</sup> ) into PAMO. Construction of three chimeras (PASTMO, PACHMO and PAMEMO1) consisting of 106 C-terminal amino acid residues of PAMO exchanged by homologous regions of the other enzymes. Characterization of all chimeras (melting temperature, substrate acceptance (using thioanisole, benzyl phenyl sulfide, <i>rac</i> -bicyclo-[3.2.0]hept-2-en-6-one, <i>rac</i> -2-phenylcyclohexanone and progesterone) and selectivity). All chimeras exhibited novel catalytic activity, especially concerning regio- and stereoselectivity, but not all activities from the parent BVMOs could be introduced into the constructs. Thermostability was significantly increased for all chimeras compared to parental BVMO.	107
CHMO <sub>Acinetobacter</sub>	Site directed mutagenesis, saturation mutagenesis	M5I, M291I, C330S, C376L, M400I, M412L, M481A, C520V	Design of mutants with enhanced oxidative stability and thermostability	Replacement of Met and Cys residues by amino acids with small hydrophobic side chains (Ile, Leu, Ala) present in PAMO and CHMO <sub>Rhodospirillum rubrum</sub> . Mutation C376L afforded the highest improvement in oxidative stability, while an M400I mutation resulted in the largest increase in thermal stability. Recombination of all improved mutants yielded two mutants with significantly increased oxidative and thermostability. While the wild-type CHMO was completely inactivated in 5 mM H <sub>2</sub> O <sub>2</sub> , mutant #16 retained >40% residual activity in 200 mM H <sub>2</sub> O <sub>2</sub> . In addition, the melting temperature of mutant #15 was increased by 7 °C compared to wild-type CHMO <sub>Acinetobacter</sub> .	87

CASTing: Combinatorial Active Site Saturation Testing; SLIC: Sequence and Ligation Independent Cloning.

hydrolysis of the formed ester by an esterase, a 1,2-diol is formed, which can react with  $\text{NaIO}_4$ . This assay operates through back titration of non-reacted  $\text{NaIO}_4$  with adrenaline yielding the chromophore adrenochrome. The method works in microtiter plates (MTPs), but is unsuitable for the determination of enzyme kinetics as it allows only endpoint measurements. More recently, an assay based on monitoring cycloalkanone consumption was shown to be applicable for qualitative screening as well as quantitative activity determination.<sup>97</sup> In alkaline solution, the enolizable ketone forms a colored complex with 3,5-dinitrobenzoic acid, which can be used to follow the decrease in absorption in case the ketone is oxidized. The method was shown to work for cycloalkanones with ring sizes between C4 and C7, but absorbance of the color decreased with the size of the cycloketone ring. Very recently, we described an assay based on the BVO of *p*-nitroacetophenone.<sup>98</sup> The resulting acetate is subsequently hydrolyzed by an esterase or NaOH to yield *p*-nitrophenolate that can easily be quantified spectrophotometrically at 410 nm. The assay principle was applied to whole *E. coli* cells containing recombinant BVMO, crude cell extract as well as to purified enzyme. Screening of mutant libraries of the 4-hydroxyacetophenone monooxygenase (HAPMO) from *Pseudomonas putida* JD1 using this assay could identify more active enzyme variants.

## Protein engineering to tailor-design BVMOs

Enzymes in nature hardly meet the demands imposed by an industrial application. For this, biocatalysts can be adapted to their required characteristics (such as substrate scope and concentration, selectivity, temperature, pH, stability) by methods of protein engineering.<sup>99–101</sup> In case the three-dimensional structure of an enzyme is available, rational protein design is often the method of choice, although it is still challenging to predict the effects of a distinct mutation. Alternatively, methods of directed evolution are used in order to improve the protein by random mutagenesis or libraries created by simultaneous saturation mutagenesis, which need to be screened with an appropriate assay to identify desired variants. A summary of the most recent protein engineering examples for BVMOs is given in Table 5. These demonstrate that activity, enantioselectivity, substrate range and stability of BVMOs could be successfully improved creating more versatile enzyme variants.

## Conclusions

In conclusion, this perspective article has shown that in recent years the number of Baeyer–Villiger monooxygenases useful for biocatalysis has substantially increased. Major reasons are novel tools to discover enzymes by protein sequence, phylogenetic and structural analysis or by identification of family relationships. This also helped to decipher possible natural functions of BVMOs and facilitated their improvement by protein engineering. Recently developed novel high-throughput assays will further contribute to identify or create novel BVMOs and to tailor-design their properties. Already, the larger “toolbox” of BVMOs available helped to substantially broaden their synthetic utility in organic chemistry. Furthermore, in the past decade,

a range of factors limiting the application of BVMOs could be identified and tools to overcome these hurdles have been developed and already led to the first large scale applications of BVMOs. Overall, these achievements and efforts strongly helped to make BVMOs versatile enzymes for numerous applications in organic synthesis.

We thank the Deutsche Forschungsgemeinschaft (Grant Bo1862/6-1), the Deutsche Bundesstiftung Umwelt (AZ13234) and the BMBF (Biokatalyse2021 cluster, FK0315175B) for financial support.

## Notes and references

- 1 H. Leisch, K. Morley and P. C. Lau, *Chem. Rev.*, 2011, **111**, 4165–4222.
- 2 D. E. Torres Pazmino, H. M. Dudek and M. W. Fraaije, *Curr. Opin. Chem. Biol.*, 2010, **14**, 138–144.
- 3 G. de Gonzalo, M. D. Mihovilovic and M. W. Fraaije, *ChemBioChem*, 2010, **11**, 2208–2231.
- 4 J. Rehdorf and U. T. Bornscheuer, in *Encyclopedia of Industrial Biotechnology: Bioprocess, Bioseparation and Cell Technology*, ed. M. C. Flickinger, John Wiley & Sons, 2010, vol. 7, DOI: 10.1002/9780470054581.eib451.
- 5 U. T. Bornscheuer, G. W. Huisman, R. J. Kazlauskas, S. Lutz, K. Robins and J. C. Moore, *Nature*, 2012, **485**, 185–194.
- 6 N. A. Donoghue, D. B. Norris and P. W. Trudgill, *Eur. J. Biochem.*, 1976, **63**, 175–192.
- 7 I. E. Conrad, R. Dubus, I. C. Gunsalus and N. York, *Biochem. Biophys. Res. Commun.*, 1961, **6**, 293–297.
- 8 J. D. Stewart, *Curr. Org. Chem.*, 1998, **2**, 195–216.
- 9 M. M. Kayser and C. M. Clouthier, *J. Org. Chem.*, 2006, **71**, 8424–8430.
- 10 K. H. Jones, R. T. Smith and P. W. Trudgill, *J. Gen. Microbiol.*, 1993, **139**, 797–805.
- 11 H. Leisch, R. Shi, S. Grosse, K. Morley, H. Bergeron, M. Cygler, H. Iwaki, Y. Hasegawa and P. C. K. Lau, *Appl. Environ. Microbiol.*, 2012, **78**, 2200–2212.
- 12 M. Kadow, K. Loschinski, S. Sass, M. Schmidt and U. T. Bornscheuer, *Appl. Microbiol. Biotechnol.*, 2012, DOI: 10.1007/s00253-011-3859-1, online.
- 13 M. Kadow, S. Sass, M. Schmidt and U. T. Bornscheuer, *AMB Express*, 2011, **1**, 13.
- 14 H. J. Ougham, D. G. Taylor and P. W. Trudgill, *J. Bacteriol.*, 1983, **153**, 140–152.
- 15 M. W. Fraaije, N. M. Kamerbeek, W. J. van Berkel and D. B. Janssen, *FEBS Lett.*, 2002, **518**, 43–47.
- 16 M. W. Fraaije, J. Wu, D. P. H. M. Heuts, E. W. van Hellemond, J. H. L. Spelberg and D. B. Janssen, *Appl. Microbiol. Biotechnol.*, 2005, **66**, 393–400.
- 17 E. Malito, A. Alfieri, M. W. Fraaije and A. Mattevi, *Proc. Natl. Acad. Sci. U. S. A.*, 2004, **101**, 13157–13162.
- 18 A. Riebel, H. M. Dudek, G. de Gonzalo, P. Stepniak, L. Rychlewski and M. W. Fraaije, *Appl. Microbiol. Biotechnol.*, 2012, DOI: 10.1007/s00253-011-3823-0, online.
- 19 C. Szolkowy, L. D. Eltis, N. C. Bruce and G. Grogan, *ChemBioChem*, 2009, **10**, 1208–1217.
- 20 H. Iwaki, S. Wang, S. Grosse, H. Bergeron, A. Nagahashi, J. Lertvorachon, J. Yang, Y. Konishi, Y. Hasegawa and P. C. Lau, *Appl. Environ. Microbiol.*, 2006, **72**, 2707–2720.
- 21 E. Beneventi, G. Ottolina, G. Carrea, W. Panzeri, G. Fronza and P. C. K. Lau, *J. Mol. Catal. B: Enzym.*, 2009, **58**, 164–168.
- 22 M. J. Fink, T. C. Fischer, F. Rudroff, H. Dudek, M. W. Fraaije and M. D. Mihovilovic, *J. Mol. Catal. B: Enzym.*, 2011, **73**, 9–16.
- 23 F. Leipold, R. Wardenga and U. T. Bornscheuer, *Appl. Microbiol. Biotechnol.*, 2012, **94**, 705–717.
- 24 J. B. van Beilen, F. Mourlane, M. A. Seeger, J. Kovac, Z. Li, T. H. Smits, U. Fritsche and B. Witholt, *Environ. Microbiol.*, 2003, **5**, 174–182.
- 25 D. G. Taylor and P. W. Trudgill, *J. Bacteriol.*, 1986, **165**, 489–497.
- 26 R. Villa, *J. Mol. Catal. B: Enzym.*, 1997, **2**, 193–197.
- 27 M. J. van der Werf, H. J. Swarts and J. A. de Bont, *Appl. Environ. Microbiol.*, 1999, **65**, 2092–2102.



- 28 E. J. McGhie, M. N. Isupov, E. Schroder and J. A. Littlechild, *Acta Crystallogr., Sect. D: Biol. Crystallogr.*, 1998, **54**, 1035–1038.
- 29 J. Fried, R. W. Thoma and A. Klingsberg, *J. Am. Chem. Soc.*, 1953, **75**, 5764–5765.
- 30 A. Świzdor, T. Kołek, A. Panek and A. Białońska, *Biochim. Biophys. Acta – Mol. Cell. Biol. L.*, 2011, **1811**, 253–262.
- 31 G. J. Grogan and H. L. Holland, *J. Mol. Catal. B: Enzym.*, 2000, **9**, 1–32.
- 32 Z. Xiong, Q. Wei, H. Chen, S. Chen, W. Xu, G. Qiu, S. Liang and X. Hu, *Steroids*, 2006, **71**, 979–983.
- 33 E. Itagaki, *J. Biochem.*, 1986, **99**, 825–832.
- 34 K. Königsberger, G. Braunnegg, K. Faber and H. Griengl, *Biotechnol. Lett.*, 1990, **12**, 509–514.
- 35 P. C. Brzostowicz, D. M. Walters, S. M. Thomas, V. Nagarajan and P. E. Rouviere, *Appl. Environ. Microbiol.*, 2003, **69**, 334–342.
- 36 Y. C. Chen, O. P. Peoples and C. T. Walsh, *J. Bacteriol.*, 1988, **170**, 781–789.
- 37 W. G. Lai, N. Farah, G. A. Moniz and Y. N. Wong, *Drug Metab. Dispos.*, 2010, **39**, 61–70.
- 38 A. Ríoz-Martínez, M. Kopacz, G. de Gonzalo, D. E. Torres Pazmiño, V. Gotor and M. W. Fraaije, *Org. Biomol. Chem.*, 2011, **9**, 1337–1341.
- 39 C. N. Jensen, J. Cartwright, J. Ward, S. Hart, J. P. Turkenburg, S. T. Ali, M. J. Allen and G. Grogan, *ChemBioChem*, 2012, **13**, 872–878.
- 40 Y. Wen, H. Hatabayashi, H. Arai, H. K. Kitamoto and K. Yabe, *Appl. Environ. Microbiol.*, 2005, **71**, 3192–3198.
- 41 J. Jiang, C. N. Tetzlaff, S. Takamatsu, M. Iwatsuki, M. Komatsu, H. Ikeda and D. E. Cane, *Biochemistry*, 2009, **48**, 6431–6440.
- 42 M.-J. Seo, D. Zhu, S. Endo, H. Ikeda and D. E. Cane, *Biochemistry*, 2011, **50**, 1739–1754.
- 43 K. Qiao, Y.-H. Chooi and Y. Tang, *Metab. Eng.*, 2011, **13**, 723–732.
- 44 A. Kirschner, J. Altenbuchner and U. T. Bornscheuer, *Appl. Microbiol. Biotechnol.*, 2007, **75**, 1095–1101.
- 45 J. Rehdorf, A. Kirschner and U. T. Bornscheuer, *Biotechnol. Lett.*, 2007, **29**, 1393–1398.
- 46 J. Rehdorf, A. Lengar, U. T. Bornscheuer and M. D. Mihovilovic, *Bioorg. Med. Chem. Lett.*, 2009, **19**, 3739–3743.
- 47 J. Rehdorf, M. D. Mihovilovic, M. W. Fraaije and U. T. Bornscheuer, *Chem.–Eur. J.*, 2010, **16**, 9525–9535.
- 48 M. J. Fink, F. Rudroff and M. D. Mihovilovic, *Bioorg. Med. Chem. Lett.*, 2011, **21**, 6135–6138.
- 49 A. Ríoz-Martínez, A. Cuetos, C. Rodríguez, G. de Gonzalo, I. Lavandera, M. W. Fraaije and V. Gotor, *Angew. Chem., Int. Ed.*, 2011, **50**, 8387–8390.
- 50 P. B. Brondani, G. de Gonzalo, M. W. Fraaije and L. H. Andrade, *Adv. Synth. Catal.*, 2011, **353**, 2169–2173.
- 51 B. P. Branchaud and C. T. Walsh, *J. Am. Chem. Soc.*, 1985, **107**, 2153–2161.
- 52 S. Colonna, N. Gaggero, G. Carrea, G. Ottolina, P. Pasta and F. Zambianchi, *Tetrahedron Lett.*, 2002, **43**, 1797–1799.
- 53 L. H. Andrade, E. C. Pedrozo, H. G. Leite and P. B. Brondani, *J. Mol. Catal. B: Enzym.*, 2011, **73**, 63–66.
- 54 J. Zhu, Y. K. Bong, S. J. Collier, M. Vogel, M. J. Nazor, D. Smith, S. Song, M. D. Clay, B. Mijts and X. Zhang, 2011, Int. Patent Application to Codexis Inc., WO/2011/071982.
- 55 H. E. M. Law, C. V. F. Baldwin, B. H. Chen and J. M. Woodley, *Chem. Eng. Sci.*, 2006, **61**, 6646–6652.
- 56 F. Secundo, S. Fialà, M. W. Fraaije, G. de Gonzalo, M. Meli, F. Zambianchi and G. Ottolina, *Biotechnol. Bioeng.*, 2011, **108**, 491–499.
- 57 G. de Gonzalo, C. Rodríguez, A. Ríoz-Martínez and V. Gotor, *Enzyme Microb. Technol.*, 2012, **50**, 43–49.
- 58 F. Schulz, F. Leca, F. Hollmann and M. T. Reetz, *Beilstein J. Org. Chem.*, 2005, **1**, 10, DOI: 10.1186/1860-5397-1-10.
- 59 C. Rodríguez, G. de Gonzalo, M. W. Fraaije and V. Gotor, *Green Chem.*, 2010, **12**, 2255–2260.
- 60 C. Rodríguez, G. de Gonzalo and V. Gotor, *J. Mol. Catal. B: Enzym.*, 2012, **74**, 138–143.
- 61 A. Kheiruloom, M. Ardjmand, M. Vossoughi and M. Kazemeini, *Biochem. Eng. J.*, 1998, **2**, 81–88.
- 62 C.-H. Wong, D. G. Drueckhammer and H. M. Sweers, *J. Am. Chem. Soc.*, 1985, **107**, 4028–4031.
- 63 C.-H. Wong and G. M. Whitesides, *J. Am. Chem. Soc.*, 1981, **103**, 4890–4899.
- 64 F. Zambianchi, P. Pasta, G. Carrea, S. Colonna, N. Gaggero and J. M. Woodley, *Biotechnol. Bioeng.*, 2002, **78**, 489–496.
- 65 J. M. Vrtis, A. K. White, W. W. Metcalf and W. A. van der Donk, *Angew. Chem., Int. Ed.*, 2002, **41**, 3257–3259.
- 66 R. Woodyer, W. A. van der Donk and H. Zhao, *Biochemistry*, 2003, **42**, 11604–11614.
- 67 D. E. Torres Pazmino, R. Snajdrova, B. J. Baas, M. Ghobrial, M. D. Mihovilovic and M. W. Fraaije, *Angew. Chem., Int. Ed.*, 2008, **47**, 2275–2278.
- 68 T. W. Johannes, R. D. Woodyer and H. Zhao, *Biotechnol. Bioeng.*, 2007, **96**, 18–26.
- 69 V. Alphand, G. Carrea, R. Wohlgemuth, R. Furstoss and J. M. Woodley, *Trends Biotechnol.*, 2003, **21**, 318–323.
- 70 S. D. Doig, H. Simpson, V. Alphand, R. Furstoss and J. M. Woodley, *Enzyme Microb. Technol.*, 2003, **32**, 347–355.
- 71 C. V. F. Baldwin, R. Wohlgemuth and J. M. Woodley, *Org. Process Res. Dev.*, 2008, **12**, 660–665.
- 72 S. D. Doig, P. J. Avenell, P. A. Bird, P. Gallati, K. S. Lander, G. J. Lye, R. Wohlgemuth and J. M. Woodley, *Biotechnol. Prog.*, 2002, **18**, 1039–1046.
- 73 H. D. Simpson, V. Alphand and R. Furstoss, *J. Mol. Catal. B: Enzym.*, 2001, **16**, 101–108.
- 74 I. Hilker, M. C. Gutierrez, R. Furstoss, J. Ward, R. Wohlgemuth and V. Alphand, *Nat. Protoc.*, 2008, **3**, 546–554.
- 75 I. Hilker, V. Alphand, R. Wohlgemuth and R. Furstoss, *Adv. Synth. Catal.*, 2004, **346**, 203–214.
- 76 B. H. Chen, S. D. Doig, G. J. Lye and J. M. Woodley, *Trans. Inst. Chem. Eng.*, 2002, **80**, 51–55.
- 77 J. Rehdorf, C. L. Zimmer and U. T. Bornscheuer, *Appl. Environ. Microbiol.*, 2009, **75**, 3106–3114.
- 78 K. Geitner, J. Rehdorf, R. Snajdrova and U. T. Bornscheuer, *Appl. Microbiol. Biotechnol.*, 2010, **88**, 1087–1093.
- 79 O. Abril, C. C. Ryerson, C. T. Walsh and G. M. Whitesides, *Bioorg. Chem.*, 1989, **17**, 41–52.
- 80 K. S. Atia, *Radiat. Phys. Chem.*, 2005, **73**, 91–99.
- 81 A. Cuetos, A. Ríoz-Martínez, M. L. Valenzuela, I. Lavandera, G. de Gonzalo, G. A. Carriedo and V. Gotor, *J. Mol. Catal. B: Enzym.*, 2012, **74**, 178–183.
- 82 S. A. Meeuwissen, A. Ríoz-Martínez, G. de Gonzalo, M. W. Fraaije, V. Gotor and J. C. M. van Hest, *J. Mater. Chem.*, 2011, **21**, 18923.
- 83 M. Hucik, M. Bucko, P. Gemeiner, V. Stefuca, A. Vikartovska, M. D. Mihovilovic, F. Rudroff, N. Iqbal, D. Chorvat, Jr. and I. Lacik, *Biotechnol. Lett.*, 2010, **32**, 675–680.
- 84 E.-H. Doo, W.-H. Lee, H.-S. Seo, J.-H. Seo and J.-B. Park, *J. Biotechnol.*, 2009, **142**, 164–169.
- 85 H. M. Kim, E. Heinzle and C. Wittmann, *J. Microbiol. Biotechnol.*, 2006, **16**, 1174–1179.
- 86 J. Y. Yun, J. E. Lee, K. M. Yang, S. Cho, A. Kim, Y. E. Kwon and J. B. Park, *Bioprocess Biosyst. Eng.*, 2012, **35**, 211–216.
- 87 D. J. Opperman and M. T. Reetz, *ChemBioChem*, 2010, **11**, 2589–2596.
- 88 R. Orru, H. M. Dudek, C. Martinoli, D. E. Torres Pazmino, A. Royant, M. Weik, M. W. Fraaije and A. Mattevi, *J. Biol. Chem.*, 2011, **286**, 29284–29291.
- 89 I. A. Mirza, B. J. Yachnin, S. Wang, S. Grosse, H. Bergeron, A. Imura, H. Iwaki, Y. Hasegawa, P. C. Lau and A. M. Berghuis, *J. Am. Chem. Soc.*, 2009, **131**, 8848–8854.
- 90 M. P. Beam, M. A. Bosserman, N. Noinaj, M. Wehenkel and J. Rohr, *Biochemistry*, 2009, **48**, 4476–4487.
- 91 M. N. Isupov and A. A. Lebedev, *Acta Crystallogr., Sect. D: Biol. Crystallogr.*, 2008, **64**, 90–98.
- 92 A. B. Watts, J. Beecher, C. S. Whitcher and J. A. Littlechild, *Biocatal. Biotransform.*, 2002, **20**, 209–214.
- 93 M. C. Gutierrez, A. Sleegers, H. D. Simpson, V. Alphand and R. Furstoss, *Org. Biomol. Chem.*, 2003, **1**, 3500–3506.
- 94 R. Sicard, L. A. Chen, A. A. Marsaioli and J.-L. Reymond, *Adv. Synth. Catal.*, 2005, **347**, 1041–1050.
- 95 D. Wahler and J. L. Reymond, *Angew. Chem., Int. Ed.*, 2002, **41**, 1229–1232.
- 96 A. Kirschner and U. T. Bornscheuer, *Appl. Microbiol. Biotechnol.*, 2008, **81**, 465–472.
- 97 J. A. Linares-Pastén, G. Chávez-Lizárraga, R. Villagomez, G. Mamo and R. Hatti-Kaul, *Enzyme Microb. Technol.*, 2012, **50**, 101–106.
- 98 S. Saß, M. Kadow, K. Geitner, M. L. Thompson, L. Talmann, D. Böttcher, M. Schmidt and U. T. Bornscheuer, *Tetrahedron*, 2012, DOI: 10.1016/j.tet.2012.05.098, online.



- 99 G. Behrens, A. Hummel, S. K. Padhi, S. Schätzle and U. T. Bornscheuer, *Adv. Synth. Catal.*, 2011, **353**, 2191–2215.
- 100 M. T. Reetz and G. P. L. Krebs, *C. R. Chim.*, 2011, **14**, 811–818.
- 101 *Engineering Handbook*, ed. S. Lutz and U. T. Bornscheuer, Wiley-VCH, 2009.
- 102 M. T. Reetz and S. Wu, *Chem. Commun.*, 2008, 5499–5501.
- 103 M. T. Reetz and S. Wu, *J. Am. Chem. Soc.*, 2009, **131**, 15424–15432.
- 104 S. Wu, J. P. Acevedo and M. T. Reetz, *Proc. Natl. Acad. Sci. U. S. A.*, 2010, **107**, 2775–2780.
- 105 H. M. Dudek, D. E. Torres Pazmino, C. Rodríguez, G. de Gonzalo, V. Gotor and M. W. Fraaije, *Appl. Microbiol. Biotechnol.*, 2010, **88**, 1135–1143.
- 106 H. M. Dudek, G. de Gonzalo, D. E. Torres Pazmino, P. Stepniak, L. S. Wyrwicz, L. Rychlewski and M. W. Fraaije, *Appl. Environ. Microbiol.*, 2011, **77**, 5730–5738.
- 107 H. L. van Beek, G. d. Gonzalo and M. W. Fraaije, *Chem. Commun.*, 2012, **48**, 3288.
- 108 M. Bučko, A. Schenk Mayerová, P. Gemeiner, A. Vikartovská, M. D. Mihovilović and I. Lacík, *Enzyme Microb. Technol.*, 2011, **49**, 284–288.

## Articles

### Article II



# Protein engineering of a thermostable polyol dehydrogenase

H. Wulf<sup>1</sup>, H. Mallin<sup>1</sup>, U.T. Bornscheuer<sup>\*</sup>

Dept. of Biotechnology & Enzyme Catalysis, Institute of Biochemistry, Greifswald University, Felix-Hausdorff-Str 4, D-17487 Greifswald, Germany

## ARTICLE INFO

### Article history:

Received 16 May 2012

Received in revised form 19 June 2012

Accepted 25 June 2012

### Keywords:

Polyol dehydrogenase

Thermostability

Protein engineering

*Deinococcus geothermalis*

Cofactor dependency

## ABSTRACT

The polyol dehydrogenase PDH-11300 from *Deinococcus geothermalis* was cloned, functionally expressed in *Escherichia coli* and biochemically characterized. The enzyme showed the highest activity in the oxidation of xylitol and 1,2-hexanediol and had an optimum temperature of 45 °C. The enzyme exhibited a  $T_{50}^{60}$ -value of 48.3 °C. The  $T_{50}^{60}$  is the temperature where 50% of the initial activity remains after incubation for 1 h. In order to elucidate the structural reasons contributing to thermostability, the substrate-binding loop of PDH-11300 was substituted by the loop-region of a homolog enzyme, the galactitol dehydrogenase from *Rhodobacter sphaeroides* (PDH-158), resulting in a chimeric enzyme (PDH-loop). The substrate scope of this chimera basically represented the average of both wild-type enzymes, but surprisingly the  $T_{50}^{60}$  was noticeably increased by 7 °C up to 55.3 °C. Further mutations in the active site led to identification of residues crucial for enzyme activity. The cofactor specificity was successfully altered from NADH to NADPH by an Asp55Asn mutation, which is located at the NAD<sup>+</sup> binding cleft, without influencing the catalytic properties of the dehydrogenase.

© 2012 Elsevier Inc. All rights reserved.

## 1. Introduction

Biocatalytic processes are frequently applied in organic synthesis and due to constant innovation in the protein engineering area, the application of biocatalysts to replace conventional chemistry is an emerging field [1,2]. Nevertheless, newly introduced biocatalysts always have to compete with established processes and need to match both chemical and economical demands. Especially thermostable enzymes are highly useful as they exhibit stability over a broad range of temperatures. This feature is essential if the advantages of elevated temperatures like better substrate solubility, reduced medium viscosity and a lowered risk of microbial contaminations [3] should be exploited.

The known structural reasons for thermostability in enzymes are due to the elevation of structural rigidity by stronger interactions like salt bridges, H-bondings and  $\pi$ - $\pi$  effects [4]. A contribution to the engineering of the thermostability was the development of the 'B-factor iterative test' (B-FIT [5]), which is based on the observation that certain residues in protein crystal structures cannot be fully resolved due to a high flexibility of these amino acids. The B-value is a measure for this flexibility and can be easily retrieved from pdb-files of protein structure data by means of

the program PyMol or the B-FIT software and consequently can help to guide the creation of more thermostable variants of enzymes by protein engineering as recently shown by Reetz et al. [5] for *Bacillus subtilis* lipase A, and by us for an esterase from *Pseudomonas fluorescens* [6].

Eijssink et al. [3] suggested three ways to access enzymes with improved thermostability: (1) isolating enzyme variants from organisms living in extreme environments, (2) rational-based mutagenesis considering all accessible structural information towards enzyme structure stabilization, and (3) directed evolution with random mutagenesis followed by screening or selection rounds [3]. Rational protein engineering strategies towards increasing thermostability of especially multimeric enzymes involve enhancement of covalent or electronic interactions of the subunits for example by introduction of disulfide bonds and reinforcement of H-bond networks or hydrophobic interactions [7].

Polyol dehydrogenases comprise a large family of oxidoreductases active towards di- or polyhydroxylated species. Their relevance in industry is due to their regio- and enantioselective catalysis leading to valuable chiral products. Here we combined approaches (1) and (2) given above for the engineering of a polyol dehydrogenase towards higher thermostability. The enzyme galactitol dehydrogenase from *Rhodobacter sphaeroides* D, which is a polyol dehydrogenase (PDH), was evolved from a chemostat culture grown at selective pressure and classified as a tetrameric short-chain dehydrogenase/reductase (SDR [8]). The enzyme is strictly dependent on NAD<sup>+</sup>, active against a broad range of polyols, with prevalence for aliphatic 1,2-diols and capable for the production of L-tagatose. Tagatose is a ketohexose C-4 fructose epimer present in

Abbreviations: PDH, polyol dehydrogenase; SDR, short chain dehydrogenase; MD, molecular dynamics.

\* Corresponding author. Tel.: +49 3834 86 4367; fax: +49 3834 86 794367.

E-mail address: [uwe.bornscheuer@uni-greifswald.de](mailto:uwe.bornscheuer@uni-greifswald.de) (U.T. Bornscheuer).

<sup>1</sup> Both authors equally contributed to this work.

nature and a potential low calorie sweetener that can be obtained by oxidation of galactitol [9,10]. The polyol dehydrogenase used within this work (PDH-158), origins from *Rhodobacter sphaeroides* DSM 158, and differs in five amino acid residues from the galactitol dehydrogenase from *R. sphaeroides* D (Fig. S1). The gene product of *Deinococcus geothermalis* (Dgeo.2865, abbreviated as PDH-11300) was annotated as SDR as well and shares 51% sequence identity with PDH-158. The radiation resistant and mesothermophilic organism *D. geothermalis* (DSM 11300) was isolated from hot springs near Naples, Italy [11]. To date, only a few enzymes from *D. geothermalis* species have been cloned, expressed and functionally characterized. The BRENDA database lists only three enzymes with *D. geothermalis* as origin (1,4- $\alpha$ -glucan branching enzyme, amylosucrase and S-ribosylhomocysteine lyase). Recently published results indicate that heterologous expressed enzymes of this strain show moderate thermostability and temperature optima from 45 to 60 °C [12–14].

This paper describes the first study towards a SDR and likewise a polyol dehydrogenase of *D. geothermalis* regarding kinetic and thermic properties and substrate scope. In order to alter and understand the substrate binding, a chimeric enzyme was constructed using PDH-11300 as scaffold. The chimera was created by substitution of a loop sequence of the PDH-11300 with the homolog loop of PDH-158, that was determined as substrate binding domain [15]. Point mutations in this newly created substrate binding site were introduced in order to evaluate the influence of these residues on the binding site hydrophobicity and the substrate scope.

In biocatalytic redox reactions the recycling of the cofactor is the crucial step in order to develop new cost effective synthesis routes. Some enzymes are strictly dependent to one cofactor of either NAD(H) or NADP(H). To broaden the cofactor specificity of an enzyme can thus contribute to a higher versatility in the application of this enzyme. In this paper a further point mutation was introduced in order to change the cofactor specificity of the enzyme. The bases of the NAD(H) dependence of SDRs and hence the incapability to use NADP(H) as cofactor is mostly due to ionic repulsion of certain residues in the cofactor binding cleft. For horse liver dehydrogenase this residue was shown to be an aspartate residue [16]. By means of homology modeling, we identified and mutated the inhibiting residue in the newly built thermostable chimeric PDH mutant, and were able to generate an enzyme with extended cofactor dependency.

## 2. Experimental

### 2.1. Chemicals

All chemicals were purchased from Sigma–Aldrich (St. Louis, USA) and Carl-Roth (Karlsruhe, Germany). Polymerases were obtained from Roboklon (Berlin, Germany), restriction enzymes and DNA ligases were obtained from Fermentas (Burlington, Canada).

### 2.2. Bacterial strains, plasmids and growth conditions

*Escherichia coli* BL21(DE3) (*B dcm ompT hsdS(r<sub>B</sub>–m<sub>B</sub>–)* *gal*) was purchased from Novagen (Darmstadt, Germany) and used as expression strain. *D. geothermalis* DSM 11300 was obtained from DSMZ (Braunschweig, Germany). *E. coli* One Shot® TOP10 cells (*F<sup>–</sup> mcrA Δ(mrr-hsdRMS-mcrBC) Φ80lacZΔM15 ΔlacX74 recA1 araD139 Δ(areau)7697 galU galK rpsL (Str<sup>R</sup>) endA1 nupG*) and vector pCR®II-TOPO® for subcloning were purchased from Invitrogen (Karlsruhe, Germany). *E. coli* strains were routinely cultured in lysogeny broth (LB) [17] at 37 °C, when necessary supplemented with ampicillin (100 µg/ml) or kanamycin (50 µg/ml). *D. geothermalis* was cultured in LB medium at 45 °C for four days. The expression plasmid pET-22b(+) was obtained from Novagen (Darmstadt, Germany) and used for heterologous enzyme expression.

### 2.3. Cloning of PDH-158 and PDH-11300

Genomic DNA (gDNA) from *E. coli* BL21 (DE3) and *D. geothermalis* was isolated using the innuPREP Bacteria DNA Kit (Analytik Jena, Jena, Germany). Plasmid isolations (Fermentas, Burlington, Canada), PCR-purification and gel extraction (Analytik

Jena, Jena, Germany) were performed according to the manufacturers protocols. Standard procedures such as DNA cloning and manipulations were performed as described by Sambrook and Russell [18]. DNA sequencing was carried out by GATC Biotech AG (Konstanz, Germany).

The gene *pdh-158* encoding for the short chain dehydrogenase (GenBank accession code: GI:77386383, locus tag RSP\_2363, (NCBI)) was amplified from genomic DNA of *R. sphaeroides* DSM 158 by PCR using the PDH-158 forward and reverse primer pair (Table S1). The SDR gene of *D. geothermalis* (GenBank accession code: GI:4074094, locus tag Dgeo.2865 (NCBI)) was amplified from genomic DNA of *D. geothermalis* DSM 11300 using the PDH-11300 forward and reverse primer pairs (Table S1). PCR products were separated in a 1.2% agarose gel from which the desired fragments were purified and cloned into the vector pCR®II-TOPO®. *E. coli* One Shot® TOP10 cells were transformed with the plasmids bearing the respective insert. The genes were sequenced and cloned into pET-22b(+) via *NdeI* and *BamHI* restriction sites (underlined). A N-terminal His<sub>6</sub>-tag was introduced simultaneously. The expression strain *E. coli* BL21(DE3) was transformed with these constructs.

### 2.4. Construction of the chimeric enzyme

The chimeric enzyme was constructed using the protein scaffold of PDH-11300 and the loop region E195–R203 of the substrate-binding domain of PDH-158. Mutagenesis was carried out by overlap extension PCR. By using a combination of primers containing the loop mutation and gene flanking primers, two fragments with overlapping ends were amplified in a first PCR. During a second PCR round with these fragments and gene flanking primers the chimeric gene was amplified (Table S1). After restriction with *NdeI* and *BamHI* the corresponding gene was ligated into pET22b(+) and transformed into chemical competent *E. coli* BL21 (DE3) cells (CaCl<sub>2</sub>/RbCl) [19]. The chimeric enzyme is abbreviated as “PDH-loop”.

### 2.5. Homology model and site-directed mutagenesis

For model prediction, design and docking studies of PDH-11300 and PDH-loop, the software YASARA structure (version 9.10.14 [20]) was used. As force field YAMBER2 [21] was taken and the best found template was the crystal structure of the GatDH of *R. sphaeroides* D (pdb code: 2WDZ). The resulting model of PDH-11300 had a z-score of –0.363, a structural coverage of 97% and an amino acid coverage of 53%. The model was refined and energy minimized. For PDH-loop the same template with comparable results was used. Energy minimizations of the PDH-loopD55N were performed after *in silico* mutation of D55N and substitution of the C2 hydroxyl group of NAD<sup>+</sup>. In a first minimization simulation using the YASARA software every residue of the objects were set as fixed, just the Asn residue and the phosphate residue were free. In the subsequent energy minimization both, the NADP<sup>+</sup> and enzyme were free.

Mutations of the active site and NAD<sup>+</sup> binding site were introduced by site-directed mutagenesis (QuikChange) using complementary primers to introduce the desired mutations. PDH-loop was taken as template for the two single (PDH-loopN99L and PDH-loopQ157A) and the double (PDH-loopV97A/N99L) mutations. The double mutant PDH-loopV97A/N99L was used as template for PDH-loopV97A/N99L/Q157A and PDH-loopV97A/N99L/Q157A acted as template for PDH-loopV97A/N99L/Q157A/N161M. For expression, all mutants were transformed into *E. coli* BL21 (DE3) chemo-competent cells.

### 2.6. Expression of PDH variants and enzyme purification

All enzyme variants were expressed in *E. coli* BL21 (DE3) cells grown at 37 °C in shaking flasks. Protein expression was induced at an OD<sub>600nm</sub> of 0.8–1.0 with 0.1 mM IPTG. After 4–6 h of protein expression at 37 °C cells were harvested by centrifugation (15 min, 3939 × g, 4 °C), washed with 100 mM sodium phosphate buffer (pH 7.5, 500 mM NaCl) and disrupted in the same buffer by sonification on ice (3 times for 5 min, 0.5 s pulse, 50% power). The supernatant was collected by centrifugation (30 min, 10,000 × g, 4 °C) and was passed through a 0.2 µm filter prior to chromatography. Affinity chromatography was performed at an ÄKTA purifier™ (GE-Healthcare, Munich, Germany) using a 5 ml Ni-Sepharose 6 Fast Flow crude column (GE Healthcare). The crude extract containing 60 mM imidazole was loaded on the column at a flow rate of 5 ml/min. The bound protein was washed with 100 mM sodium phosphate buffer (pH 7.5, 500 mM NaCl, 60 mM imidazole) and eluted with the same buffer containing 300 mM imidazole. The active fractions were pooled. For storage, the purified enzyme was subjected to gel filtration for removal of imidazole and high salt concentration using ÄKTA purifier™ equipped with a Sephadex G-25 Superfine column (26 × 110 mM). Storage of pure enzyme was performed at 4 °C or lyophilized at –20 °C. Enzyme purity and expression level were verified with SDS-PAGE (data not shown).

### 2.7. Determination of protein concentration and SDS-PAGE analysis

Polyacrylamide gel electrophoresis was carried out using 4% stacking gel and 12% resolving gel according to the method described by Laemmli [22]. Roti-Mark® STAN-DARD (Roth, Karlsruhe, M<sub>w</sub>: 14–200 kDa) was used as protein standard. The protein concentration was determined either with the BCA-assay (Uptima, Montluçon, France) or with Coomassie Brilliant-Blue using Roti®-Nanoquant (Carl-Roth, Karlsruhe, Germany) according to manufacturers protocols using BSA as standard.

## 2.8. CD-spectroscopy for the determination of $T_m$

The melting points ( $T_m$ ) of PDH variants were determined by circular dichroism (CD) spectroscopy. The purified and desalted enzyme was subjected to CD-spectroscopy in 5 mM sodium phosphate buffer (pH 7.5) using a Jasco V-650 at heat rates of 1 °C/min or 2 °C/min.

## 2.9. Enzyme assays

The dehydrogenase activity was determined spectrophotometrically at 25 or 30 °C by monitoring the rate of NADH ( $\epsilon = 5.62 \text{ mM}^{-1} \text{ cm}^{-1}$ ) or NADPH ( $\epsilon = 5.12 \text{ mM}^{-1} \text{ cm}^{-1}$ ) formation at 340 nm. The standard reaction mixture (1 ml) contained 100 mM bicine–HCl buffer (pH 9.0), 0.25 mM NAD<sup>+</sup>, 10–500 mM of different substrates and an appropriate amount of the enzyme. The reaction was started by adding NAD<sup>+</sup> to the mixture. One unit of dehydrogenase activity was defined as the amount of enzyme that catalyzes the formation of 1  $\mu\text{mol}$  NADH or NADPH per minute.

In order to determine the  $K_m$  and  $V_{max}$  values for different alcohols the spectrophotometric activity test was carried out with varying substrate concentrations at a fixed concentration of 0.25 mM NAD<sup>+</sup> or NADP<sup>+</sup> for PDH-loopD55N. Initial velocities were recorded during the first 60 s of catalytic turnover. Apparent  $K_m$  and  $V_{max}$  values were obtained by linear regression fitting according to the method of Wilkinson [23] and Duggleby [24] using the program HYPER (J.S. Easterby, <http://www.liv.ac.uk/~jse/software.html>).

The effect of temperature towards enzyme activity was determined by spectrophotometric measurements at different temperatures ranging from 20 °C to 65 °C for 3 min at pH 9.0. Stability studies were performed by incubation of purified enzyme solution for 6 h at the desired temperatures followed by activity tests after different time periods.

For determination of the  $T_{50}^{60}$  (that is the temperature where 50% of the initial activity remained after 1 h incubation) enzyme solutions were incubated in a thermocycler (Analytik Jena, Jena, Germany) at different temperatures. Depending on the studied enzyme, a temperature gradient of 30 °C was applied to 12 microreaction vessels containing enzyme solution. After 1 h incubation, residual enzyme activities were determined spectrophotometrically using a microtiterplate reader. The exact value was calculated by determination of the inflection point of a fit of the residual activities at certain temperatures to a sigmoidal plot (sigmoidal Boltzmann fit, using OriginPro 7.5).

For the determination of the effect of pH on enzyme activity, purified enzyme was measured at 25 °C for 3 min in the following buffers: 100 mM sodium phosphate (pH 5.5–8.0), bicine (pH 8–9) and glycine–NaOH (pH 9–12). For the extinction coefficient of NADH only negligible differences could be detected for the different pH and buffers.

Substrate scopes were determined in microtiter plates with 250  $\mu\text{l}$  total volume in bicine buffer at pH 9.0. The NAD<sup>+</sup> concentration was 0.5 mM and the substrate concentration for most of the substrates was 40 mM (Table 2). Different concentrations were employed for the substrates 1-phenylethanol (5 mM, 0.4% DMSO), 2-ethyl-1,3-hexanediol, 3-methyl-1-butanol (10 mM, 0.2% DMSO), cyclohexanol, cyclopentanol (10 mM, 0.4% DMSO), (10 mM, 0.2% DMSO), glyceraldehyde (20 mM), galactitol (26.6 mM).

## 3. Results

### 3.1. Cloning, mutagenesis and protein expression of polyol dehydrogenases

The enzyme PDH-11300 from *D. geothermalis* was expressed recombinantly in *E. coli* BL21 (DE3) resulting in good yields of active enzyme up to 3.16 kU (activity against xylitol) per liter culture broth. By analyzing the crystal structure of the GatDH from *R. sphaeroides* D (pdb code: 2WDZ) a loop region (195–203 aa, EMTLKMRRER) containing amino acids with high  $B$ -values could be identified, and this particular stretch was also found in the sequence of PDH-158 (Fig. 1 and Fig. S1). This loop is located next to the active site and was described as a flexible substrate binding loop, which might fit to several different substrates in the homolog enzyme from *R. sphaeroides* D [15]. Based on this knowledge a chimeric enzyme was constructed introducing this loop of PDH-158 into the PDH-11300 protein scaffold. In the alignment of the amino acid sequence of PDH-158 with the PDH-11300 sequence, this loop matched the amino acid positions 196–204 of PDH-11300 (PLTRRGLET). These amino acid residues of PDH-11300 were substituted by the loop of PDH-158 for the construction of the chimera PDH-loop. The resulting mutant PDH-loop could be expressed and

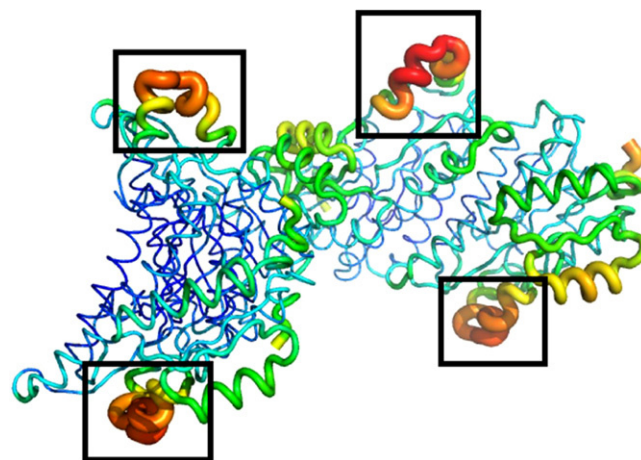


**Fig. 1.** Structure of the homotetramer of the GatDH of *R. sphaeroides* D. The amino acids 195–204 exhibited the highest  $B$ -values (highlighted in squares, color code: red depicts the highest and blue the lowest  $B$ -value). The homolog high  $B$ -value stretch of PDH-158 has the sequence: EMTLKMRRER, the homolog loop in PDH-11300 is PLTRRGLET. (For interpretation of the references to color in this figure legend, the reader is referred to the web version of the article.)

purified with yields up to 1.27 kU (activity against xylitol) per liter culture.

The substrate binding site of PDH-158 consists of a small and a large cavity [15]. The smaller part is responsible for binding specificity and the larger part may accommodate a wide variety of different substrates. The assumed 4 Å radius around the substrates of PDH-158 in the structure (PDB: 2WDZ) and the homology model of PDH-11300 covered the region surrounding the large cavity. 15 amino acid residues were identified, of which ten form the large binding pocket, and only four of the residues of PDH-11300 differed from the PDH-158 structure (Fig. 2). The large cavity of PDH-158 displays a highly apolar character whereas the large pocket of PDH-11300 shows a more polar character, which is due to the four different amino acids. These four residues therefore could represent determinants of substrate specificity and activity. To verify this assumption, four mutations (V97A, N99L, Q157A and N161M) were introduced to create mutants of PDH-11300 bearing the apolar large cavity of PDH-158. Based on the structural analysis two single mutants (PDH-loopN99L, PDH-loopQ157A), one double mutant PDH-loopV97A/N99L, one triple mutant PDH-loopV97A/N99L/Q157A and one quadruple mutant PDH-loopV97A/N99L/Q157A/N161M were constructed with PDH-loop as template, expressed and purified.

The cofactor dependency of PDH-11300 and mutants is strictly linked to NAD<sup>+</sup>. To make the biocatalysts described herein suitable for combination with NADP(H) dependent enzymes (for example as thermostable cofactor recycling enzyme), a study on the cofactor specificity was performed. Examining the homology model of the PDH-loop, aspartate residue D55 could be identified pointing towards the ribose C2 hydroxyl group of the NAD<sup>+</sup> moiety. It was assumed that this residue would repel the negatively charged phosphate group of the hypothetically bound NADP<sup>+</sup>. After substitution of the C2 hydroxyl group with the phosphate group *in silico* two subsequent energy minimizations were conducted. It could be observed that the adenosine moiety of NADP<sup>+</sup> moved far out of the binding cleft (Fig. 3) in the PDH-loop. Based on this structural analysis the single mutant D55N was created *in silico*. After introducing the given mutation and performing a MD simulation the phosphate group could be found coordinated in a binding site flanked by amide-H-bond donor groups of the backbone of Q34, L56, N57 such as the amide groups of N57 and the newly introduced N55.



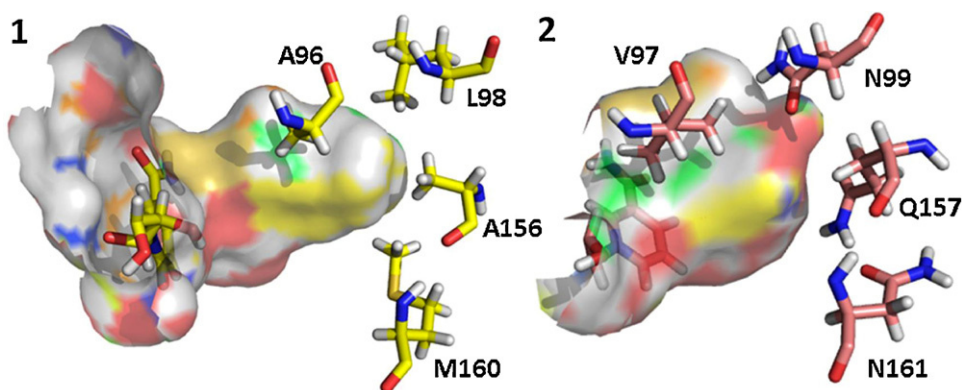


**Fig. 2.** Large binding pockets of PDH-158 (1) and PDH-11300 (2). Only the variable residues around the pockets of both enzymes and the nicotinamide ring of the NAD<sup>+</sup> are displayed.

### 3.2. Biochemical characterization: temperature- and pH-optima, stability

The temperature profiles of PDH-11300 and PDH-loop were examined using xylitol as model substrate. The activity was determined between 20 and 65 °C and both enzymes had the highest activity at 45 °C (Fig. 4). These results correspond well with the optimal growth conditions of *D. geothermalis*. At 55 °C a significant loss of activity could be found for PDH-11300 due to inactivation of the enzyme. For the loop mutant PDH-loop a broader temperature range could be determined. This mutant had 64% activity at 60 °C whereas the wild-type was not active any more. This implied a higher stability of the PDH-loop variant towards elevated temperatures. PDH-11300 showed best activity in bicine buffer at pH 9.0 and more than 80% activity remained between pH 8.5–10 during oxidations (Fig. 5). Interestingly, the PDH-loop variant was still active in the basic pH range above 9.0 and showed highest activity at pH 11 in glycine–NaOH buffer (140% compared to bicine buffer at pH 9.0).

Studies on the thermostability of PDH-11300 revealed no loss in activity during 6 h of incubation at 40 °C (Fig. 6b). During incubation at 45 °C a linear decrease in activity could be observed (12.5%

residual activity after 6 h). The mutant PDH-loop was stable for 6 h of incubation even at a temperature of 50 °C (Fig. 6c). At 55 °C the activity dropped to 6% after 2 h. These results confirm the broader temperature range and an improved thermostability of +10 °C for the loop mutant. PDH-158, in contrast, exhibits a low stability as 25 °C is the highest temperature where the enzyme remained active for 6 h (Fig. 6a). During incubation at 20 °C a “maturation” of the enzymes could be observed, resulting in an increased enzyme activity after 6 h (for PDH-11300 less characteristic visible at 35 °C).

By comparison of the melting points ( $T_m$ ) a similar ranking of the thermostability could be observed (Table 1 and Fig. S2). The PDH-158 possessed the lowest  $T_m$ , whereas the PDH-11300 showed a 5.2 °C (~48 °C) higher and the PDH-loop a 10.4 °C (~54 °C) higher melting point. Compared to the PDH-loop variant, the  $T_m$  of the cofactor mutant PDH-loopD55N was increased by 11.9 °C to 65.5 °C. For PDH-11300 and PDH-loop the  $T_{50}^{60}$  values were nearly comparable to the melting points whereas for PDH-158 and the PDH-loopD55N variant the  $T_{50}^{60}$  was about 8–9 °C lower than the  $T_m$  value. In order to evaluate the thermostability, the  $T_{50}^{60}$  is more accurate than the  $T_m$ , because it is directly linked to the enzyme activity after 1 h of incubation at certain temperatures. The  $T_{50}^{60}$  of PDH-11300 was 48 °C which was 13 °C higher than the value of

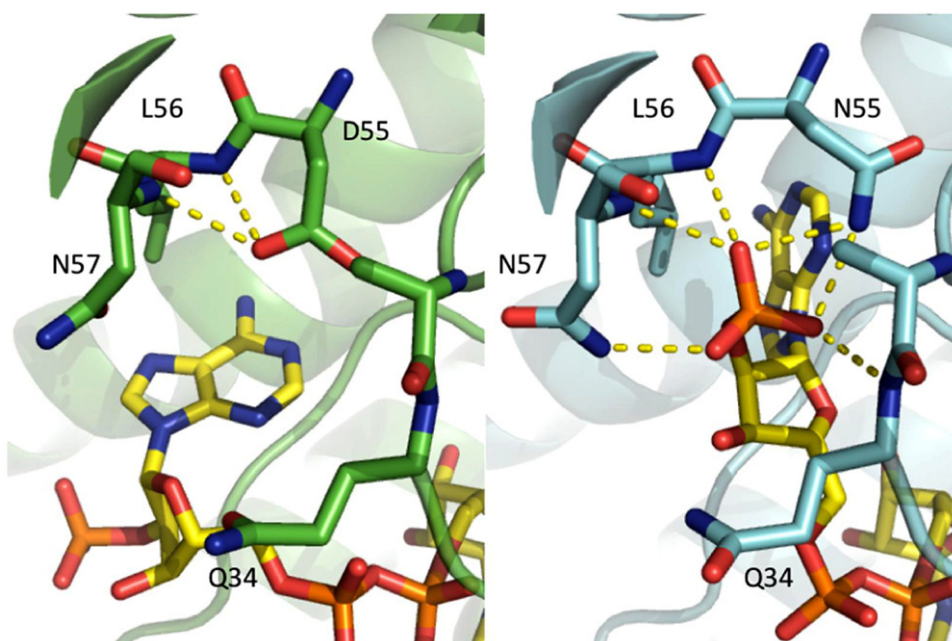


**Fig. 3.** Positioning of NADP<sup>+</sup> in the PDH-loop cofactor binding cleft (left) and NADP<sup>+</sup> bound to PDH-loopD55N (right).

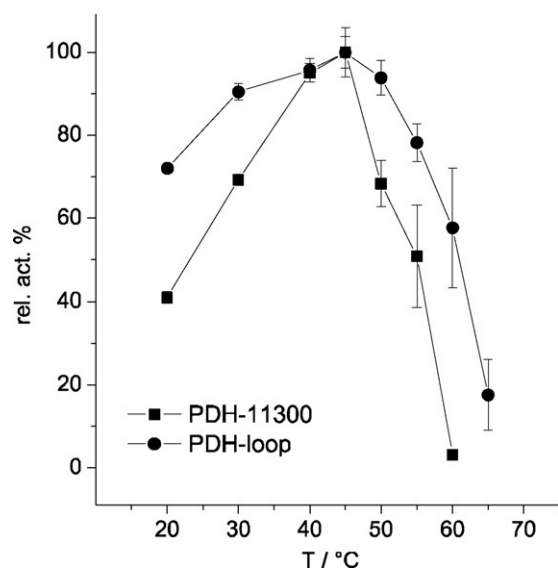


**Fig. 4.** Temperature dependency of initial velocities of PDH-11300 (■) and PDH-loop (●). 100% activity refers to 3.2 U/mg (PDH-11300) and 4.1 U/mg (PDH-loop) purified protein.

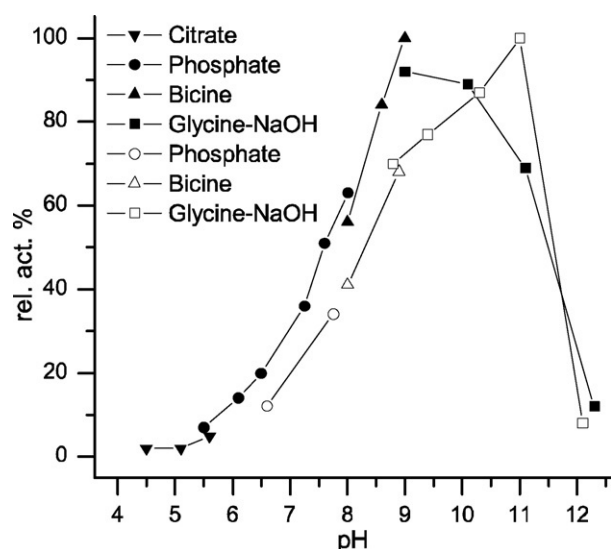


**Fig. 5.** Initial activities of PDH-11300 (filled symbols, ▼, ●, ▲, ■) and PDH-loop (empty symbols, ○, △, □) at different pH-values and buffer types. 100% activity refers to 5.5 U/mg (PDH-11300) and 2.4 U/mg (PDH-loop) purified protein.

**Table 1**  
Melting points  $T_m$  and  $T_{50}^{60}$  values of wild type and mutant polyol dehydrogenases.

PDH	$T_m$ (°C) <sup>a</sup>	$T_{50}^{60}$ (°C) <sup>b</sup>
158	43.2 ± 1.0	35.6 ± 0.4
11300	48.4 ± 0.5	48.3 ± 0.3
Loop	53.6 ± 0.2	55.3 ± 0.2
LoopD55N	65.5 ± 1.0	56.1 ± 0.2
LoopN99L	56.9 ± 0.3	nd
LoopQ157A	52.9 ± 0.2	nd
LoopV97A/N99L	53.8 ± 0.3	nd
LoopV97A/N99L/Q157A	48.5 ± 0.3	nd
LoopV97A/N99L/Q157A/N161M	48.8 ± 0.4	nd

<sup>a</sup> Melting point determined by circular dichroism spectroscopy.

<sup>b</sup> Temperature where 50% of enzyme activity remains after 60 min of incubation.

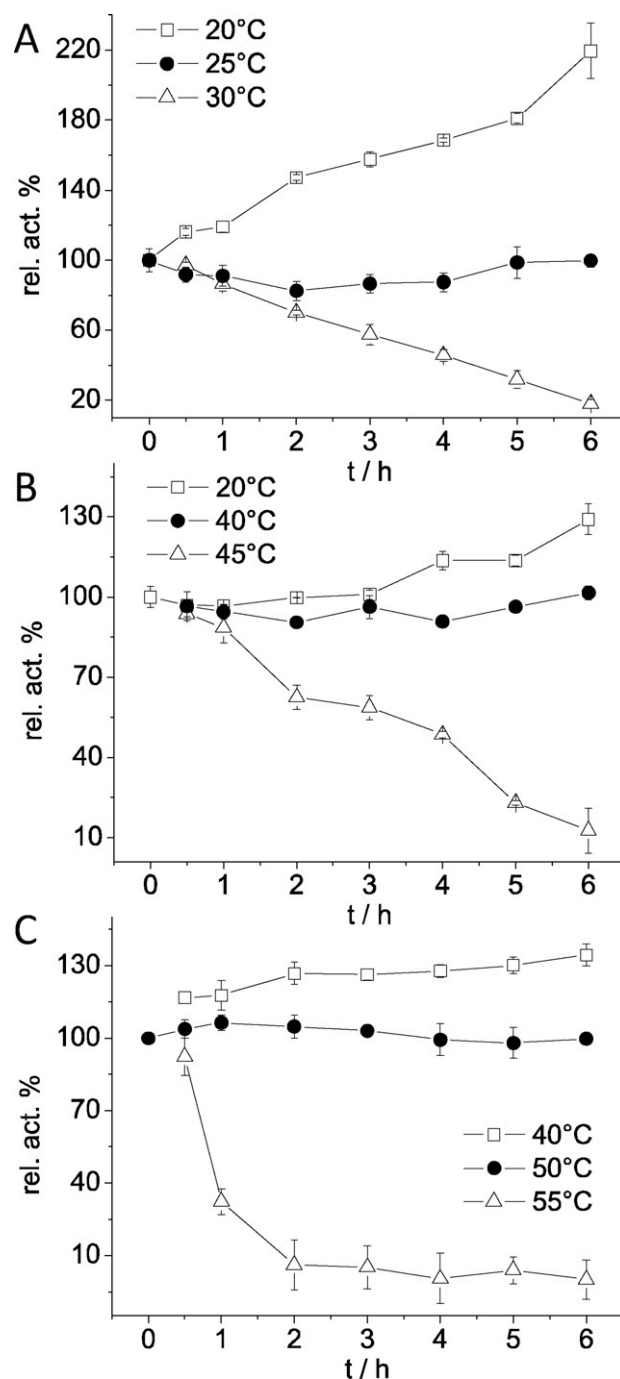


**Fig. 6.** Activity plots of A: PDH-158, B: PDH-11300 and C: PDH-loop after incubation up to 6 h at the given temperatures for elucidation of the thermostability of the enzymes. The graph with filled circles in each plot represents the highest temperature where the enzyme is stable for at least 6 h.

PDH-158. Again the thermophilic nature of PDH-11300 could be testified. The  $T_{50}^{60}$  of PDH-loop was increased by 7 °C compared to the wild type and roughly confirms findings of the stability measurements. For the active site mutants of PDH-loop only the  $T_m$  was investigated for a fast check of dramatically increased or decreased values. This was considered sufficient because the main focus of the mutant properties lay in the activity and alteration of substrate scope, and not on the stability. The  $T_m$  showed that no mutant had a melting point lower than PDH-11300. The PDH-loopQ157A and PDH-loopV97A/N99L variants showed no decreased melting point, but the mutant PDH-loopN99L had an increase of the  $T_m$  by 3 °C.

**Table 2**  
Substrate oxidation scope of PDH wild-types and mutants.<sup>a</sup>

Substrate	158	11300	loop	loopD55N	N-L <sup>b</sup>	Q-A <sup>b</sup>	2x <sup>b</sup>	3x <sup>b</sup>	4x <sup>b</sup>
1-Butanol	20	49	35	17	89	95	58	15	85
1-Methoxy-2-propanol	72	63	75	72	108	101	130	25	102
1-Phenylethanol	217	485	360	421	379	231	366	154	140
1-Propanol	23	47	43	20	81	89	82	14	79
1,2-Butanediol	3250	1013	1491	1447	901	194	736	90	95
1,2-Hexanediol	11298	2742	1960	2265	1583	389	2665	423	246
1,2-Propanediol	1028	311	403	325	405	118	323	44	110
1,3-Butanediol	146	182	74	87	166	141	141	54	127
1,3-Dihydroxyacetone	180	324	130	323	176	185	272	85	199
1,3-Propanediol	15	38	20	52	97	114	93	10	94
2-Butanol	460	303	605	349	473	456	540	367	186
2-Ethyl-1,3-hexanediol	47	120	60	21	119	127	99	25	80
2-Methyl-1-propanol	39	120	221	50	218	153	212	65	49
2-Propanol	341	142	195	88	206	159	213	112	66
2,3-Butandiol	998	664	1218	1326	1052	338	1014	210	89
3-Methyl-1-butanol	44	136	35	75	118	130	100	26	81
Cyclohexanol	305	654	1021	2076	1005	626	714	337	232
Cyclopentanol	500	383	466	207	464	427	576	343	234
Ethanol	37	55	23	53	89	131	66	17	56
Ethanolamine	30	23	23	23	86	91	61	7	54
Galactitol	263	1427	508	213	206	95	172	2	61
Glyceraldehyde	75	72	86	44	116	104	137	28	128
Glycerol	698	145	193	98	156	109	111	23	54
Hydroxyacetone	56	100	43	50	120	145	89	26	57
Sorbitol	72	936	763	400	230	102	166	19	73
Thioglycerol	221	782	1036	1459	276	147	239	40	71
Xylitol	6651	4659	1521	1435	1096	128	1722	40	60

<sup>a</sup> Activities are given in mU/mg and were determined with 0.5 mM NAD<sup>+</sup> in bicine buffer (pH 9.0; 100 mM). For mutant PDH-loopD55N NADP<sup>+</sup> was used as cofactor. Substrate concentrations are given in Section 2.

<sup>b</sup> The abbreviation refer to following PDH mutants: N-L: loopN99L, Q-A: loopQ157A, 2x: loopV97A/N99L, 3x: loopV97A/N99L/Q157A and 4x: loopV97A/N99L/Q157A/N161M.

A combination of the double mutant and mutation Q157A gave a  $T_m$  reduction by 5 °C for the PDH-loopV97A/N99L/Q157A triple mutant. Heat treatment of PDH-11300 for 10–30 min at 50 °C for purification purposes gave a 1.7-fold higher purity without loss of activity.

### 3.3. Substrate scope and steady-state kinetics for NADH/NADPH

The substrate scopes of nine PDH variants were determined to evaluate the influence of the introduced mutations. Especially the reconstruction of the hydrophobic substrate binding-cleft of PDH-158 in the PDH-loop mutant by combination of several point mutations mentioned above was investigated. Regarding the substrate spectra of all enzymes a bias towards vicinal diols was obvious. In each analysis 1,2-hexanediol, 1,2-butanediol and 1,2-propanediol (in the order of decreasing activity) were among the best substrates. 1,2-hexanediol was the best substrate for the PDH-158. In contrast, 1,2-hexanediol was only second best for PDH-11300, here xylitol was the best substrate. Galactitol, the third best substrate for PDH-11300, was a worse substrate for PDH-158, even though galactitol is the naming substrate for this enzyme subclass. By substitution of the substrate recognition loop leading to mutant PDH-loop, the order for the highest activity substrates resembled more the scope of PDH-158 than PDH-11300. The correlation coefficient between PDH-158 and

PDH-loop such as PDH-11300 and PDH-loop are  $r=0.78$  and  $r=0.77$  respectively. Comparing the activity for 1-propanol and 1-butanol with the secondary alcohols 2-propanol and 2-butanol in PDH-158 and PDH-11300, it could be derived that these enzymes (and the mutants thereof) preferably oxidize secondary than primary alcohols. The activity of PDH-loopD55N against cyclohexanol was improved remarkably. While glycerol was the sixth best substrate for PDH-158, the activity could not be recovered by rebuilding the hydrophobic binding pocket of the PDH-158 in the single or combined PDH-loop point mutants. The substrate scope of mutant PDH-loopV97A/N99L among the mutants PDH-loopN99L, PDH-loopQ157A, PDH-loopV97A/N99L/Q157A and PDH-loopV97A/N99L/Q157A/N161M with  $r=0.94$  had the highest correlation with the substrate scope of the PDH-loop variant (Table 2). As expected, the correlation of substrate scopes was also high between the PDH-loop and PDH-loopD55N ( $r=0.93$ ). The amino acid positions Q157 and N161 in the PDH-loop variant seem to have an essential role, since enzymes containing mutations at these sites exhibited decreased enzyme activities (i.e. PDH-loopQ157A, PDH-loopV97A/N99L/Q157A and PDH-loopV97A/N99L/Q157A/N161M, Table 2). The positions V97 and N99 seem to be susceptible to mutation since the variants V97A and N99L did not lead to a significant activity loss. In the case of 1,2-hexanediol the combination of these two substitutions (mutant PDH-loopV97A/N99L) improved the activity compared to the



**Table 3**  
Kinetic constants of PDH variants against the cofactor NAD<sup>+</sup> and NADP<sup>+</sup>.<sup>a</sup>

Enzyme	Cofactor	$K_m$ (mM)	$k_{cat}$ (s <sup>-1</sup> )	$k_{cat}/K_m$ (s <sup>-1</sup> μM <sup>-1</sup> )
PDH-11300	NAD <sup>+</sup>	0.15 ± 0.06	1.61	10,740
PDH-loop	NAD <sup>+</sup>	0.15 ± 0.03	2.70	17,800
PDH-loopD55N	NAD <sup>+</sup>	0.44 ± 0.26	1.53	3480
PDH-loopD55N	NADP <sup>+</sup>	0.41 ± 0.09	1.42	3450

<sup>a</sup> Activities were determined against 1,2-hexanediol.

single mutants. Despite these two mutations, introduction of further mutations for the reconstruction of the catalytic site of PDH-158 did not lead to improved enzyme activity.

The  $K_m$  of PDH-11300 and PDH-loop against NAD<sup>+</sup> is 150 μM for both enzymes. The substitution of the substrate recognition loop hence did not effected the co-substrate binding affinity, still the NAD<sup>+</sup> turnover was increased by 68% to 2.7 s<sup>-1</sup> (Table 3). Following mutagenesis and expression, activity tests of the purified mutant enzyme PDH-loopD55N showed activity towards both cofactors NAD<sup>+</sup> and NADP<sup>+</sup>. For PDH-11300, PDH-loop and PDH-loopD55N the kinetic parameters were determined for NAD<sup>+</sup> and NADP<sup>+</sup>. No activity could be found for PDH-loop and NADP<sup>+</sup>. The relaxed mutant PDH-loopD55N showed activity against both, NAD<sup>+</sup> and NADP<sup>+</sup>, all the kinetic parameters were comparable resulting in a catalytic efficiency of ~3.5 s<sup>-1</sup> mM<sup>-1</sup>. However, the catalytic efficiency of PDH-loopD55N was decreased compared to PDH-11300. Still the findings reinforce the prediction that the NADP(H) phosphate group is stabilized by polar contacts in an H-bond donor site (Fig. 3). A minor disadvantage of PDH-loopD55N was the lower expression level for soluble enzyme compared to the PDH-loop variant.

#### 4. Discussion

In this study a new polyol dehydrogenase from the mesophilic organism *D. geothermalis* 11300 (PDH-11300) was cloned, characterized and served as scaffold for a newly designed biocatalyst. The temperature optimum was examined and corresponds to the optimal growth conditions of the strain of 45 °C. Reported temperature optima of enzymes with *D. geothermalis* origin vary in a range from 45 °C to 60 °C. For instance amylosucrase of *D. geothermalis* was reported to have an optimal temperature of 50 °C and a half-life of 26 h at 50 °C [25]. The maximum half-life of the PDH-11300 characterized here was 3.5 h at 45 °C. Nevertheless, the chimeric mutant PDH-loop retained 100% of its activity for more than 6 h at 50 °C. A β-galactosidase from *D. geothermalis* was described having a half-life of 3 h at 60 °C [14]. The attempt to evaluate and compare these enzyme properties is difficult since different temperatures and timespans are used throughout different studies. It becomes obvious, that the  $T_{50}^{60}$ -values describe the thermostability of an enzyme in the most precise and unbiased manner since a fixed incubation time is applied and the  $T_{50}^{60}$ -value is determined by fitting the residual activities over several different temperatures.

The PDH-11300 showed the highest activity at pH 9.0. The properties of the enzyme were compared with the homolog PDH enzyme of *R. sphaeroides* 158 which shares high sequential and structural homology with the *D. geothermalis* enzyme. The new enzyme PDH-11300 was much more thermostable compared to PDH-158. For determination of the reasons of the different substrate scope and activity, an extensive protein engineering study on the binding site of PDH-11300 was carried out. At first a loop containing amino acids with high B-factors was identified in the crystal structure of PDH-158. It was assumed that this flexible loop highly influences the substrate

conversion, especially for larger, bulkier substrates. The newly designed chimeric enzyme PDH-loop showed a similar substrate conversion for 16 compounds compared to PDH-158, which could be explained by the new PDH-158 like active site region. The overall substrate scope was not altered seriously as seen by the correlation coefficients. The substrate scopes of PDH-158 and PDH-11300 correlate by  $r=0.81$ . In fact the correlations of PDH-loop with the PDH-158 ( $r=0.78$ ) and PDH-11300 substrate scope ( $r=0.77$ ) are slightly smaller. An explanation might be, that the loop region is not the only determinant of substrate specificity.

Interestingly, a broader pH, and temperature profile, such as a 10 °C increased thermostability of the chimera was observed compared to PDH-11300. This was a rather unexpected finding, as the mutant contained the flexible loop of the non-thermostable PDH-158 (merely stable for 6 h at 25 °C). The increase in thermostability was proven by means of the  $T_m$ , long-term stability and  $T_{50}^{60}$ . In literature the stabilization of enzymes is described as a gain of rigidity, or is reported as stabilization by substitution of flexible residues. An explanation hence might be, that the corresponding wild-type loop from PDH-11300 is much more flexible than that from PDH-158. For multimeric enzymes stabilization can also occur due to the enhancement of subunit interaction. The altered loop regions are not located at the multimerization interfaces (Fig. 1) but are located on the opposite sites. Due to the far distance no additional H-bonds or hydrophobic interactions were directly introduced. Nevertheless it might be possible, that due to interactions or repulsions between residues inside the subunits longer ranging effects influence the subunit binding. Since no crystal structure of PDH-11300 and hence the PDH-loop variant is available yet, the explanation for the elevated thermostability remains elusive. Nevertheless the chimeric enzyme PDH-loop, represents the first example of enzyme stabilization by introduction of a loop from a less thermostable to a moderately thermostable enzyme. Even if single mutations showed no effect, a combination of the mutations was shown to have a big influence on the thermotolerance.

Following the chimera design and enzyme characterization, the structure–function relationship of the enzyme regarding substrate scope and activity was elucidated by a multiple point mutational study on the active site of PDH-loop. Therefore a map of the large cavity of the substrate binding site from PDH-loop and PDH-11300 was build based upon homology modeling. The goal was to identify key residues for substrate conversion and recognition by alignment of the crystal structure of PDH-158 and the homology model of PDH-11300. A reconstruction of the apolar large cavity of PDH-158 was conducted expecting the substrate scope to approach the template substrate scope. The amino acid positions Q157 and N161 were shown to be important for conversion of 1,2-diols in PDH-loop. The positions V97 and N99 were mutated without significant activity loss, and hence might be candidates for further saturation mutagenesis studies.

We performed a protein engineering of the cofactor specificity of PDH-loop and identified mutation D55N as crucial key residue for NADP<sup>+</sup> dependency. The resulting mutant PDH-loopD55N accepted both cofactors with similar activity and affinity (Table 3), neither the chimera nor the wild-type enzymes were active with NADP<sup>+</sup>. A possible explanation for the change of cofactor activity was found by docking and energy minimization studies. Herein the aspartate residue repels the phosphate group, whereas the asparagine residue provides for additional stabilization of the phosphate.

Since 1,2-hexanediol or xylitol were among the best substrates for the newly described enzymes, we propose that the enzyme might better be designated as polyol dehydrogenases rather than galactitol dehydrogenases.

## 5. Conclusion

We have successfully cloned and characterized a new thermostable polyol dehydrogenase PDH-11300 from *D. geothermalis*. Introduction of a loop of the less thermostable homolog enzyme PDH-158 led to a thermostabilized enzyme. The substrate scope and active site of the PDHs were studied extensively. The strict NAD<sup>+</sup> dependency was expanded successfully to both cofactors (NAD<sup>+</sup> and NADP<sup>+</sup>) by a single point mutation.

## Acknowledgements

The authors thank the “Fachagentur für Nachwuchsende Rohstoffe (AZ06NR073, 22015906)”, the “Bundesministerium für Bildung und Forschung Biokatalyse2021 cluster, FK0315175B” and neoplas GmbH (Greifswald, Germany) for financial support.

## Appendix A. Supplementary data

Supplementary data associated with this article can be found, in the online version, at <http://dx.doi.org/10.1016/j.enzmictec.2012.06.006>.

## References

- [1] Behrens GA, Hummel A, Padhi SK, Schätzle S, Bornscheuer UT. Discovery and protein engineering of biocatalysts for organic synthesis. *Advanced Synthesis and Catalysis* 2011;353:2191–215.
- [2] Bornscheuer UT, Huisman G, Kazlauskas RJ, Lutz S, Moore J, Robins K. Engineering the third wave of biocatalysis. *Nature* 2012;485:185–94.
- [3] Eijssink VGH, Gäseidnes S, Borchert TV, van den Burg B. Directed evolution of enzyme stability. *Biomolecular Engineering* 2005;22:21–30.
- [4] Arnold FH, Wintrode PL, Miyazaki K, Gershenson A. How enzymes adapt: lessons from directed evolution. *Trends in Biochemical Science* 2001;26:100–6.
- [5] Reetz MT, Carballeira JD, Vogel A. Iterative saturation mutagenesis on the basis of B factors as a strategy for increasing protein thermostability. *Angewandte Chemie International Edition* 2006;45:7745–51.
- [6] Jochens H, Aerts D, Bornscheuer UT. Thermostabilization of an esterase by alignment-guided focused directed evolution. *Protein Engineering, Design and Selection* 2010;23:903–9.
- [7] Fernandez-Lafuente R. Stabilization of multimeric enzymes: strategies to prevent subunit dissociation. *Enzyme and Microbial Technology* 2009;45:405–18.
- [8] Zimmer C. Identifizierung von zwei biotechnologisch interessanten Enzymen und ihrer Gene zur stereo- und regioselektiven Modifikation von Kohlenhydraten: Benzoylsterase und Galaktitol-Dehydrogenase. Dissertation. Saarbrücken:University of Saarland;2006.
- [9] Schneider K-H, Jäkel G, Hoffmann R, Giffhorn F. Enzyme evolution in *Rhodobacter sphaeroides*: selection of a mutant expressing a new galactitol dehydrogenase and biochemical characterization of the enzyme. *Microbiology* 1995;141:1865–73.
- [10] Huwig A, Emmel S, Jäkel G, Giffhorn F. Enzymatic synthesis of L-tagatose from galactitol with galactitol dehydrogenase from *Rhodobacter sphaeroides* D. Carbohydrate Research 1997;305:337–9.
- [11] Ferreira AC, Nobre MF, Rainey FA, Silva MT, Wait R, Burghardt J, et al. *Deinococcus geothermalis* sp. nov. and *Deinococcus murrayi* sp. nov., two extremely radiation-resistant and slightly thermophilic species from hot springs. *International Journal of Systematic Bacteriology* 1997;47:939–47.
- [12] Wanarska M, Krawczyk B, Hildebrandt P, Kur J. RecA proteins from *Deinococcus geothermalis* and *Deinococcus murrayi* – cloning, purification and biochemical characterisation. *BMC Molecular Biology* 2011;12:17.
- [13] Wulf H, Perzborn M, Sievers G, Scholz F, Bornscheuer UT. Kinetic resolution of glyceraldehyde using an aldehyde dehydrogenase from *Deinococcus geothermalis* DSM 11300 combined with electrochemical cofactor recycling. *Journal of Molecular Catalysis B: Enzymatic* 2012;74:144–50.
- [14] Lee J-H, Kim Y-S, Yeom S-J, Oh D-K. Characterization of a glycoside hydrolase family 42  $\beta$ -galactosidase from *Deinococcus geothermalis*. *Biotechnology Letters* 2011;33:577–83.
- [15] Carius Y, Christian H, Faust A, Zander U, Klink BU, Kornberger P, et al. Structural insight into substrate differentiation of the sugar-metabolizing enzyme galactitol dehydrogenase from *Rhodobacter sphaeroides* D. *Journal of Biological Chemistry* 2010;285:20006–14.
- [16] Fan F, Lorenzen JA, Plapp BV. An aspartate residue in yeast alcohol dehydrogenase I determines the specificity for coenzyme. *Biochemistry* 1991;30:6397–401.
- [17] Bertani G. Studies on Lysogeny I: the mode of phage liberation by lysogenic *Escherichia coli*. *Journal of Bacteriology* 1951;62:293–300.
- [18] Sambrook J, Russell DW. *Molecular cloning: a laboratory manual*. 3rd ed. New York: Cold Spring Harbor Laboratory Press; 2001.
- [19] Hanahan D. Studies on transformation of *Escherichia coli* with plasmids. *Journal of Molecular Biology* 1983;166:557–80.
- [20] Krieger E, Koraimann G, Vriend G. Increasing the precision of comparative models with YASARA NOVA – a self-parameterizing force field. *Proteins* 2002;47:393–402.
- [21] Krieger E, Darden T, Nabuurs SB, Finkelstein A, Vriend G. Making optimal use of empirical energy functions: force-field parameterization in crystal space. *Proteins* 2004;57:678–83.
- [22] Laemmli UK. Cleavage of structural proteins during the assembly of the head of bacteriophage T4. *Nature* 1970;227:680–5.
- [23] Wilkinson GN. Statistical estimations in enzyme kinetics. *Biochemical Journal* 1961;80:324–32.
- [24] Duggleby RG. A nonlinear regression program for small computers. *Analytical Biochemistry* 1981;110:9–18.
- [25] Emond S, Mondeil S, Jaziri K, André I, Monsan P, Remaud-Siméon M, et al. Cloning, purification and characterization of a thermostable amylosucrase from *Deinococcus geothermalis*. *FEMS Microbiology Letters* 2008;285:25–32.

## Articles

### Article III



# A self-sufficient Baeyer–Villiger biocatalysis system for the synthesis of $\epsilon$ -caprolactone from cyclohexanol

H. Mallin<sup>1</sup>, H. Wulf<sup>1</sup>, U.T. Bornscheuer<sup>\*</sup>

Department of Biotechnology & Enzyme Catalysis, Institute of Biochemistry, Greifswald University, Felix-Hausdorff-Str 4, D-17487, Greifswald, Germany

## ARTICLE INFO

### Article history:

Received 30 October 2012

Received in revised form 6 December 2012

Accepted 14 January 2013

### Keywords:

Co-immobilization

$\epsilon$ -Caprolactone

Biocatalysis

Baeyer–Villiger monooxygenase

Cofactor recycling

## ABSTRACT

In order to establish a new route for  $\epsilon$ -caprolactone production from the corresponding cyclohexanol with an internal cofactor recycling for NADPH, a recently redesigned thermostable polyol dehydrogenase (PDH) and the cyclohexanone monooxygenase (CHMO) from *Acinetobacter calcoaceticus* were combined. First, the expression of PDH could be improved 4.9-fold using *E. coli* C41 with co-expression of chaperones. Both enzymes were also successfully co-immobilized on glutaraldehyde-activated support (Relizyme<sup>TM</sup> HA403). Cyclohexanol could be converted to  $\epsilon$ -caprolactone ( $\epsilon$ -CL) with 83% conversion using the free enzymes and with 34% conversion using the co-immobilized catalysts. Additionally, a preparative scale biotransformation of  $\epsilon$ -caprolactone starting from cyclohexanol was performed using the soluble enzymes. The  $\epsilon$ -CL could be isolated by simple extraction and evaporation with a yield of 55% and a purity of >99%.

© 2013 Elsevier Inc. All rights reserved.

## 1. Introduction

Researchers in biocatalysis strive to find solutions for the replacement of conventional chemical routes by application of enzymes. The advantages of biosynthetic routes are lower energy cost due to lower reaction temperatures, less or no usage of organic solvents, and fewer efforts required for workup due to the high chemo-, regio- and enantioselectivity of enzymes [1,2]. Especially useful are routes where several enzymatic steps are combined in order to achieve multistep synthesis and avoid isolation of intermediates. A further challenge is the cofactor dependency of especially NAD(P)H-dependent enzymes. We have focused here on the design of a system combining a Baeyer–Villiger monooxygenase (BVMO) with a polyol dehydrogenase in order to produce  $\epsilon$ -caprolactone ( $\epsilon$ -CL) directly from cyclohexanol (CHL, Scheme 1). On industrial scale,  $\epsilon$ -CL is synthesized by Baeyer–Villiger oxidation [3] using peracetic acid and cyclohexanone (CHO) as substrates.  $\epsilon$ -CL is used for the formation of biodegradable thermoplastic polyesters by ring opening polymerization [4] and was formerly used as precursor for  $\epsilon$ -caprolactam and hence polyamide production [5,6].

Baeyer–Villiger monooxygenases are valuable enzymes for the regio- and stereoselective formation of ester functions by introduction of molecular oxygen via Baeyer–Villiger oxidation [3,7]. BVMOs accept a broad range of substrates; particularly the NADPH-dependent cyclohexanone monooxygenases (CHMO) from *Acinetobacter calcoaceticus* [8–10] was shown to convert a vast variety of ketones of different substance classes [11,12]. In order to perform cost effective scale-up, efficient cofactor recycling must be ensured for these biotransformations. This might be performed using resting cells as described by Geitner et al. [13] or by co-expression of NADPH-regenerating enzymes like glucose-6-phosphate dehydrogenase and CHMO in whole cell systems [14]. The application of isolated enzymes as biocatalysts can be advantageous for several reasons compared to whole cells especially if the reaction comprises only one (or few) reaction steps [15]. Consequently, several recycling systems using isolated enzymes, e.g. using a phosphite dehydrogenase fused to a BVMO [16], have been developed (for a review see Torres Pazmiño et al. [17]).

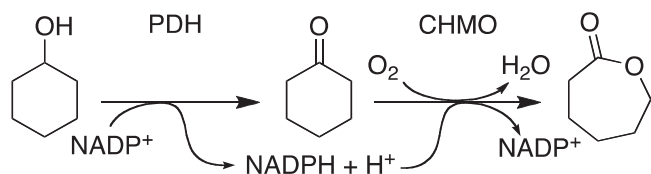
To achieve high total turnover numbers and thus to guarantee for the stability of biocatalysts, immobilization of enzymes has been applied since decades. An additional benefit of enzyme immobilization is the easier separation of the catalyst from the reaction product and eventually from the cofactor. Immobilized enzymes, mainly isomerases and hydrolases are widely used in industrial applications, and many different classes of carriers have been employed [18–20]. The CHMO of *A. calcoaceticus* could be immobilized for example on polyethylenimine-coated agarose support via adhesion or covalently bound to Eupergit<sup>®</sup> C [21].

**Abbreviations:** PDH, polyol dehydrogenase (PDH.loopN); CHMO, cyclohexanone monooxygenase from *Acinetobacter calcoaceticus*; CHL, cyclohexanol;  $\epsilon$ -CL,  $\epsilon$ -caprolactone; CHO, cyclohexanone; BVMO, Baeyer–Villiger monooxygenase; FID, flame-ionization detection; GA, glutaraldehyde.

<sup>\*</sup> Corresponding author. Tel.: +49 3834 86 4367, fax: +49 3834 86 794367.

E-mail address: [uwe.bornscheuer@uni-greifswald.de](mailto:uwe.bornscheuer@uni-greifswald.de) (U.T. Bornscheuer).

<sup>1</sup> Both authors equally contributed to this work.



**Scheme 1.** The oxidation of CHL with the cofactor NADP<sup>+</sup> catalyzed by the polyol dehydrogenase (PDH) yields CHO and the reduced cofactor NADPH. Both are then converted by the Baeyer–Villiger monoxygenase (CHMO) furnishing  $\epsilon$ -CL and NADP<sup>+</sup>; the latter being reused for the next catalysis cycle.

We have recently designed a polyol dehydrogenase PDH-loopN (here called PDH) by introducing a substrate recognition loop from a PDH from *Rhodobacter sphaeroides* into the thermostable scaffold of a *Deinococcus geothermalis* polyol dehydrogenase. The cofactor specificity was also broadened so that NADPH could now be utilized [22]. As the PDH chimera accepts CHL as substrate (with an activity of 2 U mg<sup>−1</sup>) this now enables to combine the PDH with a Baeyer–Villiger oxidation (Scheme 1) to perform a self-sufficient double oxidation of CHL to  $\epsilon$ -CL. The concept of a self-sufficient closed-loop recycling system was first reported by Willets et al. using resting cells of *A. calcoaceticus* expressing a CHMO. However, they applied isolated alcohol dehydrogenase from *Thermoanaerobium brockii* and purified *A. calcoaceticus* monoxygenase to convert bicyclic alcohols to their corresponding lactones [23]. Furthermore, in this work, we immobilized both enzymes using the Relizyme<sup>TM</sup> HA403 support to facilitate enzyme reuse and enhance stability.

## 2. Materials and methods

### 2.1. Materials

All chemicals were purchased from Fluka (Buchs, Switzerland), Sigma–Aldrich (Steinheim, Germany) and Merck (Darmstadt, Germany) unless stated otherwise. Relizyme<sup>TM</sup> HA403 was obtained from Resindion (Binasco, Italy).

### 2.2. Strains and culture conditions

The CHMO of *A. calcoaceticus* was readily cloned into pET-28a(+) in frame with a N-terminal His<sub>6</sub>-tag. The chimeric PDH was cloned into pET-22b(+) in frame with a N-terminal His<sub>6</sub>-tag. For the initial expression experiments both enzymes were expressed in *E. coli* BL21 (DE3) cells grown at 30 °C in shaking flasks. Auto-induction media ZYP-5052 [24] was used for protein expression of PDH and cells were harvested after overnight expression. CHMO expression was induced with 0.1 mM IPTG at an OD<sub>600</sub> of 0.5 at 20 °C and cells were grown in terrific broth media. After overnight expression, the cells were harvested. The cells were washed, disrupted and subsequently the protein was purified by IMAC according to a protocol previously reported [25]. The CHMO was stored in sodium phosphate buffer (50 mM, pH 7.5) including 0.1 mM FAD for stabilization [26].

### 2.3. Expression optimization

For expression optimization of the PDH different chaperones (TaKaRa Chaperone Plasmid Set #3340) and strains were examined. The chaperone kit includes the plasmids pGro7, pGKJE8, pKJE7, pGTF2 and pTF16. As strains *E. coli* BL21 (DE3), *E. coli* C41 (DE3) and *E. coli* SHuffle (DE3) were tested. Cultivation was performed in a volume of 50 ml ZYP-5052 media in a 250 ml baffled flask. After inoculation with 0.5 ml of overnight culture cells were incubated at 30 °C. After 2 h the chaperone expression was induced according to the manufacturers protocol. After expression overnight for 16 h at 30 °C OD<sub>600</sub> normalized samples were taken and disrupted in a volume of 0.5 ml sodium phosphate buffer (50 mM, pH 7.5) via sonication for 1 min. The supernatant was used for activity measurements with the NADPH assay (see below) and for analyses of the soluble fraction via SDS-PAGE. The insoluble pellet was washed and then used for analyses of the insoluble fraction via SDS-PAGE. Protein measurements were done with Roti<sup>®</sup>-Nanoquant according to the manufacturer protocol.

### 2.4. Activity assays, combined biocatalysis and GC analysis

The activity of PDH was determined spectrophotometrically at 30 °C by monitoring the formation of NADPH ( $\epsilon = 5.12 \text{ mM}^{-1} \text{ cm}^{-1}$ ) at 340 nm. The standard reaction mixture (1 ml) contained 100 mM bicine–HCl buffer (pH 9.0), 0.25 mM NADP<sup>+</sup>, 100 mM of xylitol and an appropriate amount of the enzyme. CHMO activity was

determined by spectrophotometric monitoring of the decrease of NADPH at 340 nm using the same buffer with 0.6 mM CHO. The reaction was started by addition of 0.3 mM of NADPH. One unit of dehydrogenase activity or BVMO activity was defined as the amount of enzyme that catalyzes the formation of 1  $\mu\text{mol}$  NADPH or NADP<sup>+</sup> per minute respectively. For biocatalysis, differing amounts of pure enzyme were used in 1–3 ml batches (glass vials or flasks) in 100 mM bicine–HCl buffer (pH 9.0) containing 5–10 mM CHL and a mixture of 0.3 mM of each NADP<sup>+</sup> and NADPH. Biotransformations were closed with a breathable film (AeraSeal film, Excel Scientific), shaken at 30 °C and 250  $\mu\text{l}$  samples were taken periodically. These were extracted with 500  $\mu\text{l}$  dichloromethane containing 2 mM acetophenone as internal standard. Concentrations of CHL, CHO and  $\epsilon$ -CL were determined by gas chromatography using a Shimadzu GC-14A equipped with a Hydrodex<sup>®</sup>- $\beta$ -3P column (25 m  $\times$  0.25 mm, Macherey–Nagel, Düren, Germany) and flame-ionization detection (FID). In the beginning the oven temperature was kept at 60 °C for 10 min, followed by an increase to 160 °C with a heating rate of 10 °C/min. The temperature was then held at 160 °C for ten minutes (retention times: CHO = 10.3 min, CHL = 13.3 min,  $\epsilon$ -CL = 18.6 min).

### 2.5. Preparative scale biotransformation

The biotransformation was carried out in a shake flask containing 30 ml bicine–HCl buffer (100 mM, pH 9.0), 10 mM CHL, 3.6 U PDH (one unit corresponds to the conversion of 1  $\mu\text{mol min}^{-1}$  CHL), 40 U CHMO (one unit corresponds to the conversion of 1  $\mu\text{mol min}^{-1}$  CHO) and 0.6 mM of each, reduced and oxidized cofactor. The reaction batch was extracted two times with 30 ml dichloromethane. After evaporation of the organic solvent, the extract was analyzed by GC–MS equipped with the same column used above. The same heating conditions were used except that the maximum temperature was increased to 180 °C.

### 2.6. Co-immobilization of CHMO and PDH

For co-immobilization of CHMO and PDH, 0.5–1 g (dry weight) of Relizyme<sup>TM</sup> HA403 were treated with 4–8 ml 0.125% glutaraldehyde (GA) in 50 mM phosphate buffer (pH 7.5, 2 h). Different ratios of CHMO:PDH (units) dissolved in 8 ml were added to the glutaraldehyde treated carrier and incubated for 16 h at 4 °C and 20 rpm. After washing with two times 20 ml of phosphate buffer, the immobilized enzymes were used for biocatalysis. For determination of activity, 5 mg (dry weight) of biocatalyst were used in a volume of 250  $\mu\text{l}$  reaction buffer (pH 9.0) containing different amounts of CHL and the cofactor mixture. Each concentration was measured in triplicate. After 1.5 h the whole mixture was extracted using the protocol described above. Biotransformations with 75 mg (dry weight) immobilized enzymes were carried out in 2 ml bicine–HCl buffer (100 mM, pH 9.0, 18 mU/ml) containing 0.3 mM NADP<sup>+</sup>, 0.3 mM NADPH and 10 mM CHL at 30 °C. Samples were taken periodically and were analyzed as described above. For recycling studies, 100 mg (dry weight) of biocatalyst were used in 1 ml reaction buffer (pH 9.0) containing 5 mM CHL and the cofactor mix. After 1 h, a 250  $\mu\text{l}$  sample was taken and analyzed as mentioned above. The biocatalyst was washed two times with 50 mM cold sodium phosphate buffer (pH 7.5) and was then subjected to the next cycle. For the approach with additional soluble enzyme 0.1 U ml<sup>−1</sup> of pure PDH and 1 U ml<sup>−1</sup> of pure CHMO were added to each cycle. The recovered activity was calculated by comparison of the missing units from the supernatant after immobilization and the units found on 500 mg (dry) support after immobilization.

## 3. Results

### 3.1. Expression optimization of PDH

Due to the poor expression of the PDH mutant [22] we first investigated the optimization of the overexpression of the enzyme. Because of the large insoluble fraction we tried an expression at 20 °C, which did not result in a higher total amount of PDH. Next, we used different chaperones to support folding during overexpression. Plasmids bearing five different chaperones (pGro7, pGKJE8, pKJE7, pGTF2 and pTF16 respectively) were tested and it turned out that pGro7 showed an increased volumetric activity of 4.3-fold and pGKJE8 an increase of 2-fold compared to the wild-type without chaperones (Fig. 1).

Further expression optimization was achieved by using different *E. coli* strains (BL21, C41 and SHuffle). Regarding the protein specific activity of the crude extract, the *E. coli* strain SHuffle turned out to be the most effective producer of the overexpressed enzyme (Fig. 2). Regarding the protein specific activity (crude extract), the *E. coli* strain C41 was the worst compared to the other two strains.

With *E. coli* C41 and co-expression of pGro7 chaperones (GroES–GroEL) about 1592 U L<sup>−1</sup> of culture broth could be obtained. This



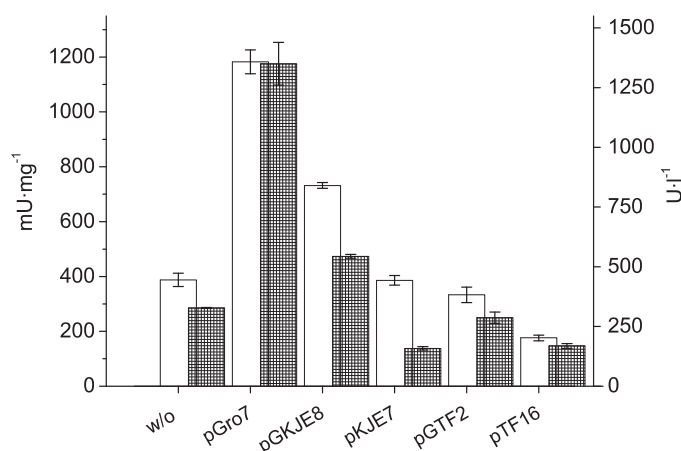


**Fig. 1.** Comparison of the specific protein activities (crude extract) of PDH expressed in BL21 using different chaperones to enhance functional protein folding. The open columns belong to the specific activity in  $\text{mU mg}^{-1}$  (left axis); the filled columns depict the volumetric activity in  $\text{U l}^{-1}$  (right axis). Activities were determined against xylitol.

corresponds to a 4.9-fold increase compared to initial conditions (Table S1) and represents the best expression system according to the obtained volumetric activity. The low specific activity found for this expression system is due to the high total protein amount of the *E. coli* C41. Furthermore the better expression was visualized by SDS-PAGE analysis where the same trend could be observed (Fig. S1).

### 3.2. Biocatalysis with dissolved enzymes and $\epsilon$ -CL synthesis

With 0.5 U (per batch) of both enzymes during biocatalysis a conversion of 84 and 80% based upon  $\epsilon$ -CL formation with 5 and 10 mM CHL, respectively, could be obtained. This conversion was observed after 2 h and only slightly increased after incubation for 4 h. For both approaches after 2 h around 95% of the substrate CHL was consumed.

To determine the rate-limiting step of the two-step reaction, three different ratios of enzyme activity were studied with 5-fold lower amounts of enzymes (Fig. 3). The highest conversion of 84% was obtained after 4.5 h with a threefold excess of CHMO over PDH (94% of CHL was consumed at this time). Equal amounts of

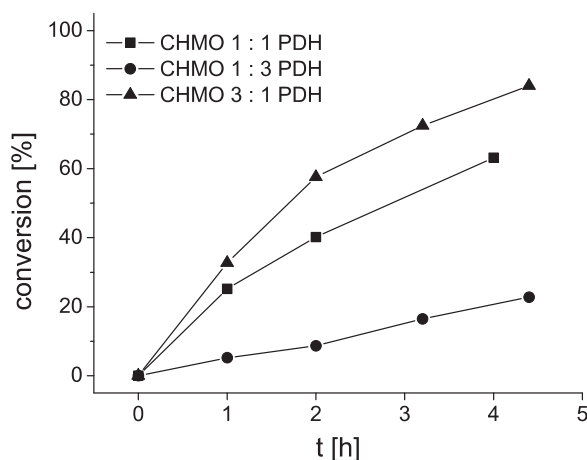


**Fig. 3.** Conversion of 10 mM CHL to  $\epsilon$ -CL using different enzyme ratios in order to determine if the rate limiting enzyme is the PDH or the BVMO.

enzymes gave a conversion of 63% and even lower conversions were obtained with CHMO in shortfall. In these cases 78% (equal amounts of enzymes) and 52% (CHMO in shortfall) of the CHL was consumed after 4 h. The bottleneck of  $\epsilon$ -CL formation thus is due to the BVMO activity.

In order to identify the reason for the reaction turnover limitation by the CHMO, the activities of the single enzymes were determined spectrophotometrically at different concentrations of CHL. The initial activity of the CHMO already drops to 30% at 10 mM CHL. The PDH on the contrary showed good performance until 70 mM and no serious activity loss at 90 mM CHL (Fig. 4). Hence the PDH compared to the CHMO works better with elevated substrate concentrations and indicates that the PDH has a higher stability in the system. As a consequence, the CHMO is the bottleneck for  $\epsilon$ -CL formation because the activity strongly decreased already at 10 mM CHL.

A preparative scale biocatalysis revealed that after 2 h no residual CHL could be detected. The  $\epsilon$ -CL product was simply extracted with dichloromethane followed by the evaporation of solvent and was isolated in 55% yield with a purity > 99%. The low yield can be attributed to the high volatility of CHL, which can easily be addressed in larger scale biocatalysis.

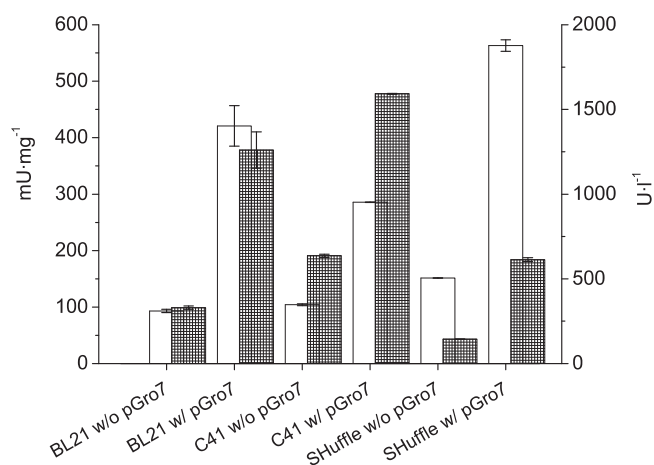


**Fig. 2.** Comparison of the specific protein activities (crude extract) of the PDH expressed from different host strains with and without pGro7 co-expression. The open columns depict the specific activity in  $\text{mU mg}^{-1}$  (left axis); the filled columns depict the volumetric activity in  $\text{U l}^{-1}$  (right axis). Activities were determined against xylitol.

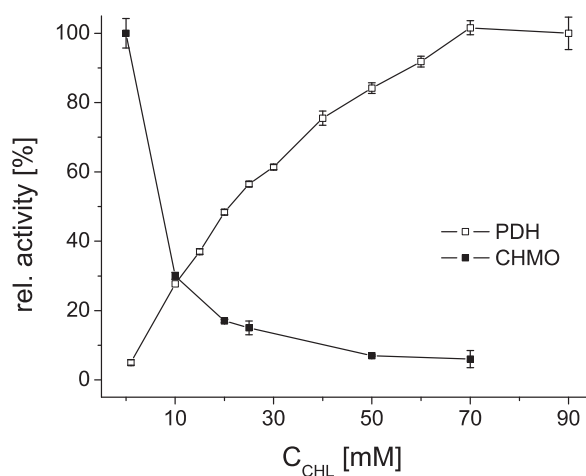


**Fig. 4.** Activity of soluble enzymes at different CHL concentrations. The activities were determined using the spectrophotometric NADPH assay. PDH activity was measured against CHL and CHMO activity was measured against 0.6 mM CHO in the presence of given concentration of CHL.

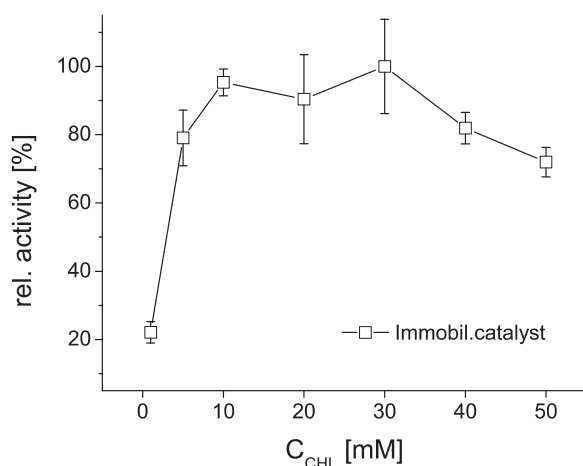


**Fig. 5.** Stability of the co-immobilized biocatalysts towards increasing CHL concentration. The error bars depict the standard deviation determined from three individual experiments. 100% relative activity was reached with 30 mM CHL and stand for formation of 3.33  $\mu\text{mol}$   $\epsilon$ -CL per liter and minute.

### 3.3. Co-immobilization of CHMO and PDH on Relizyme™ HA403

To verify the reusability of the free enzymes first a simple filtration through a 10 kDa membrane was performed for both enzymes. This led to a low residual activity of only 10% in the second cycle based on  $\epsilon$ -CL formation. Thus, immobilization experiments were carried out in order to increase the stability of the CHMO against CHL and to facilitate the reuse of both enzymes. Therefore both enzymes were covalently bound to Relizyme™ HA403 using glutaraldehyde as linker. Investigation of different ratios of the enzymes revealed that a 10:1 (CHMO:PDH) ratio led to the highest activity of the co-immobilized biocatalysts. For the combined approach an activity of 500 mU/g dry carrier with a recovered activity of 28% could be detected. Activity determination at increasing concentrations of CHL showed that CHMO was significantly stabilized against higher concentrations of CHL by immobilization as up to 40 mM CHL could now be used without significant loss of activity (Fig. 5), whereas the free CHMO retained only 15% activity at 25 mM CHL (Fig. 4).

Comparing the initial activity of immobilized and dissolved enzymes, the immobilized enzymes showed a doubled conversion after 1 h, although the free enzymes had a 2.5-fold higher starting activity. Unfortunately, the maximum conversion using the immobilized biocatalysts was only 34% at 10 mM (after 5.5 h). It was supposed that this low overall conversion is due to the low stability of the immobilized CHMO. Repeated 1 h biotransformations using the same co-immobilized biocatalyst for each batch resulted in a residual activity of 10% after the fifth cycle (Fig. 6). The first reuse step already accounts for a loss of 60% of initial activity. By addition of fresh soluble CHMO to each cycle, the loss of activity in the first cycle could be reduced to 35%. The activity of the biocatalyst just slightly decreased in this approach and a remaining activity of 53% was observed after the fifth cycle. By addition of fresh soluble PDH to each cycle no difference to the initial approach without additional enzyme could be observed.

## 4. Discussion

This paper presents a novel two-step route for the formation of  $\epsilon$ -CL from CHL and CHO. The starting point was a newly designed chimeric PDH, for which analysis of the substrate scope exhibited an increased activity of PDH against CHL. Additionally the cofactor dependency was broadened allowing for the utilization of NADP<sup>+</sup>. The reaction product of CHL oxidation, CHO, can be used

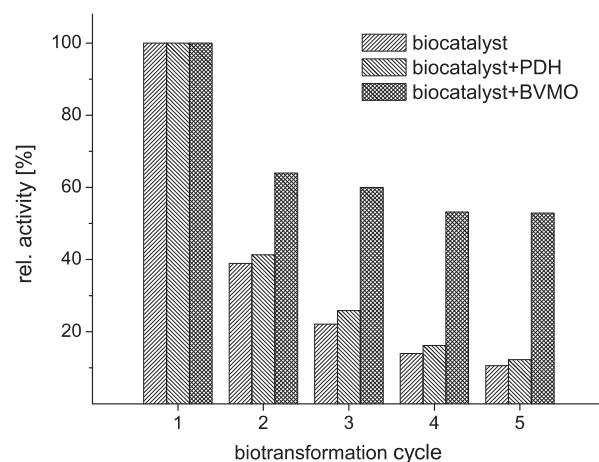


**Fig. 6.** Recycling studies of coimmobilized enzyme (biocatalysts); biocatalysts with additional soluble PDH in excess (biocatalysts + PDH) and biocatalysts with additional soluble CHMO in excess (biocatalysts + BVMO).

for a subsequent reaction with a CHO-converting Baeyer–Villiger monooxygenase, such as the CHMO of *A. calcoaceticus* used within this work. Here, the PDH forms the reduced cofactor NADPH during CHL oxidation. The PDH furthermore provides the precursor for  $\epsilon$ -CL formation, CHO. The irreversible CHMO catalyzed formation of  $\epsilon$ -CL withdraws CHO from the reversible redox interconversion of CHL and CHO. This approach thus represents a closed-loop cofactor recycling system, which might be interesting for industrial application because of its self-sufficiency.

At first an optimization of the overexpression was performed. Therefore different chaperones and strains were examined, because variation of the expression temperatures did not result in a higher amount of soluble protein. By using the pGro7 plasmid the volumetric activity could be increased 4.3-fold compared to cultivations without expression of a chaperone. When we investigated different strains it turned out that with *E. coli* C41 and pGro7 the highest volumetric productivity of active protein could be obtained (4.9-fold higher) although with *E. coli* SHuffle higher specific activities (0.6 U mg<sup>−1</sup> crude protein) were possible. The high differences in volumetric and protein specific were due to the additional expression of the chaperones and the different unspecific protein background of the used *E. coli* strains.

Using the internal cofactor recycling system by application of dissolved enzymes, conversions up to 84% at 5 mM CHL could be obtained. Here, it could be shown that the conversion is reduced by the evaporation of the substrate. This is due to the fact that no optimized reactor system was used (only flasks with breathable membranes).

The systems allows for the production of pure  $\epsilon$ -CL by simple extraction and removal of the solvent, as could be shown in a small preparative scale biotransformation. 600 mg L<sup>−1</sup> of pure  $\epsilon$ -CL (>99%) could be isolated with no residual substrate present.

The soluble PDH indicated a high stability against the organic solvent CHL whereas the soluble CHMO showed high susceptibility to CHL. The CHMO activity strongly decreased by 70% of relative activity at 10 mM CHL and above and seemed to be the bottleneck for  $\epsilon$ -CL formation. For this reason a co-immobilization in order to stabilize the CHMO was performed. The activity of CHMO against higher concentrations of CHL was strongly increased due to immobilization. Concentrations up to 3 g L<sup>−1</sup> (30 mM) CHL could now be applied with no loss of activity. Concerning the ratio of CHMO:PDH units a 10-fold excess of CHMO in covalent fixation with GA led to highest activity compared to immobilization of equal units.

Recycling the immobilized biocatalyst, we could demonstrate that the main drawback of the approach is the instability of the

CHMO. The results show that the low overall activity and low recycling stability is due to the CHMO stability but not the PDH stability. After 5 reuse cycles the PDH still had an activity of 53%, and thus seems to be a promising candidate for covalent immobilization with GA. The CHMO is sensitive to higher CHL concentration as well as it loses activity during the batch recycling steps. The activity loss of CHMO is probably due to loss of the FAD cofactor as described for immobilized oxidases other than CHMO [27,28]. The functional immobilization of *A. calcoaceticus* CHMO could be demonstrated for Relizyme™ HA403, but further stabilization of the CHMO activity on the carrier has to be carried out. Such stabilization could involve covalent bonding of the FAD either artificially or by designing or finding of a CHMO with bound cofactor like present in e.g. alditol oxidase [29]. The screening for other carriers or a protein engineering of the CHMO would be further options for optimization. This protein engineering could include the introduction of amino acid residues (for example cysteins or lysines) for a targeted, orientated immobilization of the enzyme. Further optimization of the biotransformation could involve a continuous flow system with substrate feeding of CHL in moderate concentrations.

## 5. Conclusion

In summary, our recent protein design to extend the PDH for acceptance of the cofactor NADPH enabled the possibility to combine this dehydrogenase with a BVMO for the conversion of an alcohol directly to the corresponding pure lactone (>99%) without any intermittent purification steps. Covalent immobilization of dehydrogenase and BVMO could be successfully applied, but the immobilized CHMO showed a low stability with the support used resulting in lower conversion compared to the free enzymes. With this promising proof-of-principle study we present the first example for the combination of a PDH and a BVMO in soluble and immobilized form to enable the direct formation of  $\epsilon$ -CL from CHL with no need for an additional cofactor recycling system.

## Acknowledgments

The authors thank the “Fachagentur für Nachwachsende Rohstoffe (AZ06NR073, 22015906)”, the “Bundesministerium für Bildung und Forschung Biokatalyse2021 cluster, FK0315175B”, the “Deutsche Bundesstiftung Umwelt, AZ 13234-32” and neoplas GmbH (Greifswald, Germany) for financial support. We gratefully thank B.Sc. Sten Calvelage for the lab work at the expression tests.

## Appendix A. Supplementary data

Supplementary data associated with this article can be found, in the online version, at <http://dx.doi.org/10.1016/j.enzmictec.2013.01.007>.

## References

- [1] Bornscheuer UT, Huisman GW, Kazlauskas RJ, Lutz S, Moore JC, Robins K. Engineering the third wave of biocatalysis. *Nature* 2012;485:185–94.
- [2] Clouthier CM, Pelletier JN. Expanding the organic toolbox: a guide to integrating biocatalysis in synthesis. *Chemical Society Reviews* 2012;41:1585–605.
- [3] Baeyer A, Villiger V. Einwirkung des Caro'schen Reagens auf Ketone. *Berichte der Deutschen Chemischen Gesellschaft* 1899;32:3625–33.
- [4] Köpnick H, Schmidt M, Brüggling W, Rüter J, Kaminsky W. Polyesters. In: Ullmann's encyclopedia of industrial chemistry. Weinheim: Wiley-VCH; 2000.
- [5] Breulmann M, Künkel A, Philipp S, Reimer V, Siegenthaler KO, Skupin G, et al. Polymers, biodegradable. In: Ullmann's encyclopedia of industrial chemistry. Weinheim: Wiley-VCH; 2009.
- [6] Ritz J, Fuchs H, Kieczka H, Moran WC. Caprolactam. In: Ullmann's encyclopedia of industrial chemistry. Weinheim: Wiley-VCH; 2010.
- [7] Mihovilovic Marko D, Müller B, Stanetty P. Monooxygenase-mediated Baeyer–Villiger oxidations. *European Journal of Organic Chemistry* 2002;2002:3711–30.
- [8] Donoghue NA, Norris DB, Trudgill PW. The purification and properties of cyclohexanone oxygenase from *Nocardia globerula* CL1 and *Acinetobacter* NCIB 9871. *European Journal of Biochemistry* 1976;63:175–92.
- [9] Chen YC, Peoples OP, Walsh CT. *Acinetobacter* cyclohexanone monooxygenase: gene cloning and sequence determination. *Journal of Bacteriology* 1988;170:781–9.
- [10] Walsh CT, Chen YC. Enzymic Baeyer–Villiger oxidations by flavin-dependent monooxygenases. *Angewandte Chemie International Edition* 1988;27:333–43.
- [11] de Gonzalo G, Mihovilovic MD, Fraaije MW. Recent developments in the application of Baeyer–Villiger monooxygenases as biocatalysts. *ChemBioChem* 2010;11:2208–31.
- [12] Stewart JD. Cyclohexanone monooxygenase: a useful reagent for asymmetric Baeyer–Villiger reactions. *Current Organic Chemistry* 1998;2:195–216.
- [13] Geitner K, Kirschner A, Rehder J, Schmidt M, Mihovilovic MD, Bornscheuer UT. Enantioselective kinetic resolution of 3-phenyl-2-ketones using Baeyer–Villiger monooxygenases. *Tetrahedron: Asymmetry* 2007;18:892–5.
- [14] Lee W-H, Park J-B, Park K, Kim M-D, Seo J-H. Enhanced production of  $\epsilon$ -caprolactone by overexpression of NADPH-regenerating glucose 6-phosphate dehydrogenase in recombinant *Escherichia coli* harboring cyclohexanone monooxygenase gene. *Applied Microbiology and Biotechnology* 2007;76:329–38.
- [15] de Carvalho CCCR. Enzymatic and whole cell catalysis: finding new strategies for old processes. *Biotechnology Advances* 2011;29:75–83.
- [16] Torres Pazmiño DE, Snajdrova R, Baas B-J, Ghobrial M, Mihovilovic MD, Fraaije MW. Self-sufficient Baeyer–Villiger monooxygenases: effective coenzyme regeneration for biooxygenation by fusion engineering. *Angewandte Chemie International Edition in English* 2008;120:2307–10.
- [17] Torres Pazmiño DE, Winkler M, Glieder A, Fraaije MW. Monooxygenases as biocatalysts: classification, mechanistic aspects and biotechnological applications. *Journal of Biotechnology* 2010;146:9–24.
- [18] Buchholz K, Klein J. Characterization of immobilized biocatalysts. *Methods in enzymology*. Academic Press; 1987. p. 3–30.
- [19] Bornscheuer UT. Immobilizing enzymes: how to create more suitable biocatalysts. *Angewandte Chemie International Edition in English* 2003;42:3336–7.
- [20] Buchholz K, Kasche V, Bornscheuer UT. Biocatalysts and enzyme technology. Weinheim: Wiley-VCH; 2012.
- [21] Balke K, Kadow M, Mallin H, Saß S, Bornscheuer UT. Discovery, application and protein engineering of Baeyer–Villiger monooxygenases for organic synthesis. *Organic and Biomolecular Chemistry* 2012;10:6249.
- [22] Wulf H, Mallin H, Bornscheuer UT. Protein engineering of a thermostable polyol dehydrogenase. *Enzyme and Microbial Technology* 2012;51:217–24.
- [23] Willetts AJ, Knowles CJ, Levitt MS, Roberts SM, Sandey H, Shipston NF. Biotransformation of endo-bicyclo[2.2.1]heptan-2-ols and endo-bicyclo[3.2.0]hept-2-en-6-ol into the corresponding lactones. *Journal of the Chemical Society, Perkin Transactions 1* 1991:1608.
- [24] Studier FW. Protein production by auto-induction in high-density shaking cultures. *Protein Expression and Purification* 2005;41:207–34.
- [25] Wulf H, Perzborn M, Sievers G, Scholz F, Bornscheuer UT. Kinetic resolution of glyceraldehyde using an aldehyde dehydrogenase from *Deinococcus geothermophilus* DSM 11300 combined with electrochemical cofactor recycling. *Journal of Molecular Catalysis B: Enzymatic* 2012;74:144–50.
- [26] Fraaije MW, Wu J, Heuts DPHM, van Hellemond EW, Lutje Spelberg JH, Janssen DB. Discovery of a thermostable Baeyer–Villiger monooxygenase by genome mining. *Applied Microbiology and Biotechnology* 2005;66:393–400.
- [27] Betancor L, Hidalgo A, Fernández-Lorente G, Mateo C, Rodríguez V, Fuentes M, et al. Use of physicochemical tools to determine the choice of optimal enzyme: stabilization of D-amino acid oxidase. *Biotechnology Progress* 2003;19:784–8.
- [28] Garwood GA, Mortland MM, Pinnavaia TJ. Immobilization of glucose oxidase on montmorillonite clay: hydrophobic and ionic modes of binding. *Journal of Molecular Catalysis* 1983;22:153–63.
- [29] Forneris F, Heuts DPHM, Delvecchio M, Rovida S, Fraaije MW, Mattevi A. Structural analysis of the catalytic mechanism and stereoselectivity in *Streptomyces coelicolor* alditol oxidase. *Biochemistry* 2008;47:978–85.



## Articles

### Article IV



# Immobilization of two (*R*)-Amine Transaminases on an Optimized Chitosan Support for the Enzymatic Synthesis of Optically Pure Amines

Hendrik Mallin,<sup>[a]</sup> Ulf Menyes,<sup>[b]</sup> Torge Vorhaben,<sup>[c]</sup> Matthias Höhne,<sup>[d]</sup> and Uwe T. Bornscheuer<sup>\*[a]</sup>

Two (*R*)-selective amine transaminases from *Gibberella zeae* (GibZea) and from *Neosartorya fischeri* (NeoFis) were immobilized on chitosan as a carrier to improve their application in the biocatalytic synthesis of chiral (*R*)-amines. An (*S*)-selective enzyme from *Vibrio fluvialis* (VfTA) was used for comparison. After improving the immobilization conditions, all enzymes could be efficiently immobilized. Additionally, the thermal stability of GibZea and NeoFis could be improved and also

a slight shift of the pH optimum was observed for GibZea. All enzymes showed good activity in the conversion of  $\alpha$ -methylbenzylamine. In the asymmetric synthesis of (*R*)-2-aminohexane from the corresponding ketone, a 13.4-fold higher conversion (>99%) was found for the immobilized GibZea compared to the free enzyme. Hence, the covalent binding with glutaraldehyde of these enzymes on chitosan beads resulted in a significant stabilization of the amine transaminases investigated.

## Introduction

The use of amine transaminases (ATAs), which are enzymes enabling the asymmetric synthesis of chiral amines from prosterogenic ketones, has emerged as an important alternative to traditional chemical synthesis as was recently demonstrated for the biocatalytic manufacture of the drug sitagliptin with an (*R*)-ATA created by intensive protein engineering.<sup>[1]</sup> This process turned out to be superior with respect to optical purity, yield, and waste generation compared to the already established transition-metal-catalyzed production of sitagliptin.<sup>[2]</sup>

Industrial application of enzymes usually requires immobilization of the biocatalysts as this provides many advantages such as easier downstream processing, reuse of the biocatalyst, and stabilization of the enzyme. Furthermore, in an immobilized form the catalysts can be used in continuous or fixed-bed operations.<sup>[3–6]</sup> For the immobilization of enzymes several supports are known, which have different functional groups for adsorptive or covalent attachment. Covalent binding provides the advantages of reduced enzyme leaching to the reaction

medium and better control of the binding chemistry during immobilization. A commonly used method is the formation of a Schiff base between a lysine residue of the enzyme and a free aldehyde moiety of glutaraldehyde, which is linked to another amine group on the surface of the support. Chitosan is a natural nontoxic material obtained by deacetylation of chitin<sup>[7]</sup> and well known as a suitable support for enzyme immobilization. It could be used for covalent binding (free amino group) or for adsorptive attachment (high hydrophilicity because of hydroxyl groups).

Recently, we discovered 17 novel (*R*)-ATAs using a search algorithm within >5000 protein sequences deposited in public databases.<sup>[8]</sup> We already demonstrated for 7 out of the 17 enzymes that these (*R*)-ATA are very useful for the asymmetric synthesis of a set of 12 chiral amines.<sup>[9]</sup> To improve their application in preparative biocatalysis, we used modified chitosan as a support for the immobilization of two of these enzymes: GibZea from *Gibberella zeae* and NeoFis from *Neosartorya fischeri*. Chitosan was chosen because Yi et al. could successfully immobilize the (*S*)-selective transaminase from *Vibrio fluvialis* (VfTA) on chitosan beads.<sup>[10]</sup> Therefore, we also compared the optimized chitosan support produced in this work with the previously described immobilization protocol for VfTA.<sup>[10]</sup>

## Results and Discussion

### Choice of (*R*)-selective amine transaminases

First, suitable enzyme candidates had to be chosen out of the pool of recently discovered (*R*)-ATAs. From the seven recombinantly available and biochemically characterized enzymes, GibZea and NeoFis were selected because of their high specific activity towards the model substrate (*R*)- $\alpha$ -methylbenzylamine

[a] H. Mallin, Prof. Dr. U. T. Bornscheuer  
Department of Biotechnology & Enzyme Catalysis  
Institute of Biochemistry, Greifswald University  
Felix-Hausdorff-Str. 4, 17487 Greifswald (Germany)  
Fax: (+49)-3834-86-794367  
E-mail: uwe.bornscheuer@uni-greifswald.de

[b] Dr. U. Menyes  
Enzymicals AG  
Walther-Rathenau-Str. 49a, 17489 Greifswald (Germany)

[c] T. Vorhaben  
neoplas GmbH  
Walther-Rathenau-Str. 49a, 17489 Greifswald (Germany)

[d] Prof. M. Höhne  
Institute of Biochemistry  
Greifswald University  
Felix-Hausdorff-Str. 4, 17487 Greifswald (Germany)

[(*R*)- $\alpha$ -MBA]. GibZea had an activity of  $19.6 \text{ U mg}^{-1}$  and NeoFis  $7.4 \text{ U mg}^{-1}$ .<sup>[8]</sup>

### Carrier production and optimization

After identification of suitable enzyme candidates, chitosan beads were chosen as support for immobilization. In literature, two different production protocols for chitosan beads had been reported so far and were compared first. According to Nasratun et al., dropping acidified chitosan into a NaOH solution will cause the formation of beadlike particles. These beads have been used for the immobilization of *Candida rugosa* lipase.<sup>[11]</sup> The second method was reported by Yi and co-workers for the immobilization of the (*S*)- $\omega$ -transaminase from *V. fluvialis* JS17 (VfTA).<sup>[10]</sup> Therein, an emulsion of toluene and the chitosan solution was used to form beads.

Freeze-drying of the gel-like beads obtained by both methods changed the physical properties of the carrier. This solid carrier shows a very low swelling behavior and is therefore more suitable for application. Comparison of both protocols showed that activity towards (*R*)- $\alpha$ -MBA was increased 3.8-fold (GibZea) and 2.4-fold (NeoFis) on beads produced by the emulsion method. Hence, this method was used for further optimization. The first step was the variation of the chitosan concentration. Additionally, the co-emulsifier hexanol was changed to hexane to increase the hydrophobicity of the support, which is highly hydrophilic. To investigate the effect of these optimizations, GibZea was used as model enzyme because of its higher specific activity in the crude extract and immobilized activities in the first experiments compared to NeoFis. Chitosan concentrations ranging from 0.5–2.0% were investigated, but 0.5% turned out to be below the critical concentration for bead formation. By reducing the concentration from 2 to 1%, the immobilized activity could be increased 4.1-fold to  $360 \text{ U g}^{-1}$  (Figure 1). The change of the co-emulsifier from hexanol to hexane had no significant effect on immobilized enzyme activity.

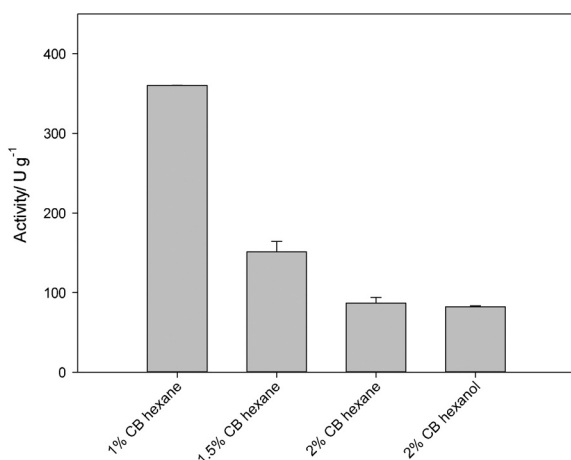


**Figure 1.** Influence of chitosan concentration and variation of the co-emulsifiers on the activity of immobilized GibZea. Activities were determined in duplicates. CB = chitosan beads.

To confirm the reproducibility of carrier production, GibZea was immobilized on three independently produced batches of chitosan beads (1% chitosan concentration). Comparison of the activities showed that, on beads of batches 1 and 3, approximately  $250 \text{ U g}^{-1}$  could be immobilized. The recovered activities were approximately 80% of the enzyme activity missing from the supernatant after immobilization. The second batch showed a slightly lower activity of approximately  $200 \text{ U g}^{-1}$ , which could be addressed to the stirring speed used during preparation of this batch. The mean of all batches was  $(246 \pm 46) \text{ U g}^{-1}$ .

### Characterization of chitosan support

Pore-size distribution and specific surface area are important criteria for efficient enzyme immobilization. Therefore, we characterized the physical properties of the chitosan beads by different methods. Scanning electron microscopy (SEM) of the support revealed a sponge-like structure with pores in different sizes (Figure 2).

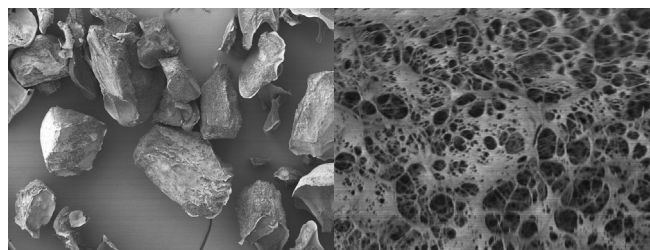


**Figure 2.** SEM images of chitosan beads (1%); magnification:  $\times 37$  (left) and  $\times 4000$  (right).

To determine the total surface area that is accessible for the enzyme solution, Brunauer–Emmet–Teller (BET) measurements were performed. From these data a specific surface area of  $(31 \pm 0.8) \text{ m}^2 \text{ g}^{-1}$  could be calculated. In addition, pore-size distribution measurements revealed that 39% of all pores have sizes between 20 and 80 nm (Table 1).

**Table 1.** Pore-size distribution of 1% chitosan beads.<sup>[a]</sup>

Pore diameter [nm]	Distribution [%]
< 6	$13.2 \pm 0.5$
6–8	$6.3 \pm 0.3$
8–10	$5.2 \pm 0.2$
10–12	$5.0 \pm 0.3$
12–16	$6.7 \pm 0.3$
16–20	$6.8 \pm 0.3$
20–80	$39.0 \pm 1.3$
> 80	$17.7 \pm 2.4$

[a] Determined by BET measurements in triplicates.

### Optimization of immobilization conditions

Next, we investigated the variation of the immobilization buffer. As immobilization of GibZea and NeoFis was done from

crude *Escherichia coli* cell extracts, 0.5 M NaCl was added to prevent polar interactions during covalent immobilization. This increased the immobilized activity for GibZea 1.6-fold compared to that in a buffer without additional NaCl but had no effect on NeoFis. From that it can be assumed that GibZea has a more polar surface and the addition of sodium chloride prevents the enzyme from disadvantageous orientations on the highly hydrophilic support. A rational approach for the immobilization of these enzymes is not possible yet because crystal structures of these enzymes are not available so far. The addition of the cofactor pyridoxal-5'-phosphate (PLP) to the buffer led to a further stabilization of these PLP-dependent transaminases. Immobilizations were performed at 4 °C and at a low orbital shaking rate to reduce shear forces, which could negatively effect enzyme stability. After two hours the maximum immobilized activity was achieved (Figure 3) and longer treat-

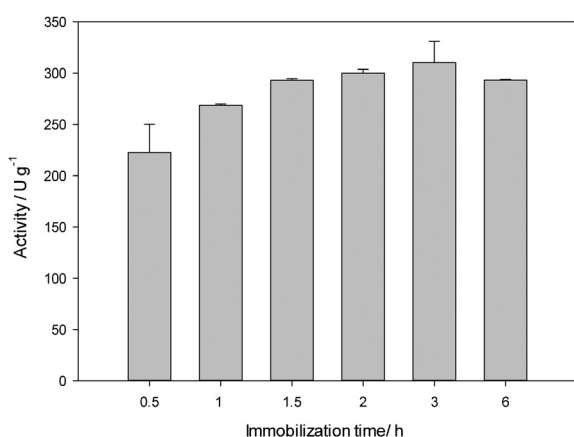


**Figure 3.** Influence of immobilization time on the bound activity as shown for GibZea as a model enzyme.

ment did not increase the immobilization yield. Under these optimized conditions the activity per gram dry support was higher for GibZea (362 U g<sup>-1</sup>) and NeoFis (216 U g<sup>-1</sup>) than for VFTA (71 U g<sup>-1</sup>). Interestingly, for VFTA a slight hyperactivation could be achieved with 120% recovered activity.

#### pH Profile of immobilized (R)-ATAs

Relative activities of free and immobilized GibZea and NeoFis were compared at different pH values (Figure 4). For the immobilized ATAs the lowest chosen pH had to be 6.5 because chitosan becomes soluble around pH 6. For NeoFis no difference in the pH optimum between the immobilized and free enzyme could be detected. However, immobilized GibZea showed a shift in its pH optimum from 7.5 to 8.0. This implies a possible conformational change in the enzyme structure.

#### Temperature profile of immobilized (R)-ATAs

Next, the activities of soluble and immobilized GibZea and NeoFis were compared at different temperatures ranging from

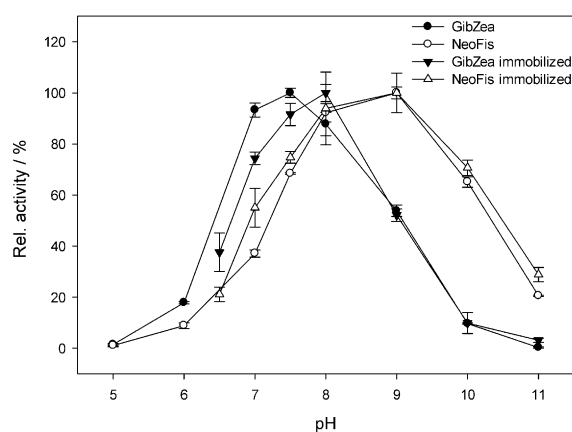


**Figure 4.** Relative activities of free and immobilized (R)-ATAs at different pH values.

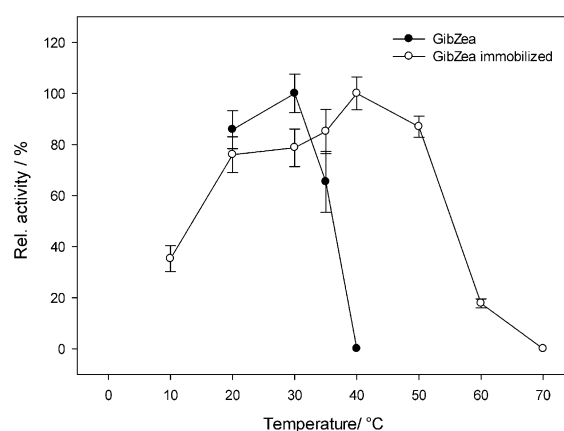


**Figure 5.** Relative initial activities of free and immobilized GibZea at different temperatures.

10 to 70 °C. For GibZea an increased optimum could be observed (Figure 5). The free enzyme has its optimum at 30 °C and is inactive at 40 °C. In contrast, immobilized GibZea has its optimum at 40 °C and is still active at higher temperatures. This indicates a strong stabilization effect owing to the covalent immobilization on chitosan-based support. NeoFis also showed an increased optimum, but the effect was less pronounced than for GibZea (Figure 6). This might be owing to the much higher stability of the free NeoFis than of the free GibZea. An increased stability of the immobilized NeoFis could be observed at 60 and 70 °C. At 60 °C the immobilized enzyme had a residual activity of 82% whereas the free enzyme had only 43%. At 70 °C the free biocatalyst was totally inactive whereas the immobilized one still had 23% residual activity.

#### Recycling of immobilized (R)-ATAs

Besides stabilization effects, immobilization of enzymes offers the main advantage that the enzyme can be reused for several consecutive biotransformations. Thus, we performed the reuse of the immobilized (R)-ATA preparations for four consecutive

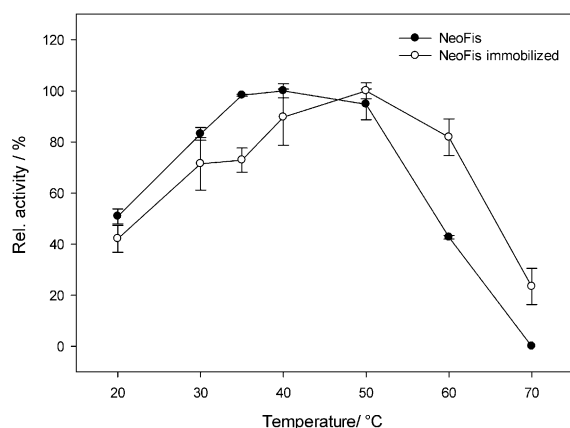


**Figure 6.** Relative initial activities of free and immobilized NeoFis at different temperatures.

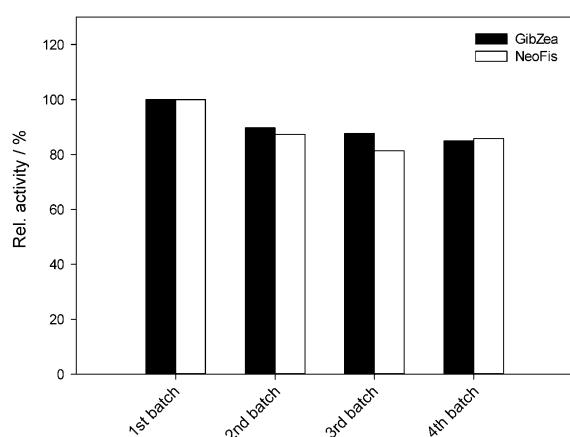


**Figure 7.** Recycling study with immobilized GibZea and NeoFis after four consecutive cycles of 1 h batches. 100% relative activity of GibZea refers to 76% conversion and 100% NeoFis refers to 72% conversion.

1 h cycles in the transamination of (*R*)- $\alpha$ -MBA to acetophenone (Figure 7). At the end of each cycle samples were taken, the immobilized enzymes were collected by filtration, and washed twice with buffer. Then the immobilized (*R*)-ATAs were subjected to the next cycle under the same conditions. During these batches the relative activity showed a slight decrease, which can be addressed to nonspecifically bound enzymes probably by hydrophobic interaction. For GibZea a reduction of 22% of the relative activity was observed after four cycles. NeoFis showed a better reuse capacity and the relative activity was decreased by only 12%. Both immobilized preparations could be reused several times, which is important for batch processes or continuous-flow or fixed-bed reactors. This small reduction of activity and good stability can be related to the covalent attachment with glutaraldehyde, which reduces the leaching of the enzymes to the reaction medium.

#### Asymmetric synthesis of (*R*)-2-aminohehexane

To investigate the selectivity of the new immobilized (*R*)-ATAs, asymmetric synthesis of (*R*)-2-aminohehexane was performed

under shaking conditions. To compare the stability and productivity of free and immobilized enzymes, the same initial activity (determined with (*R*)- $\alpha$ -MBA) was used in each experiment. In previous studies, GibZea and NeoFis reached 14 and 99% conversion in the synthesis of (*R*)-2-aminohehexane after 72 h, respectively.<sup>[9]</sup> For NeoFis no significant difference between free and immobilized biocatalyst could be detected for the conversion of 2-hexanone to (*R*)-2-aminohehexane ((79  $\pm$  13)%, free, and (71  $\pm$  3)%, immobilized), which suggests an already good stability of the free enzyme. However, for immobilized GibZea a 13.4-fold higher conversion (> (99  $\pm$  3)%) was found after 24 h than for the free enzyme. This shows a strong stabilization effect owing to the covalent binding on chitosan beads. Moreover, the immobilized GibZea showed a 1.3-fold higher activity in the synthesis of (*R*)-2-aminohehexane compared to the immobilized NeoFis. Both effects make the immobilized GibZea more suitable for an application compared to NeoFis. Furthermore, GibZea is the easiest enzyme to produce out of the seven (*R*)-ATAs used so far for asymmetric synthesis.<sup>[9]</sup>

## Conclusions

Proper selection of the chitosan carrier production and optimization of the immobilization conditions resulted in immobilized (*R*)-selective amine transaminases (ATAs), which are significantly more stable and active compared to the free enzymes. Especially for the (*R*)-ATAs from *Gibberella zeae* substantially higher conversions in the asymmetric synthesis of (*R*)-2-aminohehexane were observed.

## Experimental Section

### Materials

Chitosan [deacetylation degree > 95%, viscosity [1% (w/v) in 1% acetic acid] 500 mPas] was purchased from Heppe Medical Chitosan GmbH (Halle, Germany). All chemicals were purchased from Fluka (Buchs, Switzerland), Sigma (Steinheim, Germany), or Merck (Darmstadt, Germany), unless stated otherwise. Lyophilized (*R*)-ATAs for pretests were obtained from Enzymicals AG. Crude extracts of (*R*)-ATAs were obtained by overexpression in *E. coli* as described previously,<sup>[9]</sup> but in terrific broth instead of lysogeny broth media. Cells were disrupted by sonication to obtain crude extracts of GibZea, NeoFis, and VfTA. Additionally, VfTA was purified after cell disruption by immobilized metal ion affinity chromatography through its His-tag to obtain pure enzyme preparation.<sup>[12]</sup>

### Preparation of chitosan beads

Chitosan beads were prepared by the emulsion method according to Yi et al. with slight modifications.<sup>[10]</sup> Different concentrations of chitosan (0.5 to 2.0% w/v) were dissolved in 250 mL of 1% acetic acid. The solution was slightly stirred and degassed in a sonication bath. The oil phase was prepared with 300 mL toluene, 2.2 g Span 80 and 1.2 mL hexane and stirred for 2 h at RT. Degassed chitosan solution was poured into the oil phase and stirred slightly for 10 min. Then the resulting emulsion was poured slowly into 1.5 L NaOH solution (3 M) and stirred for further 3 h. Then the mixture was filtered and the beads were washed twice with 3 L of deionized water. The beads were filtered again and washed until the



flow-through showed a neutral pH. Chitosan beads produced by the dropping method were produced as reported<sup>[11]</sup> but at a chitosan concentration of 1.5% (w/v). All wet beads were dried under vacuum overnight to obtain a solid and physically stable support. Dried beads were stored at RT.

### Characterization of chitosan supports

All BET and pore-size distribution measurements were performed with dried chitosan beads using a Beckman Coulter SA 3100 (Beckman Coulter, Krefeld, Germany). SEM pictures were recorded with a JOEL JSM-7500F field emission scanning electron microscope. Measurements were done in triplicates.

### Immobilization of transaminases

Immobilization of ATAs was performed with 50 mg dry chitosan beads, which were activated with 2.5% (v/v) glutaraldehyde in deionized water in a total volume of 4 mL (20 °C, 180 rpm, 1.5 h). Activated beads were filtered and washed twice with deionized water. Then, crude extracts of GibZea or NeoFis (varied from 18 to 43 U towards (R)- $\alpha$ -MBA) were incubated with the glutaraldehyde-activated carrier in a total volume of 5 mL sodium phosphate buffer (50 mM, pH 7.5, 0.1 mM PLP, 0.5 M NaCl) for 3 h at 4 °C. Then, samples were taken from the supernatant, the beads were filtered and washed twice with the immobilization buffer. The wet beads were then used for further experiments. The activity of the supernatants was determined with the acetophenone assay (see below) and protein content was measured with a Roti-Nanoquant. The recovered activity was calculated by comparison of the missing units from the supernatant after immobilization and the units found on 50 mg (dry) support after immobilization. Depending on the starting activity used, the efficiency varied from 40% (high activity) to 80% (low activity).

### Enzyme assays

Enzyme activities were determined by using the acetophenone assay by measuring the increase in absorbance at 245 nm<sup>[12]</sup> in a 96-well UV-microtiter plate (Greiner) at 30 °C. For soluble enzymes, 10  $\mu$ L enzyme solution were mixed with 90  $\mu$ L sodium phosphate buffer (50 mM, pH 7.5). Afterwards, 100  $\mu$ L reaction solution (sodium phosphate buffer, 50 mM, pH 7.5, 5 mM (R)- or (S)- $\alpha$ -MBA, 5 mM pyruvate, and 0.5% DMSO) was added and the measurement was started immediately. Activity was determined over 10 min and the slope was used to calculate the activity. For immobilized enzymes the same assay was used in a 24 deep-well plate, which was incubated in a shaker at 30 °C. 10 to 20 mg of wet immobilized enzyme was used for each measurement. The reaction was started by adding 5 mL of prewarmed reaction solution (sodium phosphate buffer, 50 mM, pH 7.5, 2.5 mM (R)- or (S)- $\alpha$ -MBA, 2.5 mM pyruvate, and 0.25% DMSO). Then, 200  $\mu$ L samples were taken and the absorbance was measured as described above at 245 nm. The slope was determined and the activity was calculated.

The pH profile was determined in a pH range of 5–11. Reaction conditions for the soluble enzymes were the same as described above for the free and immobilized enzymes, but with 100 mM Davies<sup>[13]</sup> buffer instead of sodium phosphate buffer. The temperature profile was determined by using the same photometric assay. To obtain optimal temperature conditions, the assay was performed for the free and immobilized enzymes in a volume of 2 mL

in a thermoshaker at the desired temperatures ranging from 10–70 °C. The reaction solution (sodium phosphate buffer, 50 mM, pH 7.5, 2.5 mM (R)- $\alpha$ -MBA, 2.5 mM pyruvate, and 0.25% DMSO) was preheated prior to the reaction. Then 5 mg wet immobilized enzyme or 20  $\mu$ L of free enzyme was incubated with the reaction solution. 100  $\mu$ L samples were taken periodically and diluted 1:2 in sodium phosphate buffer (50 mM, pH 7.5) to a final volume of 200  $\mu$ L in a UV microtiter plate. The absorbance was measured and the slope was used to calculate the activity, as described above. Recycling studies were performed in a volume of 3 mL (sodium phosphate buffer, 50 mM, pH 7.5, 2.5 mM (R)- $\alpha$ -MBA, 2.5 mM pyruvate, and 0.25% DMSO) for 1 h per cycle. 60 mg wet catalysts were used for GibZea and NeoFis for each approach. After 1 h, a 500  $\mu$ L sample was taken and, after extraction with 500  $\mu$ L ethylacetate, the organic phase was analyzed by gas chromatography by using a Shimadzu GC-14 A equipped with a Hydrodex- $\beta$ -3P column (25 m  $\times$  0.25 mm, Macherey–Nagel, Düren, Germany) and flame-ionization detector. In the beginning, the oven temperature was kept at 60 °C for 10 min, followed by an increase to 160 °C with a heating rate of 10 °C min<sup>-1</sup>. The temperature was then held at 160 °C for 10 min (retention time: 16.2 min). The immobilized enzyme was washed twice with sodium phosphate buffer (50 mM, pH 7.5) and then subjected to the next cycle.

### Asymmetric synthesis of (R)-2-aminohexane

Asymmetric synthesis of (R)-2-aminohexane was performed using the GDH/LDH system as described previously.<sup>[9]</sup> Reactions were performed in a 1 mL volume using sodium phosphate buffer (100 mM, pH 7.5, 0.1 mM PLP) containing 2-hexanone (50 mM), NADH (1 mM), D-alanine (250 mM), and D-glucose (150 mM). 2 U (towards (R)- $\alpha$ -MBA) of transaminase (immobilized or free) were used for each approach using lactate dehydrogenase (88 U mL<sup>-1</sup>) and glucose dehydrogenase (15 U mL<sup>-1</sup>) for shifting the equilibrium and cofactor recycling. All experiments were performed in triplicates. After 24 h 150  $\mu$ L samples were taken and analyzed as described previously.<sup>[9]</sup>

### Acknowledgements

We are grateful to the BMBF (Bonn, Germany) within the cluster Biokatalyse2021 (FK0315175B) for financial support and Dagmar Jasinski for her help in the laboratory.

**Keywords:** asymmetric synthesis • chitosan beads • enzyme catalysis • immobilization • transaminase

- [1] C. K. Savile, J. M. Janey, E. C. Mundorff, J. C. Moore, S. Tam, W. R. Jarvis, J. C. Colbeck, A. Krebber, F. J. Fleitz, J. Brands, P. N. Devine, G. W. Huisman, G. J. Hughes, *Science* **2010**, 329, 305–309.
- [2] A. A. Desai, *Angew. Chem.* **2011**, 123, 2018–2020; *Angew. Chem. Int. Ed.* **2011**, 50, 1974–1976.
- [3] C. Mateo, J. M. Palomo, G. Fernandez-Lorente, J. M. Guisan, R. Fernandez-Lafuente, *Enzyme Microb. Technol.* **2007**, 40, 1451–1463.
- [4] R. A. Sheldon, *Adv. Synth. Catal.* **2007**, 349, 1289–1307.
- [5] K. Buchholz, V. Kasche, U. T. Bornscheuer, *Biocatalysts and Enzyme Technology*, 2nd ed., Wiley-VCH, Weinheim, **2012**.
- [6] U. T. Bornscheuer, *Angew. Chem.* **2003**, 115, 3458–3459; *Angew. Chem. Int. Ed.* **2003**, 42, 3336–3337.
- [7] B. Krajewska, *Enzyme Microb. Technol.* **2004**, 35, 126–139.
- [8] M. Höhne, S. Schätzle, H. Jochens, K. Robins, U. T. Bornscheuer, *Nat. Chem. Biol.* **2010**, 6, 807–813.



- [9] S. Schätzle, F. Steffen-Munsberg, M. Thotowi, M. Höhne, K. Robins, U. T. Bornscheuer, *Adv. Synth. Catal.* **2011**, 353, 2439–2445.
- [10] S. S. Yi, C. W. Lee, J. Kim, D. Kyung, B. G. Kim, Y.-Sik Lee, *Proc. Biochem.* **2007**, 42, 895–898.
- [11] M. Nasratun, A. S. Hasrul, A. Sureena, M. A. Nurul Aini, A. R. Ruwaida, M. S. Shalyda, A. Ideris, A. S. Rozaimi, J. H. Sharifuddin, N. I. A. Ahamad Nordin, *J. Appl. Sci.* **2010**, 10, 2701–2704.
- [12] S. Schätzle, M. Höhne, E. Redestad, K. Robins, U. T. Bornscheuer, *Anal. Chem.* **2009**, 81, 8244–8248.
- [13] M. T. Davies, *Analyst* **1959**, 84, 248–251.

---

Received: June 28, 2012

Published online on October 9, 2012

## Articles

### Article V



Contents lists available at ScienceDirect

Journal of Biotechnology

journal homepage: [www.elsevier.com/locate/jbiotec](http://www.elsevier.com/locate/jbiotec)



# Immobilization of (R)- and (S)-amine transaminases on chitosan support and their application for amine synthesis using isopropylamine as donor

H. Mallin<sup>a</sup>, M. Höhne<sup>b</sup>, U.T. Bornscheuer<sup>a,\*</sup>

<sup>a</sup> Department of Biotechnology & Enzyme Catalysis, Institute of Biochemistry, Greifswald University, Felix-Hausdorff-Str 4, D-17487 Greifswald, Germany

<sup>b</sup> Protein Biochemistry, Institute of Biochemistry, Greifswald University, Felix-Hausdorff-Str 4, D-17487 Greifswald, Germany

## ARTICLE INFO

### Article history:

Received 16 February 2014

Received in revised form 14 May 2014

Accepted 19 May 2014

Available online xxx

Dedicated to Prof. Karl-Erich Jaeger on the occasion of his 60th birthday.

### Keywords:

Asymmetric synthesis

Biocatalysis

Immobilization

Enzyme activation

Transaminase

## ABSTRACT

Transaminases from *Aspergillus fumigatus* ((R)-selective, AspFum), *Ruegeria pomeroyi* ((S)-selective, 3HMU) and *Rhodobacter sphaeroides* 2.4.1 ((S)-selective, 315T) were immobilized on chitosan with specific activities of 99, 157, and 163 U/g and acceptable yields (54, 21, and 23%, respectively) for glutaraldehyde (GA) immobilization. Besides GA, also divinylsulfone was used as linker molecule leading to a similar efficient immobilization for two enzymes, GibZea and NeoFis, whereas GA was superior in the other cases. Storage of the GA-immobilized enzymes for one month resulted in increased relative activities between 120 and 180%. The thermal stability was improved, especially for the GA-immobilized AspFum compared to the free enzyme after incubation for 4 h at 60 °C (10% vs. 235% residual activity). Especially after incubation of AspFum (free or immobilized) for 2 h at 50 °C a strongly increased activity was observed (up to 359% of the initial activity). This effect was studied in more detail, revealing that one heat activation prior and one after immobilization increased the overall immobilization efficiency. Recycling of the immobilized ATAs resulted only in a small reduction of activity after four batches. Asymmetric synthesis of (R)- or (S)-1-methyl-3-phenylpropylamine from the prostereogenic ketone using isopropylamine (IPA) as amino donor was applied with conversions up to 50% (AspFum) or 75% (3HMU). Except for NeoFis, all immobilized ATAs showed higher conversions compared to the free enzyme.

© 2014 Elsevier B.V. All rights reserved.

## 1. Introduction

In the last decades biocatalysis became an emerging field in chemical synthesis due to technical and scientific advancements (Bornscheuer et al., 2012). Especially for advanced pharmaceutical intermediates (API), biocatalytic routes are desired to replace traditional chemical processes. The application of biocatalysts in industry reduces the commonly large amounts of waste, rendering a process more cost effective and environmentally friendly (Pollard and Woodley, 2007; Woodley, 2008). Especially amine transaminases (ATAs) turned out to be interesting enzymes for the asymmetric synthesis of enantiomerically pure amines and in

cascade reactions (Höhne and Bornscheuer, 2009, 2012; Kohls et al., 2014; Mathew and Yun, 2012; Simon et al., 2013). For example Savile and co-workers created a transaminase by extensive protein engineering for the production of sitagliptin using isopropylamine as amino donor. The new process replaced the chemical asymmetric hydrogenation, considerably reduced the waste, and increased the overall yield and optical purity compared to the chemical process (Desai, 2011; Savile et al., 2010). For further process optimization an immobilized ATA was developed, enabling the use in organic solvents (Truppo et al., 2012). This further increased the productivity, the catalyst was used in long-term operations and the downstream process was simplified due to an easy filtration of the catalyst. Thus, immobilization is an important part of process development in biocatalysis, because of often increased stability, easier downstream processing, reuse of the catalysts and the possibility for applications in continuous or fixed-bed operations (Bornscheuer, 2003; Brena et al., 2013; Buchholz et al., 2012; Mateo et al., 2007; Sheldon, 2007). So far no general concept was identified to immobilize an enzyme (Hanefeld et al., 2009; Liese and Hilterhaus, 2013). For ATAs, several immobilization methods were reported in literature, including covalent binding, sol-gel

**Abbreviations:** ATA, amine transaminase; GA, glutaraldehyde; DVS, divinylsulfone; IPA, isopropylamine; 1-PEA, 1-phenylethylamine; PLP, pyridoxal-5'-phosphate; DMSO, dimethylsulfoxide; GibZea, ATA from *Gibberella zeae*; NeoFis, ATA from *Neosartorya fischeri*; AspFum, ATA from *Aspergillus fumigatus*; 3HMU, ATA from *Ruegeria pomeroyi*; 315T, ATA from *Rhodobacter sphaeroides* 2.4.1.

\* Corresponding author. Tel.: +49 3834 86 4367; fax: +49 3834 86 794367.

E-mail address: [uwe.bornscheuer@uni-greifswald.de](mailto:uwe.bornscheuer@uni-greifswald.de) (U.T. Bornscheuer).

<http://dx.doi.org/10.1016/j.jbiotec.2014.05.015>

0168-1656/© 2014 Elsevier B.V. All rights reserved.

preparations or cell flocculation using chitosan (Koszelewski et al., 2010; Mallin et al., 2013a; Ni et al., 2012; Pääviö and Kanerva, 2013; Rehn et al., 2013, 2012; Truppo et al., 2012; Yi et al., 2007). Chitosan was used in several immobilization approaches due to its useful properties such as amino- and hydroxyl groups for covalent binding, high hydrophilicity for adsorptive attachment, easy production of a desired form of the carrier and a porous structure (Krajewska, 2004) suggesting that it could be also a suitable carrier for transaminases.

Recently, we reported the immobilization protocol for two (R)-selective transaminases from *Gibberella zeae* (GibZea) and from *Neosartorya fischeri* (NeoFis) on optimized chitosan support resulting in highly active and stable immobilized transaminase preparations (Mallin et al., 2013a). So far, two (R)-ATAs (GibZea and NeoFis) and one (S)-ATA (from *Vibrio fluvialis*, VFTA (Yi et al., 2007)) were covalently immobilized on chitosan. Thus we decided to prove this immobilization procedure for three further transaminases, where no immobilization had been described: the (R)-ATA from *Aspergillus fumigatus* (AspFum) and the (S)-ATAs from *Ruegeria pomeroyi* (3HMU) and *Rhodobacter sphaeroides* 2.4.1 (3IST) (Höhne et al., 2010; Steffen-Munsberg et al., 2013; Thomsen et al., 2014). (S)- and (R)-ATAs were chosen as they belong to two different folds: PLP fold classes I and IV, respectively (Jansonius, 1998). Owing to their different homodimeric, tertiary structures, it was not expected that the chitosan support is equally suited for (S)- and (R)-ATAs in general. Furthermore, we already showed that the free enzymes could be used for the production of various chiral amines from prochiral ketones (Schätzle et al., 2011; Steffen-Munsberg et al., 2013). The immobilization of these enzymes would make them more suitable for different reactor types as already demonstrated for the chitosan-immobilized GibZea (Mallin et al., 2013b). As the variation of the linker can lead to changed properties of the immobilized enzyme, we also investigated divinylsulfone (DVS) as an alternative to GA in this study. Whereas the latter reacts with different functional groups of an enzyme (mainly with the  $\epsilon$ -amino groups of lysine at a pH around 7.5) (Migneault et al., 2004), DVS additionally links thiol and hydroxyl groups of cysteine and serine with the functional groups present on the carrier (Friedman and Finley, 1975; Masri and Friedman, 1988; Morales-Sanfrutos et al., 2010).

## 2. Experimental

### 2.1. Materials

Chitosan (deacetylation degree >95%, viscosity [1% (w/v) in 1% acetic acid] 500 mPa s) was purchased from Heppe Medical Chitosan GmbH (Halle, Germany). All chemicals were purchased from Fluka (Buchs, Switzerland), Sigma–Aldrich (Steinheim, Germany), Merck (Darmstadt, Germany) or ABCR (Karlsruhe, Germany) unless stated otherwise. GA stock solution was purchased in a concentration of 25% (v/v). Crude extracts of (R)-ATAs were obtained by overexpression in *Escherichia coli* as described previously (Schätzle et al., 2011), but cell growth was performed in terrific broth instead of lysogeny broth to obtain higher cell densities. For 3HMU and 3IST, expression was performed overnight at 30 °C in auto-induction media ZYP-5052 (Studier, 2005). Cells were disrupted in sodium phosphate buffer (50 mM, pH 7.5, 0.1 mM PLP, 0.5 M NaCl) by sonication (10 ml volume, 20 min on ice, 0.5 s pulse, 50% power) to obtain crude extracts of GibZea, NeoFis, AspFum, 3IST and 3HMU after centrifugation (16 000  $\times$  g, 20 min, 4 °C). Chitosan beads (1%) were produced using the emulsion method (Mallin et al., 2013a).

### 2.2. Immobilization of transaminases using glutaraldehyde

Immobilization of ATAs was done using 25–300 mg of dry chitosan beads, which were activated using 1.5% (v/v) of the GA stock solution in a volume of 2–24 ml deionized water (1.5 h,

20 °C, 180 rpm). Activated beads were washed twice with deionized water and were then incubated with the different transaminase crude extracts under the same conditions as described in our recent publication (Mallin et al., 2013a). The enzyme activity used for immobilization was determined with (R)- or (S)-1-phenylethylamine (1-PEA) (Xie et al., 2013) and set to 10 U/ml for 10 mg dry, activated carrier. Samples, which were taken from the supernatant after immobilization, were used for the activity determination using the acetophenone assay and the protein content was determined using the Roti®-Nanoquant assay. The recovered activity was determined as described previously (Mallin et al., 2013a). The immobilized enzymes were obtained by filtration and washed twice with 20 ml of buffer (50 mM, pH 7.5, 0.1 mM PLP, 0.5 M NaCl). To exclude enzyme deactivation, the enzyme solutions were incubated without carrier under the same immobilization conditions.

### 2.3. Immobilization of transaminases using divinylsulfone

The immobilization of ATAs using DVS (Friedman and Finley, 1975) was performed under the same conditions as described for the immobilization using GA. The concentration of DVS was set to 2.5% (v/v) in deionized water and then the solution was basified (pH >13) using 10 N sodium hydroxide solution (1/10 of total volume). This solution was then used during the activation step of the beads for 1.5 h (20 °C, 180 rpm). To exclude enzyme deactivation, the enzyme solutions were incubated without carrier under the same immobilization conditions.

### 2.4. Enzyme assays

Activities of free enzymes were determined using the acetophenone assay by measuring the increase in absorbance at 245 nm in a 96-well UV-microtiter plate (Greiner) at 30 °C (Schätzle et al., 2009). The buffers employed in the assay were varied for the individual enzymes to ensure optimal enzyme performance: 50 mM sodium phosphate (pH 7.5), CHES (pH 9.5), or Bicin (pH 9.5) buffers were used for activity determination of the (R)-selective ATAs (Schätzle et al., 2011), 3HMU (Steffen-Munsberg et al., 2013) and 3IST, respectively.

For activity determination using the immobilized enzymes, a discontinuous variant of the acetophenone assay was performed (in triplicates). The same conditions were applied as given in our previous publication (Mallin et al., 2013a), except that the sample volume was reduced: from the enzymatic reaction 100  $\mu$ l samples were taken every 2 min (for a 10 min total time) from the supernatant and mixed with 100  $\mu$ l of the respective precooled buffer in a 96-well microtiter plate on ice. Then the absorbance at 245 nm was determined using a Tecan Infinity 200Pro spectrophotometer.

### 2.5. Characterization of ATAs

The storage stability was studied by incubating the soluble enzymes at 4 °C in sodium phosphate buffer (50 mM, pH 7.5, 0.1 mM PLP, 0.5 M NaCl). The immobilized enzymes were stored in a wet state in a closed vessel at 4 °C. After different time periods samples were taken and the activity was determined in triplicate as described above. For the soluble enzyme a centrifugation step for 1 min at 16 000  $\times$  g was performed to remove denatured proteins before activity determination.

To obtain the temperatures profiles of the free and immobilized ATAs, the initial activities at temperatures ranging from 15 to 80 °C (for 10 min) were determined as described earlier (Mallin et al., 2013a) with the following modifications: reaction buffers for the enzymes were chosen as described above and the total reaction volume was reduced to 1.8 ml. For AspFum, 3HMU and 3IST, the

**Table 1**Specific activity<sup>a</sup> and recovered activity<sup>b</sup> of GibZea immobilized on chitosan beads at different GA- or DVS-concentrations.

GA concentration [% (v/v)]	Activity	Recovered activity	DVS concentration [% (v/v)]	Activity	Recovered activity
1.5	319 ± 25	42 ± 1	1.0	280 ± 22	47 ± 7
2.0	298 ± 26	40 ± 1	2.5	407 ± 20	47 ± 2
2.5	285 ± 8	37 ± 4	5.0	372 ± 6	51 ± 5
3.0	241 ± 34	30 ± 2			

<sup>a</sup> Activities are given in U g<sub>dry</sub><sup>-1</sup> against the model substrate R-1-PEA.<sup>b</sup> Refers to the percentage of activity bound to the carrier after immobilization.

GA-immobilized and for GibZea and NeoFis the DVS-immobilized ATAs were used.

Stability of AspFum was determined by incubating the soluble or immobilized enzyme at various temperatures (40, 50 and 60 °C) for 4 h. For the free enzyme, samples were taken periodically, cooled down to 4 °C, centrifuged (1 min, 16 000 × g, 4 °C) and then the activity was determined as described above at 30 °C. For the immobilized enzyme, 15 mg wet catalysts was weighed in a 2 ml Eppendorf tube for each measurement (performed in triplicates) and incubated in 200 µl sodium phosphate buffer at the given temperatures (50 mM, pH 7.5 adjusted at 20 °C, 0.1 mM PLP, 0.5 M NaCl). For activity determination, the incubated immobilized enzyme was cooled down on ice for 2 min and was then incubated at 30 °C in a thermoshaker for 1 min. 1.6 ml of pre-warmed (30 °C) reaction solution (sodium phosphate buffer, 50 mM, pH 7.5, 2.8 mM (R)-1-PEA, 2.8 mM pyruvate and 0.28% DMSO) was added to the start the reaction. The reaction was run for 10 min and 100 µl samples were taken every 2 min. After dilution of the sample activity was determined as described above.

Recycling studies were performed in a volume of 3 ml (appropriate buffer, 50 mM, pH 7.5 (or 9.5), 100 mM *rac*-1-PEA, 100 mM pyruvate, 0.1 mM PLP and 2% DMSO) for 1 h in a thermoshaker (30 °C, 220 rpm). Each experiment was done in triplicate with wet catalysts: 1.2 U GibZea, 0.9 U NeoFis, 0.8 U AspFum (not activated), 1.6 U 3HMU and 2 U 315T. At the end of each cycle a 250 µl sample was taken and analyzed by GC as described earlier (Mallin et al., 2013b) to calculate the conversion. Then, the catalysts were washed twice with 10 ml sodium phosphate buffer (50 mM, pH 7.5, 0.1 mM PLP) and were subjected to the next reaction cycle. Heat activation of immobilized AspFum was performed by incubating 1 g of wet catalyst in a volume of 5 ml (sodium phosphate, 50 mM, pH 7.5, 0.1 mM PLP, 0.5 M NaCl) in a closed vessel for 2 h in a 50 °C water bath. After filtration, the wet catalyst could be used.

### 2.6. Asymmetric synthesis of (R)- or (S)-1-methyl-3-phenylpropylamine

The reactions were performed in triplicate in a volume of 1 ml solution (ATA specific buffer, 50 mM, pH 7.5 (or 9.5), 10 mM 4-phenyl-2-butanone, 300 mM isopropylamine, 1 mM PLP and 10% DMSO) in a thermoshaker (30 °C, 1000 rpm). 1 U ATA (soluble or immobilized, acetophenone assay) was used in each biocatalysis. After 40 h a 50 µl sample was taken and diluted with 150 µl of the ATA specific buffer used in the reaction. Then the samples were analyzed by HPLC as described previously (Schätzle et al., 2011).

## 3. Results and discussion

The three ATAs AspFum, 3HMU and 315T were chosen for this study because they had high specific activity towards (R)- or (S)-1-phenylethylamine [(R) or (S)-1-PEA] and an interesting substrate scope in the asymmetric synthesis of amines (Schätzle et al., 2011; Steffen-Munsberg et al., 2013). However, immobilization was not yet established for these enzymes and therefore we aimed to extend the previously established protocol for this purpose. Furthermore,

the (R)-selective ATAs GibZea and NeoFis were included in this study as we wished to investigate the effect of the linker DVS compared to GA, which was used in our previous study for immobilizing GibZea and NeoFis (Mallin et al., 2013a). For the (R)-selective enzymes sodium phosphate buffer (pH 7.5) was used as described by Höhne et al. (2010). For 3HMU, CHES buffer at pH 9.5 gave the highest activity (Steffen-Munsberg et al., 2013), but for 315T Bicin buffer at pH 9.5 turned out best as a doubled activity was found compared to the use of CHES buffer at the same pH.

For the immobilization of the ATAs chitosan beads were used as carrier matrix. The preparation of the beads was performed as reported elsewhere (Mallin et al., 2013a). Prior to the immobilization studies different concentrations of GA or DVS were investigated using GibZea as model enzyme (Table 1). A concentration of 1.5% (v/v) GA turned out to be the best in terms of enzyme activity loading. This concentration was used for all further experiments. GibZea was also used as model enzyme to identify that 2.5% (v/v) DVS was best for optimal activity loading on the chitosan support (Table 1). Immobilization times of 3 h were found optimal for all enzymes leading to active immobilized ATAs (Table 2). GibZea and NeoFis showed nearly the same immobilized activities with both linkers. With NeoFis, the recovered activity was 15% higher using DVS. In the other cases, the GA-immobilized enzymes showed ~2–3-fold higher specific activities compared to the DVS-immobilized ones.

### 3.1. Influence of immobilization on stability and temperature profiles

Storage stability is an important property of an immobilized biocatalyst for commercial use (i.e., for shipment, production of large batches) and was examined for the free and the immobilized enzymes over one month (Fig. 1A–C). Using GA as linker for immobilization the storage stability of the enzymes was in general increased and in a few cases also a slight hyperactivation was observed, which was quite significant for 3HMU. Only 315T was rather unstable, even as immobilized preparation. For GibZea, independently of the linker equal stabilities were found, whereas the other enzymes showed a lower stability with DVS compared to GA. The temperature profiles determined from 15 to 80 °C for all immobilized enzymes gave similar profiles compared to the

**Table 2**Specific<sup>a</sup> and recovered activities<sup>b</sup> of different (R)- and (S)-ATA immobilized covalently on chitosan beads with GA or DVS as linker molecules.

Enzyme	Activity [GA]	Recovered activity [GA]	Activity [DVS]	Recovered activity [DVS]
GibZea	322 ± 22	63 ± 4	291 ± 29	38 ± 4
NeoFis	165 ± 6	39 ± 2	168 ± 15	54 ± 5
AspFum <sup>c</sup>	99 ± 7	54 ± 2	51 ± 3	85 ± 6
3HMU	157 ± 2	21 ± 0	52 ± 22	26 ± 11
315T	163 ± 8	23 ± 3	50 ± 6	9 ± 1

<sup>a</sup> Activities are given in U g<sub>dry</sub><sup>-1</sup> against the model substrate (R)- or (S)-1-PEA.<sup>b</sup> Refers to the percentage of activity bound to the carrier after immobilization.<sup>c</sup> Before heat activation.



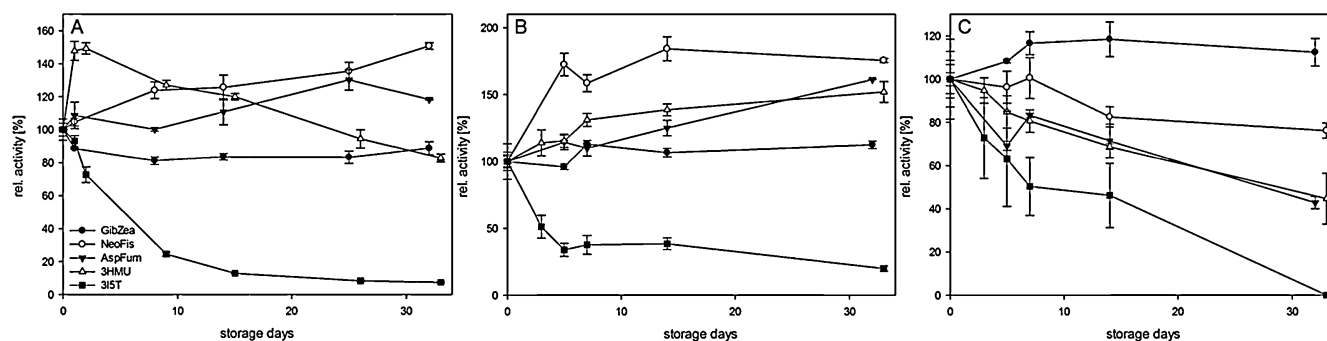


**Fig. 1.** (A–C) Storage stability at 4 °C for the free (A), the glutaraldehyde (B) or divinylsulfone (C) immobilized transaminases on chitosan support. Activity was determined at 30 °C as described in Section 2.

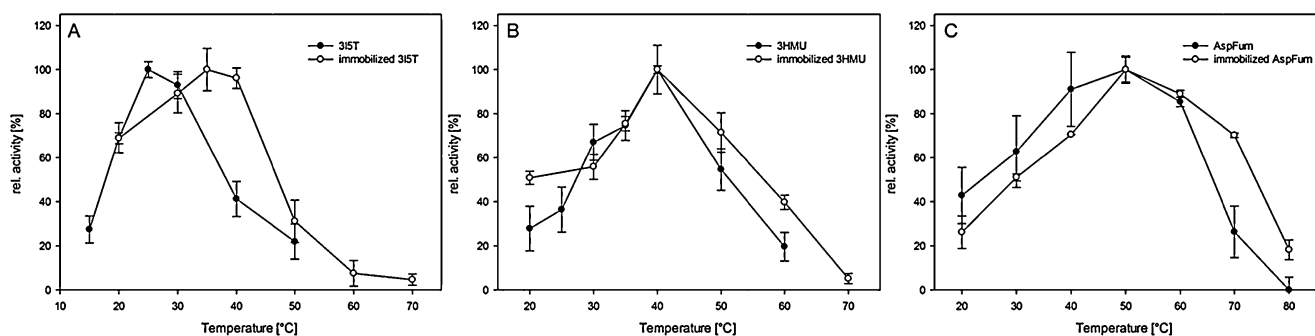


**Fig. 2.** (A–C) Relative initial activities of free and GA-immobilized 315T (A), 3HMU (B) or AspFum (C) at different temperatures. 100% relative activity refers to: A = 1.9 U/ml for free enzyme and 61 U/g<sub>dry</sub> for the immobilized enzyme, B = 4.2 U/ml for free enzyme and 146 U/g<sub>dry</sub> for the immobilized enzyme, C = 1.9 U/ml for free enzyme and 110 U/g<sub>dry</sub> for the immobilized enzyme.

corresponding free enzymes (Fig. 2A–C). For 315T a shift of the temperature optimum was observed due to the immobilization, but as the enzyme showed low stability, this effect was only of modest importance. Interestingly, GA-immobilized AspFum was significantly more active at 70 °C compared to the free enzyme (70% compared to 26%). This indicates a stronger stabilization of the enzyme due to the covalent attachment to the chitosan support. Further investigation for this enzyme with incubation at 40, 50 and 60 °C for 4 h showed a strong activation of GA-immobilized AspFum (Fig. 3) with up to 3.6-fold higher activities at 50 °C. At 60 °C

the free AspFum was unstable, whereas the immobilized enzyme showed a strong activation after 4 h.

### 3.2. Recycling of immobilized transaminases

Besides the advantage of stabilization effects, other main advantages of immobilized enzymes are their easy downstream processing by simple filtration and the possibility for reuse of the catalyst. Consecutive batch experiments were investigated for the GA-immobilized 315T, 3HMU and AspFum and for the DVS-immobilized GibZea and NeoFis. For four batches the residual conversion for the transamination of *rac*-1-PEA (12.1 g l<sup>-1</sup>, 0.1 M) to acetophenone was determined after 1 h (Fig. 4). At the end of each batch a sample was taken and analyzed by GC after extraction with dichloromethane followed by derivatization with trifluoroacetic anhydride. Then the immobilized preparations were filtered, washed twice with buffer and were then subjected to the next cycle. A decrease of the relative activities to 37–85% remaining activity was observed for different enzyme preparations. Reasons could be leaching of non-specifically bound enzymes, a slow deactivation of exposed enzyme layers or the slow accumulation of inhibiting reaction compounds. The GA-immobilized 3HMU and AspFum were applied four times in biotransformations with low reductions in the conversion, making both biocatalysts usable for different reactor types and long-term operations. Especially, due to the covalent attachment the leaching to the reaction media can be reduced compared to adsorptive immobilized enzymes, which could be a reason for the good stability and small reduction of activity for the 3HMU and AspFum after several reuses. 315T was strongly deactivated after several reuse, supporting the already found modest stability of this enzyme. The DVS-immobilized GibZea and NeoFis showed a constant decrease in activity until the fourth batch. This is in contrast to the good recycling performance of the

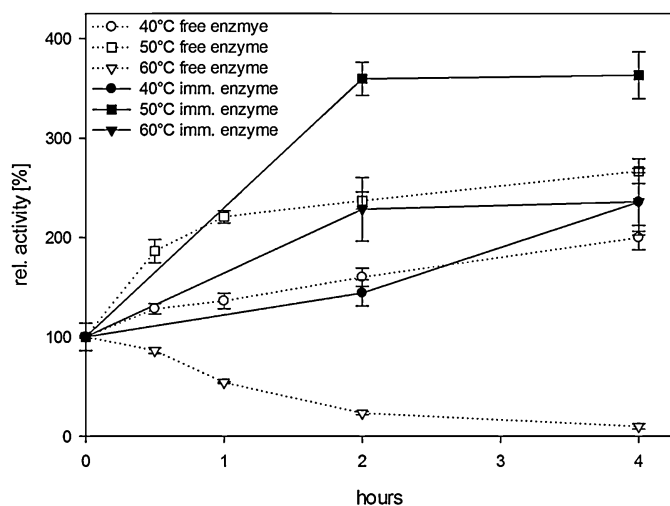


**Fig. 3.** Relative initial activities of free (dots) and GA-immobilized (line) AspFum at 30 °C after incubation at 40 °C, 50 °C and 60 °C for 4 h. For incubation conditions see Section 2. 100% relative activity refers to: 0.4 U/ml for free enzyme and 24 U/g<sub>dry</sub> for the immobilized enzyme.



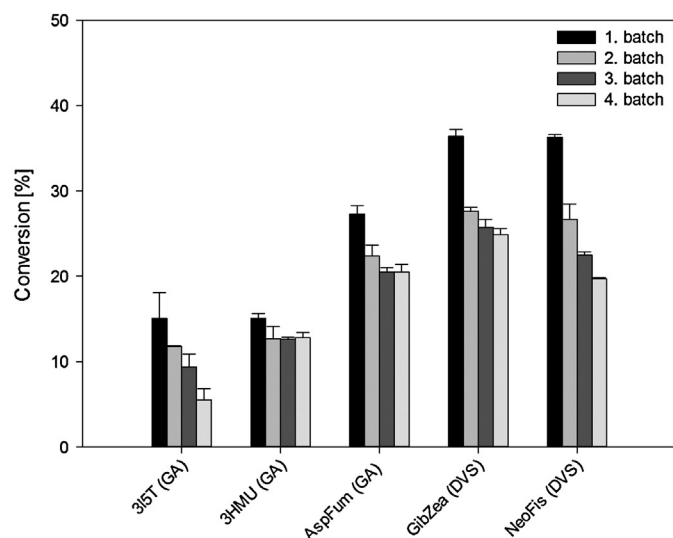


**Fig. 4.** Recycling study with GA immobilized 3IST, 3HMU and AspFum and DVS immobilized GibZea and NeoFis for four consecutive cycles of 1 h batches in the kinetic resolution of *rac*-1-PEA.

GA-immobilized GibZea and NeoFis reported earlier (Mallin et al., 2013a). Because of these results the DVS variants were not used for the asymmetric synthesis experiment.

#### Scheme 1.

### 3.3. Asymmetric synthesis with isopropylamine as amino donor

ATAs can use isopropylamine (IPA) as amino donor in asymmetric synthesis. IPA displays many advantages because it is cheap and the equilibrium can be shifted by applying high equivalents of IPA or via removal of the acetone formed. In general, wild-type enzymes showed only a low acceptance for IPA, making improvements by protein engineering necessary to generate a useful biocatalyst for this application (Savile et al., 2010). Therefore we investigated the performance of free and immobilized enzymes in the asymmetric synthesis of (*R*)- or (*S*)-1-methyl-3-phenylpropylamine using IPA as amino donor (Table 3). IPA was used in a 30-fold excess to shift the

**Table 3**

Conversions<sup>a</sup> observed in biocatalysis<sup>b</sup> using the free and GA immobilized enzymes. As amino donor IPA was used in 30-fold excess to shift the equilibrium.

Enzyme	Free enzyme	Immobilized enzyme
GibZea	<1	36 ± 2
NeoFis	46 ± 2	17 ± 0
AspFum <sup>b</sup>	44 ± 2	50 ± 1
3HMU	67 ± 1	75 ± 1
3IST	10 ± 0	18 ± 1

<sup>a</sup> Conversion in % after 40 h as determined by HPLC for (*R*)- or (*S*)-1-methyl-3-phenylpropylamine produced.

<sup>b</sup> Heat activated.

equilibrium. Slightly higher conversions were found for the immobilized AspFum, 3HMU, and 3IST compared to the free enzymes (Table 3). In the latter case, only 18% conversion could be reached using the GA-immobilized enzyme, due to the lower stability of 3IST as demonstrated above. Furthermore, we verified our previously immobilized ATAs GibZea and NeoFis for the acceptance of IPA as amine donor. Here, we demonstrated again a 120-fold increased conversion (36 ± 1.9%) in the asymmetric amine synthesis for the immobilized GibZea compared to the free enzyme (Mallin et al., 2013a). In stark contrast, the free NeoFis showed a 2.7-fold higher conversion (46 ± 1.5%) compared to the GA-immobilized NeoFis, demonstrating that chitosan immobilization does not generally increase ATA performance for all applications.

### 4. Conclusion

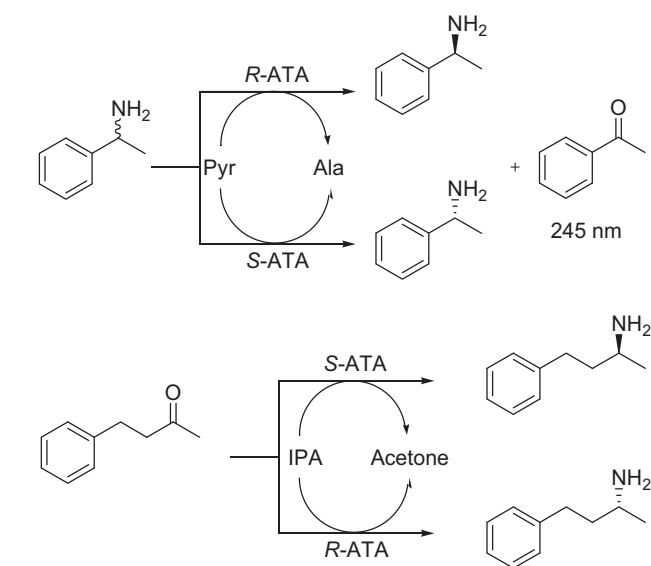
In this study we expanded our protocol for the immobilization of GibZea and NeoFis on chitosan support using glutaraldehyde as linker molecule to three further transaminases ((*R*)-ATA: AspFum; (*S*)-ATAs: 3HMU and 3IST). All enzymes could be immobilized in active form, which shows that ATAs from different fold classes can be immobilized with the same protocol on chitosan. The immobilized enzymes showed excellent storage stabilities, increased stabilities, good recycling performance, they can be used in asymmetric synthesis with IPA as amino donor and in case of AspFum also displayed a hyperactivation.

### Acknowledgement

The authors thank the “Bundesministerium für Bildung und Forschung Biokatalyse2021 cluster, FK0315175B” for financial support.

### References

- Bornscheuer, U.T., 2003. Immobilizing enzymes: how to create more suitable biocatalysts. *Angew. Chem. Int. Ed.* 42, 3336–3337.
- Bornscheuer, U.T., Huisman, G.W., Kazlauskas, R.J., Lutz, S., Moore, J.C., Robins, K., 2012. Engineering the third wave of biocatalysis. *Nature* 485, 185–194.
- Brena, B., González-Pombo, P., Batista-Viera, F., 2013. Immobilization of enzymes: a literature survey. In: Guisan, J.M. (Ed.), *Immobilization of Enzymes and Cells*. Humana Press, pp. 15–31.
- Buchholz, K., Kasche, V., Bornscheuer, U.T., 2012. *Biocatalysts and Enzyme Technology*, 2nd ed. Wiley-VCH, Weinheim.
- Desai, A.A., 2011. Sitagliptin manufacture: a compelling tale of green chemistry, process intensification, and industrial asymmetric catalysis. *Angew. Chem. Int. Ed.* 50, 1974–1976.
- Friedman, M., Finley, J.W., 1975. Reactions of proteins with ethyl vinyl sulfone. *Int. J. Pept. Protein Res.* 7, 481–486.
- Hanefeld, U., Gardossi, L., Magner, E., 2009. Understanding enzyme immobilisation. *Chem. Soc. Rev.* 38, 453–468.
- Höhne, M., Bornscheuer, U.T., 2009. Biocatalytic routes to optically active amines. *ChemCatChem* 1, 42–51.
- Höhne, M., Bornscheuer, U.T., 2012. Application of transaminases in organic synthesis. In: May, O., Gröger, H., Drauz, W. (Eds.), *Enzyme Catalysis in Organic Synthesis*. Wiley-VCH, Weinheim, pp. 779–820.
- Höhne, M., Schätzle, S., Jochens, H., Robins, K., Bornscheuer, U.T., 2010. Rational assignment of key motifs for function guides in silico enzyme identification. *Nat. Chem. Biol.* 6, 807–813.



**Scheme 1.** Reactions catalyzed by the different transaminases. The kinetic resolution of *rac*-1-PEA or the asymmetric synthesis of (*R*)- or (*S*)-1-methyl-3-phenylpropylamine using isopropylamine (IPA) as amino donor were studied.

- Janssonius, J.N., 1998. Structure, evolution and action of vitamin B6-dependent enzymes. *Curr. Opin. Struct. Biol.* 8, 759–769.
- Kohls, H., Steffen-Munsberg, F., Höhne, M., 2014. Recent achievements in developing the biocatalytic toolbox for chiral amine synthesis. *Curr. Opin. Chem. Biol.* 19, 180–192.
- Koszelewski, D., Müller, N., Schrittwieser, J.H., Faber, K., Kroutil, W., 2010. Immobilization of  $\omega$ -transaminases by encapsulation in a sol-gel/celite matrix. *J. Mol. Catal. B: Enzym.* 63, 39–44.
- Krajewska, B., 2004. Application of chitin- and chitosan-based materials for enzyme immobilizations: a review. *Enzyme Microb. Technol.* 35, 126–139.
- Liese, A., Hilterhaus, L., 2013. Evaluation of immobilized enzymes for industrial applications. *Chem. Soc. Rev.* 42, 6236–6249.
- Mallin, H., Menyes, U., Vorhaben, T., Hohne, M., Bornscheuer, U.T., 2013a. Immobilization of two (R)-amine transaminases on an optimized chitosan support for the enzymatic synthesis of optically pure amines. *ChemCatChem* 5, 588–593.
- Mallin, H., Muschiol, J., Byström, E., Bornscheuer, U., 2013b. Efficient biocatalysis with immobilized enzymes or encapsulated whole cell microorganism by using the SpinChem reactor system. *ChemCatChem* 5, 3529–3532.
- Masri, M.S., Friedman, M., 1988. Protein reactions with methyl and ethyl vinyl sulfones. *J. Protein Chem.* 7, 49–54.
- Mateo, C., Palomo, J.M., Fernandez-Lorente, G., Guisan, J.M., Fernandez-Lafuente, R., 2007. Improvement of enzyme activity, stability and selectivity via immobilization techniques. *Enzyme Microb. Technol.* 40, 1451–1463.
- Mathew, S., Yun, H., 2012.  $\omega$ -Transaminases for the production of optically pure amines and unnatural amino acids. *ACS Catal.* 2, 993–1001.
- Migneault, I., Dartiguenave, C., Bertrand, M.J., Waldron, K.C., 2004. Glutaraldehyde: behavior in aqueous solution, reaction with proteins, and application to enzyme crosslinking. *Biotechniques* 37, 790–802.
- Morales-Sanfrutos, J., Lopez-Jaramillo, J., Ortega-Munoz, M., Megia-Fernandez, A., Perez-Balderas, F., Hernandez-Mateo, F., Santoyo-Gonzalez, F., 2010. Vinyl sulfone: a versatile function for simple bioconjugation and immobilization. *Org. Biomol. Chem.* 8, 667–675.
- Ni, K., Zhou, X., Zhao, L., Wang, H., Ren, Y., Wei, D., 2012. Magnetic catechol-chitosan with bioinspired adhesive surface: preparation and immobilization of  $\omega$ -transaminase. *PLOS ONE* 7, e41101.
- Päiviö, M., Kanerva, L.T., 2013. Reusable  $\omega$ -transaminase sol-gel catalyst for the preparation of amine enantiomers. *Process Biochem.* 48, 1488–1494.
- Pollard, D.J., Woodley, J.M., 2007. Biocatalysis for pharmaceutical intermediates: the future is now. *Trends Biotechnol.* 25, 66–73.
- Rehn, G., Grey, C., Branneby, C., Adlercreutz, P., 2013. Chitosan flocculation: an effective method for immobilization of *E. coli* for biocatalytic processes. *J. Biotechnol.* 165, 138–144.
- Rehn, G., Grey, C., Branneby, C., Lindberg, L., Adlercreutz, P., 2012. Activity and stability of different immobilized preparations of recombinant *E. coli* cells containing  $\omega$ -transaminase. *Process Biochem.* 47, 1129–1134.
- Savile, C.K., Janey, J.M., Mundorff, E.C., Moore, J.C., Tam, S., Jarvis, W.R., Colbeck, J.C., Krebber, A., Fleitz, F.J., Brands, J., Devine, P.N., Huisman, G.W., Hughes, G.J., 2010. Biocatalytic asymmetric synthesis of chiral amines from ketones applied to sitagliptin manufacture. *Science* 329, 305–309.
- Schätzle, S., Höhne, M., Redestad, E., Robins, K., Bornscheuer, U.T., 2009. Rapid and sensitive kinetic assay for characterization of  $\omega$ -transaminases. *Anal. Chem.* 81, 8244–8248.
- Schätzle, S., Steffen-Munsberg, F., Höhne, M., Robins, K., Bornscheuer, U.T., 2011. Enzymatic asymmetric synthesis of enantiomerically pure aliphatic, aromatic and arylaliphatic amines with (R)-selective amine transaminases. *Adv. Synth. Catal.* 353, 2439–2445.
- Sheldon, R.A., 2007. Enzyme immobilization: the quest for optimum performance. *Adv. Synth. Catal.* 349, 1289–1307.
- Simon, R.C., Richter, N., Busto, E., Kroutil, W., 2013. Recent developments of cascade reactions involving  $\omega$ -transaminases. *ACS Catal.* 4, 129–143.
- Steffen-Munsberg, F., Vickers, C., Thontowi, A., Schätzle, S., Tumilirsch, T., Svedendahl, H.M., Land, H., Berglund, P., Bornscheuer, U.T., Höhne, M., 2013. Connecting unexplored protein crystal structures to enzymatic function. *ChemCatChem* 5, 150–153.
- Studier, F.W., 2005. Protein production by auto-induction in high-density shaking cultures. *Protein Exp. Purif.* 41, 207–234.
- Thomsen, M., Skalden, L., Palm, G.J., Hohne, M., Bornscheuer, U.T., Hinrichs, W., 2014. Crystallographic characterization of the (R)-selective amine transaminase from *Aspergillus fumigatus*. *Acta Crystallogr. Sect. D* 70, 1086–1093.
- Truppo, M.D., Strotman, H., Hughes, G., 2012. Development of an immobilized transaminase capable of operating in organic solvent. *ChemCatChem* 4, 1071–1074.
- Woodley, J.M., 2008. New opportunities for biocatalysis: making pharmaceutical processes greener. *Trends Biotechnol.* 26, 321–327.
- Xie, J., Xu, P., Li, H., Xue, Q., Jin, H., Cheng, Y., Zhu, C., 2013. A room temperature decarboxylation/C–H functionalization cascade by visible-light photoredox catalysis. *Chem. Commun.* 49, 5672–5674.
- Yi, S.-S., Lee, C.-w., Kim, J., Kyung, D., Kim, B.-G., Lee, Y.-S., 2007. Covalent immobilization of  $\omega$ -transaminase from *Vibrio fluvialis* JS17 on chitosan beads. *Process Biochem.* 42, 895–898.

## Articles

### Article VI

# Efficient Biocatalysis with Immobilized Enzymes or Encapsulated Whole Cell Microorganism by Using the SpinChem Reactor System

Hendrik Mallin,<sup>[a]</sup> Jan Muschiol,<sup>[a]</sup> Emil Byström,<sup>\*,[b]</sup> and Uwe T. Bornscheuer<sup>\*,[a]</sup>

Nowadays, biocatalysis is an established method for the enzymatic synthesis of chiral building blocks for organic compounds and pharmaceuticals, compounds for the flavor and fragrance industry, the production of bulk chemicals, and the modification of lipids for the food industry.<sup>[1]</sup>

Biocatalysis has become highly competitive with classical (asymmetric) chemical routes that use transition-metal catalysts, especially in combination with new methods for enzyme discovery and protein engineering,<sup>[2]</sup> as recently shown for the synthesis of the drug Sitagliptin.<sup>[3]</sup> The cost-effective application of enzymes, in particular for the synthesis of cheap products, requires immobilization of the biocatalyst (or the encapsulation of whole cells) to enhance their long-term stability<sup>[4,5]</sup> and facilitate their reuse. At the same time, immobilization of the biocatalyst should enable the use of established reactor setups, such as fixed-bed reactors (FBRs), instead of simple stirred-tank reactors (STRs, Figure 1).<sup>[1b,6]</sup> FBRs are used, for instance, for the large-scale production of chiral amines<sup>[7]</sup> or emollient esters for the cosmetic sector<sup>[8]</sup> by using lipase catalysts. However, several disadvantages are encountered with FBRs, which depend on, for example, the length, diameter, and particle size in the reactor, the

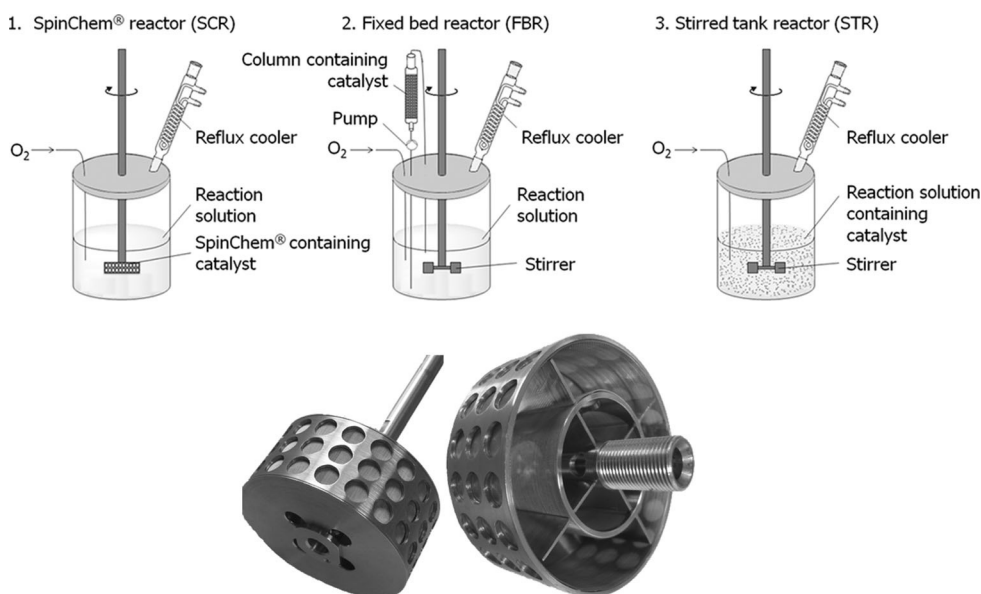


**Figure 1.** Top: Schematic representation of the three reactor setups that were investigated. Bottom: Photograph of the SpinChem device (reflux cooler and oxygen supply only for BVMO reaction).

flow rate, the pressure drop within the column, and reactant and pH gradients, as well as inactivation profiles after extended use. In contrast, the more operationally simple STR encounters mechanical challenges for the carrier, which results in abrasion of the biocatalyst material and severe damage of encapsulated whole cells beside the fact that the recycling of the immobilized biocatalyst is rather laborious.

Herein, we have investigated the use of an alternative setup for the application of immobilized enzymes and encapsulated whole cells. This SpinChem reactor (SCR; SpinChem is a registered trademark by Nordic ChemQuest AB, Umeå, Sweden) enables the simultaneous stirring and efficient percolation of a liquid through packed particle beds, which is implemented by a hollow stirring device that allows the solid reaction chamber to be located inside the stirring element itself. The SCR can be seen as an evolution of the standard basket reactor.<sup>[9,10]</sup> The basket reactor, first published by Carberry in 1964, is a setup in which four baskets rotate inside a well for gas/solid reactions. This concept was later developed as the “annular spinning basket reactor” by Mahoney et al. in 1978. However, in the SpinChem reactor, the solid phase (such as an immobilized enzyme) is present in the stirring element itself in up to four separate compartments, which provides greater mixing and flexibility compared to the basket reactors.

[a] H. Mallin,<sup>+</sup> J. Muschiol,<sup>+</sup> Prof. Dr. U. T. Bornscheuer  
Institute of Biochemistry  
Dept. of Biotechnology & Enzyme Catalysis  
Greifswald University  
Felix-Hausdorff-Str. 4, 17487 Greifswald (Germany)  
Fax: (+49) 3834-86-794367  
E-mail: uwe.bornscheuer@uni-greifswald.de

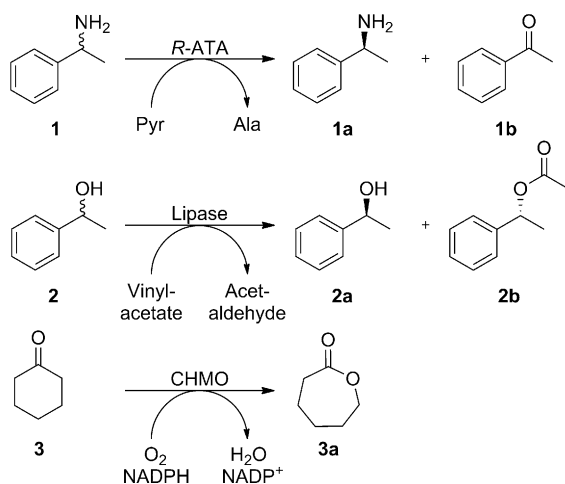
[b] Dr. E. Byström  
Nordic Chemquest AB  
Box 7958, S-907 19 Umeå (Sweden)  
E-mail: emil.bystrom@nordicchemquest.com

[<sup>+</sup>] These authors contributed equally to this work.

Supporting information for this article, including all of the experimental details, is available on the WWW under <http://dx.doi.org/10.1002/cctc.201300599>.

In this way, a variety of heterogeneous operations (catalysis, solid-phase reactions, scavenging, etc.) can be performed in an efficient and convenient fashion, because the material is contained in the overhead stirring device and is not subject to mechanical wear or filtration problems. By rotating the SCR, the liquid inside is “thrown out” through a centrifugal effect and the new liquid will be drawn into the SCR from both the bottom and the top (Figure 1). The main advantages of the SpinChem system are easier downstream processing and simple recycling of the biocatalyst, because the compartment that contains the immobilized enzyme can be easily separated from the bulk reaction solution.

To verify the properties of the SCR compared to established reactor systems for biocatalysis, we have investigated 1) the kinetic resolution of (*R,S*)-1-phenylethylamine by using an immobilized (*R*)-transaminase from *Gibberella zeae* (GibZea)<sup>[11]</sup> and 2) the kinetic resolution of (*R,S*)-1-phenylethanol by using an immobilized *Candida antarctica* lipase B (CAL-B,<sup>[12]</sup> Novozyme 435, N435) in *n*-hexane (Scheme 1).



**Scheme 1.** Biocatalytic reactions that were studied by using the different reactor systems. R-ATA = (*R*)-amine transaminase, CHMO = cyclohexanone monooxygenase.

Furthermore, 3) calcium-alginate-encapsulated *Escherichia coli* whole cells that harbor the cyclohexanone monooxygenase (CHMO) from *Acinetobacter calcoaceticus* NCIMB 9871<sup>[13]</sup> were used for the production of  $\epsilon$ -caprolactone from cyclohexanone (Scheme 1). Stability has been a particularly challenging issue for  $O_2$ -consuming enzymes, which still has to be addressed. Furthermore, in FBRs, the  $O_2$  supply is a difficult issue and, thus, an alternative reactor system is sought.

The reactions in the SCR and the STR were performed with a volume of 0.5 L in a New Brunswick BioFlo 110 Fermentor/Bioreactor (total volume: 0.9 L). In the FBR reactions a reservoir with a volume of 0.5 L was used. In all three setups, we used identical amounts of enzyme (based on units of activity; for details, see the Supporting Information). For the lipase and transaminase reactions, we operated at high substrate concentrations of  $122.17 \text{ g L}^{-1}$  (1 M) and  $16.12 \text{ g L}^{-1}$  (0.133 M), respectively.

Because Baeyer–Villiger monooxygenases work best at lower substrate concentrations, only  $1.96 \text{ g L}^{-1}$  (0.02 M) cyclohexanone was used for the CHMO-catalyzed reaction. To ensure an optimal mass transfer, we first determined the optimal stirring speed for the SCR, which was found to be 500 rpm for all three reactions that were studied (the range 100–1000 rpm was investigated; see the Supporting Information, Table S6).

In the transaminase-catalyzed kinetic resolution (Scheme 1, Figure 2, and Table 1), the SCR and the STR gave the same con-

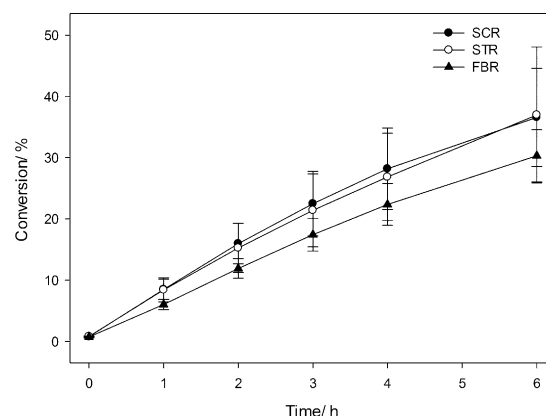


**Figure 2.** Kinetic resolution of (*R,S*)-1-phenylethylamine to afford (*S*)-1-phenylethylamine by using the immobilized GibZea (*R*)-transaminase.

versions after 6 h, whereas the FBR gave a 1.2-fold-lower conversion. For the lipase-catalyzed kinetic resolution (Scheme 1, Figure 3, and Table 1), almost-identical conversions (close to 50%) were determined after only 4 h, even at a substrate concentration of 1 M. The production of  $\epsilon$ -caprolactone catalyzed

**Table 1.** Conversions that were achieved with three different reactor systems.

Enzyme	Conversion [%]		
	SCR	STR	FBR
transaminase <sup>[a]</sup>	37 ± 8.0	37 ± 11	30 ± 4.3
lipase <sup>[b]</sup>	45 ± 1.0	46 ± 1.0	n.d.
CHMO <sup>[c]</sup>	36 ± 6.1	35 ± 6.0	4 ± 0.2

[a] After 6 h; [b] after 4 h; [c] after 24 h; n.d. = not determined.

by the CHMO also showed the same conversions (35%) after 24 h in both the SCR and the STR (Scheme 1, Figure 4, and Table 1). In contrast, for the FBR, a significant nine-fold-lower conversion was obtained. This dramatic slowdown could be explained by the decreased oxygen supply in the column. Thus, SCR and STR enable similar conversions for CHMO-, lipase-, and transaminase-catalyzed reactions, thus indicating that, for these reactors, mass transfer is not a limiting issue.

Next, reuse and downstream processing were studied in the SCR and the STR under identical conditions. In the case of the SCR, this study was simply performed by taking the stirrer out of the reactor and washing it three times in small beakers

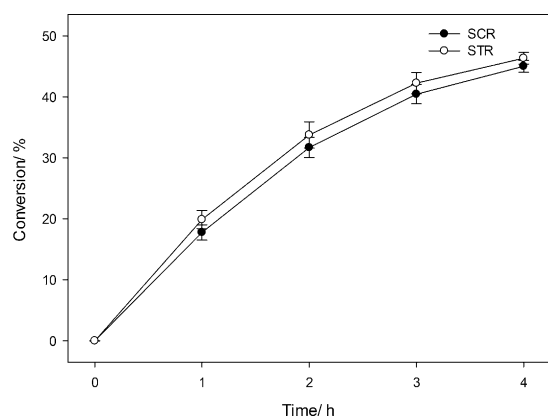


**Figure 3.** Transesterification of (*R,S*)-1-phenylethanol into the corresponding (*R*)-acetate by using immobilized lipase CAL-B in the SCR and the STR.

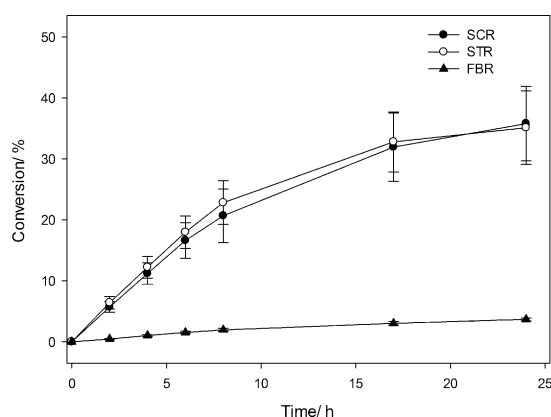


**Figure 4.** Formation of  $\epsilon$ -caprolactone by using alginate-encapsulated resting *E. coli* cells that harbored a CHMO.

under stirring for 30 s. Then, the biocatalysts that were present in the SpinChem compartment were ready to use in the next cycle. In the STR, the reaction solution was first filtered, followed by washing the immobilized catalyst before the next cycle was started. These recycling studies revealed that, for the transaminase reaction, the SpinChem system was superior: 93% relative activity was recovered in the SCR compared to only 62% in the STR (Figure 5).

This result suggested that the immobilized transaminase was better protected from mechanical forces in the SpinChem device. In the lipase-catalyzed kinetic resolution, the SCR was slightly superior until the fourth cycles; after the sixth cycle, both systems gave similar conversions (Figure 6).

Notably, CAL-B is a highly robust lipase and, hence, losses in activity are difficult to observe because the immobilized biocatalyst is typically stable for several months under process conditions. Furthermore, this initial decrease in activity could be caused by accumulation of the reaction compounds on the carrier or in the enzyme environment. In the oxidation reactions that were catalyzed by CHMO whole cells, the SCR was clearly superior and showed 41% residual activity after six cycles (versus 14% relative activity in the STR). Furthermore,

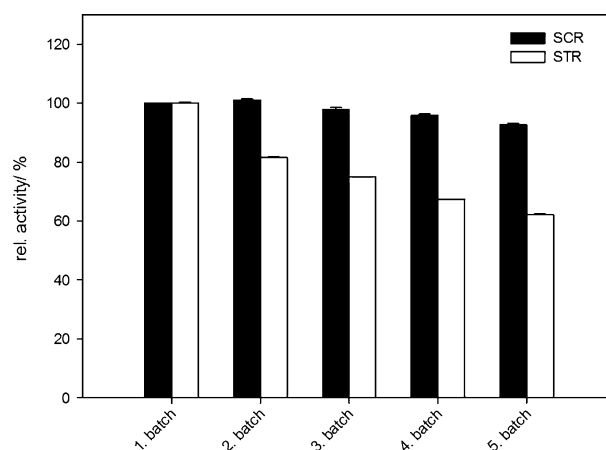


**Figure 5.** Recycling study with immobilized GibZea (*R*)-transaminase (2 h per batch) in the SCR and the STR; 100% relative activity refers to 19% conversion of (*R*)-1-phenylethylamine in the first batch.

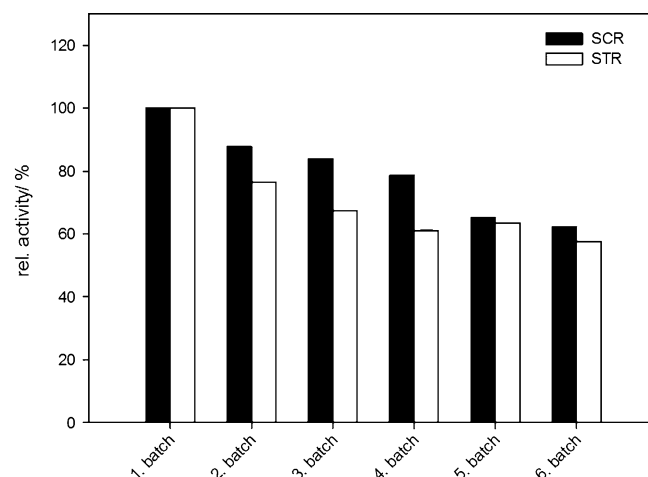


**Figure 6.** Recycling study with immobilized lipase CAL-B (2 h per batch) in the SCR and the STR; 100% relative activity refers to 33% (SCR) and 39% conversions (STR) of (*R,S*)-1-phenylethanol in the first batch.

between the fourth and fifth cycles, the encapsulated cells were stored overnight at 4 °C (Figure 7). The cells in the SCR showed no significant loss of activity, whereas, in contrast, only half of the relative activity was determined for the cells in the STR. In addition, for successful recycling of the alginate capsules, the presence of 10 mM CaCl<sub>2</sub> in the reaction and washing solution was necessary. Without this additive, the beads completely dissolved after the second cycle, owing to removal of the Ca<sup>2+</sup> ions from the calcium-alginate complex (data not shown).

In conclusion, we have developed an alternative reactor concept for the use of immobilized enzymes or whole cells in biocatalysis. The SCR was shown to be equivalent to—or even superior to—conventional setups. In particular, recycling experiments in consecutive batch reactions are facilitated and the activity loss was reduced in the SCR. The SCR does not require special laboratory equipment because, in essence, only the stir-



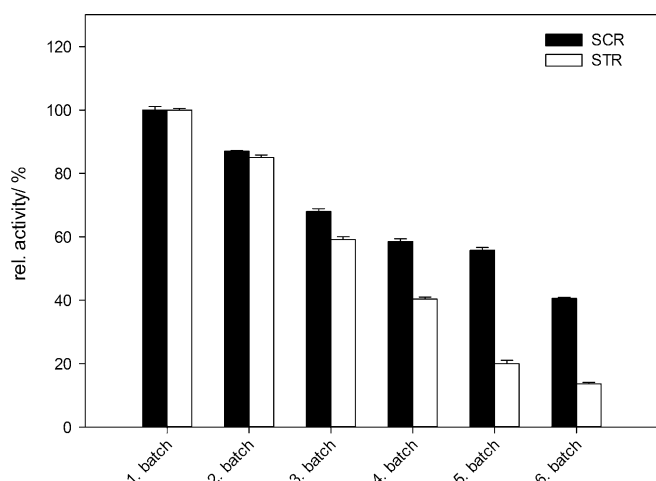


**Figure 7.** Recycling study with encapsulated resting *E. coli* cells that expressed the CHMO in the SCR and the STR (2 h per batch); 100% relative activity refers to 7.5% conversion of cyclohexanone in the first batch.

rer needs to be modified with the Spin-Chem compartment chamber.

## Acknowledgements

We thank the "Bundesministerium für Bildung und Forschung" for financial support within the "Biokatalyse 2021" cluster (FKZ: 0315175A) and the "Deutsche Forschungsgemeinschaft" (Bo1862/6-1) for financial support. We are also grateful to the mechanical workshop at Greifswald University for their support in constructing the reactor setups.

**Keywords:** biocatalysis • enzymes • immobilization • kinetic resolution • microreactors

- 43, 788–824; b) K. Buchholz, V. Kasche, U. T. Bornscheuer, *Biocatalysts and Enzyme Technology*, 2nd ed., Wiley-VCH, Weinheim, **2012**; c) *Enzyme Catalysis in Organic Synthesis*, Vol. 1–3, 3rd ed. (Eds.: O. May, H. Gröger, K. Drauz), Wiley-VCH, Weinheim, **2012**; d) S. Wenda, S. Illner, A. Mell, U. Kragl, *Green Chem.* **2011**, 13, 3007–3047; e) *Industrial Biotransformations*, 2nd ed. (Eds.: A. Liese, K. Seelbach, C. Wandrey), Wiley-VCH, Weinheim, **2006**.
- [2] U. T. Bornscheuer, G. W. Huisman, R. J. Kazlauskas, S. Lutz, J. C. Moore, K. Robins, *Nature* **2012**, 485, 185–194.
- [3] a) C. K. Savile, J. M. Janey, E. C. Mundorff, J. C. Moore, S. Tam, W. R. Jarvis, J. C. Colbeck, A. Krebber, F. J. Fleitz, J. Brands, P. N. Devine, G. W. Huisman, G. J. Hughes, *Science* **2010**, 329, 305–309; b) A. A. Desai, *Angew. Chem.* **2011**, 123, 2018–2020; *Angew. Chem. Int. Ed.* **2011**, 50, 1974–1976.
- [4] C. Mateo, J. M. Palomo, G. Fernandez-Lorente, J. M. Guisan, R. Fernandez-Lafuente, *Enzyme Microb. Technol.* **2007**, 40, 1451–1463.
- [5] P. V. Iyer, L. Ananthanarayan, *Process Biochem.* **2008**, 43, 1019–1032.
- [6] a) U. T. Bornscheuer, *Angew. Chem.* **2003**, 115, 3458–3459; *Angew. Chem. Int. Ed.* **2003**, 42, 3336–3337; b) L. Cao, *Carrier-Bound Immobilized Enzymes*, Wiley-VCH, Weinheim, **2005**; c) P. Adlercreutz, *Chem. Soc. Rev.* **2013**, 42, 6406–6436; d) R. DiCosimo, J. McAuliffe, A. J. Poulou, G. Bohlmann, *Chem. Soc. Rev.* **2013**, 42, 6437–6474; e) U. Hanefeld, L. Cao, E. Magner, *Chem. Soc. Rev.* **2013**, 42, 6211–6212; f) A. Liese, L. Hiltnerhaus, *Chem. Soc. Rev.* **2013**, 42, 6236–6249; g) R. A. Sheldon, S. van Pelt, *Chem. Soc. Rev.* **2013**, 42, 6223–6235.
- [7] F. Balkenhohl, K. Ditrach, B. Hauer, W. Ladner, *J. Prakt. Chem.* **1997**, 339, 381–384.
- [8] G. Hills, *Eur. J. Lipid Sci. Technol.* **2003**, 105, 601–607.
- [9] J. J. Carberry, *Ind. Eng. Chem.* **1964**, 56, 39–46.
- [10] J. A. Mahoney, K. K. Robinson, E. C. Myers, *Chemtech* **1978**, 8, 758–763.
- [11] a) M. Höhne, S. Schätzle, H. Jochens, K. Robins, U. T. Bornscheuer, *Nat. Chem. Biol.* **2010**, 6, 807–813; b) H. Mallin, U. Menyes, T. Vorhaben, M. Höhne, U. T. Bornscheuer, *ChemCatChem* **2013**, 5, 588–593; c) S. Schätzle, F. Steffen-Munsberg, A. Thontowi, M. Höhne, K. Robins, U. T. Bornscheuer, *Adv. Synth. Catal.* **2011**, 353, 2439–2445.
- [12] E. M. Anderson, K. M. Larsson, O. Kirk, *Biocatal. Biotransform.* **1998**, 16, 181–204.
- [13] a) N. A. Donoghue, D. B. Norris, P. W. Trudgill, *Eur. J. Biochem.* **1976**, 63, 175–192; b) J. D. Stewart, *Curr. Org. Chem.* **1998**, 2, 195–216.

Please note: Minor changes have been made to this manuscript since its publication in ChemCatChem. The Editor.

- [1] a) M. Breuer, K. Ditrach, T. Habicher, B. Hauer, M. Keßeler, R. Stürmer, T. Zelinski, *Angew. Chem.* **2004**, 116, 806–843; *Angew. Chem. Int. Ed.* **2004**,

Received: July 23, 2013

Published online on October 11, 2013

# Affirmation

## Affirmation

Hiermit erkläre ich, dass diese Arbeit bisher von mir weder an der Mathematisch-Naturwissenschaftlichen Fakultät der Ernst-Moritz-Arndt-Universität Greifswald noch einer anderen wissenschaftlichen Einrichtung zum Zwecke der Promotion eingereicht wurde.

Ferner erkläre ich, dass ich diese Arbeit selbständig verfasst und keine anderen als die darin angegebenen Hilfsmittel und Hilfen benutzt und keine Textabschnitte eines Dritten ohne Kennzeichnung übernommen habe.

Greifswald, 22.08.2014

*H. Mall-*

# Curriculum Vitae

## Curriculum Vitae

### Current Position

03/14-current Employee at the University of Basel in the working group of Prof. Dr. T. Ward (topic: artificial metalloenzymes)

### PhD Thesis

01/11-02/14 PhD Thesis in the field of „Biotechnology and Enzyme catalysis“ supervised by Professor Dr. U.T. Bornscheuer (Institute of Biochemistry, University of Greifswald, Germany),

*Development of Enzymes for Biocatalytic Applications: Protein Engineering, Immobilization and Reactor Concepts*

### Education

2005-2010 Diploma in biochemistry at Ernst-Moritz Arndt University of Greifswald with specialization on biotechnology und immunology (Grade: 1.9).

Diploma thesis in the working group of Prof. U.T. Bornscheuer:

*Characterization and Mutagenesis of Galactitol-Dehydrogenases* (Supervisor: Dr. Hauke Wulf)

- 08-10 Main studies, Degree: Diplom Biochemist (equally to Master)
- 05-08 General studies, Degree: Vordiplom Biochemistry (equally to bachelor)

### Practical experience

02/09-05/09 Industrial placement at Lonza AG, Visp, Switzerland

*Investigation and Fermentation of probiotic products*, Project: Development of a new product

### Social Service

2004-2005 Social health care service as caregiver for mentally ill people

### School

1995-2004 High school “Friedrich-Franz-Gymnasium Parchim“, Degree: „Abitur“ (Advanced courses: mathematics and biology)

# Acknowledgements

## Acknowledgements

Mein größter Dank gilt dir Uwe für die tolle Zeit während meiner Doktorarbeit und Diplomarbeit. Neben dem spannenden Thema habe ich es sehr genossen, dass du es mir stetig ermöglicht hast meiner Kreativität freien Lauf zu lassen und mich dabei tatkräftig unterstützt hast. Auch die vielen Möglichkeiten, auf Konferenzen teilzunehmen, die tollen Gruppenausflüge oder sich auch einfach mal auf ein Bierchen im Huscheck oder in der Kulturbrauerei mit Dir zu treffen. Nicht zuletzt auch für den Aufenthalt bei der Lonza AG oder meiner momentanen Stelle in Basel. Vielen Dank für all dies und vieles mehr!

Ich bedanke mich ebenfalls beim Bundesministerium für Bildung und Forschung (BMBF) innerhalb des Clusters Biokatalyse2021 für die Finanzierung der Projekte.

Hauke, danke für die tolle und produktive Zusammenarbeit mit Dir während unserer Projekte, das Bier am Abend oder der Mensabesuch.

Maria und Stefan auch Euch besonderen Dank für die immer tolle Zeit, die netten Gespräche und die herzliche Aufnahme im Büro. An dieser Stelle möchte ich mich weiterhin für die immer tolle und lustige Atmosphäre im Büro sowie der Kaffeepausen während meiner Ära im Büro B022 bedanken (Maria, Stefan, Sebastian, Jan, Christin, Kathleen und Lilly).

Vielen Dank auch an Euch Leona, Alberto und Hannes für die lustigen Kaffeepauschen und Gespräche!

An dieser Stelle möchte ich mich ganz besonders bei Jan für die tolle Zusammenarbeit während unserer Projekte, Pausen und den abendlichen Ausflügen bedanken.

Liebe Arbeitsgruppe, danke für die schöne Zeit und das gute Arbeitsklima! Vielen Dank auch an Ina, Angelika, Anita und Dominique, dass Ihr alles im Labor am Laufen haltet. Vielen Dank auch Dir, Torge für viele anregende Diskussionen!

Weiterhin möchte ich mich auch bei all meinen PraktikantInnen und AustauschwissenschaftlerInnen bedanken, die ich während meiner Zeit betreuen durfte.

Auch danke ich der Laborcrew (Timo, Jan, Sandy, Micha, Stefan) für das tolle Arbeitsklima in unserem Labor!

Auch danke ich Helge, der mich während meiner Praktikantenzeit in die Welt der Molekularbiologie und Biotechnologie eingewiesen hat!

Von ganzem Herzen danke ich meiner Familie, die mich immer tatkräftig unterstützt hat und stetig mit beruhigenden Worten zur Seite stand. Ihr habt mir als dies ermöglicht, immer an mich geglaubt und wart immer für mich da.

Marie, auch Dir danke ich, dass du immer geduldig und immer da warst, auch wenn ich die Abende in meiner Doktorarbeit versunken war. Ich bin froh, dass es Dich gibt!